

Vinyl Ether Functional Polyurethanes as Novel Photopolymers

Dissertation
zur Erlangung des Grades
„Doktor der Naturwissenschaften“
im Promotionsfach Chemie

am Fachbereich Chemie, Pharmazie und Geowissenschaften
der Johannes Gutenberg-Universität Mainz

Stefan Kirschbaum

geboren in Köln

Mainz, 2015

Dekan:

1. Berichterstatter:

2. Berichterstatter:

Tag der mündlichen Prüfung: 17. Dezember 2015

Ich versichere, die als Dissertation vorliegende Arbeit selbstständig angefertigt zu haben und alle verwendeten Quellen und Hilfsmittel kenntlich gemacht zu haben.

Die vorliegende Arbeit wurde von Oktober 2012 bis November 2015 unter Betreuung von _____ in Kooperation zwischen dem Max-Planck-Institut für Polymerforschung in Mainz und der Henkel AG und Co. KGaA in Düsseldorf angefertigt.

Max-Planck-Institut für Polymerforschung
Max Planck Institute for Polymer Research



Table of Content

1	Introduction.....	1
2	Theoretical Background.....	5
2.1	Basic Considerations of Photocuring.....	5
2.1.1	Photoinitiation and Electronic States.....	6
2.1.2	Cationic Photoinitiators.....	11
2.1.3	Photoinduced Cationic Polymerization.....	14
2.1.4	Photoinduced Radical Polymerization of Acrylates.....	19
2.1.5	Photoinduced Thiol-Ene Curing.....	22
2.2	Chemistry of Vinyl Ethers.....	25
2.2.1	Technical Synthesis and Availability.....	25
2.2.2	Properties and Reaction Capabilities.....	29
2.3	Chemistry of Polyurethanes.....	32
2.3.1	Technical Considerations.....	36
2.3.2	Polyhydroxyurethanes (PHUs).....	38
2.4	Chemistry of Benzoxazines.....	42
3	Characterization Techniques.....	47
3.1	Differential Scanning Calorimetry (DSC).....	47
3.1.1	Temperature Modulated DSC.....	48
3.1.2	Photo-DSC.....	49
3.2	Real Time (Near) Infrared Spectroscopy.....	50
3.3	Rheology.....	51
3.3.1	Photorheology.....	52
3.3.2	UV/NIR-Rheology.....	53
4	Results and Discussion.....	55
4.1	Unique Curing Properties through Living Polymerization in Crosslinking Materials: Polyurethane Photopolymers from Vinyl Ether Building Blocks.....	57
4.1.1	Motivation.....	58
4.1.2	Synthesis of VEPUs.....	59
4.1.3	Radiation Curing of VEPUs.....	60
4.1.4	Vitrification Induced Curing Time Out and Thermal Post-Curing.....	65
4.1.5	Durability of Trapped Cationic Chain-Ends.....	66
4.1.6	Influence of the Curing Conditions on the Network Structure.....	67
4.1.7	Conclusion and Outlook.....	68
4.2	Vinyl Ether Functional Polyols as Building Blocks for UV-Curable Polyurethanes and Isocyanate-Free Polyhydroxyurethanes.....	69

4.2.1	Motivation	70
4.2.2	Synthesis of Urethane Containing VEOHs	71
4.2.3	Synthesis and UV-Curing of Novel VEPUs	73
4.2.4	Polyhydroxyurethanes via Thiol-Ene Addition of Urethane Containing VEOHs	76
4.2.5	Conclusion and Outlook	78
4.3	Synergistic and Sequential Dual Curing Mechanism for Vinyl Ether Functional Polyurethanes	79
4.3.1	Motivation	80
4.3.2	Synthesis and Curing of Isocyanate Terminated VEPUs	82
4.3.3	Conclusion and Outlook	86
4.4	Cationic Phototransfer Polymerization: pH-Responsive Acetal-Based Polymer Networks	87
4.4.1	Motivation	88
4.4.2	Mechanism of Cationic Phototransfer Polymerization	89
4.4.3	Addition of Difunctional Alcohols	91
4.4.4	Addition of Monofunctional Alcohols	93
4.4.5	Conclusion and Outlook	98
4.5	Cationic Phototransfer Polymerization of Photocurable Polyhydroxyurethanes	99
4.5.1	Motivation	99
4.5.2	Synthesis of the VEPHU	102
4.5.3	Cationic Curing of the VEPHU	105
4.5.4	Conclusion and Outlook	110
4.6	Synthesis and Thermal Curing of Benzoxazine Functionalized Polyurethanes	111
4.6.1	Motivation	112
4.6.2	Synthesis and Oligomerization of the P-m	114
4.6.3	Benzoxazine Functionalization of the Polyurethane	121
4.6.4	Curing of the Polyurethane/Benzoxazine-Hybrids	123
4.6.5	Conclusion and Outlook	124
5	Experimental Section	126
5.1	Unique Curing Properties through Living Polymerization in Crosslinking Materials: Polyurethane Photopolymers from Vinyl Ether Building Blocks	126
5.1.1	Materials	126
5.1.2	Synthesis of Vinyl Ether Polyol (VEOH)	126
5.1.3	Synthesis of the Hydrogenated Vinyl Ether Polyol (h-VEOH)	128
5.1.4	General Synthesis Procedure for Vinyl Ether Functionalized Polyurethanes (VEPUs)	128
5.1.5	Formulation of the VEPUs with Photoinitiator	130
5.1.6	Size Exclusion Chromatography (SEC)	130
5.1.7	UV/NIR-Rheology	131
5.1.8	Differential Scanning Calorimetry (DSC)	132
5.1.9	Comparability of UV/NIR-Rheology and Photo-DSC	132
5.2	Vinyl Ether-Functional Polyols as Building Blocks for UV-Curable Polyurethanes and Isocyanate-Free Polyhydroxyurethanes	134

5.2.1	Materials.....	134
5.2.2	Synthesis of 4-Glycidylether Butyl Vinyl Ether (GEBVE).....	134
5.2.3	Synthesis of 4-Glycidylcarbonate Butyl Vinyl Ether (GCBVE).....	135
5.2.4	Synthesis of 1,4-Butanedioldiglycidylcarbonate (BDDGC).....	136
5.2.5	Synthesis of di-Trimethylolpropanedicarbonate (di-TMPDC).....	137
5.2.6	Synthesis of the Vinyl Ether Polyol P1.....	138
5.2.7	Synthesis of the Vinyl Ether Polyol P2.....	139
5.2.8	Synthesis of the Vinyl Ether Polyol P3.....	140
5.2.9	Synthesis of the Vinyl Ether Functionalized Polyurethanes PU1, PU2, PU3.....	142
5.2.10	Synthesis of the Linear Polyhydroxyurethane PHU3.....	142
5.2.11	Synthesis of the Crosslinked Polyhydroxyurethane c-PHU3.....	143
5.2.12	UV/NIR-Rheology.....	143
5.2.13	IR Spectroscopy.....	144
5.2.14	GC-FID Analysis.....	146
5.2.15	¹ H NMR Spectroscopy.....	146
5.2.16	¹³ C NMR Spectroscopy.....	146
5.2.17	HPLC-MS Analysis.....	146
5.2.18	SEC Analysis.....	148
5.3	Synergistic and Sequential Dual Curing Mechanism for Vinyl Ether Functional Polyurethanes.....	149
5.3.1	Materials.....	149
5.3.2	Synthesis of the Vinyl Ether Functional Polyol (VEOH).....	149
5.3.3	Synthesis of the Reactive Vinyl Ether Functional Polyurethane (rVEPU).....	149
5.3.4	UV/NIR-Rheology.....	150
5.4	Cationic Phototransfer Polymerization: pH-Responsive Acetal-Based Polymer Networks.....	151
5.4.1	Materials.....	151
5.4.2	Synthesis of the Vinyl Ether Functional Polyol (VEOH).....	151
5.4.3	Synthesis of the Vinyl Ether Functional Polyurethane (VEPU).....	151
5.4.4	UV/NIR-Rheology.....	152
5.4.5	Differential Scanning Calorimetry (DSC).....	153
5.4.6	Solid State ¹³ C NMR Spectroscopy.....	153
5.4.7	Extractable Alcohol Content (GC Analysis).....	154
5.5	Cationic Phototransfer Polymerization of Photocurable Polyhydroxyurethanes..	155
5.5.1	Materials.....	155
5.5.2	Synthesis of 4-Glycidylcarbonate Butyl Vinyl Ether (GCBVE).....	155
5.5.3	Synthesis of the VEOH.....	155
5.5.4	Synthesis of the Vinyl Ether Diglycidylcarbonate (VEDGC).....	155
5.5.5	Synthesis of the Vinyl Ether Functionalized Polyhydroxyurethane (VEPHU) and Subsequent Amine-scavenging.....	156
5.5.6	Amine-scavenging Study.....	157
5.5.7	¹ H NMR Spectroscopy.....	157
5.5.8	Solid State ¹³ C NMR Spectroscopy.....	158
5.5.9	IR Spectroscopy.....	159
5.5.10	UV/NIR-Rheology.....	159

5.5.11	Differential Scanning Calorimetry (DSC).....	160
5.6	Synthesis and Thermal Curing of Benzoxazine Functionalized Polyurethanes	161
5.6.1	Materials.....	161
5.6.2	Synthesis of 3,4-Dihydro-3-methyl-2H-1,3-benzoxazine (P-m)	161
5.6.3	Oligomerization of P-m.....	161
5.6.4	Vacuum Distillation of P-m	162
5.6.5	Polymerization Study of P-m	162
5.6.6	Synthesis of N,N-bis(3,5-dimethyl-2-hydroxybenzyl)methylamine (DMP ₂ -m)	163
5.6.7	Indirect Potentiometric Titration	164
5.6.8	Synthesis of PU/BOX-Hybrids.....	165
5.6.9	Curing of PU/BOX-Hybrids and Rheological Investigation	166
5.6.10	HPLC-MS Analysis.....	167
6	Summary	168
7	References	173
8	Appendix	VIII
8.1	List of Abbreviations and Symbols	VIII
8.2	Scientific Contributions	X
8.3	Danksagung (Acknowledgement)	XIII
8.4	Lebenslauf (Curriculum Vitae).....	XV

1 Introduction

And God said, "Let there be light," and there was light.

God saw that the light was good, ... [Genesis 1,3-4]

Sun radiation is the primary energy source of the earth. The absorption of the electromagnetic energy and transformation into heat results in the ambient climate that enables life. Nature has further utilized direct radiation energy in photosynthesis to grow plants or algae. In this process organic chemical structures of comparatively high energy are mainly generated from water and carbon dioxide.¹ Therefore, they serve as food and energy source for various living organisms. Over millions of years excess biomass has been anaerobically carbonized under increasing pressure of sedimentary deposition to form fossil fuels such as coal, crude oil and gas.² Within the last centuries technical developments enabled the exploitation of these subterranean deposits to a large extent. However, the continuously increasing energy demand of a growing population and the limited availability of fossil fuels in combination with global warming issues as a result of exhaust gas pollution led to the awareness that a more balanced energy budget needs to be achieved. Over the last decades, extensive efforts were made towards environmental cautiousness, renewable energy sources, energy efficiency and ecological sustainability.

For the so-called energy turnaround the generation of energy from renewable sources plays an important role and particularly photovoltaics, which turns light into electric power represents an important share. On the other hand an efficient use of energy is as important as its generation. Light is the foundation for the human visual sense and provides convenience, orientation and safety. Therefore, when the sun goes down large areas on earth are illuminated by artificial light. Unfortunately, the artificial generation of light is often very inefficient and accompanied by heat generation. Nowadays, more efficient light sources such as light emitting diodes (LED) or laser diodes are available. Exemplary, the Nobel Prize in Physics 2014 was awarded for the invention of efficient blue light emitting diodes, which have enabled bright and energy-saving white light sources.³ In this context, the European Union has enacted regulations to gradually ban

inefficient light bulbs and halogen lamps since 2009.^{4, 5} Recognizing how light-based technologies promote sustainable development and provide solutions to global challenges the UN proclaimed 2015 as the “*International Year of Light and Light-based Technologies*” to focussing on the topic of light science and its applications.⁶

A growing field of research is photochemistry that deals with the utilization of light as energy source to drive chemical processes or convert light energy into chemical energy, following the example of photolysis.^{7, 8} Generally, photochemical excitation provides molecules with sufficient energy for certain desired transitions and enables reaction pathways that would not be accessible from the ground state.⁹ Furthermore, photocatalysts or photosensitizers can be applied to transfer energy to molecules that do not absorb light energy. Consequently, several scientists all over the world devote their research activities towards chemical reactions assisted by light.

One particular photochemical technology that has become commercialized on a large scale is photocuring. Several applications such as coatings, adhesives or sealants necessitate materials that can be easily applied as a liquid and convert to a solid to fulfill its requirements. In the early days mainly thermal curing or solvent based materials were used. The associated setting procedures are accompanied by large energy consumption and may cause environmental pollution. Photocuring provides a great alternative as latent reactive formulations cure fast and selective in the irradiated area. This process is characterized by a comparatively low energy consumption, even if artificial light sources are used and provides a valuable contribution towards various more sustainable production processes.

In 1972, photoinduced radical polymerization was undergoing rapid development as replacement for thermal curing or solvent based coatings.¹⁰ As the costs estimated for an UV-induced enamel production line including a nitrogen purging system to avoid oxygen inhibition of radically polymerizing systems were too expensive, James Vincent Crivello started looking for alternatives and got interested in cationic polymerization, which offers manifold new reaction characteristics such as fast polymerization without oxygen inhibition, a non-terminating reaction mechanism and the utilization of heterocyclic monomers. At that time Crivello came across a publication that described photosensitivity of diaryliodonium salts and realized that any pathway he could imagine

for the photolysis of this compounds would involve the generation of a highly reactive cationic species. In the following, he prepared several types of onium salt based photoinitiators and applied them for the polymerization of various heterocyclic and activated vinyl monomers. With his pioneering work, he lay the foundation for the technical application of cationic polymerizations. Previous to the development of cationic photoinitiators, conventional cationic polymerization was typically induced by direct addition of the initiating species and instantaneous gelation was observed upon mixing these initiators into multifunctional monomers. First, the latent reactivity of onium salts enabled well-controlled, cationic mass polymerization that is essential for reliable processes. The onium salt itself is not capable to induce the reaction and can be dissolved in photocuring formulation. Polymerization is subsequently initiated simultaneously in the entire radiated volume.

Among cationically polymerizable monomers epoxides and vinyl ethers are often mentioned to be most interesting owing to their high reactivity and the variety of available monomers. However, vinyl ether monomers are rarely used in commercial applications due to their comparatively high costs and poor product properties,¹¹ whereas epoxides are widely applied as coatings, adhesives, inks, photoresists and holographic data storage. Also recent, exciting additive manufacturing methods such as stereolithography and 3D-inkjet printing use photocuring epoxy resin.¹² Nevertheless, concerning reactivity and sensitivity towards nucleophilic groups vinyl ethers are vastly superior in comparison to epoxides and provide an enormous potential that has not been fully utilized yet.

Thus the objective of this work are vinyl ether functionalized polyurethanes that provide adjustable curing profiles and high performance properties and complementary introduce a photoinduced, cationic curing mechanism to polyurethane chemistry. This conceptually new materials overcome the structural limitations associated with low molecular weight vinyl ethers and in contrast to state-of-the-art photocuring polyurethane acrylates the cationic mechanism is not inhibited by oxygen and shows a considerable *dark curing* behavior, which means that the polymerization reaction continues after the light source was switched off, due to the absence of an inherent termination mechanism. Moreover, vinyl ether functional polyurethanes with additional

functional groups are prepared and the curing process was altered by the introduction of special transfer agents.

Furthermore, novel benzoxazine functionalized polyurethanes were prepared, which provide a thermal curing mechanism for polyurethanes and may be applicable as toughener in benzoxazine resins or stand-alone materials. A more detailed introduction to the particular work presented in this thesis is provided in the abstracts section.

This thesis is based on six publications or publication drafts, which are discussed separately in the Chapter 4.1 - 4.6. Every section represents a coherent research project and individual abstracts are provided at the beginning. However, all sections are related to each other and the most basic work is presented first.

2 Theoretical Background

2.1 Basic Considerations of Photocuring

Photocuring can be defined as light induced conversion of a liquid material to the solid state.¹³⁻¹⁷ This conversion is generally achieved via radical or cationic polymerization of multifunctional monomers, oligomers or prepolymers to yield crosslinked polymers. Photocuring materials are typically applied as bulk systems that rapidly change from liquid to solid state without application of solvents or thermal treatment. The use of radiation as energy source provides an energy efficient and environmentally benign setting mechanism, selectively in the irradiated volume. Photocurable formulations often consist of three main components. Oligomers or prepolymers that comprise functional groups for the curing reaction, low molecular weight reactive diluents and a suitable photoinitiating system. The prepolymer backbone, which often comprises ether, ester or urethane repeating units largely contributes to the final material properties. Reactive diluents are low molecular weight mono- or multifunctional monomers, which are used to adjust the viscosity of the formulation and the crosslinking density of the cured product. Photoinitiators are applied to generate initiating species capable to start the curing reaction upon light absorption of defined wavelength. The photophysical and photochemical processes involved are discussed in Chapter 2.1.1. Often photosensitizers or coinitiators are applied along with photoinitiators to adopt the absorption characteristics to a given light source and improve the efficiency of the initiation process.

Photocuring reactions mostly proceed via chain growth, whereas either radical or cationic polymerization mechanisms are applied depending on the polymerizable groups. Most commonly, acrylates and methacrylates are polymerized via radical mechanism due to their high reactivity, low costs and large variety of available monomers. Hence, they are frequently considered as benchmark in photocuring technologies.^{14, 18} Moreover, other unsaturated monomers also polymerize via radical mechanism. Exemplarily the copolymerization of unsaturated polyester with styrene that finds application in glass fiber reinforced composites should be mentioned.^{14, 19}

The radical mediated thiol-ene is a unique type of reaction, as it proceeds via a step growth mechanism. Among cationic polymerizations, only epoxides have made their way to significant commercial applications. These different types of photocuring reactions are discussed in Chapter 2.1.3 and the following.

Because of their obvious advantages, photocurable materials serve a wide variety of applications,^{10, 11} such as decorative, protective or functional coatings, adhesives, printing inks, photoresists and insulations for microelectronics, stereolithography,^{12, 20} nanoimprint lithography,²¹⁻²³ holographic data storage^{24, 25} and dental fillings.^{26, 27} Due to the instantaneous solidification, high spatial resolution, and the environmentally benign curing procedure, photocuring materials seem to enjoy an ever growing field of applications facilitated by the continuous development of efficient laser and light emitting diodes (LED) light sources, novel application processes, and tailored photopolymers.

2.1.1 Photoinitiation and Electronic States

Photoinitiators are molecules that generate reactive species, capable to initiate radical or cationic polymerization upon irradiation.¹³ Therefore, they comprise chromophores that absorb light of a certain wavelength. The electromagnetic spectrum is shown with an emphasis on the regions of interest in Figure 2.1.

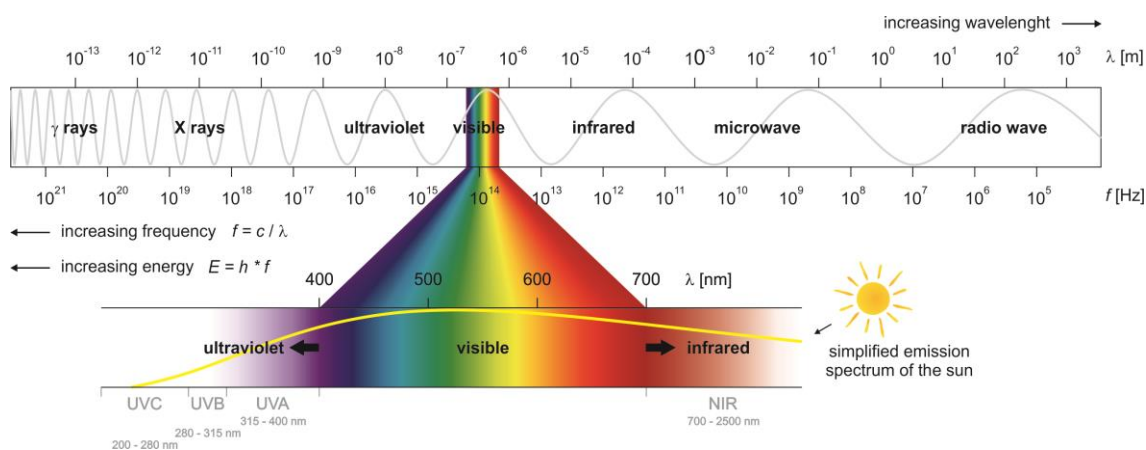


Figure 2.1. The electromagnetic spectrum.

The visible light spectrum and adjacent ultraviolet and near infrared regions are highlighted as they are of high importance for photoinitiation processes as well as characterization methods applied in this thesis.

Ideally, the absorption spectrum of a photoinitiator correlates with the emission spectrum of the light source used.²⁸ The absorption process and subsequent photophysical and photochemical processes are reviewed in detail in the literature^{13, 14, 29-33} and a basic overview is provided hereafter.

Molecules may absorb light of an appropriate energy via excitation of an electron. The energy required for electronic excitation generally corresponds to ultraviolet, visible or in rare cases near infrared light, whereas pure changes in the vibrational or rotational energy levels are stimulated by significantly lower energies via absorption in the infrared or microwave spectral region. Consequently, electronic excitation is generally accompanied by transitions in the vibrational and rotational molecular energy levels and hence results in a broad, band-like absorption. The corresponding energy scheme of a molecule is shown in Figure 2.2.

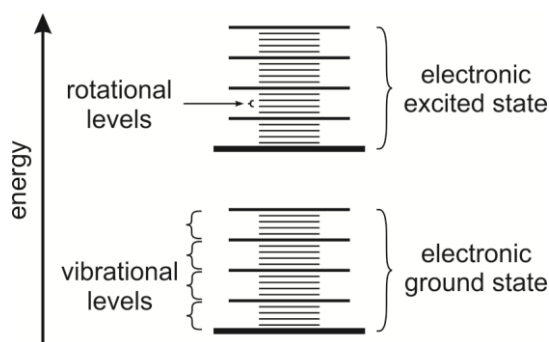


Figure 2.2. Energy scheme for the superimposition of electronic, vibrational and rotational states.

Electronic excitation is generally accompanied by transitions in the vibrational and rotational molecular energy levels.

Accordingly, the total excitation energy ΔE consists of three terms for the transitions of the electronic, the vibrational and the rotational state (Equation 1).

$$\Delta E = \Delta E_{elect.} + \Delta E_{vibr.} + \Delta E_{rot.} \quad (1)$$

The electronic transition can occur among various orbitals. However, the lowest energy and thus the most important transitions are the promotion of bonding π -electron in carbon-carbon double bonds ($\pi\pi^*$ -excitation) or the promotion of a non-bonding n-electron from the lone pairs of heteroatoms, e.g. oxygen in carbonyl groups ($n\pi^*$ -excitation) to an unoccupied antibonding π -orbital π^* of substantially higher

energy. If chromophores are connected to electron donating substituents or consist of conjugated unsaturated systems, the energy difference between the highest occupied molecular orbital (HOMO) and the lowest unoccupied molecular orbital (LUMO) is narrowed and the absorption is shifted towards longer wavelengths (red-shifted).

Most unexcited molecules exist in a singlet ground state (S_0), which means that they exhibit paired electrons of antiparallel spin. Generally, electronic excitation occurs with retention of the electron spin to any of the excited singlet states (S_1 - S_n). The absorption process proceeds within 10^{-15} s and is followed by internal conversion (IC) and vibrational relaxation (VR) to the excited singlet state of lowest energy (S_1) within about 10^{-12} s. Due to this fast relaxation of excess energy excitation and decay processes originate almost exclusively from the vibrational ground state of each electronic level (Kasha's rule). The first excited singlet state may decay via emission of a photon and returns to any vibrational level of the electronic ground state and is again followed by a series of vibrational relaxations to the vibrational ground state. This process is called fluorescence and is depicted in Figure 2.3.

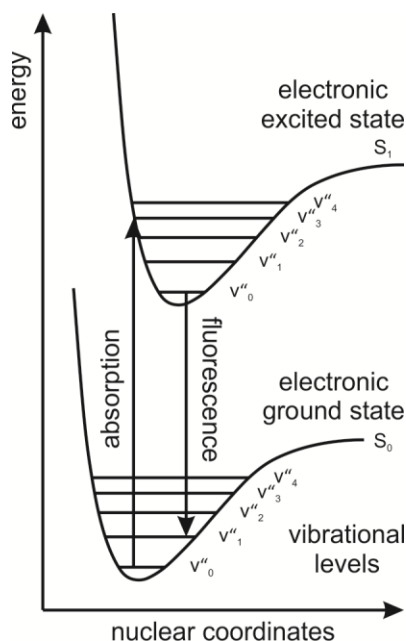


Figure 2.3. Franck-Condon energy diagram.

Electronic excitation generally occurs from the vibrational ground level to any vibrational level of the excited state with different probabilities depending on the overlap of their wave functions.

Following the Franck-Condon principle, the change in electronic energy levels is so fast that it occurs without changes in the relative atomic position and hence the electronic

excitation is more likely if the wave functions of both electronic states overlap. This vibrational fine structure may result in shoulders or asymmetric bands in the absorption or emission spectrum.

Instead of fluorescence, the first excited singlet state can also undergo intersystem crossing (ISC) to the first excited triplet state (T_1) of the same potential energy via spin inversion. The unpaired electrons exhibit parallel spins in the triplet state. The molecular orbital scheme for different electronic states of ethylene is shown in Figure 2.4.

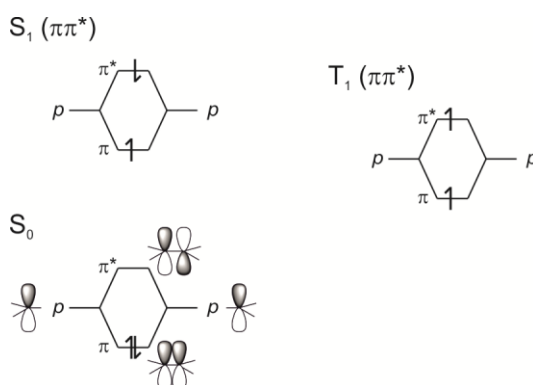


Figure 2.4. Molecular orbital scheme of ethylene.

Generally, triplet states are of lower energy as the corresponding singlet states. Therefore, ISC proceeds to a promoted vibrational level in the triplet state, where the potential energy of both states intersect. This vibrational level subsequently dissipates via vibrational relaxation just as it has been described for the singlet state. Figure 2.5 shows ISC in the potential energy diagram.

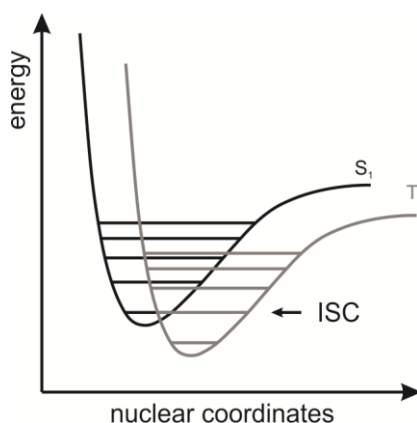


Figure 2.5. Potential energy diagram for the intersystem crossing process.

Intersystem crossing occurs when the potential energy of the singlet and triplet states intersect.

Due to the parallel spins, the decay of the triplet state is quantum mechanically forbidden and therefore improbable. However, also the excited triplet state can decay via emission of a photon with significantly lower probability. This process is called phosphorescence and the lower energy difference in comparison to fluorescence results in an emission of longer wavelength. Furthermore, the prolonged life time of the triplet state results in a long-lived emission of up to 10^3 s. Both electronically excited states are highly reactive, whereas photochemical reactions compete with other decay mechanisms. Hence, the majority of photochemical reactions occur from the excited triplet state due to its long lifetime. Finally, both excited states can decay to the ground state radiation less via energy transfer to other molecules. This process is of high importance for photosensitization or quenching processes. A summary of the processes that can occur as a consequence of light absorption is provided in the Jablonski diagram in Figure 2.6.

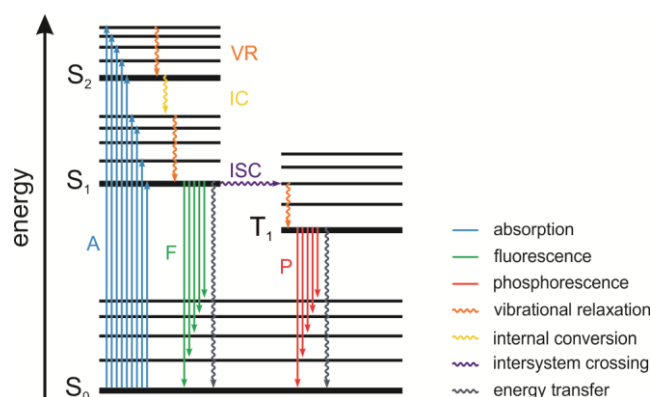


Figure 2.6. Jablonski diagram.

Possible decay mechanisms for electronically excited states upon light absorption.

Several processes that may take place upon light absorption compete with each other. The probability of any photophysical or photochemical process depends on the molecular structure and can be expressed by the quantum yield, which is defined as quotient of the number of a specific event and the number of absorbed photons. The quantum yield for the generation of initiating species is hence defined as moles of initiating species that are generated per Einstein (one mole photons) absorbed light and sufficiently describes the efficiency of a photoinitiator. By definition, the quantum yield exhibits values between 0 and 1 unless decomposition by-products are capable to induce dissociation of further photoinitiator molecules in a chain reaction.

Electromagnetic radiation of higher energy such as short UV-rays (< 200 nm), X-rays and γ -rays may be ionizing as they free electrons from atoms and molecules depending on their specific ionization energy. Therefore, ionizing radiation is also capable to induce polymerization active species directly from the monomer without the need of photoinitiators. Besides electromagnetic radiation also particle radiation of sufficient energy acts ionizing and especially electron beams have been applied in photoinitiator free radiation curing.³⁴ However, for safety considerations and energy efficiency recent developments focus on lower energy initiation, particularly in the visible light spectrum.

2.1.2 Cationic Photoinitiators

Photoinitiators are molecules that generate radical, cationic or anionic species capable to induce chemical reactions upon light absorption. Radical photoinitiators are by far the most important ones, as they are widely applied to induce curing of acrylate formulations. However, the work in hand mainly deals with cationic curing reactions. Therefore, this chapter is devoted to cationic photoinitiators. Detailed information on radical photoinitiators is available in the respective literature.^{14, 35-37}

Several types of cationic photoinitiators including halonium salts, sulfonium salts diazonium salts and organometallic complexes are described in the literature.^{14, 38} Among these, diaryliodonium salts and triarylsulfonium salts are most frequently applied^{28, 39-41} and were exclusively used in this work. They are thermally stable, non-hygroscopic and exhibit efficient quantum yields. Brønsted acids are generated as initiating species upon photolysis. Thus they are also referred to as photoacid generators (PAGs). The basic structures of diaryliodonium and triarylsulfonium salts are shown in Figure 2.7.

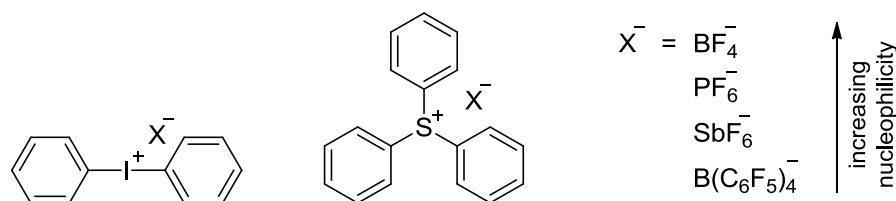


Figure 2.7. Basic structure of diaryliodonium salts and triarylsulfonium salts.

The solubility and absorption characteristics of onium salts are largely influenced by their substituents. The ion pair separation and consequent polymerization kinetics largely depends on the nucleophilicity of the counter anion.

The absorption maxima are located at about 230 nm for simple diphenyliodonium salts and 260 nm for simple triphenylsulfonium salts. The aryl groups of the cation are often substituted to red-shift the absorption maximum and increase the molar extinction coefficient. Furthermore, the solubility of generally polar salts in nonpolar monomers can be significantly improved by long-chain alkyl substituents. Finally, the residue influences volatility, odor and toxicity of arene or sulfur containing cleavage products that may be released upon photolysis. In general, triarylsulfonium salts exhibit better absorption characteristics, increased quantum yields and an improved heat stability in comparison to diaryliodonium salts. On the contrary they are more prone to yellowing, may exhibit a sulfur-like odor and are less soluble in nonpolar monomers. Exemplarily, the structure and absorption spectra of 4,4'-dimethyl-diphenyliodonium hexafluorophosphate (Omnicat 440) and 10-[1,1'-Biphenyl]-4-yl-2-(1-methylethyl)-9-oxo-9*H*-thioxanthenium hexafluorophosphate (Omnicat 550) as commercially available photoinitiators that have particularly been used in this thesis are shown in Figure 2.8.

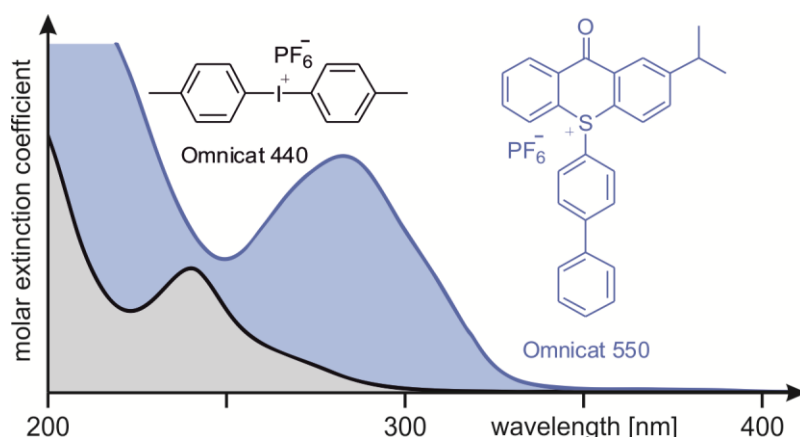


Figure 2.8. Structure and spectra of particular onium salt initiators.

The absorption spectrum of the sulfonium salt is red-shifted due to its enhanced chromophore system. Both initiators comprise the harmless hexafluorophosphate anion.

The counter anion is particularly characterized by its size and electron density. Large anions with a relatively low electron density are non-nucleophilic and lead to a good ion pair separation and hence rapid propagation. In contrast, more nucleophilic anions are less separated and may even be added to the monomer or dissociate. The nucleophilicity decreases in the order: $\text{BF}_4^- > \text{PF}_6^- > \text{SbF}_6^- > \text{B}(\text{C}_6\text{F}_5)_4^-$. Therefore, the choice of the anion has a great impact on the propagation rate and the structure of the polymer. However, the tetrakis(pentafluorophenyl)borate anion is very expensive and the

hexafluoroantimonate anion is toxic. Consequently, the hexafluorophosphate anion is increasingly used in commercial photocuring applications.

The decomposition mechanism of diaryliodonium salts is exemplarily discussed in the following. Albeit, triarylsulfonium decomposes via a similar mechanism. The photolysis of diaryliodonium salts involves the scission of the C-I-bond. The cleavage can be homolytic or heterolytic to form either a phenyliodine and a phenyl cation or a phenyliodonium radical cation and a phenyl radical. These pairs of cleavage products are formed together, surrounded by a “cage” of solvent molecules (mainly monomer and polymer) and stays in close proximity for a finite time period. In that time period the pair undergoes a series of contacts before it escapes and separate. Therefore, in cage reactions like recombination, intrapair electron transfer or other reactions of the pair are favored, especially in viscous media.¹⁴ The bond scission occurs either from the excited singlet state, or the excited triplet state, whereas the triplet state only cleaves homolytically. Radicals formed from the dissociation of a triplet state cannot recombine due to their parallel spins, until they undergo intersystem crossing to form a singlet radical pair. In addition to in-cage reactions protons may also be generated via out-of-cage processes in the presence of hydrogen donors. A simplified decomposition mechanism is shown in Figure 2.9.

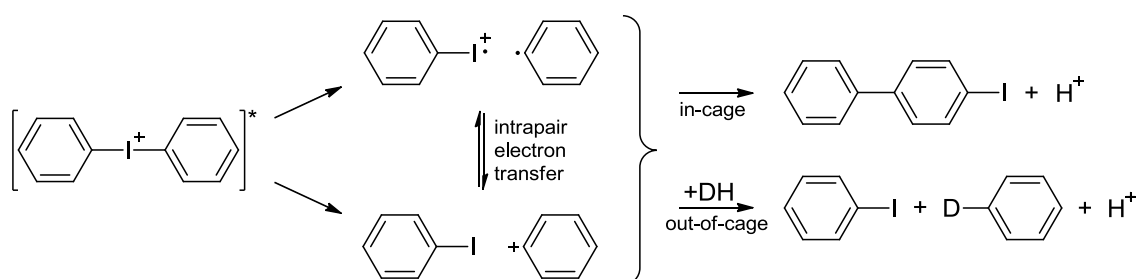


Figure 2.9. Simplified decomposition mechanism of the excited diphenyliodonium cation.

Cleavage of the C-I-bond can be homolytic or heterolytic and the initiating Brønsted acid is generated via in-cage rearrangement or out-of-cage reactions with hydrogen donors.

Additionally, reactions of the primary photolysis products occur with solvent, monomer or further initiator molecules, whereas radical intermediates may induce the decomposition of further initiator molecules via electron transfer. The generated free Brønsted acid is the main initiating species for the subsequent cationic polymerization.

Furthermore, the absorption and decomposition characteristics of a photoinitiating system can be significantly enhanced by the addition of sensitizers or coinitiators. Hydrogen donors can be intentionally applied as coinitiator species to facilitate the out-of-cage decomposition mechanism. On the other hand, sensitizers are molecules that absorb light of longer wavelength and accordingly lower energy and induce the decomposition of the actual photoinitiator. Due to their low reduction potential the most efficient sensitization mechanism for onium salts proceed via electron-transfer. Prominent photosensitizer are anthracenes,^{42, 43} which absorb in the visible range, slightly above 400 nm, and radical photoinitiator with good absorption characteristics. This approach is the so-called free radical promoted cationic polymerization, whereas the electron transfer does occur from the released radicals rather than from the excited state.⁴⁴ The use of sensitizers is an efficient way to adjust the absorption characteristics towards harmless, low energy and low cost light sources such as highly efficient LEDs and lasers (Blu-ray laser and efficient LEDs emit at 405 nm) or sunlight, which makes photocuring more appropriate to the masses.⁴⁵ Particularly, blue LEDs enable the application in consumer products like household 3D-printer without extensive safety regulations. Moreover, initiation with longer wavelengths allow curing through transparent substrates that strongly absorb in the UV-range like glass or polycarbonates and enables the application of thicker films via deeper light penetration into the material.

2.1.3 Photoinduced Cationic Polymerization

This chapter provides a brief overview on cationic polymerization under consideration of photocuring conditions and with a focus on the most important monomers in photocuring applications. More detailed explanations on cationic polymerization in general can be found in several reviews^{40, 46} and text books.^{47, 48}

Cationic polymerization is a chain growth reaction that is initiated by addition of a cation to a monomer and characterized by the consecutive addition of further monomer units to the propagating, cationic chain-end. Monomers that can be polymerized via cationic mechanism include heterocycles, vinyl monomers with electron rich double bonds and compounds with a double bond to heteroatoms such as carbonyls. Figure

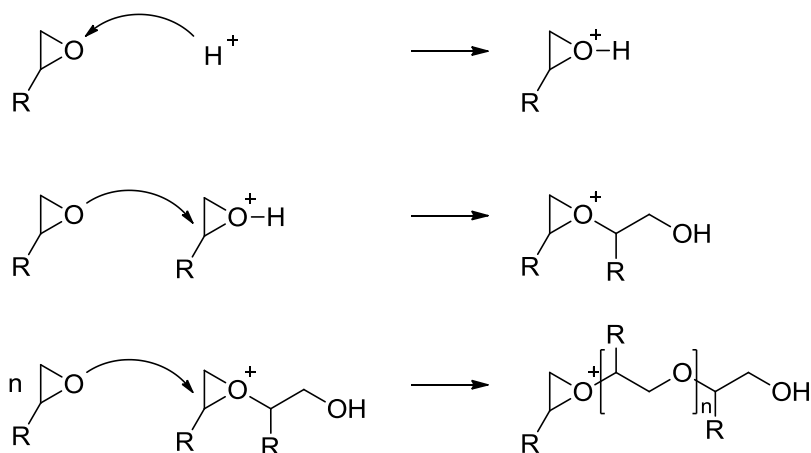


Figure 2.11. Cationic polymerization mechanism of epoxides.

The epoxide is activated via proton addition to form an oxonium cation. The consecutive addition of further epoxides appears through attack at the electron deficient α -carbon and ring-opening.

In contrast, vinyl ethers polymerize via carbenium ions. These carbenium ions are generally less solvated in comparison to oxonium ions and the activation energy of monomer addition is lower. Therefore, the cationic polymerization of vinyl ether proceeds with rates similar to those of acrylates polymerizing via a free radical mechanism. Additionally, resonance stabilization renders the carbocation relatively stable and less prone to side-reactions. It has been shown that the polymerization of vinyl ether proceeds well in the presence of several weak nucleophiles like amides or urethanes that already inhibit the polymerization of epoxides.^{40, 51} This is a very important aspect as it is a basic requirement for the cationic polymerization of vinyl ether functionalized polyurethanes, which are presented in this work. The polymerization mechanism of vinyl ethers is depicted in Figure 2.12.

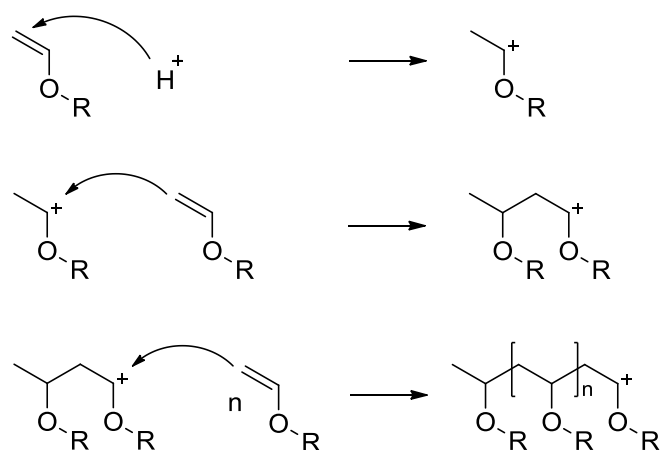


Figure 2.12 Cationic polymerization mechanism of vinyl ether.

Cationic polymerization is initiated via addition of a proton to the electron rich double bond. The resulting carbocation propagates via addition of further monomers. The cationic polymerization of vinyl ether proceeds very fast in comparison to epoxides. Furthermore, the reaction tolerates the presence of weak nucleophiles such as amides or urethanes.

As initiators, Brønsted acids, Lewis acids, or carbenium salts can be applied. Each cationic species is accompanied by non-nucleophilic counter ions, which exhibit a considerable influence on the polymerization reaction. The activated species at the chain-end may exist in several forms starting from a polarized covalent bond via counter associated ions, ion pairs or solvated ion pairs up to free ions. The separation of the ion pair has a drastic influence on the reaction kinetics and product structure. In well controlled solvent based cationic polymerization the separation of a specific ion pair is largely dependent on the dielectric constant of the solvent. However, photocuring is generally performed in bulk, hence the reaction medium consists of monomers and polymer. Therefore, the reaction progress is mainly defined by the monomer and counter ion structure, which is introduced by the initiator as well as the temperature and the mobility of reactants in the formulation.

Evenly charged, ionic chain-ends exhibit mutual repulsion and hence lack a compelling, natural termination mechanism. As a consequence, the chain-ends remain “*living*” throughout the entire polymerization and after complete conversion in the absence of termination and transfer reactions. The concept of living polymerizations was introduced by Szwarc⁵² and is further characterized by an initiation rate much faster than the propagation rate. This allows an almost simultaneous initiation and a similar chain growth of all polymer chains, which remain living after complete conversion and continue to propagate upon further addition of monomer. The simultaneous chain

growth and the absence of termination and transfer reactions result in a narrow, Poisson-like molar mass distribution and a linear increase of the average molecular weight over the conversion. Hence, the final degree of polymerization X_n can be predicted from the monomer concentration $[M]$ and the initiator concentration $[I]$ via.

$$X_n = [M] / [I] \quad (2)$$

Moreover, sequential monomer addition provides an efficient method for the synthesis of block copolymers, whereas the intentional addition of termination agents allows the synthesis of polymers with defined end-groups. The first example of a living cationic polymerization was the polymerization of isobutyl vinyl ether initiated by HI/I_2 .⁵³ However, cationic propagating species are generally not very stable and easily undergo transfer and termination reactions. Therefore, truly living cationic polymerizations are rare and will only be obtained at very low temperatures and with a wisely chosen initiator system in the absence of nucleophiles. In contrast, the initiating species generated via photolysis of onium salts are simple protonic acids and for application reasons photocuring is usually performed at ambient or elevated temperatures. Consequently, transfer and termination reactions cannot be excluded. Furthermore, the prolonged initiation process caused by photolysis over the entire irradiation period results in a broadened molecular weight distribution. Nevertheless, the polymerizing species is still long living and allows the curing reaction to continue after the irradiation is stopped. This behavior is called “*dark cure*” and is contrary to radical photocuring reactions where conversion stops immediately in the dark.

The differentiation of transfer and termination reactions is a pure kinetic consideration. Transfer reactions also terminate a growing chain, but the thereby generated cation is capable to start a new propagating chain. Transfer reactions are more often than a true termination of the kinetic chain. Termination and transfer reactions that may occur upon photopolymerization of vinyl ether comprise proton transfer under formation of unsaturated end groups, addition of counter ions and fragments, hydride abstraction, or the reaction with traces of water or other nucleophiles. These reactions are shown in Figure 2.13.

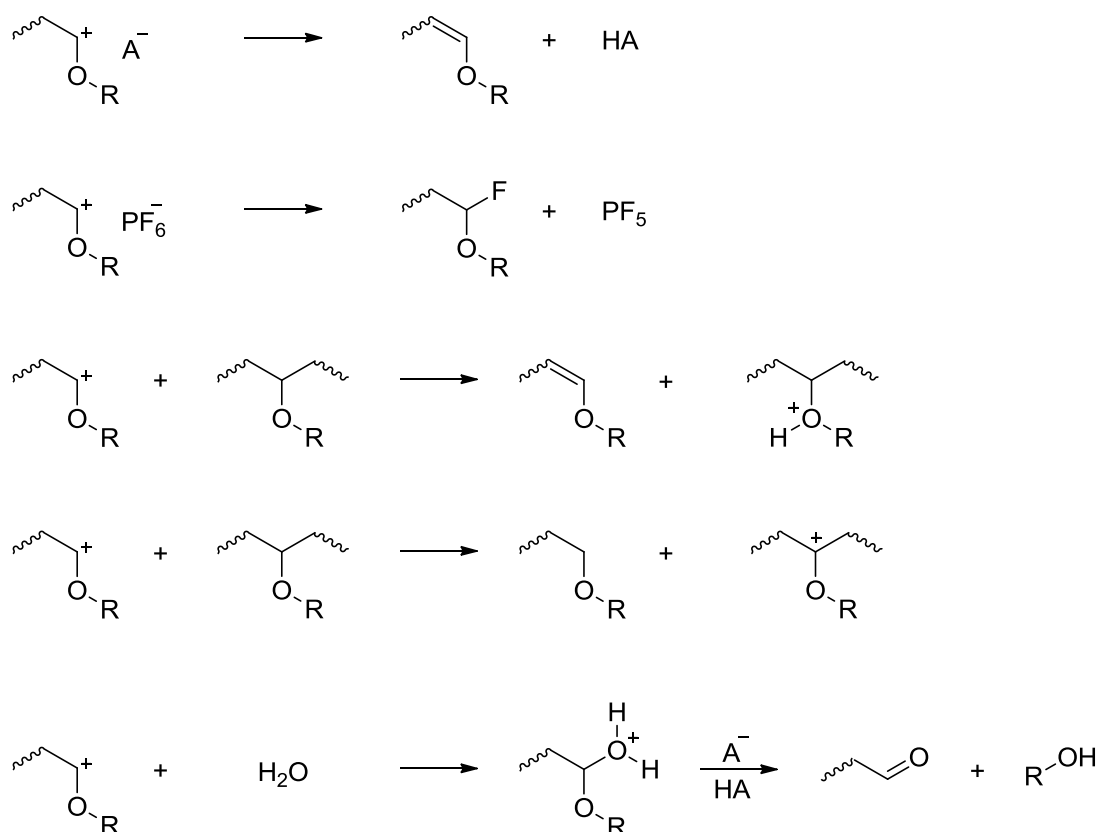


Figure 2.13. Termination and transfer reactions upon photopolymerization of vinyl ether.

Cationic polymerization is sensitive towards a number of nucleophiles, these reactions are also described in Chapter 2.2.2. Especially the transfer reaction with hydroxyl groups is discussed and utilized in Chapter 4.4 and Chapter 4.5. However, highly reactive vinyl ether monomers actually tolerate weakly nucleophilic functional groups like amides or urethanes⁵¹ and in contrast to radical polymerization, cationic polymerization is particularly not inhibited by oxygen.

2.1.4 Photoinduced Radical Polymerization of Acrylates

The vast majority of photocuring systems consists of radical curing (meth)acrylate based monomers and oligomers.^{14, 18} Because of its importance, the mechanism for radical polymerization of acrylates is shown in Figure 2.14.

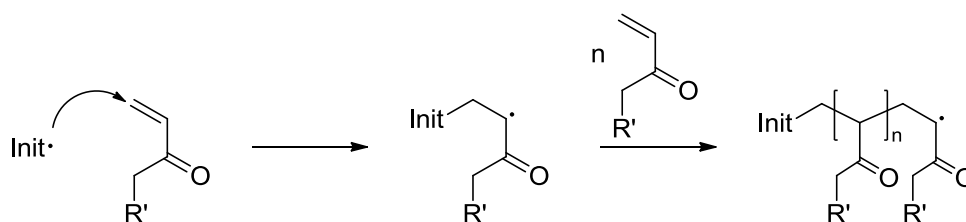


Figure 2.14. Radical polymerization of acrylates.

The initiator radical adds to the acrylic double bond and forms a monomer radical. The monomer radical propagates via further addition of monomers to form a polymer. However, in contrast to cationic polymerization the growing radical chain-ends readily terminate each other in fast radical combination or disproportionation reactions. Therefore, the reaction abruptly stops, if no more initiating radicals are generated after irradiation as is illustrated in Figure 2.15.

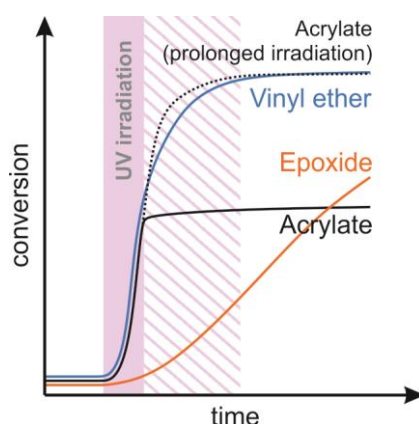


Figure 2.15. Schematic reaction progress during and after irradiation.

The radical polymerization of acrylates abruptly stops after irradiation. Hence, the sample needs to be irradiated for the entire curing process (prolonged irradiation is indicated by the dashed background). On the contrary, cationic curable formulations exhibit significant dark curing (the polymerization proceeds in the absence of light after initial photoinitiation). Furthermore, vinyl ether polymerize with rates similar to those of acrylates, whereas epoxides polymerize comparatively slow.

The success of acrylates substantially relies on the large commercial availability and straightforward functionalization reactions using acrylic acid or hydroxyethyl acrylate as reactive precursors. Besides various low molecular weight crosslinkers and reactive diluents, there is also a huge variety of (meth)acrylate functionalized based oligomers and prepolymers with polyether, polyester, epoxy resins, or polyurethane backbones readily available. Figure 2.16 exemplarily shows the functionalization reaction of polyurethane prepolymers containing terminal isocyanate groups with hydroxyethyl acrylate.

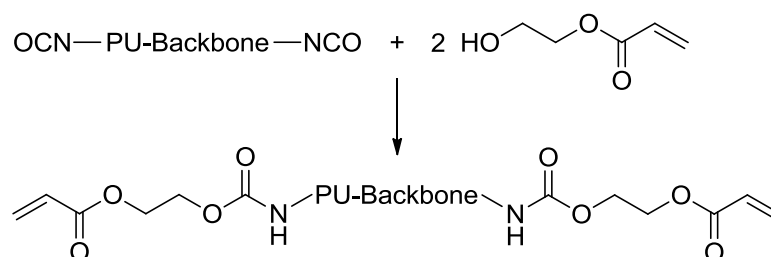


Figure 2.16. Synthesis of polyurethane acrylates (PUA).

Polyurethane acrylates are frequently used as UV-curable materials.

Furthermore, various acrylates and methacrylates can be easily copolymerized, the polymerization proceeds very fast (often within seconds) and is tolerant towards several functional groups. However, especially low molecular weight acrylates are volatile, exhibit a strong odor and show irritating properties.¹⁴ Furthermore, radical polymerization is generally sensitive towards oxygen inhibition and various, partial costly procedures like nitrogen purging lines are implemented to circumvent the effect of oxygen inhibition.⁵⁴

The electronic configuration of oxygen exhibits two antibonding electrons of parallel spin in different orbitals. Therefore, oxygen molecules exhibit a triplet ground state (t_0) with biradical character that is the reason for the inhibiting effect on radical polymerization. Two mechanisms can be observed. First, the triplet oxygen is readily excited via energy transfer from an excited photoinitiator molecule before it decomposes. This effect is known as quenching. However, it is minor for very efficient photoinitiators that decompose with very short life times. Second, due to the biradical character oxygen easily adds to initiator or propagating radicals to form a peroxy radical. The peroxy radical is significantly less reactive and incapable to add further monomer. Instead the peroxy radical readily combines with other radical to terminate another polymer chain as indicated in Figure 2.17.

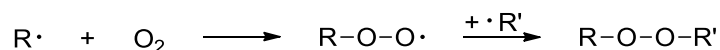


Figure 2.17. Oxygen inhibition through addition of radicals.

The propagation inactive peroxy radical readily combines with other radicals to terminate a second initiator or propagating radical.

It is important to mention that dissolved oxygen is consumed very fast and oxygen inhibition is largely caused by diffusing oxygen. Therefore, applications with large

surfaces areas that are typical for photocuring materials are particularly prone to oxygen inhibition. The effect of oxygen inhibition on the reaction progress is shown in Figure 2.18.

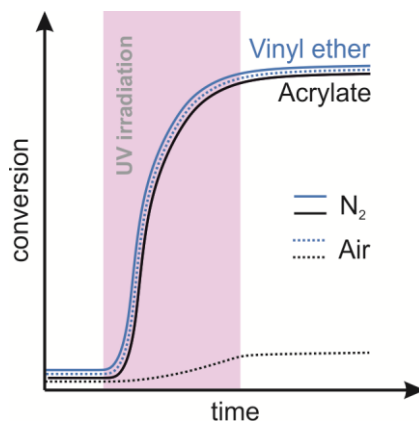


Figure 2.18. Schematic illustration of the oxygen inhibition effect on the conversion plot.

Radical polymerization is largely affected by oxygen inhibition. Therefore, the reaction is often conducted under inert gas atmosphere. In contrast, cationic polymerization is generally not inhibited by oxygen.

A chemical approach to significantly reduce oxygen inhibition is the addition of thiols, which is discussed in the following chapter. However, the easiest way to circumvent oxygen inhibition is the application of a non-radical curing mechanism such as cationic polymerization.

2.1.5 Photoinduced Thiol-Ene Curing

Radical mediated thiol-ene addition represents a rigorous modification of radical polymerization via pronounced transfer reactions.^{14, 55-59} Various unsaturated monomers are reactive in this reaction and are summarized as “enes”. The mechanism of thiol-ene reactions can be described as follows and is shown in Figure 2.19.

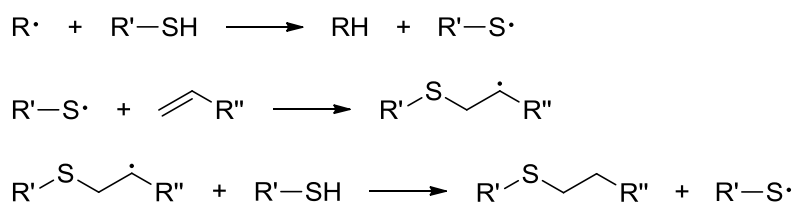


Figure 2.19. Radical mediated thiol-ene addition.

The weak sulphur-hydrogen-bond of thiols is readily cleaved in radical transfer reactions.

The initiator radical easily abstracts a hydrogen radical from the weak sulfur-hydrogen-bond of a thiol and forms a thiyl radical. Subsequently, the thiyl radical adds to the carbon-carbon double bond of the ene monomer. The newly formed carbon-centered radical abstracts a hydrogen radical from another thiol to regenerate a thiyl radical in a transfer reaction. The alternating addition and transfer process is successively continued until the kinetic chain is terminated via radical combination. The net reaction is a simple addition of the thiol to the double bond similar to other addition reactions. Consequently, thiol-ene addition of multifunctional thiols and enes proceeds via step growth, which is in accordance with other polyaddition or polycondensation reactions and in contrast to the chain growth mechanism of classical radical polymerization. Accordingly, the molecular weight evolves successive with the conversion and high molecular weights are only obtained at high conversions,^{47, 60, 61} whereas in free radical polymerization high molecular weight polymer chains are generated and terminated within very short time periods while only the number of polymer chains increases proportional with the conversion. Therefore, gelation and vitrification occurs delayed to higher conversions in radical mediated thiol-ene reactions and result in the formation of more uniform networks that exhibits a narrowed glass transition regime and a reduced internal shrinkage-stress. In contrast, to other polyaddition reactions the thiol-ene addition proceeds radical mediated, which allows to trigger the initiation process through the application of various radical initiators.

Low concentrations of thiol transfer agents are frequently applied in free radical polymerization of linear polymers to reduce and control the molecular weight.⁶² Although they show high chain transfer constants and are well suited as molecular weight regulator, they do not completely avoid homopolymerization of ene monomers even if they are applied in stoichiometric amounts. Hence, an ideal thiol-ene reaction can only be observed for monomers that do not readily homopolymerize such as norbornenes or vinyl ethers. Both are particularly suitable for thiol-ene reactions as they additionally provide outstanding reactivities owing to their strained or electron rich double bond. If homopolymerizations are excluded, the thiol-ene addition also qualifies as “*click*” reaction with respect to the definition of Sharpless.^{57, 63, 64} Therefore, thiol-ene reactions with monofunctional thiols are increasingly used for highly efficient polymer modification.^{65, 66} The thiol-ene reaction of vinyl ether is particularly discussed

in Chapter 2.2.2. In contrast, the prevailing thiol-ene curing reaction of acrylates and methacrylates proceeds in a mixed mode as depicted in Figure 2.20.

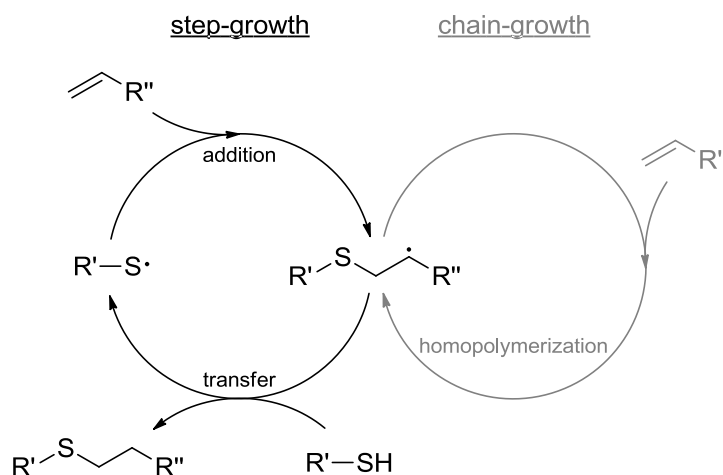


Figure 2.20. Thiol-ene addition reaction with additional homopolymerization of the ene monomer.

The combination of step growth and chain growth enables a broad range of material properties. For example the network homogeneity and conversion at gel point can be adjusted. Oxygen inhibition is reduced by addition of small quantities of thiol, but not completely prevented.

The active carbon-centered radicals can either undergo chain transfer or propagate via addition of ene monomers. The relative kinetics of both reactions are largely predefined for a specific combination of thiol and ene components. However, they depend on the oxygen level. The oxygen biradical efficiently combines with propagating radicals to form a polymerization inactive peroxy radical. However, thiols even transfer hydrogen radicals to peroxy radicals and generate new thiyl radicals.⁵⁴ This reaction significantly reduces the effect of oxygen inhibition in thiol-ene reactions, whereas the presence of oxygen reduces the relative contribution of homopolymerization. The combination of thiols with (meth)acrylates makes a broad range of material properties available and utilizes several benefits that are brought in by the presence of thiols, namely reduced oxygen inhibition, reduced shrinkage-stress and narrowed glass transitions. However, oxygen inhibition cannot be completely prevented in radical polymerization. Another limitation may be residual thiol as a consequence of hardly predictable reaction pathway (thiol-ene reaction vs. homopolymerization). Therefore, ternary systems with an additional ene that does not or barely homopolymerize allow the manipulation of the polymerization process and the final material properties. Variations in the relative content of the enes allow to shift the contribution of chain and step growth and hence

control the network homogeneity as well as the conversion at gel point and the crosslinking density.

A similar system that combines the cationic chain growth polymerization of vinyl ether with a step growth polyaddition through cation transfer reactions with hydroxyl groups is introduced and discussed in Chapter 5.4.

2.2 Chemistry of Vinyl Ethers

Vinyl ethers represent highly reactive functional groups for a number of chemical reactions including cationic polymerization, nucleophilic addition or radical mediated thiol-ene addition. The work in hand involves the synthesis of novel vinyl ether functional polyol building blocks, designed for the incorporation into polyurethanes. Furthermore, the mentioned reactions were utilized for both, vinyl ether functional polyols and polyurethanes. Therefore, this chapter reviews common synthetic pathways and available structures of vinyl ether monomers as well as their reaction capabilities.

2.2.1 Technical Synthesis and Availability

In the 1930s, Walter Reppe and his research group developed the acetylene based synthesis of vinyl ethers to extend the range of polymerizable monomers and produce unsaponifiable derivatives of poly(vinyl alcohol).^{67, 68} First, vinyl ethers were successfully synthesized from vinyl chloride and alkoxides as shown in Figure 2.21.⁶⁹

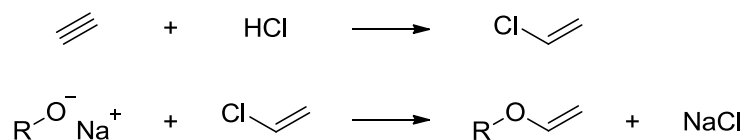


Figure 2.21. Synthesis of vinyl ethers from vinyl chloride and alkoxides.

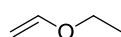
In the following it has been figured out that vinyl ethers can be similarly obtained directly from acetylene and alcohols in a vinylation reaction as depicted in Figure 2.22.⁷⁰



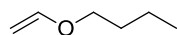
Figure 2.22. Vinylation of alcohols with acetylene.

The addition reaction is conducted at temperatures of 150 °C - 200 °C using alkaline hydroxide, especially potassium hydroxide, as catalyst and pressurized acetylene is charged to the reaction vessel.⁶⁷ The product is separated from the alkaline reaction mixture via distillation. Purification is a crucial process step as even traces of residual base would inhibit cationic polymerization.⁷¹ However, only low molecular weight products can be readily distilled and hence easily prepared via this method. Unfortunately, low boiling monomers may cause volatility and odor issues. A choice of monomers that are manufactured via direct vinylation of alcohols with acetylene on a commercial scale are shown in Figure 2.23.⁷²

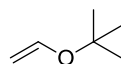
Mono vinyl ether



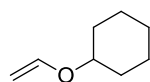
Ethyl vinyl ether



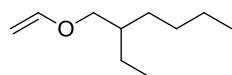
n-Butyl vinyl ether



tert.-Butyl vinyl ether

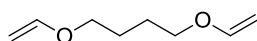


Cyclohexyl vinyl ether

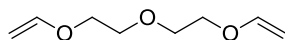


2-Ethylhexyl vinyl ether

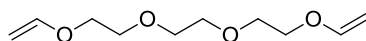
Divinyl ether



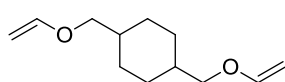
Butanediol divinyl ether



Diethylenglycol divinyl ether

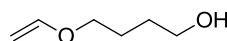


Triethylenglycol divinyl ether

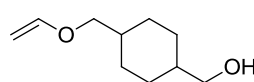


1,4-Cyclohexanedimethanol divinyl ether

Hydroxy functional vinyl ether



Hydroxybutyl vinyl ether (HBVE)



1,4-Cyclohexanedimethanol mono vinyl ether

Figure 2.23. Vinyl ether monomers synthesized via vinylation of alcohols with acetylene.

A representative selection of vinyl ether monomers that are commercially available.

In Addition to mono- and difunctional vinyl ethers, also hydroxyl functional vinyl ethers are prepared by incomplete conversion of diols and fractional distillation.⁷¹ Many commercially available vinyl ethers exhibit structures that are well known from (meth)acrylate monomers. However, some popular structures derived from 1,3-diols such as trimethylolpropane, pentaerythritol or neopentyl glycol cannot be synthesized,

as the formation of six-membered, cyclic acetals is preferred.⁷¹ Generally, the yield of divinyl ethers depend on the distance between the hydroxyl groups and the reaction conditions. For example, the vinylation of ethylene glycol at about 200 °C quantitatively yields 2-methyl-1,3-dioxolane, whereas at rather low reaction temperatures the mono- and divinyl ether can be obtained (see in Figure 2.24).

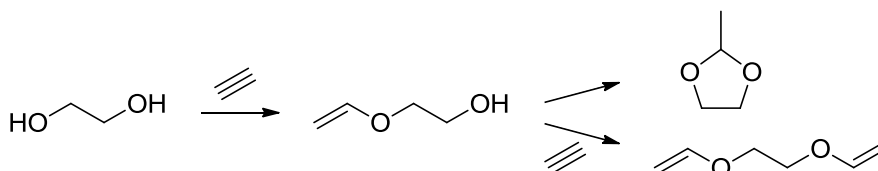


Figure 2.24. Vinylation of ethylene glycol.

Depending on the vinylation conditions and the distance between the hydroxyl groups, cyclic acetals may be formed from the intermediate monovinyl ethers.

Furthermore, only backbones that withstand the hot, alkaline conditions are accessible via direct vinylation. Therefore, more polar vinyl ethers monomers have been prepared via addition or condensation reactions starting from hydroxyl functional vinyl ethers.⁷¹ Ester containing structures of higher molecular weight have been prepared via esterification with carboxylic acid derivatives as shown in Figure 2.25.

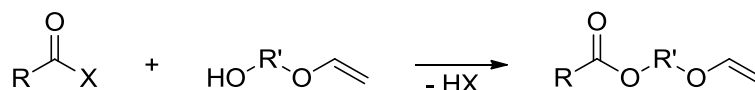


Figure 2.25. Esterification of hydroxyl functional vinyl ethers.

Vinyl ethers with ester backbones that would not withstand the hot, alkaline vinylation conditions are synthesized via esterification of hydroxyl functional vinyl ethers.

A particularly attractive method to synthesize ester containing vinyl ethers is the transesterification with methyl- or ethyl esters as they do not involve acidic educts or side-products that may cause addition, hydrolysis or polymerization reactions. The released alcohols are volatile and can be readily removed from the reaction equilibrium. Urethane containing vinyl ethers can be easily prepared by addition of hydroxyl functional vinyl ethers to common isocyanates or isocyanate terminated oligomers (see Figure 2.26).

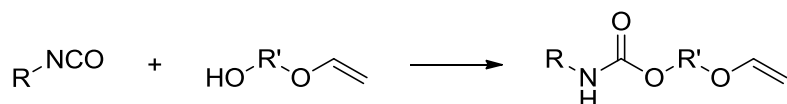


Figure 2.26. Synthesis of vinyl ether functional urethanes.

Figure 2.27 shows a representative selection of vinyl ether functional esters and urethanes that have been commercially available by Allied Signal Inc. and Vertellus under the tradename Vectomer and are currently available by Sigma Aldrich.⁷³

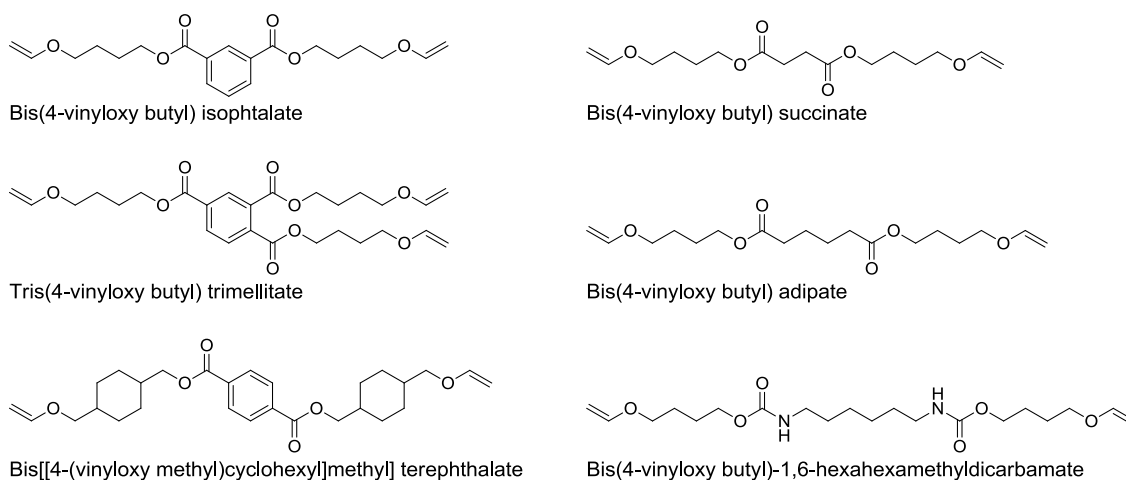


Figure 2.27. Selection of ester or urethane group containing vinyl ether monomers.

These monomers are available by a fine chemical supplier.

Although not applied commercially, another convenient method to synthesize vinyl ether structures that are not accessible otherwise is catalytic transvinylation. The vinyl moiety is transferred from a simple vinyl ester^{74, 75} or vinyl ether⁷⁶⁻⁷⁸ to a new alcohol using transition metal complexes as shown in Figure 2.28.

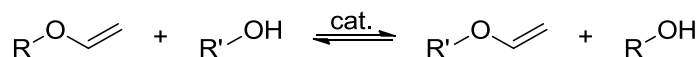


Figure 2.28. Catalytic transvinylation reaction of vinyl esters or vinyl ethers with alcohols.

Several other methods mainly applicable for the laboratory scale synthesis of vinyl ethers have recently been reviewed.⁷⁹ Generally, the commercial availability of vinyl ether monomers with additional functional groups is limited to hydroxyl functional vinyl ethers. Additionally, 3-aminopropyl vinyl ether (APVE) is currently available as R&D product on a pilot-plant scale.⁷² It can be synthesized similarly the already

described low molecular weight vinyl ethers via vinylation with acetylene as shown in Figure 2.29.⁸⁰



Figure 2.29. Vinylation of 3-aminopropanol.

3-Aminopropyl vinyl ether (APVE) is currently available as pilot-plant product.

Furthermore, the synthesis of vinyl ethers with other functional groups like epoxides⁸¹ or cyclic carbonates⁸² on the laboratory scale have been reported. Similar structures were also prepared and utilized in the course of this thesis. Nevertheless, vinyl ether monomers containing more than one additional functionality for the integration in conventional polyaddition or polycondensation products have not been reported yet. In the presented work, vinyl ether functional polyols (VEOHs) have been successfully prepared and serve as key components.

2.2.2 Properties and Reaction Capabilities

Vinyl ethers are the combination of an alkene with an ether group in α -position. Hence, it can be assumed that they show reaction capabilities related to the individual functionalities. However, the electron rich oxygen atom significantly increases the electron density of the double bond and results in a unique reactivity. The delocalization of the electron density is indicated by resonance structures in Figure 2.30.

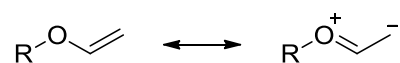


Figure 2.30. Resonance structures of vinyl ethers.

Ether groups are relatively inert but the electron rich, unsaturated double bond is particularly reactive in nucleophilic addition reactions. The π -bond is easily polarizable and can be readily activated by electrophiles, protons or radicals. In the presence of water, vinyl ether are stable in alkaline or neutral solution. However, even slightly acidic conditions result in hydrolytic cleavage and quantitatively yield the corresponding alcohols and acetaldehyde via hemiacetal intermediates. Several other functional groups such as carboxylic acids,⁸³ alcohols,⁸³ phenols^{84, 85} or thiols⁸⁶ can be covalently attached to the vinyl ether under dry, acidic reaction conditions.^{68, 87} Also the

addition of hydrogen halides or halogens proceeds smoothly without further catalysis and should be conducted at low temperatures and sufficient dilution to avoid polymerization and thermal decomposition of the reaction product.⁸⁸ Moreover, vinyl ethers can be readily hydrogenated in the presence of catalytically active metals to yield ethyl ethers.⁸⁹

If strong acids with non-nucleophilic anions are applied to vinyl ether, they polymerize via a cationic mechanism as depicted in Figure 2.31 and described in more detail in Chapter 2.1.3.

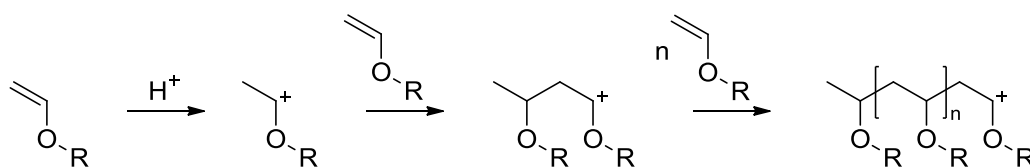


Figure 2.31. Cationic polymerization of vinyl ethers.

A proton adds to the double bond to form a resonance stabilized carbocation and if the counter ion is stable enough it does not add to the vinyl ether. Instead, another electron rich vinyl ether monomer can be added to form a new carbocation. Further vinyl ether molecules add consecutively to the growing chain and yield a poly(vinyl ether). However, the polymerization active chain-ends exhibits a similar structure to proton activated vinyl ethers in acid catalyzed addition reaction. Therefore, the addition of nucleophiles, if present, competes with the addition of monomer and interferes with the polymerization. The addition of nucleophiles with labile protons result in cationic species that stabilize themselves via proton separation. Hence, the growing chain becomes terminated but the released proton is capable to start a new polymerizing chain. Therefore, many nucleophiles can be considered as transfer agents in the cationic polymerization. One particular group of transfer agents that is particularly utilized in the course of this thesis are alcohols. The transfer reaction with alcohols under formation of acetal groups in the cationic polymerization of vinyl ethers is depicted in Figure 2.32.

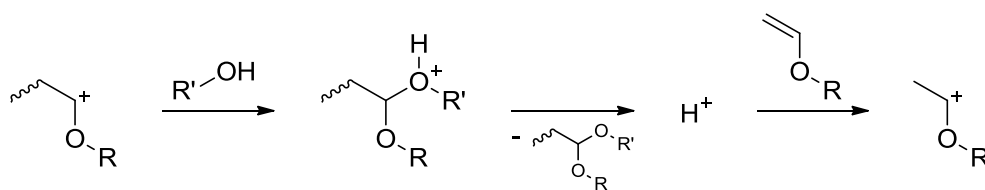


Figure 2.32. Transfer reaction with alcohols in the cationic polymerization of vinyl ethers.

It is well known, that vinyl ethers do not homopolymerize under radical conditions.⁴⁷ The reactivity of vinyl ethers towards free radicals is comparatively low and vinyl ether radicals formed upon addition of initiating radicals are highly reactive. This high reactivity derives from a deviation of the planar sp^2 -conformation due to the high electron density of the neighboring oxygen atom.^{90, 91} Therefore, side and transfer reactions are pronounced if vinyl ether are treated with considerable amounts of radicals and only low quantities of vinyl ether oligomers could be obtained after long reaction times.⁹² However, the high reactivity of vinyl ether radicals can be utilized in copolymerizations with e.g. acrylates,⁹³ methacrylates or styrene.⁹⁴ Expectably, the radical copolymerization parameter that were obtained for such mixtures are $r_{\text{vinyl ether}} \approx 0$ and $r_{\text{comonomer}} > 1$. This means that radical vinyl ether chain-ends exclusively add acrylates, whereas radical chain-ends of the comonomer preferably add another comonomer but also vinyl ether monomers to a lower extent. Therefore, the resulting polymer contains a little share of isolated vinyl ether units. However, the high reactivity of vinyl ether radicals leads to an acceleration of the overall polymerization kinetics. Additionally, these systems offer the possibility of simultaneous or subsequent cationic polymerization of excess vinyl ether, if suitable photoinitiators or mixtures of photoinitiators are applied.⁹³

Furthermore, vinyl ethers can be copolymerized with electron deficient monomers that do not homopolymerize as well, such as maleic anhydride or unsaturated polyesters based on maleates or fumarates.⁹⁵⁻⁹⁷ Strictly alternating copolymers are obtained in a fast polymerization. Besides cross-propagation of the free monomers also the addition of donor-acceptor-complexes contributes to the polymerization mechanism. Low concentrations of these donor-acceptor-complexes are formed in equilibrium with the free monomer mixture. These complexes also absorb UV-light and are capable to initiate the polymerization without the need of an additional photoinitiator.

The radical mediated addition reaction of thiols and vinyl ether is classified as click-type reaction as it exhibits all the desirable features associated with click chemistry.⁶³ The reaction proceeds rapid at ambient conditions, is highly selective and the product is formed in good purity at high yields.⁵⁷ This reaction can be utilized to modify vinyl ether functional precursors or in thiol-ene curing compositions if multifunctional materials are applied.

2.3 Chemistry of Polyurethanes

Polyurethanes were initially discovered by Otto Bayer in 1937⁹⁸ and their chemistry has recently been described in several reviews.⁹⁹⁻¹⁰² They are conventionally prepared via polyaddition of diisocyanates and diols as depicted in Figure 2.33.

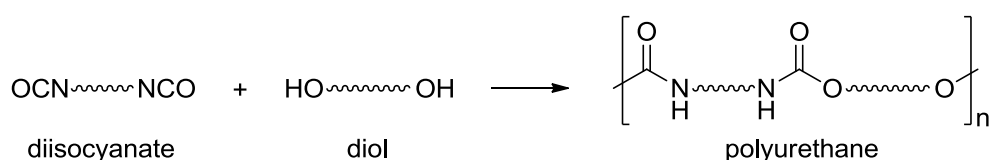


Figure 2.33. Polyurethane synthesis from diisocyanates and diols.

A striking feature of polyurethane chemistry is the extraordinary reactivity of isocyanates that allow the reaction to proceed up to high conversions even under mild conditions and in viscous media. The reactivity of the isocyanate group is based on the high polarization induced by the electronegative oxygen and nitrogen atoms in the heterocumulene. The delocalized electron density is illustrated by the resonance structures of the isocyanate group in Figure 2.34.



Figure 2.34. Resonance structures of the isocyanate group.

The carbon atom is very electron deficient and can be easily attacked by nucleophiles.

Additionally, the particular reactivity of isocyanates is largely affected by the attached group (R). Electron withdrawing groups further reduce the electron density at the carbon atom and significantly enhance the reactivity of aromatic isocyanates over aliphatic isocyanates. The electron deficient carbon atom can be easily attacked by hydrogen active nucleophiles, followed by transfer of the hydrogen atom to the nitrogen

atom. Besides alcohols also amines, thiols, or water easily add to the isocyanate function. Typical reactions of isocyanates are shown in Figure 2.35.

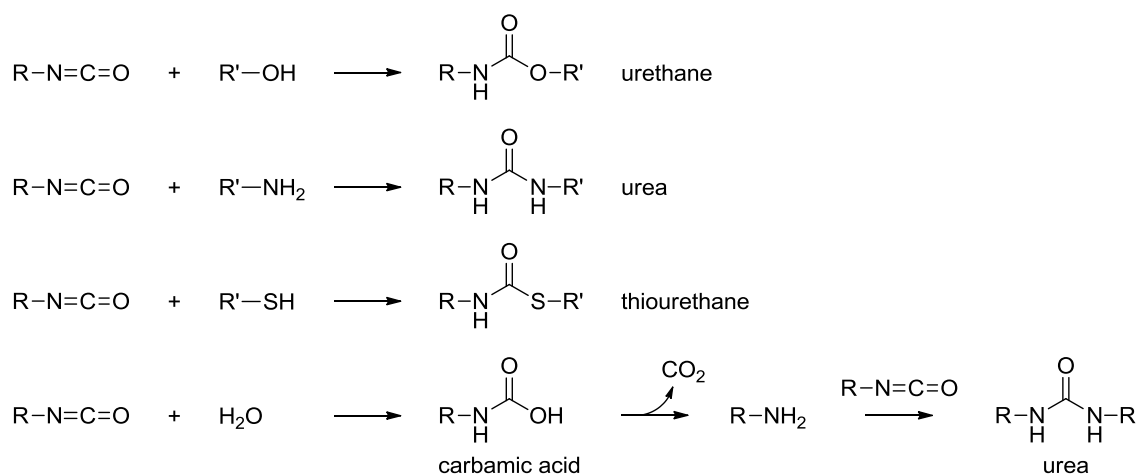


Figure 2.35. Reaction of isocyanates with hydrogen active nucleophiles.

Generally, polymers based on addition reactions of isocyanates are frequently described as polyurethanes, although they do not exclusively contain urethane groups. The addition of water results in the formation of carbamic acid groups, which are unstable and dissociate into carbon dioxide and the respective amine. Due to its higher reactivity towards isocyanate groups the generated amines directly add to further isocyanates under formation of urea groups. This reaction is often utilized for moisture-curable polyurethanes or to autonomously generate carbon dioxide as blowing agent in the production of foams. Additionally, less nucleophilic functional groups may also react with isocyanates. For example increasing amounts of urethanes or ureas are generated throughout the polyurethane synthesis. Their nitrogen atoms are comparatively less nucleophilic and hence less reactive, due to the neighboring carbonyl groups. However, they may cause branching via secondary reactions at elevated temperatures as depicted in Figure 2.36.

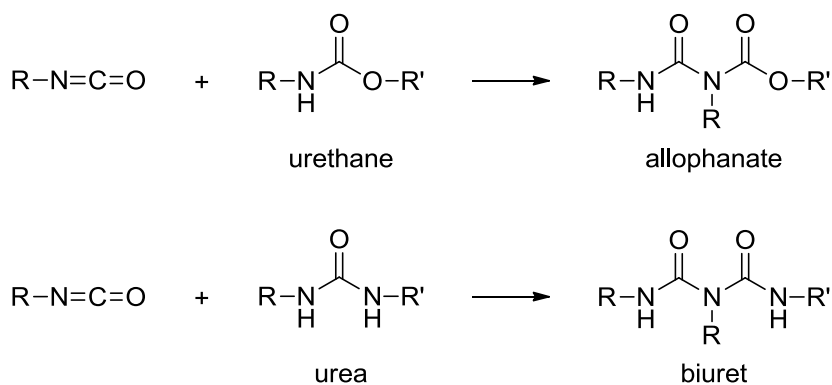


Figure 2.36. Reaction of isocyanates with urethanes or ureas.

These reactions may be utilized on purpose to increase crosslinking in thermosetting polyurethanes, they are strongly undesired in the synthesis of thermoplastic polyurethanes or linear prepolymers. Therefore, all reactions in this thesis were carried out under mild conditions (at 80 °C for aliphatic isocyanates). The relative reactivities of some nucleophiles towards isocyanates are summarized in Table 2.1 as a rule of thumb.⁹⁹

Table 2.1. Relative reactivity of hydrogen active compounds towards isocyanates.

hydrogen active compound	relative reactivity
aliphatic primary amine	1000
primary alcohol	1
water	1
urea	0.15
urethane	0.001

In many cases the reactivity of amines is too high to achieve a satisfying reaction control. The reaction of ureas and urethanes proceeds relatively slow, at elevated temperatures and preferably if an excess of isocyanate is available.

The polyurethane synthesis can be readily catalyzed with non-nucleophilic bases or Lewis acids. Two classes of catalysts are commonly applied. First, organometallic compounds are applied as Lewis acid catalysts, whereof dibutyltin dilaurate (DBTL) is the most popular representative. The Lewis acid coordinates with the isocyanate and further increases its polarization to facilitate a nucleophilic attack. Currently, efforts are

made to substitute toxic mercury or tin based catalysts by bismuth or titan based organometallic compounds. However, the presented research was carried out using dimethyltin dineodecanoate (Fomrez UL-28) as well-established and reliable catalyst.

Second, tertiary amines are applied as alkaline catalysts. 1,4-Diazabicyclo[2.2.2]octane (DABCO) represents a widely applied amine catalyst with low steric hindrance at the nitrogen atom and its free electron pair. It needs to be mentioned that some catalysts may influence the relative reactivity of different functional groups. A good example is 2,2'-dimorpholinyl diethyl ether (DMDEE) that forms chelates with water molecules and hence favors the reaction of isocyanate with water over the reaction with alcohols. This catalyst is often applied as so-called blowing catalyst in foam preparation. The structures of typical isocyanate catalysts are shown in Figure 2.37.

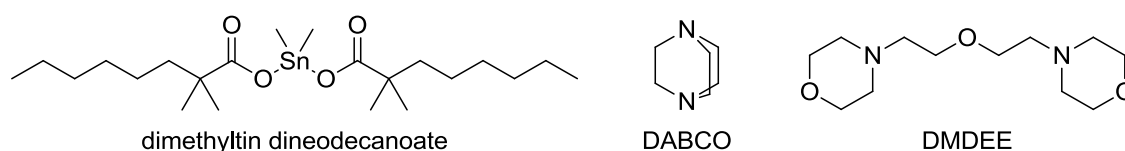


Figure 2.37. Typical isocyanate catalysts.

In general, polyurethanes are thermally unstable as they contain weak bonds. Possible decomposition reactions are shown in Figure 2.38.

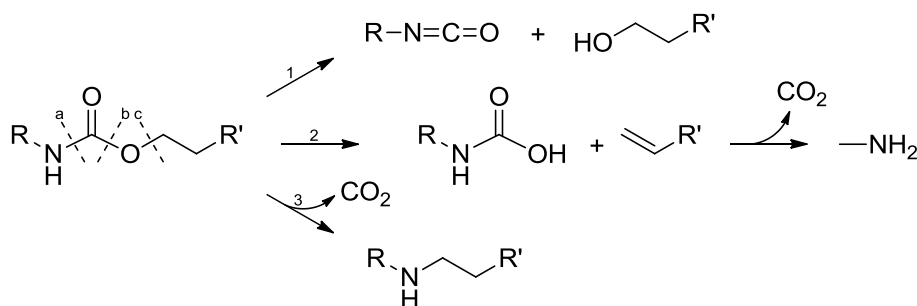


Figure 2.38. Thermal decomposition reactions of urethane groups.

Dissociation of bond b represents the main decomposition pathway (1) for most urethanes as it exhibits the lowest activation energy.

The dissociation of the bond b, which regenerates the initial educts in a reverse reaction (reaction path 1) exhibits the lowest activation energy and represents the main decomposition mechanism for most urethanes. The other pathways occur more slowly and at higher temperatures. The particular thermal stability of urethanes group depends

on their electron density and generally follows the order presented in Table 2.2 with approximated decomposition temperatures.¹⁰³

Table 2.2. Thermal stability order of urethanes.

urethane composition	thermal stability
alkyl-NCO / alkyl-OH	250 °C
aryl-NCO / alkyl-OH	200 °C
alkyl-NCO / aryl-OH	180 °C
aryl-NCO / aryl-OH	120 °C

However, in the presence of stronger nucleophiles transcarbamoylation reactions may occur at much lower temperatures than indicated. Similarly, other isocyanate adducts such as ureas, allophanates and biurets thermally dissociate. Their relative thermal stability is described as follows: allophanates < biuret < urethane < urea.¹⁰³ The thermal reversibility of isocyanate derivatives is a very characteristic feature of isocyanate chemistry and is utilized in so-called blocked isocyanates, which readily dissociate at elevated temperatures to regenerate the free isocyanate in a latently reactive formulation.¹⁰⁴⁻¹⁰⁶ The most important blocked isocyanates are adducts of isocyanates with phenols, aromatic amines, oximes, or amides like ϵ -caprolactam. Phenols are of particular interests as their deblocking temperature can be easily adjusted via electron withdrawing or electron donating substituents. In the course of this work isocyanate prepolymers were blocked with benzoxazine oligomers. However, these bonds are rather stable, as aliphatic isocyanates were used and benzoxazines represent relatively electron rich phenols.

2.3.1 Technical Considerations

Polyurethanes are generally synthesized in a modular reaction starting from only a few polyisocyanates and a variety of diols. The diisocyanates are predominantly synthesized via phosgenation of the corresponding amines as depicted in Figure 2.39.

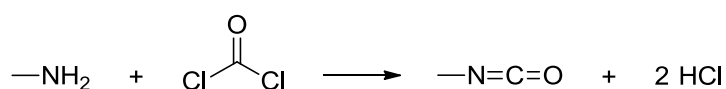


Figure 2.39. Synthesis of isocyanates via phosgenation of amines.

The use of phosgene in the synthesis of polyurethanes is considered as major drawback with respect to environmental, health and safety considerations. In the last decades also technical processes to produce aliphatic isocyanates without the use of phosgene in an urea based multistep synthesis were developed and commercialized.¹⁰⁷ However, aromatic isocyanates account for about 95% of the isocyanate market,¹⁰⁸ whereas the more expensive and less reactive aliphatic isocyanates are only used if their properties justify the increased costs. The reduced reactivity towards water renders them useful for waterborne applications, the absence of aromatic chromophores results in an improved weatherability and is beneficial for photocuring applications and the electron rich urethane groups result in a superior thermal stability. The most important diisocyanates are methylene diphenyl diisocyanate (MDI), toluene diisocyanate (TDI), hexamethylene diisocyanate (HDI) and isophorone diisocyanate (IPDI). The structures of their most prominent isomers are shown in Figure 2.40.

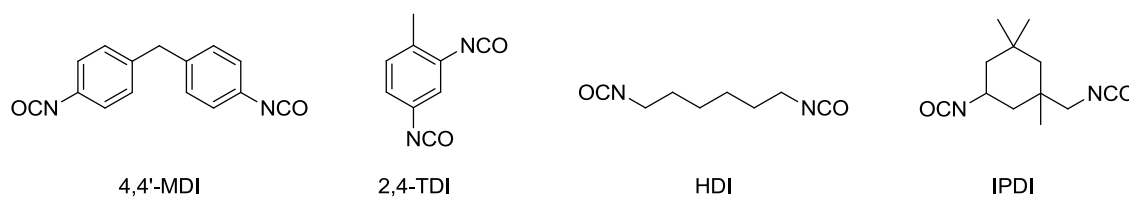


Figure 2.40. Most important diisocyanates.

The aromatic isocyanates MDI and TDI account for about 95% of the isocyanate market. HDI and IPDI are the most commonly used aliphatic isocyanates and find applications in waterborne and photocuring applications. Furthermore, they may be used to improve weatherability and thermal stability.

The aliphatic isocyanates IPDI and HDI were exclusively used in the presented studies, as UV-transparency and temperature resistance were required within the different projects. On the opposite, there is a variety of polyols such as polyether, polyester, polycarbonates and low molecular weight polyols available. Often a mixture of polyols is applied. A macrodiol with a molecular weight of a few thousand g/mol and a short diol (chain extender), which can also be applied after the initial prepolymer synthesis to increase the molecular weight due to its high mobility. The resulting polyurethanes can be seen as segmented blockcopolymers, whereas urethane group rich segments comprising of isocyanates and short polyols constitute the so-called *hard segments* (HS) and the less polar macrodiols constitute *soft segments* (SS). Upon polymerization the HS become incompatible with the SS and tend to phase separate. The SS are usually amorphous with glass transition temperatures (T_g) below room temperature, whereas HS

domains are often semicrystalline and exhibit high glass transition and crystalline melting temperatures due to rigid structures and intense hydrogen binding. However, also crystalline or high T_g soft segments are used for special applications.¹⁰⁹ The resulting microphase morphology represents a physical crosslinking mechanism and results in high toughness, good abrasion resistance and high performance mechanical properties of polyurethanes. Tailor-made material properties can be synthesized via variation of block length and composition in a highly modular tool box like approach. Linear polyurethanes can be designed as thermoplastic elastomers through physical crosslinking. They behave elastic at ambient conditions but can be processed like thermoplasts above the melting temperature of the HS. Furthermore, higher functional polyols or isocyanates can be utilized to introduce chemical crosslinking and allow the synthesis of high modulus and high strength thermosetting polyurethanes suitable for structural applications.

A major concern regarding polyurethanes is the pronounced toxicity of isocyanates. Therefore, many products are sold as isocyanate terminated prepolymers or blocked isocyanate prepolymer formulations that were cleaned from low molecular weight isocyanates. This approach is tedious but efficiently reduces volatility and toxicity while maintaining similar reactivity to low molecular weight formulations.⁹⁹ The prepolymers finally cure via addition of short diols or as one-pot formulations via moisture diffusion or thermal treatment. Furthermore, acrylate terminated polyurethanes are widely used as photopolymers (PUA). The work in hand extend these approaches by photocurable, vinyl ether functional polyurethanes (VEPU) and benzoxazines functionalized, thermally curable polyurethanes that do not release blocking agents.

2.3.2 Polyhydroxyurethanes (PHUs)

Recently, increasing attention was paid to phosgene and isocyanate free synthetic routes towards polyurethanes.^{99, 108} The resulting PUs are classified as non-isocyanate polyurethanes (NIPU). The most prominent approach is ring-opening addition of aliphatic amines to cyclic carbonates, which has been summarized in recent reviews.¹¹⁰⁻¹¹³ In contrast to other alternative procedures via polycondensation, this reaction proceeds without release of volatile by-products and exhibits relatively high reactivity, allowing the reaction to proceed at ambient conditions without the necessity of

catalysts. The reaction of a five-membered cyclic carbonate with a primary amine is shown in Figure 2.41.

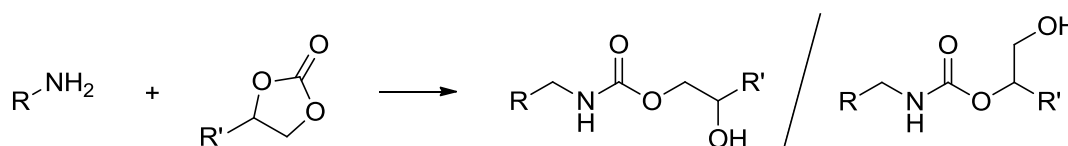


Figure 2.41. Aminolysis of a pentacyclocarbonate.

The reaction yields urethanes with a hydroxyl group in β -position. Depending on the ring-opening direction isomers with primary or secondary hydroxyl groups are formed. PHUs can be prepared starting from polyfunctional amines and polyfunctional cyclic carbonates.

The resulting polyurethanes contain free hydroxyl groups. Depending on the direction of the ring-opening reaction either primary or secondary hydroxyl group containing structures are generated. Typically, the secondary hydroxyl group is favored with a ratio of about 70/30.¹¹⁰ Five-membered cyclic carbonates are commonly applied, as they can be readily prepared via carbon dioxide insertion to a variety of commercially available epoxides. This practical and sustainable reaction (see Figure 2.42) is conducted using common quaternary ammonium or metal salt catalysts at elevated temperature and can be realized under atmospheric pressure.^{114, 115}

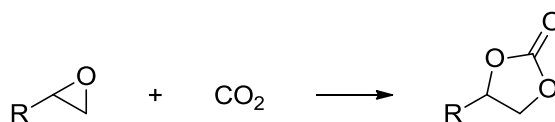


Figure 2.42. Synthesis of five-membered cyclic carbonates via CO₂ insertion to epoxides.

Carbon dioxide fixation represents an environmentally benign process and various commercially available epoxides can be utilized as precursors.

Another, frequently reported preparation method of multifunctional cyclic carbonates is the esterification of commercially available glycerine carbonate with various carboxylic ester precursors (see Figure 2.43).

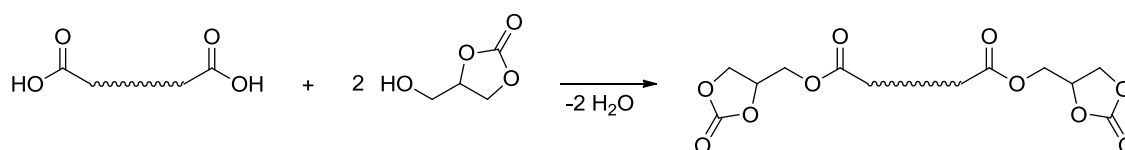


Figure 2.43. Synthesis of polycarbonates via esterification of glycerine carbonates.

The aminolysis reaction of five membered cyclic carbonates initially proceeds with a fast rate even under ambient conditions. However, the reaction kinetics drops off significantly as the reactant concentration decreases and the viscosity increases, especially in bulk reactions. The drastically reduced reaction rates at high conversion despite initially high reactivity can be explained by the observation that the reaction follows a second order kinetic with respect to both the amine and the cyclic carbonate concentration. It has been proposed that a second amine molecule can catalyze the ring-opening reaction via formation of hydrogen bond stabilized intermediates. Consequently, the reaction rate is exponentially affected by the educt concentrations and therefore high conversion often require temperatures of 60 °C - 80 °C, the application of catalysts and reaction times of several hours up to a few days. As a result, only low molecular weight products, often below $3 \cdot 10^4$ g/mol are obtained for difunctional systems leading to linear polymers.¹¹⁰ Therefore, PHUs are often considered to be mainly suitable for the preparation of prepolymers or crosslinking materials.

In contrast, six-membered cyclic carbonates exhibit a significantly higher reactivity by a factor of 29 - 62 in the relevant temperature range of 30 °C - 70 °C.¹¹⁶ The difference in reactivity can be attributed to the increased ring tension of six-membered cyclic carbonates. Although, it is counterintuitive that six-membered cyclic compounds exhibit a higher ring strain energy compared to five-membered rings, this situation arises from the mixture of sp^2 - and sp^3 -hybridized carbon atoms along with the presence of oxygen atoms in the ring. The increased ring strain also facilitates cationic ring-opening polymerization of six-membered cyclic carbonates, which is hardly observed for its five-membered counterparts.¹¹⁴ Originating from 1,3-diol precursor, six-membered cyclic carbonates are often substituted at the β -carbon atom. The molecule is therefore symmetric and ring-opening results in only one constitutional isomer, containing primary hydroxyl groups that are sterically more favorable in terms of subsequent modification reactions. However, the variety of oxetanes or 1,3-diols as precursors is limited and six-membered cyclic carbonates are much more difficult to synthesize due to the comparatively low reactivity of oxetanes compared to epoxides in conjunction with the reduced stability of more strained six-membered cycles. Possible synthetic pathways via transesterification with dimethyl carbonate (DMC)¹¹⁷ or carbon dioxide

insertion to oxetanes¹¹⁸ and aminolysis reaction of six-membered cyclic carbonates are shown in Figure 2.44.

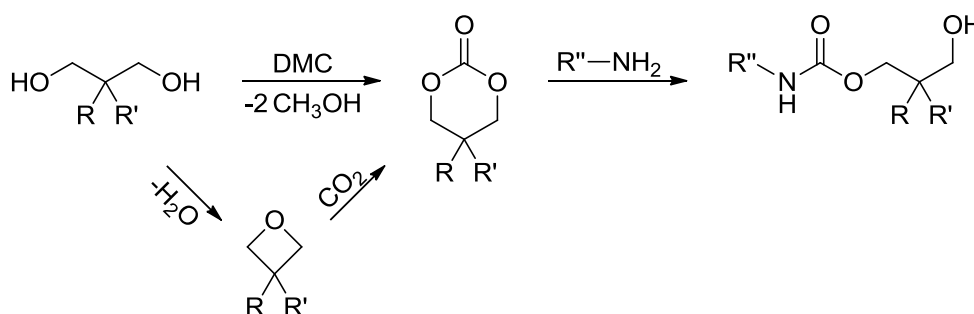


Figure 2.44. Possible synthetic pathways and aminolysis reaction of six-membered cyclic carbonates. Six-membered cyclic carbonates are of significantly higher reactivity due to their increased ring strain over five-membered cyclic carbonates. However, their synthesis starting from less reactive compounds is more difficult and the availability of oxetanes and 1,3-diols is limited.

The reactivity of the amine differs according to its nucleophilicity, steric hindrance, and mobility.¹¹⁹ It was shown that steric effects are pronounced and thus, the reactivity of secondary amines is significantly reduced. Furthermore, the reactivity of primary amines at a primary carbon atom is increased over amines with secondary α -carbon atoms. Finally, the reactivity decreases with increasing molecular weight of the amine compound, especially in bulk reactions. Therefore, it can be considered that the even evolution of molecular weight in step growth reactions is disadvantageous for high conversions. The distinct reactivity graduation even among different aliphatic amines indicates that less reactive nucleophiles such as water or hydroxyl groups require drastic conditions to react with cyclic carbonates and hence do not show a significant impact on the synthesis of PHUs.¹²⁰ Therefore, pore-free films can be obtained even on wet surfaces and polyurethanes bearing free hydroxyl groups or secondary amine groups are accessible, which could not be prepared based on nonselective isocyanate chemistry. Especially, the inherent free hydroxyl groups of PHUs were subjected to a number of post modification reactions such as silylation, esterification, or urethanization and were further utilized as transfer agents in the cationic polymerization of vinyl ether.¹¹⁰

The properties of polyhydroxyurethanes are similar to those of conventional polyurethanes. However, some distinct differences arise from the free hydroxyl groups and shall be briefly discussed. The free hydroxyl groups in close proximity to the urethane group is capable to form intramolecular hydrogen bonds as shown in Figure

2.45. This behavior is especially pronounced for PHUs derived from five-membered cyclic carbonates where the hydroxyl group is located in β -position to the urethane.

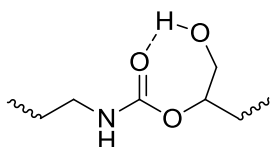


Figure 2.45. Intramolecular hydrogen bonding in β -polyhydroxyurethanes.

The urethane group is stabilized and shielded by the hydrogen bond, which results in an improved chemical and hydrolytic stability.

The urethane group is hence stabilized and sterically hindered, which leads to substantially improved hydrolysis- and chemical resistance at the expense of significantly higher water uptake of up to more than 30%. The thermal stability of PHUs was reported to be similar to conventional PUs of comparable structure, but generally benefits from the exclusively aliphatic structure and the absence of allophanate and biuret groups.

2.4 Chemistry of Benzoxazines

Benzoxazines are molecules with an oxazine attached to a benzene.¹²¹ Oxazines are six-membered heterocycles that contain one oxygen atom and one nitrogen atom. Different benzoxazines structures are possible, depending on the position of the heteroatoms. 1,3-benzoxazines are of particular interest, as they can polymerize via ring-opening addition (see Figure 2.46). The traditional nomenclature of benzoxazines is very complex, thus they are usually abbreviated referring to their educts. For example, the benzoxazine derived from phenol and methylamine is abbreviated as P-m whereas the corresponding traditional names are 3,4-dihydro-3-methyl-2*H*-1,3-benzoxazine or 3-methyl-2*H*,4*H*-benzo[e]1,3-oxazine (IUPAC name).

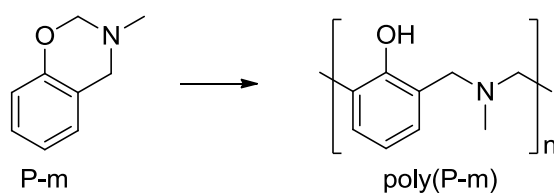


Figure 2.46. Polymerization of 1,3-benzoxazines.

As already indicated, these 1,3-benzoxazines are typically prepared from phenols, primary amines and formaldehyde in a stoichiometry of 1:1:2, whereas formaldehyde is usually applied as paraformaldehyde.¹²¹⁻¹²⁴ Formaldehyde evaporates easily, instead paraformaldehyde is a low molecular weight polyoxymethylene that slowly generates formaldehyde *in-situ* via thermal depolymerization and hence is beneficial in terms of stoichiometry and toxicity. The synthesis is shown in Figure 2.47.

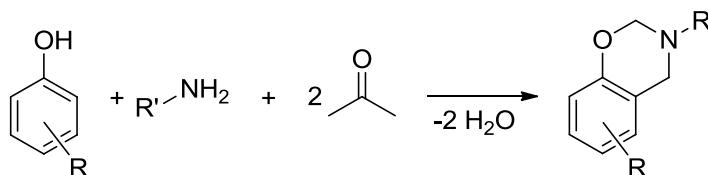


Figure 2.47. Typical synthesis of 1,3-benzoxazines from phenols, primary amines and formaldehyde. Oligomeric, Mannich bridged by-products are generally obtained. Nevertheless, benzoxazines are often applied as resins without further removal of these oligomeric species.

First, formaldehyde reacts with the amine to form a *N,N*-dimethylolamine, which condenses to the benzene and subsequently ring-closes via condensation with the phenol. However, besides the expected benzoxazine also various multi-substituted or Mannich bridged, oligomeric structures may be obtained. The exact composition of the product mixture is influenced by several variables such as the structure of the amine and phenol component, the solvent polarity and the reaction temperature and time. Purification of benzoxazines is often complicated and intricacy increases with functionality and molecular weight of the intended product. Therefore, benzoxazine resins are often applied without further purification from oligomeric species. Benzoxazine oligomers are discussed in more detail in Chapter 4.6, where the free hydroxyl content of benzoxazine oligomers is subjected to functionalization reactions with isocyanates.

Molecular modeling proposed that the oxazine ring shows a distorted semi-chair structure.¹²⁵ The ring strain arising from this structure provides the driving force for the ring-opening reaction. However, it is not substantial and thus high temperatures are necessary. The ring-opening reaction is catalyzed by acidic species. The mechanism is still not entirely established. However, there are evidences that the reaction proceeds via an iminium ion mechanism, if Brønsted acids are the catalytically active species. If Lewis acids are applied the reaction may proceed via traditional cationic polymerization

mechanism to an aryl ether structure. However, aryl ethers are thermally unstable and undergo structural transformation at elevated temperatures. Both mechanisms are depicted in Figure 2.48.^{121, 126}

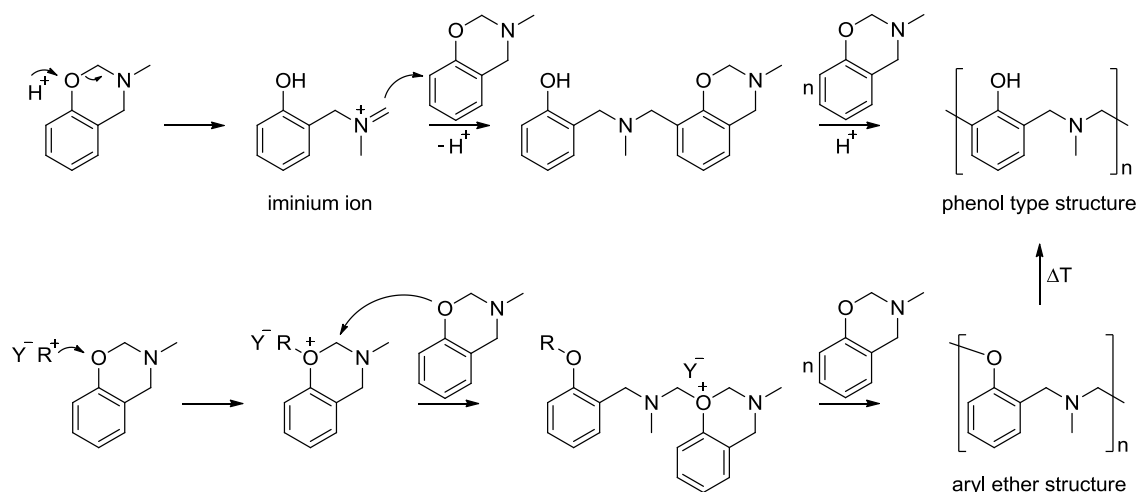


Figure 2.48. Supposed polymerization mechanisms of benzoxazines.

The upper mechanism is catalyzed via Brønsted acids and proceeds via iminium ion intermediates to polybenzoxazines of the phenol type structure, whereas the lower mechanism is initiated by Lewis acids and yields aryl ether structures. The aryl ethers are thermally unstable and undergo structural transformation to the phenol type structure at elevated temperatures.

If no catalyst is applied, phenols act as catalytic species. These phenols may be provided from residues, Mannich bridge by-products or via thermal dissociation of benzoxazines. Consequently, purified benzoxazines that contain less free phenolic hydroxyl groups polymerize at higher temperatures and due to the formation of phenolic products the reactions exhibits an auto-acceleration.

A large difference in reactivity is observed between benzoxazines derived from aliphatic and aromatic amines. Benzoxazines derived from aromatic amines polymerize at significantly higher temperature, as the benzene ring is capable to resonance stabilize the iminium ion intermediate. In principal, the iminium ion can attack benzoxazines in ortho or para position. However, it has been demonstrated that the reaction proceeds preferentially in ortho position due to the formation of intermolecular hydrogen bridge intermediates.¹²³ Furthermore, the formation of very strong intramolecular six-membered hydrogen bond between the phenolic hydroxyl group and the neighboring Mannich base competes with the propagation reaction so that for monofunctional benzoxazines only linear or branched polymers with molecular weights

of a few hundred to a few thousand can be obtained.¹²¹ Therefore, di- or multifunctional benzoxazines are predominantly applied. Beyond that, extensive inter- and intramolecular hydrogen bonding and particularly the formation of six-membered hydrogen bonds as depicted in Figure 2.49 results in unique properties of polybenzoxazines^{121, 127} and has a strong impact on the reactivity of the phenolic hydroxyl groups (see Chapter 4.6).^{128, 129}

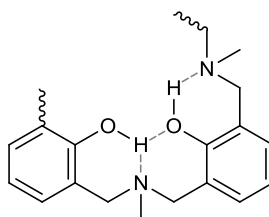


Figure 2.49. Intramolecular hydrogen bonds in polybenzoxazines.

Curing of multifunctional benzoxazines results in the formation of three-dimensional polymer networks and was introduced just about 20 years ago by the group of Ishida as a new class of thermosetting materials.¹³⁰ Meanwhile, benzoxazines find applications as composite materials and coatings in high technology industries such as aerospace or electronics. Consequently, the properties of benzoxazines are discussed in comparison to other thermosetting materials like epoxy/amine or phenol/formaldehyde resins. In general, thermosets provide high mechanical strength and dimensional stability along with good thermal and chemical resistance. These properties arise from the rigid and tightly crosslinked network structure and the absence of weak bonds. The thermal stability of benzoxazine resins is similar to those of traditional phenolic resins, despite the fact that usual Mannich bridges already degrade at moderate temperatures. This surprisingly good thermal stability of at least 260 °C has been ascribed to the stabilizing effect of intramolecular OH-N hydrogen bonds.^{131, 132} Also the mechanical modulus of benzoxazines is largely affected by intermolecular hydrogen bonds and is generally higher as it would be expected only from the crosslinking density. The glass transition temperature of thermosetting resins is usually closely related to the curing temperature. The molecular motion becomes restricted as soon as T_g exceed the curing temperature and hence the reactions stops. However, benzoxazines often exhibit T_g s that are significantly higher than their curing temperatures (in extreme cases even up to 160 °C higher).^{133, 134} Also this observation can be interpreted by subsequent formation of hydrogen bridges, which result in an reduced free volume through closer packing and

hence lead to increased T_g s. Particularly, intramolecular OH-N hydrogen bonds may be stable even above 300 °C.¹³⁵ The final glass transition temperatures of benzoxazines range from 160 °C to 400 °C and are largely dependent on the bulkiness of the amine. Nevertheless, it may be observed that mechanical properties gradually decrease over a wide temperature range below T_g . Also this behavior is a result of hydrogen bonds of different thermal stability. Another property that is beneficially influenced by the hydrogen bonding structure is the low water uptake despite the high hydroxyl group content. Typically, the presence of polar groups causes large water absorption of 3 - 20 wt.% for common epoxy or phenol resins.¹²¹ However, many benzoxazines absorb less than 2 wt.% of water as the strong intramolecular hydrogen bonds render the polybenzoxazine less hydrophilic in comparison to free hydroxyl groups. It is important to mention that the strength of OH-N hydrogen bonds is related on the basicity of the incorporated amine. Therefore, aliphatic and aromatic benzoxazines behave significantly different, whereas the described effects are much more pronounced for aliphatic benzoxazines.

Additionally, the ring-opening addition reaction of benzoxazines provides further advantages over the condensation of phenolic resins such as almost no release of volatile by-products and near zero volume shrinkage/expansion, which reduces optical distortion, warping or residual stress. However, the most striking feature of benzoxazines is their molecular design flexibility from various cheap phenols and amines. Originating from the unique and beneficial properties in combination with low costs it is obvious that polybenzoxazines are not just applied as simple replacement for phenol resins or more technical epoxy resins but also enable new applications. Therefore, benzoxazine functional polyurethane prepolymers are introduced in this thesis to provide a novel thermal curing mechanism for polyurethanes and likewise provide an adjustable toughener for polybenzoxazines. This work is related to previous work in our group.¹³⁶⁻¹³⁹

3 Characterization Techniques

UV-curing reactions proceed within seconds or even fractions of seconds and typically yield crosslinked materials. Therefore, it is difficult to investigate physical and chemical transitions that occur during the reaction. Particular methods that have been applied in this thesis for reaction monitoring and determination of critical parameters are described in the following.

3.1 Differential Scanning Calorimetry (DSC)

Differential scanning calorimetry is a dynamic method to determine thermal events corresponding to physical or chemical transitions in a sample.¹⁴⁰⁻¹⁴³ Typical events that can be observed are shown in Figure 3.1.

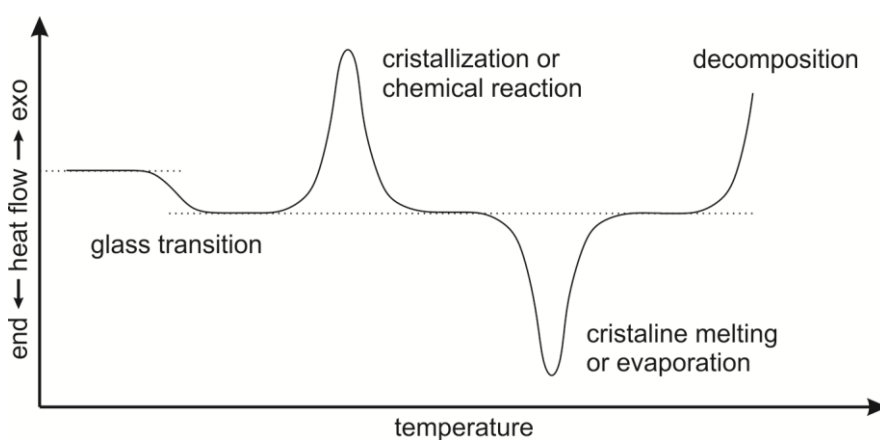


Figure 3.1. Thermal events in a DSC plot.

The most common measurement setup is the heat flow DSC, where the sample and the reference pan are located on two temperature sensors within one oven as depicted in Figure 3.2.

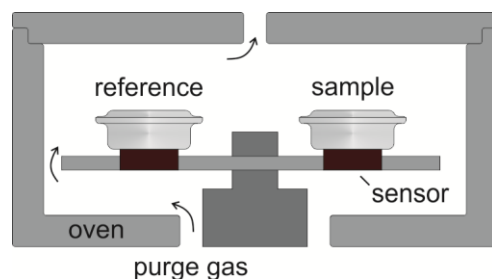


Figure 3.2. Setup of a heat flux DSC.

The heat flow between the sample and the tempered environment can be calculated from the temperature difference of the sensors and is directly proportional to the heat capacity of the sample. Upon glass transition a polymer changes from the glass like, energy elastic state to the rubber like, entropy elastic state. Transitional and rotational motions of the polymer chains take place above T_g , but become practically impossible below T_g (vitrification). This relaxation transition is not characterized by a transition enthalpy as it is the case for classical first order phase transitions. However, it is accompanied by a change in the heat capacity and the free volume. Consequently, the glass transition temperature can be observed as a step in the DSC-curve.

Instead, classical first order phase transitions like crystallization and evaporation or chemical transitions show endothermic or exothermic peaks. The corresponding change in enthalpy can be calculated from the integrated peak areas. With respect to the work presented in the following, the determination of glass transition temperatures and the observation of exothermic chemical reactions is of particular interest.

3.1.1 Temperature Modulated DSC

A temperature modulated DSC experiment allows the differentiation between reversible effects such as glass transition (follows modulation) and irreversible effects like crystallization, crosslinking, evaporation or decomposition (do not follow modulation).¹⁴⁰⁻¹⁴³ This method is particularly beneficial, if reversible and irreversible effects overlap or appear in a narrow temperature range as it may be the case for supercooled and vitrified amorphous orientations that recrystallize upon glass transition or vitrified chemical reactions that continue to proceed above glass transition.

A periodical (usually sinusoidal) heating rate is added to the basic constant heating rate. Therefore, the actual heating rate oscillates around the average heating rate (see Figure 3.3a). The measured modulated heat flow can be differentiated into the total, average heat flow and its reversible and irreversible contributions via Fourier transformation. The total heat flow is consistent with the signal of a conventional DSC measurement, whereas the reversible and irreversible contributions allow the independent evaluation of the individual effects. An example is shown in Figure 3.3b.

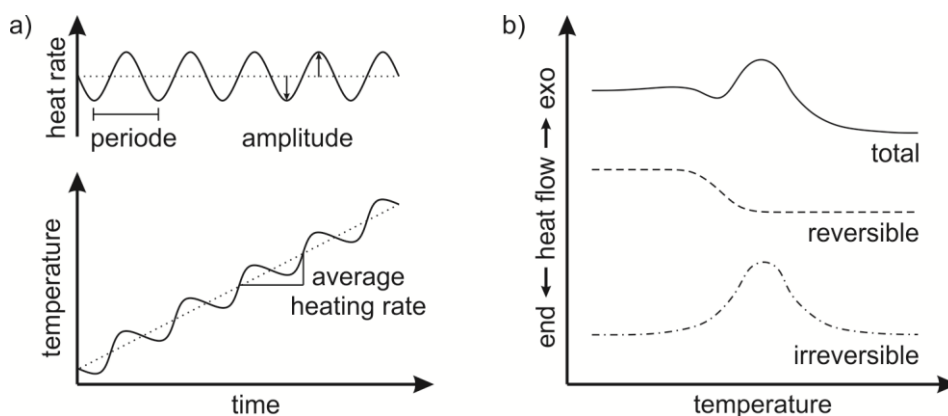


Figure 3.3. Temperature modulated DSC.

a) Heat rate in temperature modulated DSC. b) Reversible and irreversible contributions of the total heat flow curve. Reversible and irreversible effects can be differentiated and evaluated separately.

3.1.2 Photo-DSC

The reaction enthalpy of light induced reactions can be investigated via photo-DSC.¹⁴²⁻¹⁴⁵ The instrumental setup is basically equivalent to that of a regular heat flux DSC, except for the two light guides that are mounted into the lid of the measuring cell.¹⁴⁶ Both light guides are connected to the same light source via a beam splitter. The sample is prepared in open pan and can be irradiated from the top during the measurement as depicted in Figure 3.4.

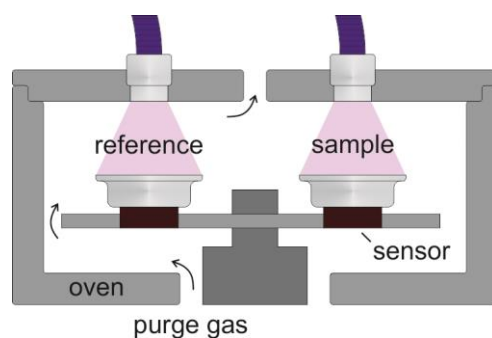


Figure 3.4. Setup of a photo-DSC.

Samples are prepared in open pans and can be irradiated from the top during the measurement.

The samples are typically irradiated several times under isothermal conditions to ensure completeness of the reaction. The resulting heat flow during irradiation needs to be corrected for the energy input through absorption via subtraction of a later irradiation cycle to give the reaction enthalpy. If complete conversion can be assumed or the entire theoretical reaction enthalpy is known, one can correlate the evolution of reaction enthalpy with the conversion of functional groups and hence gain kinetic information. The combination of isothermal photocuring segments with common or temperature modulated ramped segments in a complex measurement profile allows to evaluate thermal properties of the educt and product within a single measurement as well as photo- or thermally induced curing and post-curing reactions.

3.2 Real Time (Near) Infrared Spectroscopy

Direct structural information can be obtained from vibrational spectroscopy. The intensity of a characteristic absorption band is proportional to the concentration of the corresponding functional group and its conversion can be calculated in relation to the starting value. Modern Fourier transform infrared (FTIR) spectrometer allow sampling rates much greater than 100 s^{-1} and hence are capable to record a sufficient number of spectra within the time scale of a photoinduced curing reaction.¹⁴⁷⁻¹⁴⁹ Spectra can be recorded via ATR-technique or in transmission through thin films, while the sample can be easily irradiated with UV-light in both instrumental setups. The curing kinetics and the influence of various variables can be studied via monitoring the conversion of an involved functional group throughout irradiation. Any impact that result from sample shrinkage or deformation may be subtracted using an absorption band of a functional group that does not participate in the reaction as internal reference.

In recent years, cost efficient and easy to use near infrared (NIR) spectroscopy was increasingly applied to monitor photocuring reactions.^{150, 151} The key advantage of NIR spectroscopy over conventional mid IR spectroscopy is that many glass and polymeric optics and fibers are largely transparent in the NIR spectral range. On the other hand absorption bands in the NIR spectrum are generally overtone- and combination vibrations, which exhibit a comparatively weak intensity and can hardly be correlated to the individual functional groups. Therefore, NIR spectroscopy is mainly applied in comparative quality analysis. However, vinyl ethers show a well separated absorption band at about 6200 cm^{-1} corresponding to the first overtone of the C-H stretching vibration and weak intensities can be compensated by an increased film thickness.^{150, 152}

3.3 Rheology

Rheology is a mechanical characterization technic that deals with the flow behavior and deformation of liquid and solid materials.^{153, 154} As such it is perfectly suited to monitor mechanical and viscoelastic properties throughout phase transition between these states. Typically, deformation and frequency are fixed in oscillatory experiments and mechanical properties, including the complex shear modulus ($G^* = G' + G''$), storage and loss modulus (G' and G''), the damping factor ($\tan\delta = G''/G'$) or the complex viscosity (η^*) are reported. Isothermal rheology may be performed to accurately determine key figures. However, often temperature ramps are applied to observe structural or phase transitions. A phase transition such as the glass transition has a drastic effect on the mechanical properties of a polymer. The vitrified polymer chains result in a rigid and brittle consistency below T_g , whereas more flexible elastic or liquid like behavior is observed above T_g , depending on the crystallinity or crosslink density. Consequently, G' rapidly decreases at T_g , whereas G'' shows a maximum of energy dissipation. Typical rheological plots for the temperature dependence of G' and G'' are shown in Figure 3.5.

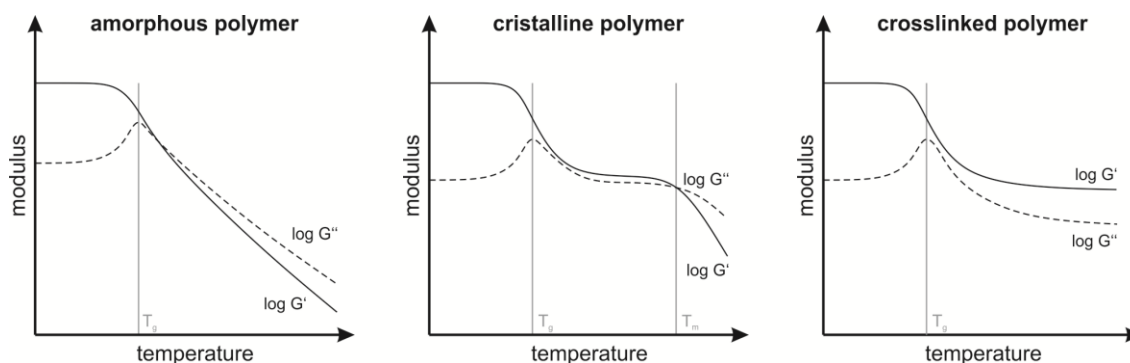


Figure 3.5. Temperature dependence of G' and G'' for different types of polymers.

The glass transition temperature can be determined best from the peak maximum in the loss modulus.

3.3.1 Photorheology

Also chemical reactions like polymerization or crosslinking have a distinct effect on the mechanical properties. Rheological experiments are again perfectly suited to in-situ monitor these processes that involve transition from liquid to solid state. The plate/plate geometry represents a common measurement setup in oscillatory rheology. However, the plates cover the largest surface of the sample. Therefore, at least one plate has to be replaced by a quartz glass optic to allow a reliable and homogeneous irradiation for the investigation of photoinduced curing reactions. The first photorheology setup was reported by Kahn *et al.* to monitor the gelation behavior of photocuring materials.¹⁵⁵ In contrast to well-established photo-DSC and real time vibrational spectroscopy, photorheology provides information that are of high interest for technical processes and applications such as, pot life, open time, plateau modulus and the viscosity profile. A typical plot of G' , G'' and $\tan\delta$ of a photocurable material upon irradiation is shown in Figure 3.6.

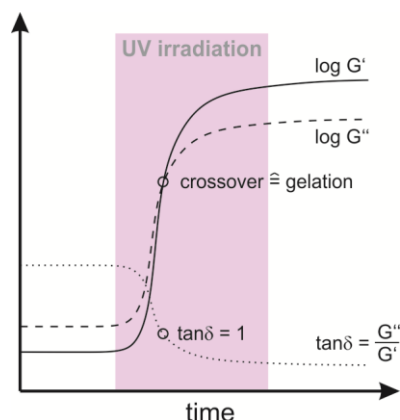


Figure 3.6. Rheological plot of a UV-curing material.

The purple highlighted background indicates the irradiation period and can be found in several photorheology and photo-DSC plots throughout this thesis. Gelation of the sample is observed when the curves of G' and G'' crossover (sol-gel transition).¹⁵⁶ By definition the damping factor ($\tan\delta = G''/G'$) becomes 1 at that point. Before gelation ($G'' > G'$) the sample behaves more liquid like, whereas after gelation ($G' > G''$) the solid character dominates.

3.3.2 UV/NIR-Rheology

The coupling of photorheology and near infrared (NIR) spectroscopy enables the simultaneous measurement and hence the direct correlation of mechanical properties and molecular information.^{157, 158} Several instrumental setups with different arrangements of the UV-source and the NIR probes were proposed. The setup described by the group of Scherzer¹⁵⁷ was replicated for this thesis and is shown in Figure 3.7.

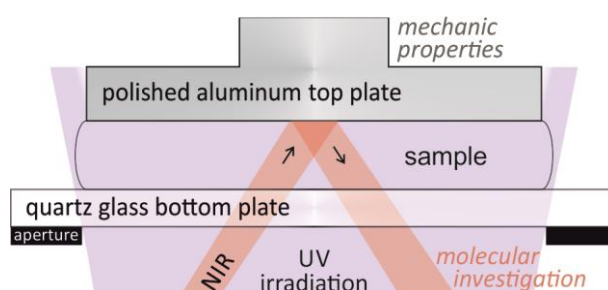


Figure 3.7. Setup of the UV-and NIR coupled rheometer.

The UV-coupling allows to photoinduce chemical reactions and the coupled NIR spectrometer enables the structural investigation of the material upon curing. Hence the mechanical data acquired from the rheological experiment can directly be correlated to the conversion and the reaction kinetics.

The rheometer is equipped with a quartz glass bottom plate that is transparent in a broad spectral range including both UV and NIR light. The UV-irradiation is performed perpendicular to the sample surface to ensure a homogeneous illumination and an even curing reaction, whereas the NIR probes are placed angular to the sample surface. Spectra are recorded in transfection, using the aluminum top plate as reflector. Significantly improved signal no noise ratios can be obtained, when the aluminum top plate is manually polished to mirror finish.

4 Results and Discussion

Chapter 4.1 - 4.6 represent coherent research projects, which are related to each other. The overall context and the intersection between different chapters are discussed referring to Figure 4.1.

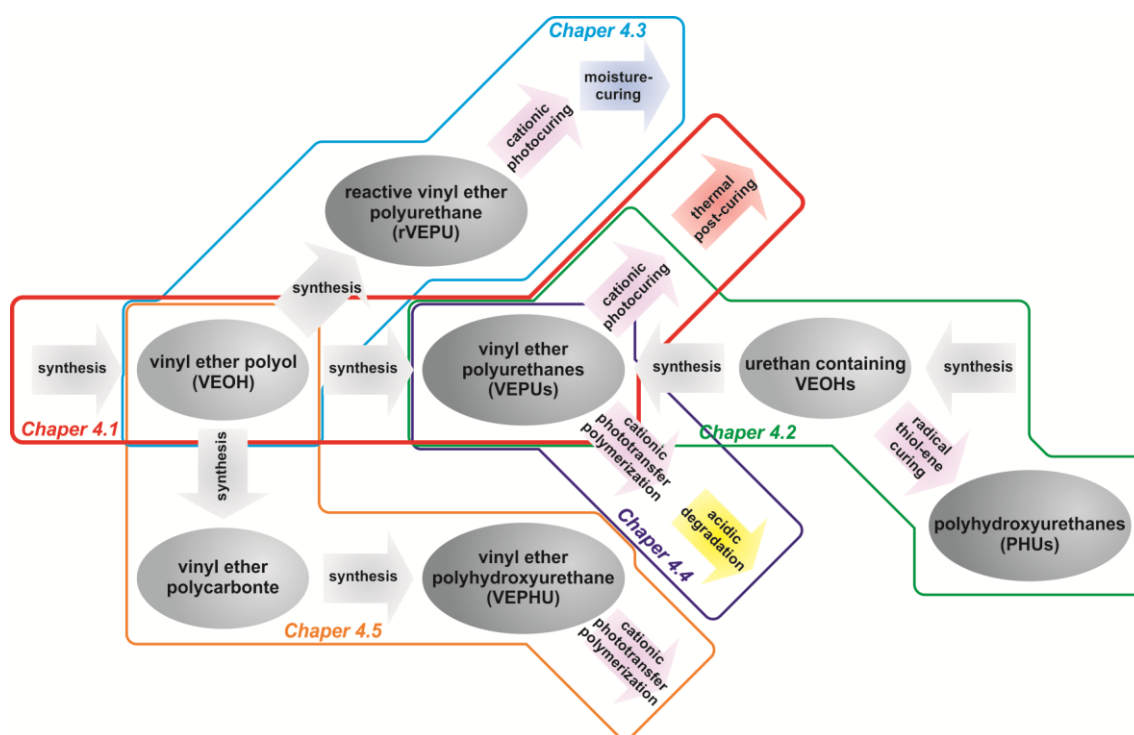


Figure 4.1. Overview of the content presented in Chapter 4.1 - 4.5.

VEOHs and VEPUs enable a number of selective reaction pathways and structures with high value for material chemistry.

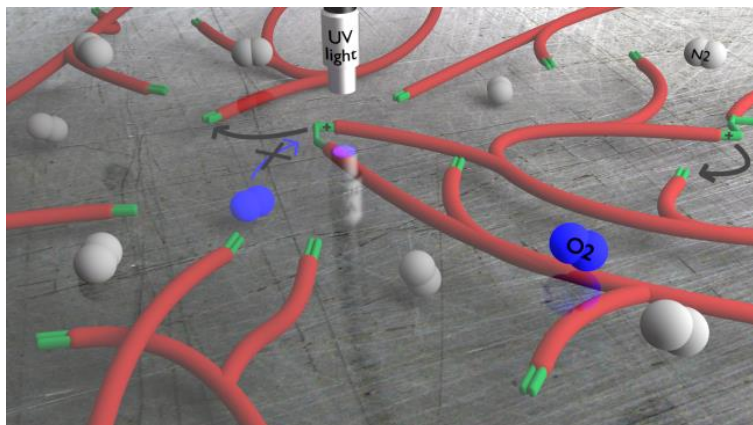
Chapter 4.1 introduces the elementary synthesis of a vinyl ether polyol (VEOH) and its incorporation into a highly vinyl ether functional polyurethane prepolymer (VEPU). Subsequently, the VEPU was photocured under cationic conditions. The curing and post-curing processes were investigated in detail to provide a fundamental understanding. Starting from this fundament the following chapter utilize numerous specific reactions to prepare and cure VEOHs, VEPUs or related materials.

Chapter 4.2 deals with a simplified and scalable synthesis of alternative vinyl ether polyols. These urethane containing VEOHs were evaluated for cationic photocuring in polyurethane prepolymers and also as raw materials for polyhydroxyurethanes (PHU)

via radical mediated thiol-ene addition. The objective of Chapter 4.3 was to prepare reactive vinyl ether polyurethane prepolymers with terminal isocyanate groups (rVEPU). These materials provide a synergistic dual cure mechanism comprising of cationic photocuring and moisture-curing. In Chapter 4.4 VEPU were formulated with different hydroxyl group containing transfer agents. The resulting cationic phototransfer reaction was carefully investigated with an emphasis on the formation of acetal groups in crosslinked polymer networks. Furthermore, the acidic degradation and release efficiency of hydroxyl component were evaluated. This concept was successfully transferred to a vinyl ether polyhydroxyurethane (VEPHU) as one component system comprising vinyl ether and hydroxyl groups in Chapter 4.5. Cationic phototransfer polymerization of VEPHUs was shown to consume inherent hydroxyl groups.

A benzoxazine functionalized polyurethane was prepared in Chapter 4.6. This project is not directly related to the vinyl ether approach but the material also introduces a novel curing mechanism for polyurethanes.

4.1 Unique Curing Properties through Living Polymerization in Crosslinking Materials: Polyurethane Photopolymers from Vinyl Ether Building Blocks*



Photopolymers with unique curing capabilities are introduced by combining living cationic polymerization with network formation and restricted polymer motion. A vinyl ether diol is synthesized as functional building block and reacted with isophorone diisocyanate to form a highly vinyl ether functional polyurethane as model system with high crosslinking ability. In combination with cationic photoinitiators fast polymerization is observed upon short UV-irradiation. Curing proceeds in the absence of light and under ambient conditions without oxygen inhibition. Cationic active sites become trapped, dormant species upon network-induced vitrification and surprisingly remain living for several days. The polymerization can be reactivated, triggered by additional UV-irradiation and/or temperature. The curing behavior was studied in detail using UV and FT-NIR coupled rheology and photo-DSC to simultaneously observe spectroscopic and mechanical information as well as thermal effects.

* This section is based on the publication “*Unique Curing Properties through Living Polymerization in Crosslinking Materials: Polyurethane Photopolymers from Vinyl Ether Building Blocks*” by Stefan Kirschbaum, Katharina Landfester and Andreas Taden, published in *Angew. Chem. Int. Ed.* **2015**, 54, 5789-5792. Reprinted with permission. Copyright 2015 Wiley-VCH Verlag GmbH & Co. KGaA, Weinheim.

4.1.1 Motivation

The desire for novel photopolymers with facile, robust curing conditions and highly adjustable mechanical properties is sparked by the broad availability of energy efficient, light emitting diodes^{159, 160} and recent exciting technological developments, like stereolithography,²⁰ 3D inkjet printing¹² or nanoimprint lithography.²¹⁻²³ One of the most important classes of photopolymers are polyurethanes carrying terminal (meth)acrylic units, designed for UV-initiated radical crosslinking reactions.¹⁶¹⁻¹⁶³ They can combine various attractive properties like chemical and mechanical resistance, fast polymerization, adjustable strength and absence of volatile organic contents. This wide range of accessible material properties is generally recognized as a striking feature of polyurethane chemistry and accordingly various applications can be addressed. However, the radical polymerization mechanism is sensitive towards oxygen inhibition. In particular, thin films with large surface area are prone to termination reactions and defects under ambient conditions.^{99, 100}

To overcome this issue, an alternative curing mechanism has to be employed. Since the development of onium salts, the UV-initiated cationic polymerization of epoxides and vinyl ethers received increasing attention.^{10, 164} Although cationic polymerization is sensitive towards a number of functional groups, it provides several advantages over free radical polymerization such as propagation without self-termination. Hence, once initiated, the polymerization proceeds in the absence of light. This so-called “*dark cure*” behavior is technologically relevant, for example to assemble non-transparent substrates. Additionally, the absence of oxygen inhibition eliminates the need of nitrogen purging.^{40, 165, 166} Unfortunately, the cationic polymerization of epoxides is not compatible with urethane groups due to undesired transfer reactions.⁵¹ and polymerization kinetics are rather slow.⁵⁰ Furthermore, compared to polyurethane systems the mechanical properties cannot be tailored over a wide range.

In contrast, the cationic polymerization of vinyl ethers is generally less sensitive towards nucleophilic functional groups and proceeds in the presence of urethanes. Even living polymerization conditions can be achieved due to mesomeric stabilization of the propagating species.^{53, 167} Moreover, the high electron density results in reaction rates similar to free radical polymerization of acrylates.¹¹ Unfortunately, the highly

exothermic reaction leads to vigorous heat release, which hinders the use of low molecular weight vinyl ether in technical applications. As a consequence urethane functionalized or blended vinyl ether systems were investigated.^{50, 168} It was found, that interactions with urethane groups can lead to reduced polymerization rates or yield products with reduced molecular weight and broadened polydispersity, indicating that transfer reactions cannot be completely prevented. Vinyl ether terminated urethane prepolymers^{51, 169} with cationic curing ability were synthesized, but still require blending with multifunctional reactive diluents to obtain higher crosslinking densities and a more distinct mechanical modulus increase upon polymerization. Recently, the first polymer systems bearing vinyl ether moieties along the backbone were reported, prepared as biocompatible polyether⁸¹ and polyphosphorester¹⁷⁰ templates for post-polymerization modification using thiol-ene click reactions. In these reports neither UV-initiated crosslinking nor mechanical properties were discussed.

We herein describe for the first time the synthesis of highly functionalized polyurethanes carrying vinyl ether side-chains. In contrast to the previous work, we focus on photocuring and mechanical properties and introduce unique curing capabilities.

4.1.2 Synthesis of VEPUs

A vinyl ether diol (VEOH) was synthesized as functional building block and reacted with an excess of isophorone diisocyanate (IPDI) to yield a prepolymer. Terminal isocyanate groups were subsequently converted with 4-hydroxybutyl vinyl ether (HBVE). The resulting side-chain functionalized polyurethane prepolymer (sc-VEPU) was estimated to have a vinyl ether functionality of 16.5 and a number average molecular weight (M_n) of 5000 g/mol. For comparison, the VEOH was hydrogenated to obtain a vinyl ether terminated polyurethane with a similar but inactive backbone structure (hsc-VEPU). In addition, vinyl ether and alkyl end-capped polyurethanes (t-VEPU and i-PU) were synthesized from IPDI and polypropylene glycol using HBVE and 1-heptanol respectively as end-capping reagents. An overview on the synthetic pathway is provided in Figure 4.2 and more detailed information can be found in Chapter 5.1 in the Experimental Section.

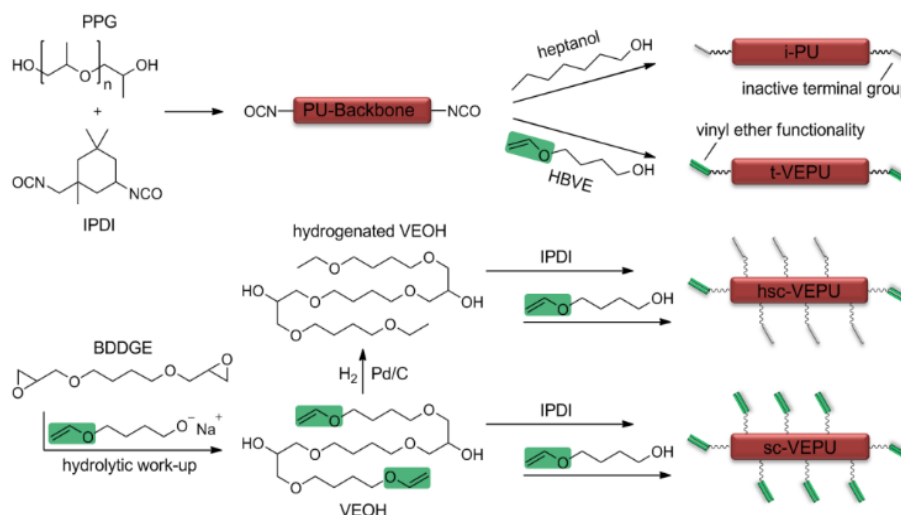


Figure 4.2. Synthesis of polyurethanes with different backbone and vinyl ether functionality.

4.1.3 Radiation Curing of VEPUs

The polyurethanes were subsequently formulated with 1 wt% cationic photoinitiator, 4,4'-dimethyl-diphenyliodonium hexafluorophosphate. UV/NIR-rheology¹⁵⁷ was then used to simultaneously monitor the evolution of mechanical properties and the conversion of vinyl ether groups upon UV-irradiation. Figure 4.3a illustrates the instrumental setup (details can be found in Chapter 5.1.7). Figure 4.3b shows a picture of the cured and highly transparent sc-VEPU on a glass slide. Rheometric plots are provided in Figure 4.3c. The irradiation period of 10 s is indicated by the purple colored background in the diagram.

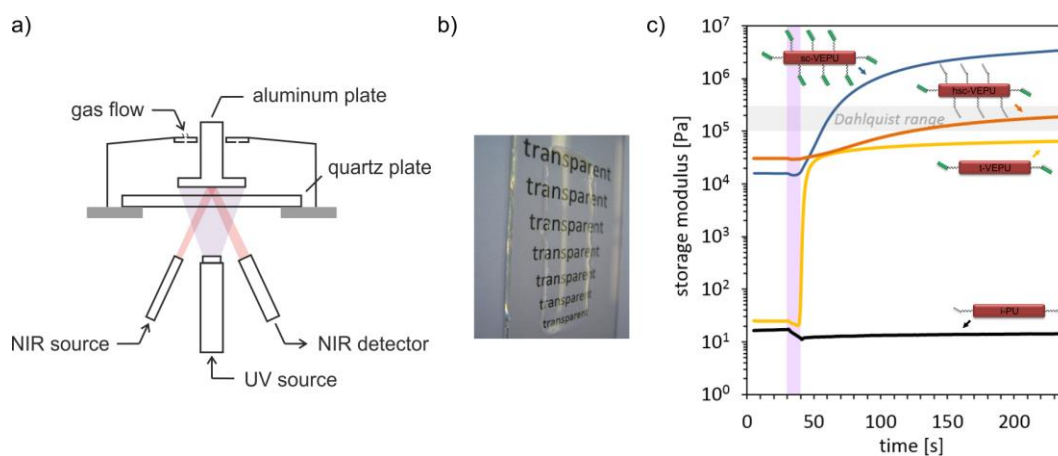


Figure 4.3. Radiation induced curing of VEPUs

a) Illustration of the rheometer setup. b) Picture of the sc-VEPU cast onto a glass slide and cured. c) Rheometric plots of the polyurethanes upon 10 s UV-irradiation (purple background) at room temperature. The Dahlquist range needs to be exceeded to obtain tack-free films.

As expected, the i-PU does not show any storage modulus increase and instead a slight, thermally induced decline in the storage modulus can be observed upon irradiation. The t-VEPU shows an inhibition period of 9 s after initial exposure, followed by a rapid increase in the storage modulus. This behavior can be explained by traces of stabilizer impurities, such as potassium hydroxide from HBVE, and is also observed under dry nitrogen atmosphere as shown in Figure 4.4.

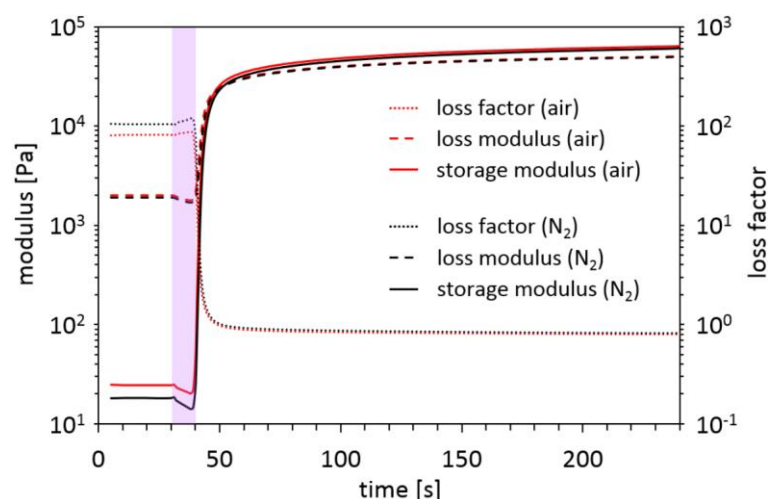


Figure 4.4. Rheometric plot of the t-VEPU cured under instrumental air and nitrogen atmosphere.

The presence of oxygen does not show an effect on the curing profile. The deviation in the initial storage moduli probably derives from an overfilled gap or gas bubbles within one sample and is rather low but pronounced by the logarithmic scale.

Both of the polypropylene glycol based samples (i-PU and t-VEPU) consist of about 82 wt% soft segment and show relatively low initial storage moduli. Therefore, upon UV-curing the storage modulus of the t-VEPU can increase over several orders of magnitude, but does not exceed the Dahlquist criterion, representing the marginal value required to obtain tack-free films.^{171, 172} The tackiness of the film indicates that the flexible polymer chains do not have sufficient crosslink density to set solely via terminal reactive sites.

The hsc-VEPU demonstrates the effect of different polyurethane backbones. It has a high content of urethane hard segments due to the short polyol structure, which results in stronger intermolecular interactions and increased viscosity. For comparison, the initial complex viscosities of all samples are reported in Table 4.1.

Table 4.1. Initial, complex viscosities

Sample	T_{curing} [°C]	$\eta^*_{t=0}(T_{curing})$ [Pa*s]
i-PU	25	29
t-VEPU	25	32
hsc-VEPU	25	827
sc-VEPU	25	728
sc-VEPU	40	253
sc-VEPU	60	43

The initial sample viscosity was determined within the UV/NIR-rheology experiment and exemplifies the major difference in molecular mobility between polyurethanes synthesized from the PPG 2000 compared to the polyurethanes synthesized either from the VEOH or the hydrogenated VEOH.

Accordingly, the initial storage modulus of the hsc-VEPU is significantly increased and, upon UV-initiation, evolves at a lower rate. The slower polymerization kinetics are attributed to limited mobility of the functional groups in viscous media, as it is described in the literature for macromonomers.^{173, 174} Moreover, the curing plot of the hsc-VEPU clearly demonstrates the dark cure behavior, as the majority of the modulus increase occurs after irradiation. Although the cured hsc-VEPU shows a higher storage modulus compared to the t-VEPU it still remains soft and slightly tacky. In contrast, the highly functionalized sc-VEPU with similar backbone structure cures to a tack free film and exhibits a superior storage modulus as direct consequence of the significantly enhanced crosslinking ability.

The vinyl ether conversion can be observed *in situ* via NIR spectroscopy. However, integration of the C-H stretching band at about 6200 cm⁻¹ was only performed for the sc-VEPU sample. The concentration of vinyl ether groups in solely terminal functionalized samples was too little to get reliable signal to noise ratios. Exemplarily the NIR spectra of the sc-VEPU cured at 60 °C are shown in Figure 4.5. Please note, that the vinyl ether peak is located in a convex area of the spectrum. Therefore, slightly negative values for the residual vinyl ether concentration may arise upon total disappearance of the peak.

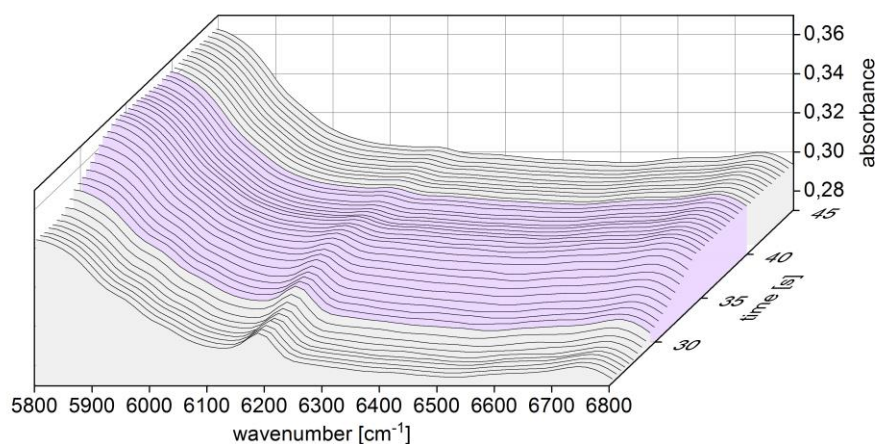


Figure 4.5. NIR spectra of the sc-VEPU upon UV-initiated curing at 60 °C.

The sample was irradiated from 30 - 40 s. The increasing background intensity at that time correlates with the sample shrinkage of 3.7% but could also be due to a change in the optical density. Unfortunately, no reference peak is available in the NIR spectrum so that these effects cannot be eliminated.

Figure 4.6 shows the overlaid storage moduli and vinyl ether conversion plots for the sc-VEPU prepolymer composition cured at 25 °C, 40 °C and 60 °C.

Increasing polymerization rates and lower initial moduli were observed with increasing temperatures. The accelerated polymerization rates are a consequence of higher mobility of the reactive sites at higher temperatures. Curing at 25 °C and 40 °C resulted in incomplete conversions of about 45% and 75% after the first exposure to UV. A second exposure further increased the conversion to about 70% and 90%, respectively.

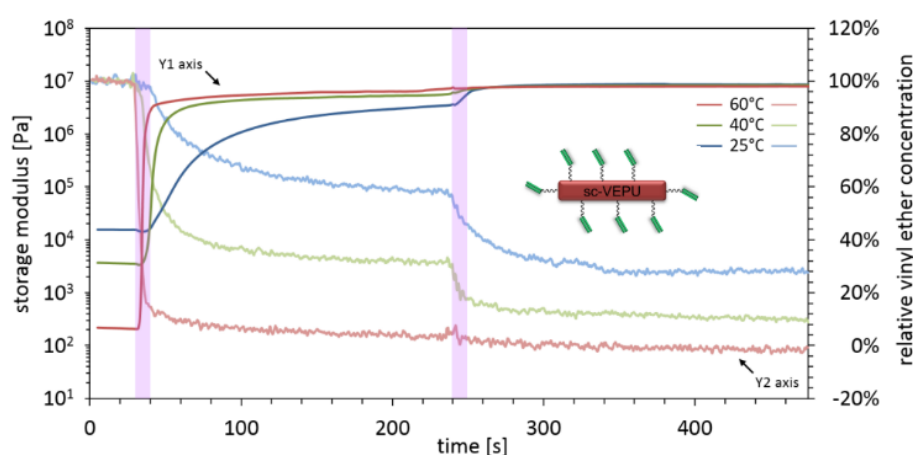


Figure 4.6. Photocuring and dark cure of the side-chain functionalized polyurethane (sc-VEPU) at different temperatures. Evolutions of the mechanical modulus (full color lines) and the vinyl ether concentration (pale color lines) were recorded simultaneously. The purple colored background indicates UV-exposure.

Similar results were obtained using isothermal photo-DSC as depicted in Figure 4.7.

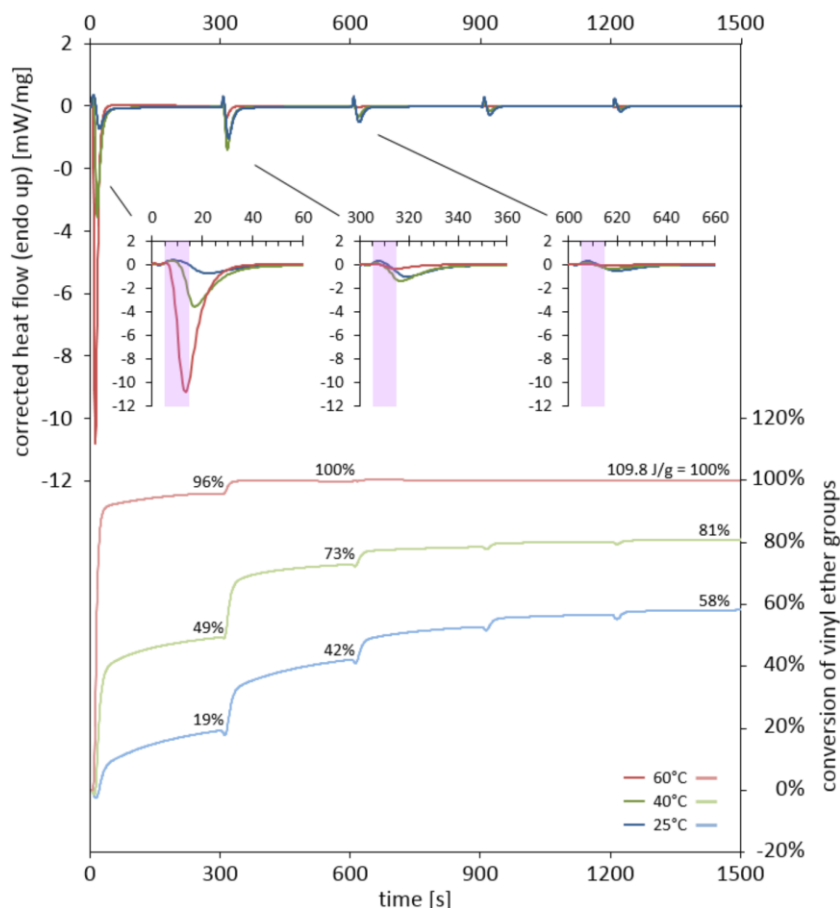


Figure 4.7. Reaction enthalpy and conversion of the sc-VEPU upon isothermal UV-exposure at different curing temperatures.

The corrected heat flow of the samples upon irradiation is plotted in the top of the diagram. The heat flow during the tenth irradiation was subtracted from the previous irradiations to eliminate the energy input through absorption. In accordance with the UV/NIR-rheology one can observe that the sample releases more energy with increasing curing temperature and hence cures faster and to a higher degree. Also post-curing and curing upon further irradiation of the samples was monitored. Furthermore, the integral of the corrected heat flow can be correlated to the reaction enthalpy and hence to the conversion, which is plotted at the bottom of the diagram. The comparatively small endothermal effect upon irradiation can be assigned to decomposition of the photoinitiator via comparison of the i-PU with and without photoinitiator and slightly distorts the conversion data. Unfortunately, the conversions cannot directly be compared with those from the rheology experiment as the intensities of the initiation effective UVC range differ in both instrumental setups (see Chapter 5.1.9). The terminal

functionalized samples are not plotted in this content as the measurable enthalpy is rather low and does not allow reliable conclusions.

4.1.4 Vitrification Induced Curing Time Out and Thermal Post-Curing

The isothermal photo-DSC was performed in a complex measurement profile (see Chapter 5.1.8) that also included temperature modulated segments to determine thermal events before and after curing. Figure 4.8 exemplarily shows the total heat flow as well as its reversing and non-reversing contributions in the first temperature modulated heating run of the sc-VEPU after curing at 25 °C.

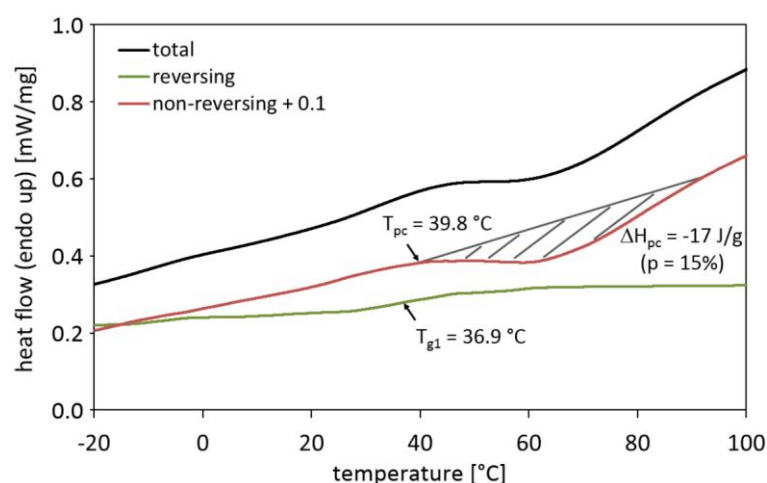


Figure 4.8. First temperature modulated heating run of the sc-VEPU after UV-exposure at 25 °C.

The reversing and non-reversing contributions allow the independent determination of the glass transition temperature before post-curing (T_{g1}) and the onset temperature of the post-curing reaction (T_{pc}) as well as a more accurate determination of the post-curing enthalpy (ΔH_{pc}). The non-reversing curve was shifted by +0.1 in the graph to improve clarity.

The total heat flow indicates a glass transition followed by a broad exothermic peak. The overlapping of the signals makes it difficult to accurately assign the post-curing enthalpy and the temperatures of both effects. However, the modulated DSC experiment allows to separate the reversible glass transition and the irreversible curing reaction and determine them independent from each other. The exothermic peak was assigned with an onset temperature (T_{pc}) and integrated to calculate the reaction enthalpy (ΔH_{pc}), whereas the glass transition temperature before post-curing was defined as T_{g1} . The results of the complex photo-DSC measurements are summarized in Table 4.2.

Table 4.2. Thermal properties of the VEPUs samples.

Sample	$T_{g0}^{[a]}$ [°C]	$T_c^{[b]}$ [°C]	$\Sigma\Delta H^{[c]}$ [J/g]	$T_{g1}^{[a]}$ [°C]	T_{pc} [°C]	ΔH_{pc} [J/g]	$T_{g2}^{[a]}$ [°C]
i-PU	-57.9	25	-	-58.0	-	-	-58.1
t-VEPU	-58.5	25	n.d.	-58.7	-	-	-58.3
hsc-VEPU	-12.1	25	n.d.	-5.0	-	-	-4.6
sc-VEPU	-12.0	25	-65	36.9	39.8	-17	64.2
sc-VEPU	-11.1	40	-89	55.0	59.8	-5	77.1
sc-VEPU	-10.9	60	-110	74.7	-	-	85.6

^[a] T_{g0} , T_{g1} , T_{g2} are the glass transition temperatures determined before curing and within two consecutive heating runs after curing. ^[b] T_c is the curing temperature. ^[c] $\Sigma\Delta H$ is the entire reaction enthalpy over several irradiations.

The energy input from the lamp caused a short temporary temperature increase of about 6 °C at the sensor and explains why the glass transition temperatures after polymerization (T_{g1}) are similarly higher than the curing temperatures (T_c s) for all samples. However, the relation of T_{g1} and T_c reveals that the polymer vitrifies and the curing reactions stops when the increasing T_g of the photopolymer exceeds the ambient temperature. Mechanistically, the active chain-ends become trapped in crosslinked, vitrified regions and inaccessible to residual vinyl ether groups. A subsequent exposure for UV-generates new, more mobile polymerizing species (and heat), which further increases the conversion. Vitrification of the living polymerization is induced by tight network formation and hence only possible in systems with high crosslinking capability. The reactivation of the living but otherwise dormant cationic sites by simple thermal treatment represents a novel and unique post-curing mechanism. As a consequence of the increased conversion upon irradiation at higher temperature, the extent of thermally induced post-curing decreases. At 60 °C, the sc-VEPU prepolymer composition cures rapidly to essentially complete conversion and consequently does not show thermally induced post-curing.

4.1.5 Durability of Trapped Cationic Chain-Ends

To investigate the durability of the trapped cationic chain-ends and the post-curing ability, thermal treatment was performed after various storage times. Onset

temperatures and enthalpies of the thermally induced post-curing are plotted as a function of the time between initial curing and thermal treatment in Figure 4.9.

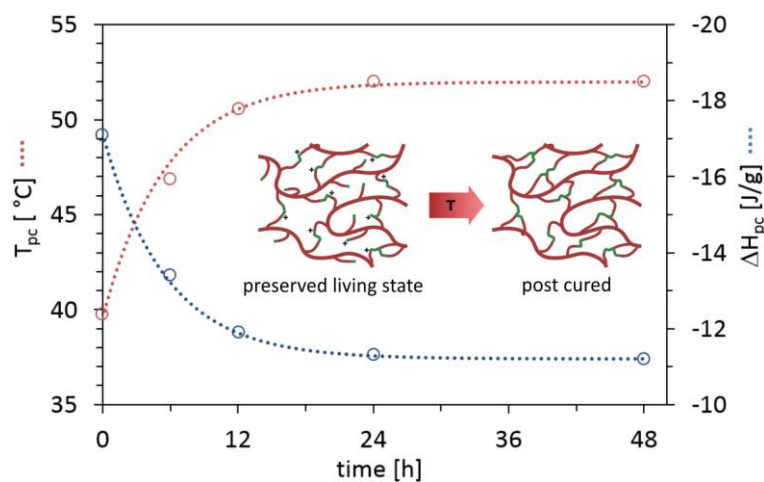


Figure 4.9. Durability of the post-curing ability of the sc-VEPU pre-cured at 25 °C.

The results indicate that dark curing proceeds slowly over several hours up to a certain limit. After about 24 h dark curing came to stagnation, while an accordingly reduced post-curing ability is constantly preserved over days. It can be concluded, that the trapped cationic species remain active for days under technical air conditions at room temperature.

4.1.6 Influence of the Curing Conditions on the Network Structure

Despite thermal treatment of all samples, higher T_{g2} values are observed for samples cured at higher temperature within fewer irradiations (see Table 4.2). Increased quantities of photoinitiator are decomposed, when a samples is submitted to additional UV-exposure to increase conversion, at low temperatures. Additional propagating species become generated, which in average leads to shorter kinetic chain lengths and correspondingly reduced crosslinking densities. This behavior is schematically depicted in Figure 4.10 and can explain the variations in T_{g2} through altered network structures.

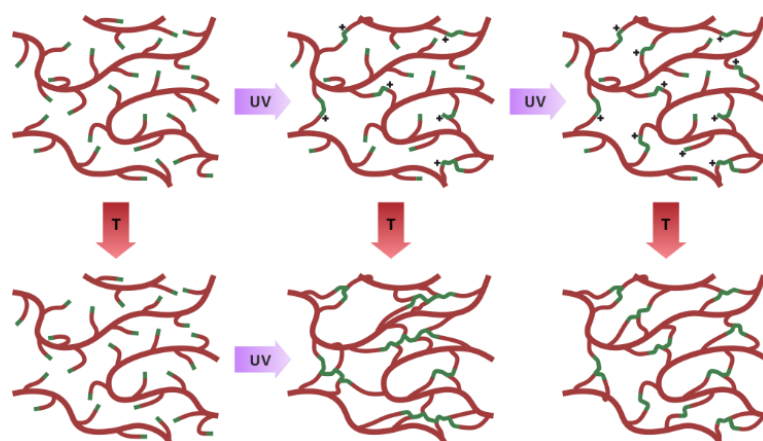


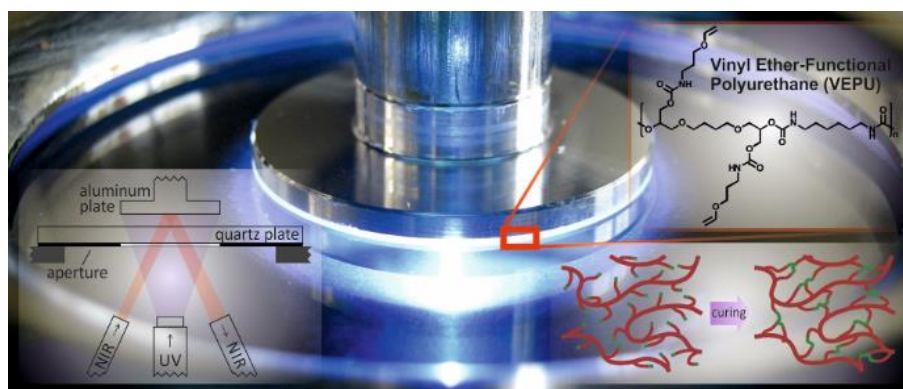
Figure 4.10. Schematic curing and post-curing abilities

4.1.7 Conclusion and Outlook

The polyurethane model system chosen for this study exhibits a comparatively high starting storage modulus and viscosity. However, polyurethane chemistry is highly modular and the VEOH can be utilized as functional building block to create various different photopolymer structures with adjustable properties. In addition, vinyl ethers are highly reactive in thiol-ene “click” reactions due to their high electron density and the absence of radical homopolymerization.⁵⁷ Such systems could be adopted as alternative curing mechanism to the cationic system described in this section.

In summary, we described the first synthesis of vinyl ether polyols and highly functionalized vinyl ether polyurethanes and demonstrated their use as novel class of photopolymers with unique and adjustable curing capabilities. Our modular synthetic approach is compatible with standard polyaddition and polycondensation reactions and therefore enables a wide range of new photopolymers with tunable mechanical properties. Originating from the living cationic polymerization, curing can proceed in the absence of light and is not inhibited by oxygen. Materials with high crosslinking capability can deliver trapped, vitrified active sites, which remain living, but dormant due to restricted mobility. Simple heating and/or repeated UV-initiation leads to the reactivation of the polymerization reaction and hence enables numerous new engineering solutions and processes. The overall material and (post)curing characteristics can be customized for various applications and are expected to stimulate new applications and push existing technologies.

4.2 Vinyl Ether Functional Polyols as Building Blocks for UV-Curable Polyurethanes and Isocyanate-Free Polyhydroxyurethanes*



Vinyl ether functional polyols (VEOHs) are key components for advanced photopolymer systems and additionally provide facile modification capabilities via thiol-ene chemistry. A novel synthetic route towards VEOHs based on the ring-opening reaction of cyclic carbonates with amines is introduced. This procedure yields oligomer free products with improved physical properties through integrated urethane groups. The synthetic approach is easily scalable and avoids tedious purification steps. The respective synthetic procedures and reaction products are discussed in detail. Three new polyol structures were incorporated into polyurethane photopolymers and UV-cured in a UV/NIR-rheology setup. Furthermore, we exemplarily describe the preparation of linear and crosslinked polyhydroxyurethanes (PHUs) via thiol-ene polyaddition as alternative synthesis method compared to the frequently applied aminolysis of cyclic carbonates, maintaining an isocyanate and phosgene free synthetic route. This approach enables the photoinduced, fast curing of polyhydroxyurethane systems.

* This section is based on the publication manuscript “*Vinyl Ether Functional Polyols as Building Blocks for UV-Curable Polyurethanes and Isocyanate-Free Polyhydroxyurethanes*” by Stefan Kirschbaum, Katharina Landfester and Andreas Taden. Publication was withheld for the submission of the patent “*Herstellung oder Härtung von Polymeren mittels Thiol-En Polyadditionsreaktionen*“, filed on 11.11.2015, filing no. EP 15194064.0, internal no. PT033463.

4.2.1 Motivation

As already discussed, photopolymers are important technology enablers, which seem to enjoy ever-growing interest. In Chapter 4.1, we introduced vinyl ether functionalized polyurethanes (VEPUs) as a novel class of photopolymers with unique curing capabilities. They are prepared from vinyl ether functional diol building blocks (VEOHs) in a polyaddition reaction with isocyanates. Consequently, VEOHs constitute crucial key components for this new class of photopolymers and accordingly, there is a strong need for efficient and scalable synthesis methods towards VEOHs to completely exploit the potential of VEPUs. The previously reported vinyl ether functional diol was obtained through the addition of sodium 4-(vinylloxy) butanolate to 1,4-butanediol diglycidyl ether in a technically difficult procedure that involves formation of an alkoxide in an excess of 4-(vinylloxy)-1-butanol, neutralization of the reaction product, elution of the resulting salt load and vacuum distillation of residual 4-(vinylloxy)-1-butanol.¹⁷⁵ The synthesis is depicted in Figure 4.11. Upon ring-opening of the epoxide the product is generated as an alkoxide, and depending on the reaction procedure further epoxy units may be added and yield oligomeric side-products with increased polyol functionality. For most applications the formation of these oligomers is unfavorable, as they potentially cause branching or crosslinking of subsequently synthesized polyurethane prepolymers.

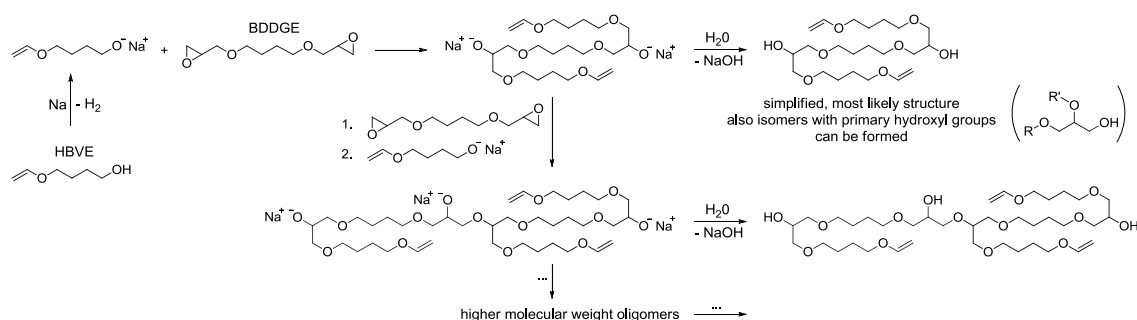


Figure 4.11. Synthesis of a vinyl ether functional polyol via ring-opening addition of an alkoxide to a multifunctional epoxide. The generation and structure of oligomeric by-products and isomers is indicated.

To obtain a more defined product structure in a straightforward synthetic procedure we herein introduce the synthesis of VEOHs based on the ring-opening reaction of cyclic carbonates with amines. The increased reactivity graduation of primary amines over hydroxyl groups is expected to suppress the formation of oligomers. Furthermore, the

use of symmetric six-membered cyclic carbonates allows the preparation of a uniform product structure that comprises solely of one constitutional isomer characterized by sterically favorable primary hydroxyl groups. The technical effort of this new synthetic approach is much lower and circumvents difficult purification procedures like salt elution or vacuum distillation. Furthermore, the respective polyol structures already contain urethane moieties, which can contribute to the final product properties in a beneficial way and allow to reduce the isocyanate quantity required to obtain the desired urethane group content of the VEPU.

Finally, the vinyl ether functionality is highly suited for thiol-ene “*click*” chemistry, which enables an additional set of modification and polymerization possibilities. The high reactivity of vinyl ether in thiol-ene reactions is related to the electron-rich double bond and the reluctance of radical homopolymerization results in a high selectivity.⁵⁷ Therefore, VEOHs can also serve as building blocks in the radical mediated thiol-ene addition reactions that yield polyhydroxyurethanes (PHUs) via an isocyanate and phosgene free synthetic route. This chemistry is of particular interest as a novel route towards PHUs, and might overcome molecular weight limitations of “*classical*” PHU synthesis based on the aminolysis of cyclic carbonates.¹¹³

In this section we describe the synthesis of novel, urethane group containing VEOHs and their incorporation into VEPUs for the sake of photocuring. Furthermore, the VEOHs are applied in polyaddition reactions with polythiols to introduce a conceptually different synthetic approach towards environmentally friendly PHUs.

4.2.2 Synthesis of Urethane Containing VEOHs

Three vinyl ether functional polyols (P1 - P3) were prepared following different synthetic pathways (see Figure 4.12) to expand the structural variety of VEOHs and access differentiated material characteristics.

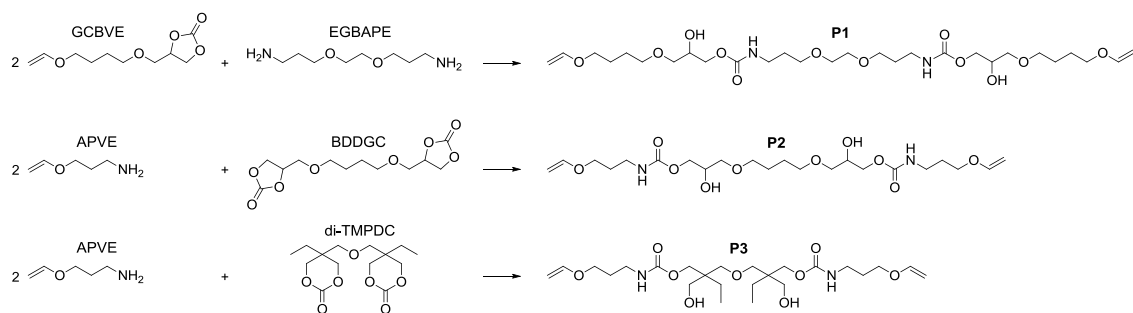


Figure 4.12. Synthesis of the vinyl ether functional polyols P1 - P3 via ring-opening addition of amines to cyclic carbonates. For P1 and P2 only the most likely isomeric structures are shown, other isomeric structures are described and quantified in Chapter 5.2.17. P3 comprises solely of one constitutional isomer.

P1 was synthesized from ethylene glycol bis(3-aminopropyl) ether (EGBAPE), an abundant and commercially available primary diamine, and 4-glycidylcarbonate butyl vinyl ether (GCBVE), which is accessible through epoxidation of 4-hydroxybutyl vinyl ether (HBVE) with epichlorohydrin and subsequent CO₂ insertion. The general reaction pathway is well-established and technically feasible as several commercial epoxy resins are synthesized following the same epoxidation route on an annual 10⁶ t scale.¹⁷⁶ The CO₂ insertion is a very selective, straightforward and scalable synthesis with high yields. The desire for cyclic carbonates as raw materials for the phosgene and isocyanate free synthesis of polyhydroxyurethanes (PHUs) as emerging alternative for common polyurethane in combination with carbon footprint efforts are currently seen as strong drivers for the industrialization of this process.^{82, 113} The synthetic pathway starting from a difunctional amine and a vinyl ether functional carbonate yields a polyol with urethane groups located between the two hydroxyl groups and consequently along the backbone of a subsequent polyurethane (see Figure 4.13).

In contrast, the polyols P2 and P3 are synthesized from 3-aminopropyl vinyl ether (APVE) as amine functional vinyl ether source and a difunctional cyclic carbonate. Consequently, the urethane groups are located outside of the diol backbone and subsequent polyurethanes have urethane groups incorporated within the vinyl ether functional side-chains. Another structural difference is that a symmetric six-membered cyclic carbonate is used in the synthesis of P3, which results in only one constitutional isomer, exclusively containing sterically more favorable, primary hydroxyl groups, independent from the direction of the ring-opening reaction. Furthermore, six-membered cyclic carbonates show a significantly increased reactivity towards

amines over its five-membered analogs.¹¹⁶ However, it needs to be mentioned that two chiral centers in one molecule result in different enantiomers and diastereomers. The polyol structures including their different types of isomers were characterized via ¹H NMR and ¹³C NMR spectroscopy and HPLC analysis, which are discussed in Chapter 5.2.

4.2.3 Synthesis and UV-Curing of Novel VEPUs

The polyols P1 - P3 were reacted with HDI and terminated with methanol each to yield polyurethanes with a number average molecular weight of about $M_n = 2000$ g/mol. The molecular weight was verified via IR spectroscopic end group analysis. 3 wt% of 10-[1,1'-biphenyl]-4-yl-2-(1-methylethyl)-9-oxo-9H-thioxanthenium hexafluorophosphate were added as photoinitiator. The resulting polyurethanes PU1 - PU3 were subjected to UV/NIR-rheology. The corresponding repeating units of the polyurethanes are depicted in Figure 4.13. Depending on the molecular weight of the polyol segments the average degree of polymerization is about $n = 2.5 - 3$ resulting in an average vinyl ether functionality of $f = 5 - 6$, which is of certainly high enough to obtain crosslinked materials upon photocuring.

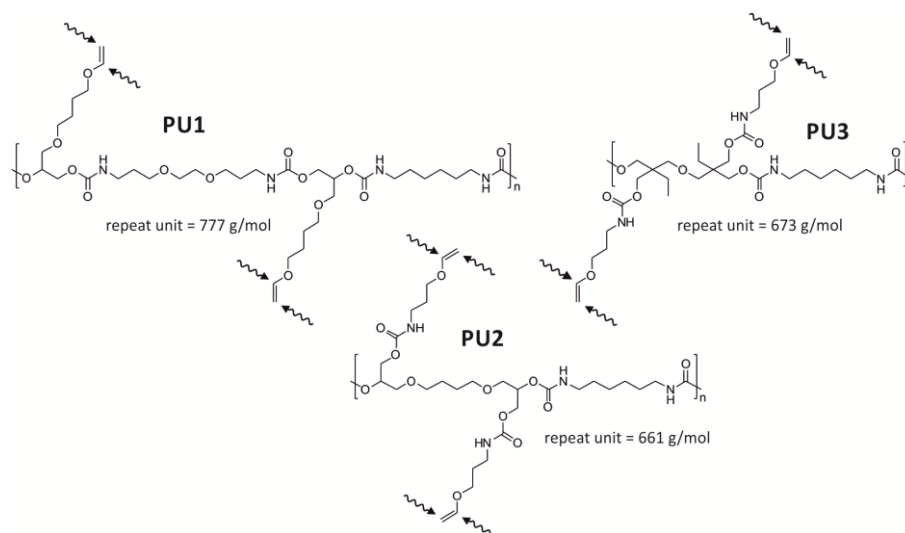


Figure 4.13. Repeating units of the vinyl ether functionalized polyurethanes PU1 – PU3.

Possible crosslinking points are indicated by the curved arrows to provide an impression of the cured network structure.

Figure 4.14 shows a plot of the storage moduli and the reaction progress on a molecular scale, determined via integration of the vinyl ether absorption band in the NIR spectrum

over the time. The curing reaction was performed at 75 °C, which is above the final glass transition temperatures of the cured materials (see Figure 4.15) to avoid stagnation of the reactions caused by vitrification and trapped cationic species.

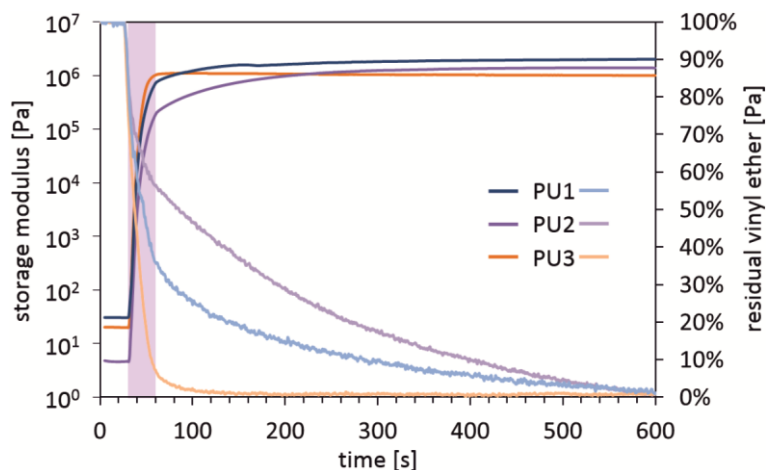


Figure 4.14. Mechanical and molecular curing profiles of the polyurethanes PU1 - PU3 upon UV-irradiation. The purple background indicates the irradiation period of 30 s.

All curves show a fast evolution of the sample moduli upon irradiation and similarly high plateau moduli of about 10^6 Pa at 75 °C. However, it was observed that PU1 and PU2 polymerize significantly slower in terms of conversion. It can be speculated that the reduced reaction rates originate from a reduced concentration of propagating species, caused by basic amine groups in the sample, which neutralize initiating cations. Of course, residual primary amine groups are highly unlikely after polyurethane synthesis, but low quantities of residual epoxides (only present in GCBVE and BDDGC) can generate secondary and tertiary amines during the synthesis of P1 and P2. Especially, traces of tertiary amines are expected to remain in the vinyl ether functional polyurethanes PU1 and PU2, as they are not reactive towards isocyanates and consequently inhibit polymerization or lead to reduced reaction kinetics. In contrast, the six-membered cyclic carbonate used for the synthesis of P3 did not involve an epoxide as intermediate so that PU3 is completely free of tertiary amines. In fact, we observed that PU3 in contrast to PU1 and PU2 efficiently polymerizes even at lower photoinitiator concentrations.

Subsequent to the curing reaction, the samples were subjected to a temperature ramp of 2 °C/min in the rheometer setup to investigate their thermomechanical properties, for example the glass transition temperature (T_g) and the related mechanical moduli

dependency of the cured materials. The mechanical moduli and the loss factor are plotted dependent on the temperature in Figure 4.15.

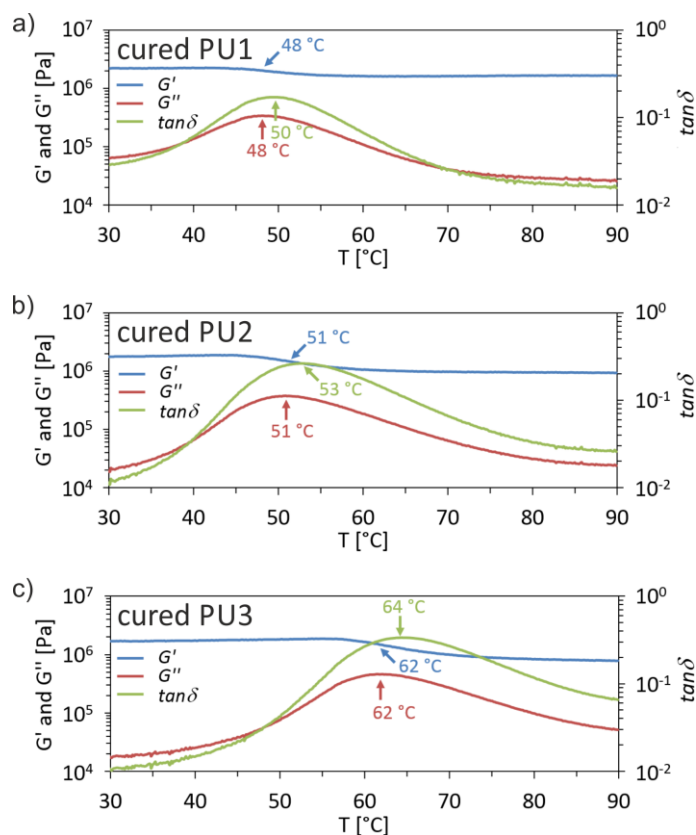


Figure 4.15. Thermal properties of the cured polyurethanes PU1 - PU3.

The small decline of the storage modulus (G') and the high plateau value of about 10^6 Pa is typical for highly crosslinked materials and signifies a tight network structure, which can bear high mechanical loads.¹⁷⁷ Additionally a maximum in the loss modulus, curve (G'') indicates the glass transition. Consequently, glass transition temperatures of 48 °C, 51 °C and 62 °C were determined for the cured polyurethanes PU1, PU2 and PU3 via the G'' -peak method, according to ASTM D4065. The glass transition temperatures inversely correlate with the chain length of flexible structures. However, the hexyl chain from the HDI structure largely contributes to the overall chain mobility and hence distinct differences may only be obtained if more rigid isocyanates such as IPDI were used.

4.2.4 Polyhydroxyurethanes via Thiol-Ene Addition of Urethane Containing VEOHs

The primary structure of the presented VEOHs, comprising two vinyl ether groups as well as two hydroxyurethane moieties renders them perfectly suitable for the synthesis of linear and crosslinked polyhydroxyurethanes (PHUs) via thiol-ene addition with di- and multifunctional thiols. Currently, the most pursued approach towards sustainable polyurethanes that does not involve highly reactive and toxic phosgene or isocyanates as intermediates, is the preparation of PHUs through aminolysis of cyclic carbonates.¹¹¹ However, one drawback of the corresponding PHUs is their comparatively low molecular weight, as a result of the second order aminolysis kinetics with respect to both, the amine and the cyclic carbonate,^{110, 113} as well as the generally low reactivity of higher molecular weight amines created during the initial stages of the polyaddition reaction.^{99, 119}

The utilization of thiol-ene polyaddition of strictly difunctional vinyl ether compounds with dithiols can overcome this limitation and potentially lead to higher molecular weight polymers compared to the aminolysis of cyclic carbonates. Therefore, P3 and dimercapto-1,8-dioxa-3,6-octane (DMDO) were mixed in approximately equimolar amounts for a proof of concept. Figure 4.16 shows the reaction equation and the corresponding size exclusion chromatograms.

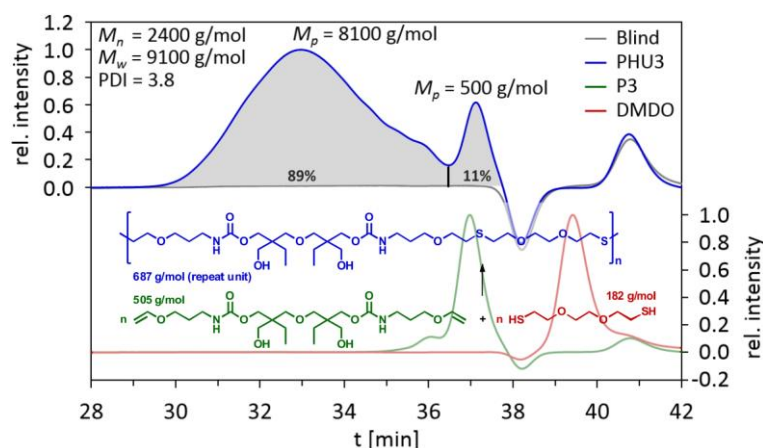


Figure 4.16. SEC plots of the PHU thiol-ene polyaddition of P3 and DMDO.

The overlay clearly indicates that a polymerization takes place. The reaction product shows a broad molecular weight distribution with a peak molecular weight of

$M_p = 8050$ g/mol. The consumption of vinyl ether and thiol functional groups is also verified via IR spectroscopy (see Chapter 5.2.10). These results clearly indicate the feasibility of PHU syntheses via thiol-ene polyaddition of urethane containing VEOHs. However, residues with a similar molecular weight to P3 were observed, which with respect to the IR spectrum do not contain vinyl ether groups any more. Therefore, we assume the consumption of vinyl ether in a side-reaction, which alters the effective stoichiometry and functionality and limits the molecular weight. To obtain high molecular weight products in a linear polyaddition reaction a very precise functionality and stoichiometry of the educts is necessary and needs to be maintained throughout the reaction. However, in crosslinking reactions with higher functional thiols, the strict observance of functionality is not as relevant as for linear polymers.

Figure 4.17 shows a plot of the mechanical property evolution and the consumption of vinyl ether groups in the photoinduced, radical mediated thiol-ene addition reaction of P3 with pentaerythritoltetra(3-mercaptopropionat) (PETMP).

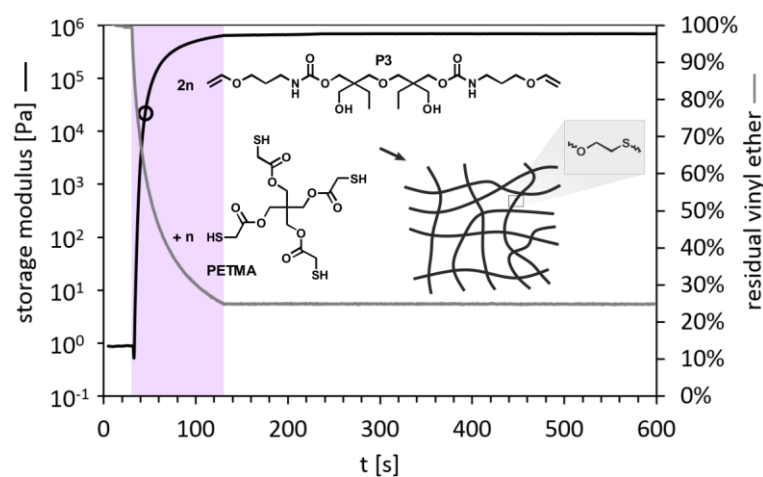


Figure 4.17. Mechanical and molecular curing profiles of the crosslinked PHU.

The purple background indicates the irradiation period of 100 s. Gelation is indicated by the hollow circle.

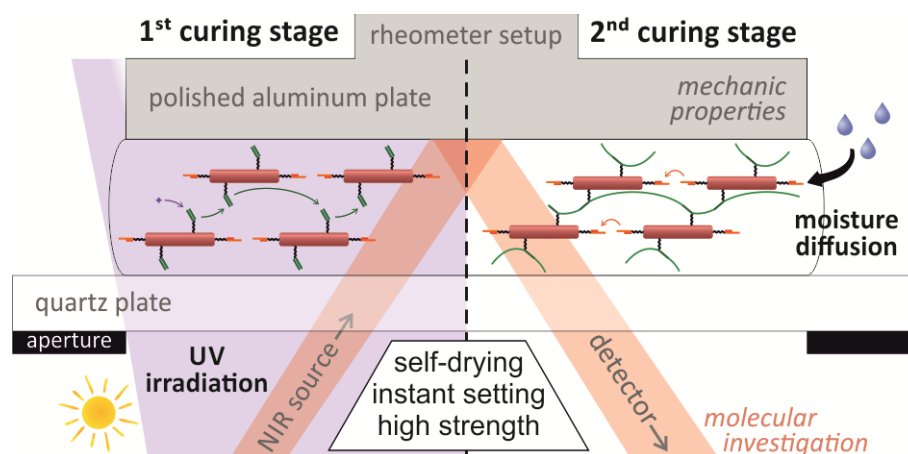
To the best of our knowledge, this reaction represents the first photoinduced synthesis of crosslinked polyhydroxyurethanes and nicely shows the benefits of the introduced thiol-ene reaction mechanism on the preparation of PHUs. First, the latent reactivity of the photoinducible thiol-ene reaction circumvents pot life issues that generally go along with crosslinking reactions. Second, after irradiation the thiol-ene mechanism leads to rapid network formation and solidification within seconds. Furthermore, it can be seen

that the cured material obtains a high modulus, which is an important prerequisite for engineering purposes.

4.2.5 Conclusion and Outlook

In summary, we have introduced an alternative synthetic route towards vinyl ether functional polyols that can be prepared in a technically facile way and inherently provide urethane moieties, which beneficially contribute to the product properties of vinyl ether polymer systems. Cyclic carbonates and amines of different ring-size and structure were utilized and the corresponding products were characterized thoroughly with respect to their structure and present isomers. Furthermore, these polyols were incorporated into polyurethanes and subjected to UV-induced cationic curing. Finally, the urethane containing vinyl ether polyols were used to prepare linear and crosslinked polyhydroxyurethanes via photoinduced, radical mediated thiol-ene addition, which represents an alternative mechanism compared to the frequently applied aminolysis of cyclic carbonates. In principle, our novel approach toward polyhydroxyurethanes can offer substantial benefits, like improved reactivity that results in drastically accelerated curing reactions or the formation of higher molecular weight species. The utilization of photoinitiation relates to storage-stable, latent reactive polyhydroxyurethane systems with triggered polymerization capability. This energy-efficient, environmental friendly, non-hazardous and fast reaction is highly desired for a variety of applications. The related material structures and properties can principally be tailored over a wide range, and the formation of a highly crosslinked, high-modulus polyhydroxyurethanes within seconds was exemplarily shown. In any case, the presented results represent a significant advancement in photopolymer chemistry and certainly should stimulate new applications and processes, including the substitution of solvent-based coatings and adhesives.

4.3 Synergistic and Sequential Dual Curing Mechanism for Vinyl Ether Functional Polyurethanes*



Polyurethanes comprising vinyl ether side-chain functionality and terminal isocyanate groups are introduced as novel dual cure materials. The vinyl ether groups are susceptible to cationic photopolymerization while the NCO-functionalities enable moisture-induced, step growing via urea formation. This dual cure chemistry is highly synergistic, because the presence of isocyanate groups ensures low levels of free nucleophiles (“*self-drying*”) and hence provides extraordinary robust conditions for cationic chain growth. Furthermore, the isocyanate functionalization can contribute to increased adhesion with various substrates. In contrast to radical photopolymer systems, photoinitiated cationic polymerization proceeds without any oxygen inhibition and continues even in the absence of light (“*dark cure*”). Thickening or setting of the material can be adjusted upon a short, initial irradiation period, while subsequent moisture-curing proceeds over several hours or days. The dual cure process was investigated spectroscopically and mechanically *via* simultaneous UV/NIR-rheology and transparent, high strength, tough materials were obtained.

* This section is based on the publication manuscript “*Synergistic and Sequential Dual Curing Mechanism for Vinyl Ether Functional Polyurethanes*” by Stefan Kirschbaum, Katharina Landfester and Andreas Taden. Publication was withheld for the submission of the patent “*Härtungsverfahren für Polyurethane*“, filed on 11.11.2015, filing no. EP 15194065.7, internal no. PT033407.

4.3.1 Motivation

Moisture-curing polyurethanes are an important class of reactive, one component materials, which are industrially applied in a wide range of applications such as coatings, adhesives and sealants.^{100, 178} Moisture-curability can easily be provided by terminal isocyanate groups of polyurethane prepolymers, which react with ambient humidity to generate primary amines upon cleavage of carbon dioxide. These amines are highly reactive towards residual isocyanate groups and preferably react further to form urea bonds (see Figure 4.18).⁹⁹ High molecular weight or crosslinked structures formed in these curing reactions can provide excellent mechanical properties including high strength and modulus in conjunction with flexibility and toughness, due to micro phase separation in soft and hard segments. Frequently, these materials are described as polyurethanes, although they may contain significant amounts of urea groups. However, long curing times are a major limitation of moisture-curable polyurethanes resulting in weak adhesion, mechanical strength and dimensional stability over hours or days, until a certain degree of curing is achieved. To overcome this drawback we present a novel dual cure mechanism characterized by an almost immediate thickening or setting of the material upon irradiation *via* cationic polymerization of vinyl ether side-chains, followed by a protracted moisture-curing reaction.

The concepts of dual cure refers to the combination of two different curing mechanisms at different stages.¹³ In contrast, hybrid cure describes two different curing mechanisms proceeding simultaneously. Several dual and hybrid cure systems involving radiation curing have been described. Most prominent examples are the combination of photoinduced radical and cationic polymerization^{179, 180} or radical photopolymerization of acrylates combined with thermally or moisture-curing systems.¹⁸¹⁻¹⁸⁴ However, to the best of our knowledge no system combining rapid photoinduced cationic polymerization of vinyl ethers with subsequent moisture-curing of isocyanates has been described.

In Chapter 4.1, we introduced the cationic curing reaction of vinyl ether side-chain functionalized polyurethanes (VEPUs). Moreover, a variety of different vinyl ether polyol structures (VEOHs), which can be utilized in standard polyurethane syntheses has been reported in Chapter 4.2. The modular synthetic approach of polyurethane

chemistry enables a broad flexibility in polymer design and the facile adjustment of desired material properties. Consequently, VEOHs can easily be integrated in isocyanate terminated polyurethane prepolymers and were already prepared as intermediates in Chapter 4.1.2. The cationic polymerizations are generally sensitive towards various nucleophilic functional groups, whereas exemplarily the presence of water causes hydrolysis of carbenium ion intermediates and hence affect or inhibit the polymerization. For that reason, most cationic polymerization reactions require thorough drying procedures. Therefore, the combination of reactive isocyanate groups, which can be seen as intrinsic moisture-scavenger, and vinyl ether groups in one system is highly beneficial and represents a “*self-drying*” reaction environment for the cationic polymerization. In this respect, the dual cure system ensures and maintains an adequately dry reaction medium over a long time. Moreover, isocyanates are highly reactive towards a number of other nucleophiles like alcohols, thiols or amines. These groups are known to interfere with the cationic polymerization of vinyl ether through transfer reactions or neutralization of the strongly acidic initiators. The isocyanate groups rapidly consume such nucleophiles and yield less nucleophilic carbonyl structures like urethanes, which do not hinder the cationic vinyl ether polymerization.⁵⁰ Furthermore, if these groups are present on the substrate surface, the resulting covalent attachment can even improve the adhesion. Figure 4.18 illustrates the sequential dual curing mechanism as well as the monitoring techniques that are employed to simultaneously record changes in the viscoelastic properties (rheometry) and functional group conversions (NIR), which occur during both curing stages.

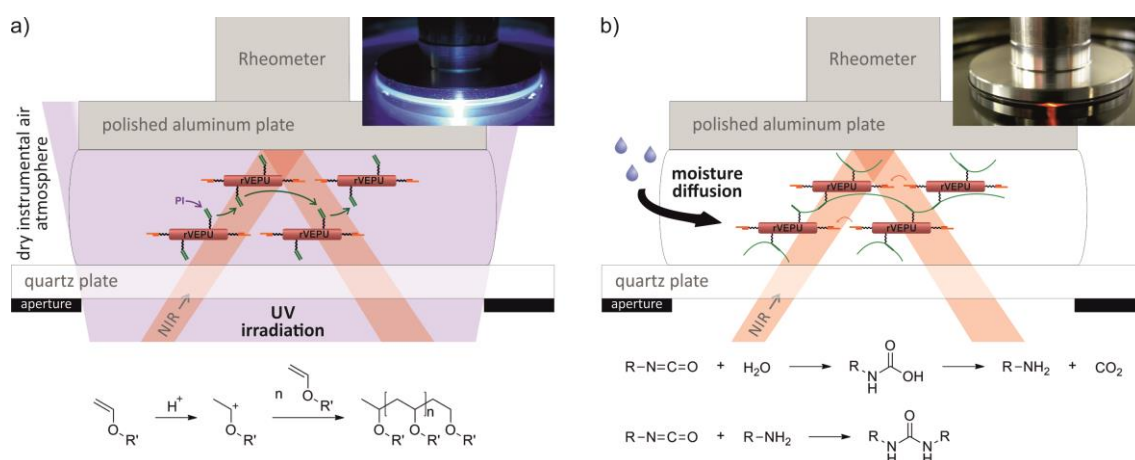


Figure 4.18. Sequential dual curing mechanism.

a) First stage: light induced cationic curing of vinyl ether side-chains. b) Second stage: moisture-curing of terminal isocyanate moieties.

4.3.2 Synthesis and Curing of Isocyanate Terminated VEPUs

A rVEPU resin with a theoretical molecular weight of $M_n = 5000$ g/mol and an average vinyl ether functionality of 1.94 was synthesized from a vinyl ether functional polyol (VEOH), a polypropylene glycol (PPG) and hexamethylene diisocyanate (HDI) as depicted in Figure 4.19 and formulated with 1 wt% of 4,4'-dimethyl-diphenyliodonium hexafluorophosphate as photoacid generator (for detail see Chapter 5.3.3).

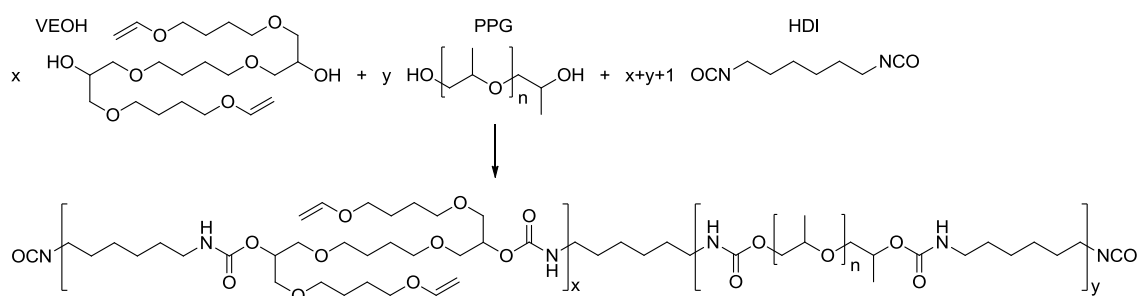


Figure 4.19. Synthesis of the rVEPU.

The sequential cationic and moisture-curing of the rVEPU resin was then monitored in a UV/NIR-rheology setup upon photoinduced curing at 60 °C. The sample was irradiated for 50 s under instrumental air atmosphere to initiate the cationic photopolymerization that continues in the dark. After 1800 s (30 min) the rheometer covering was opened to allow the diffusion of ambient moisture into the sample. Figure 4.20 displays the complex viscosity (η^*) and the loss factor ($\tan\delta$) of the sample over time.

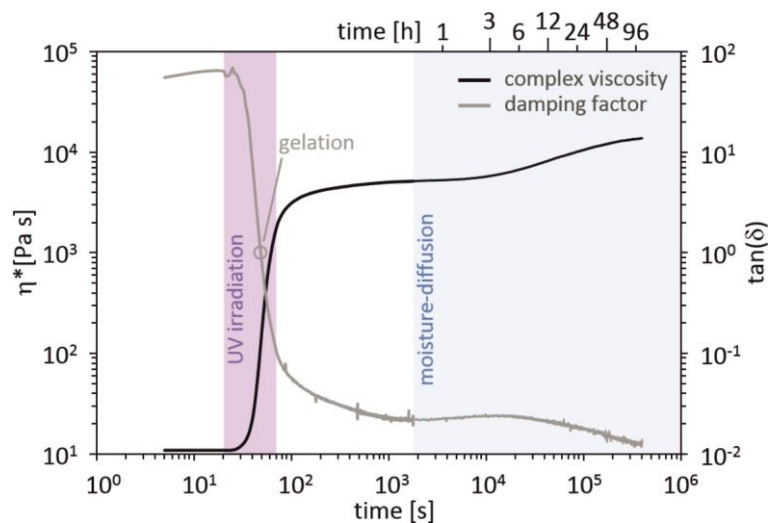


Figure 4.20. Rheological plot of the sequentially dual curing rVEPU at 60 °C.

The reaction temperature of 60 °C was applied to speed up both the cationic polymerization and the moisture-curing reaction and to allow an improved differentiation in the rheological plot. The time scale is plotted logarithmically to illustrate both curing mechanisms in one diagram. The cationic curing reaction upon UV-irradiation leads to an increase of the complex viscosity over more than two orders of magnitude, despite the low vinyl ether functionality and causes gelation of the sample ($\tan\delta = 1$) within 29 s. The temporary plateau of the complex viscosity curve at about 10^3 s indicates the ending of this reaction. Accordingly, the slow, subsequent increase of the complex viscosity can be attributed to the moisture-curing reaction of isocyanate groups. The long curing time was expected and is in the same order as reported earlier for moisture-curing polyurethanes based on aliphatic isocyanates.¹⁷⁸ However, the moisture-curing process may even be retarded by the small accessible surface area and the relatively long diffusion path length of moisture from the edges of the film to the inside. It should be noted that although the viscosity increase upon moisture-curing appears minor on the logarithmic scale, it has a strong effect on the final material properties. For a certain time after irradiation the film can be readily removed from the rheometer setup but is weak and friable and does not adhere well to either the quartz or aluminum surfaces of the rheometer plates. We attribute this behavior to poor cohesion originating from the low crosslinking density and weak intermolecular interactions. In contrast, after a few days of humidity curing, the film was relatively strong and difficult to remove. When a sufficient force was applied, failure occurred at the interfaces and the detached film exhibited a drastically improved abrasion resistance as a consequence of the increased crosslinking density and strong intermolecular hydrogen bond interactions arising from the increased urea content.

Complementary to the mechanical evaluation, Figure 4.21 shows the simultaneously recorded NIR spectroscopic information.

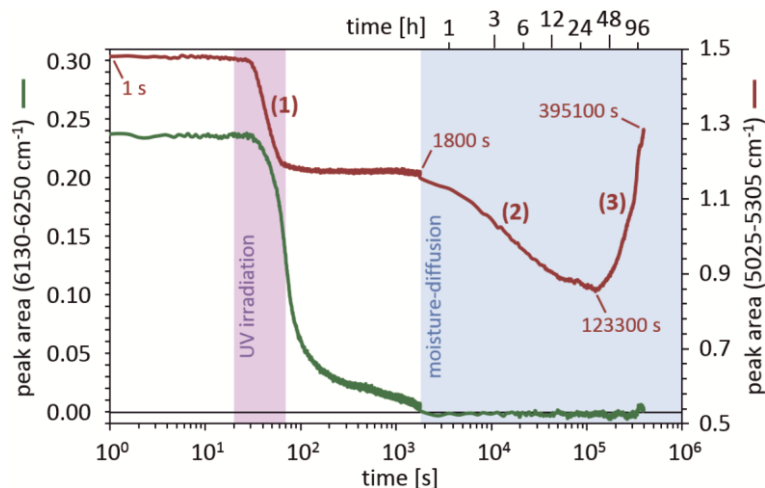


Figure 4.21. Selected NIR absorption peak areas of the sequentially dual curing rVEPU over the reaction time.

The green line indicates the peak area in the range of 6130 - 6250 cm^{-1} , which is assigned to the first overtone of the C-H-stretching vibration and inversely correlates to the conversion of vinyl ether functional groups. In accordance with the rheological plot, the vinyl ether conversion indicates a short inhibition period followed by a fast reaction to high conversion and a slower dark curing process to complete conversion. The red line represents the peak area in the range of 5025 - 5305 cm^{-1} . The interpretation is more difficult and hence the curve was divided in 3 sections for the discussion. The small isocyanate absorption band at 5215 cm^{-1} appears in an uneven spectral region that is shown in Figure 4.22 and is therefore hard to quantify in an absolute manner.

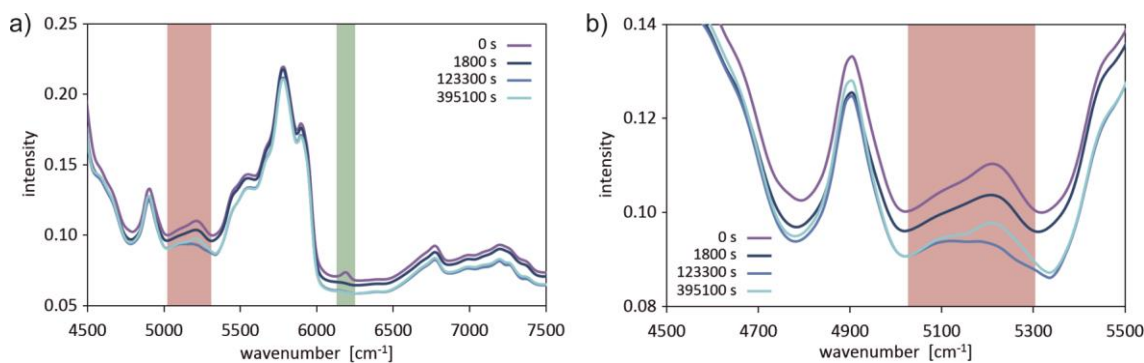


Figure 4.22. NIR spectra of the rVEPU in different curing stages.

a) Spectral range of 4500 - 7500 cm^{-1} . b) Enlarged spectral region of 4500 - 5500 cm^{-1} .

Moreover, besides the isocyanate combination band a broad and very intense (several times more intense) moisture absorption band appears in the same spectral region. Reference spectra are shown in Figure 4.23.

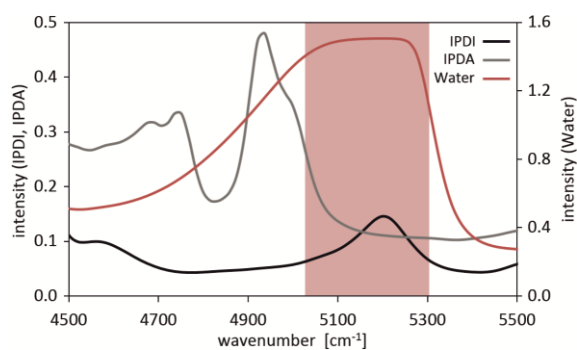


Figure 4.23. NIR spectra of IPDI, isophorone diamine (IPDA) and water.

Unfortunately, the water absorption is very intense and overlaps with the isocyanate absorption band. Therefore, even traces of water in the sample show a distinct influence on the peak integration values.

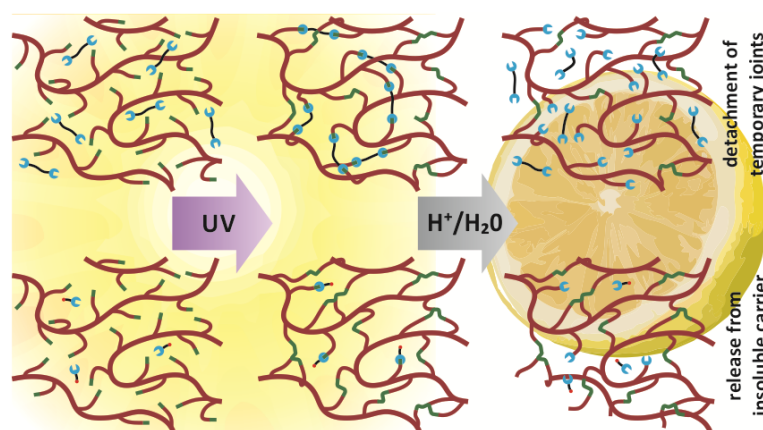
In section (1) of Figure 4.21, the peak area of the red curve decreases upon UV-irradiation. However, this decrease is much smaller than that of the vinyl ether curing reaction and can be attributed to water consumption through hydrolysis of the protonated vinyl ether cations. Similar observations have already been reported in the literature upon cationic polymerization of low molecular weight vinyl ethers¹⁸⁵ and cycloaliphatic epoxides.¹⁵⁰ The observation of water in the hydrophilic polyurethane sample, after exposure to humid atmosphere or absorbed water from the glass surface, was not expected due to the presence of isocyanates. However, the moisture level observed, despite the presence of isocyanate groups, seems to be very low, and does not lead to significant curing inhibition, although the fraction of vinyl ether in the system is very low. Furthermore, it can be speculated that more reactive aromatic isocyanates would be more effective in moisture-scavenging, especially at low temperatures. After the cationic polymerization of vinyl ether groups was completed, the sample appeared to be completely dry and moisture was allowed to diffuse into the sample. Shortly thereafter, the expected consumption of isocyanate took place, as shown in section (2) of the reaction profile. After several hours the monitored peak area shows a minimum, when the residual isocyanate concentration was significantly reduced and further diffusion of water into the polymer network becomes faster than its consumption. This situation explains the course of the graph in section (3), where the peak area increases, while at the same time the complex viscosity indicates the slowdown of the moisture-curing reaction.

4.3.3 Conclusion and Outlook

The presented dual curing concept based on cationic polymerization and moisture-curing is expected to be easily transferred to other moisture-curable functional groups such as aromatic isocyanates or silanes. The increased reactivity of such groups could further reduce the maximum dissolved water concentration before photocuring and increase the rate of the later moisture-curing reaction. Thus, these improved systems will be a focus of future investigations.

In summary, we have introduced a vinyl ether functional, isocyanate terminated prepolymer that may be cured by two independent mechanisms, which complement each other in a synergistic manner. The system may be considered as a prototype for a new class of dual cure materials and represents an important extension to conventional moisture-curing polyurethanes or photocuring polymers. These new systems will enable various new processes and applications. Moisture-curable rVEPU of low viscosity can be synthesized and easily applied. After rapid, radiation induced, cationic polymerization of vinyl ether groups, the rVEPUs resins yield highly viscous or gelled materials, which hold their shape, even when difficult geometries or fast moving substrates are involved. They may be joined subsequently, before extensive moisture diffusion results in the complete setting of the material. In contrast to other photocuring polymers, low application viscosities can be obtained by shifting the molecular weight build-up and controlling the evolution of strong intermolecular interactions after the photocuring reaction. Thus, low molecular weight prepolymers with reduced fractions of polar groups can now be applied in processes that require low viscous materials, such as inkjet printing without causing disadvantageous product properties. Additionally, the isocyanate groups inherently provide an almost nucleophile free, *self-drying* reaction medium. Correspondingly, low concentrations of photoinitiator can be applied in a robust and efficient photoinitiation and polymerization process. Moreover, the reactive isocyanate groups can increase the adhesion to various substrates or between multilayers through covalent bonding and significantly contribute to the final mechanical properties, which are adjustable through the modular prepolymer synthesis.

4.4 Cationic Phototransfer Polymerization: pH-Responsive Acetal-Based Polymer Networks*



Vinyl ether functional polyurethanes (VEPUs) were combined with mono- or difunctional alcohols and subjected to photoinduced, cationic polymerization. The hydroxyl compounds become covalently incorporated into the resulting polymer network via formation of acetal linkages in a nucleophilic addition reaction followed by proton transfer. The resulting curing mechanism is an interplay between cationic polymerization and polyaddition, and is hence introduced and discussed as cationic phototransfer polymerization. Highly adjustable acetal-containing polymer networks were obtained, which enable pH-responsive degradation and controlled release of the hydroxyl components. After acetal hydrolysis the materials remain crosslinked, which is expected to facilitate different applications, ranging from insoluble drug carriers to engineering materials with debonding on command properties. UV/NIR-rheology was utilized to evaluate the curing reaction and mechanical property dependencies. ¹³C MAS NMR spectroscopy and extractive GC analysis were used to verify the formation of acetal groups and investigate the release efficiency and kinetics under different pH-conditions.

* This section is based on the publication manuscript “Cationic Phototransfer Polymerization: pH-Responsive Acetal-Based Polymer Networks” by Stefan Kirschbaum, Robert Graf, Katharina Landfester and Andreas Taden. Publication is withheld for the submission of the patent “Kationische Phototransferpolymerisation“, internal no. PT033452.

4.4.1 Motivation

Acetals are well-established protective groups in organic chemistry for hydroxyl moieties. One particular synthetic method is the addition reaction with vinyl ether under dry, acidic conditions. Being stable under neutral and basic conditions, the acetal functionality becomes easily hydrolyzed in aqueous, acidic media for deprotection.¹⁸⁶ Because of the facile and convenient chemistry, acetal groups have also been integrated into polymers via polyaddition of divinyl ether and dialcohols^{187, 188} or by polyaddition of hydroxyl functional vinyl ethers^{189, 190} to obtain pH-responsive materials with improved degradability. Similar to low molecular weight protective groups the corresponding polyacetals are stable over a wide pH-range from alkaline to mild acidic media, and readily can be hydrolytically cleaved under stronger acidic conditions. Based on the same principle more complex polymers with acetal structures were designed. Vinyl ether side-chain functionalized polyethers⁸¹ and polyphosphoesters¹⁷⁰ were modified with hydroxyl functional molecules and reported as pH-sensitive drug carriers for targeted release. Furthermore, acetal units were incorporated into polyethers to provide defined, cleavable points^{191, 192} and to improve biodegradability.¹⁹³

Vinyl ethers enable this facile chemistry due to their extraordinary electron-rich double bond. For the same reason they are also highly reactive in cationic polymerization. They can be protonated under strong acidic conditions and the corresponding cationic centers propagate in a chain growth reaction in the absence of water.^{46, 53} With respect to the technical applicability of cationic polymerization the development of onium salt based photoacidgenerators (PAGs) by Crivello et al.^{10, 11, 164} was a milestone achievement. The respective photoinitiators can be dissolved in a monomer mixture without premature gelation and long shelf life, but upon UV-exposure readily create so-called “*super acids*” as highly active species for cationic polymerization. However, cationic polymerization is highly sensitive towards nucleophilic functional groups. Hydroxyl groups act as transfer agents via addition to the propagating carbocation and regeneration of the initiating proton.¹⁹⁴ The rate of this transfer reaction is very fast and almost exclusive acetal formation has been described in the literature if a stoichiometric amount of alcohol is present.¹⁹⁰ The reaction scheme for cationic vinyl ether polymerization as well as for the formation and hydrolysis of acetal groups under acidic conditions is shown in Figure 4.24.

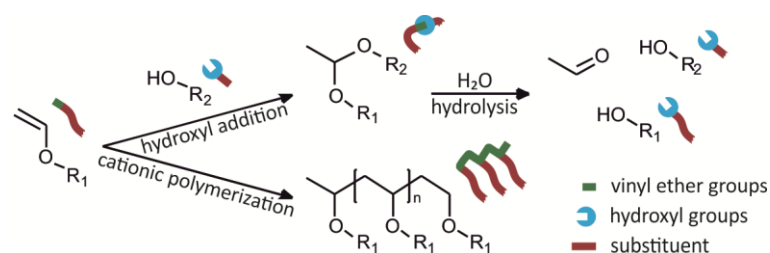


Figure 4.24. Reaction scheme for vinyl ethers and alcohols under strong acidic conditions.

In the presence of hydroxyl groups, acetal units are created, which later on can be easily hydrolyzed. In absence of nucleophilic reagents cationic polymerization takes place.

A cationic polymerization of vinyl ether that is largely affected by transfer reactions significantly differs from pure chain growing polymerizations. A good example for such reactions is the thiol-ene addition, where consecutive thiol addition to an unsaturated double bond and radical transfer reactions take place. Consequently, an ideal stoichiometric thiol-ene polymerization shows characteristics of a step growing polyaddition reaction rather than a radical polymerization and results in more uniform network structures.⁵⁷ Furthermore, mixed-mode reaction that involve both, radical homopolymerization and thiol-ene addition are of particular interest as the curing profile and product properties can be tailored by shifting the relative contributions of each mechanism. This concept is expected to be transferable to the cationic phototransfer polymerization comprising of cationic homopolymerization and the addition reaction of vinyl ethers and alcohols under cationic conditions.

In Chapter 4.1, we reported the synthesis of VEPUs as novel class of photopolymers. Inspired by afore mentioned work, this chapter deals with the introduction of transfer reactions to cationic curing of VEPUs, to alter the resulting network structure via addition of alcohols. The corresponding cationic phototransfer polymerization yields flexibilized products, which enable partial degradation via selective hydrolysis. The improved degradability is important in terms of environmental cautiousness, and can furthermore be utilized to intentionally release active ingredients or to provide a debonding on demand mechanism for temporary joint.

4.4.2 Mechanism of Cationic Phototransfer Polymerization

Curing reactions were performed using different stoichiometries and functionalities. Sub-stoichiometric amounts of hydroxyl groups are preferred to allow cationic chain

propagation and provide polymer networks that remain solid after hydrolysis. Mechanistically, a polymer network becomes formed via an interplay between cationic polymerization and polyaddition as schematically depicted in Figure 4.25.

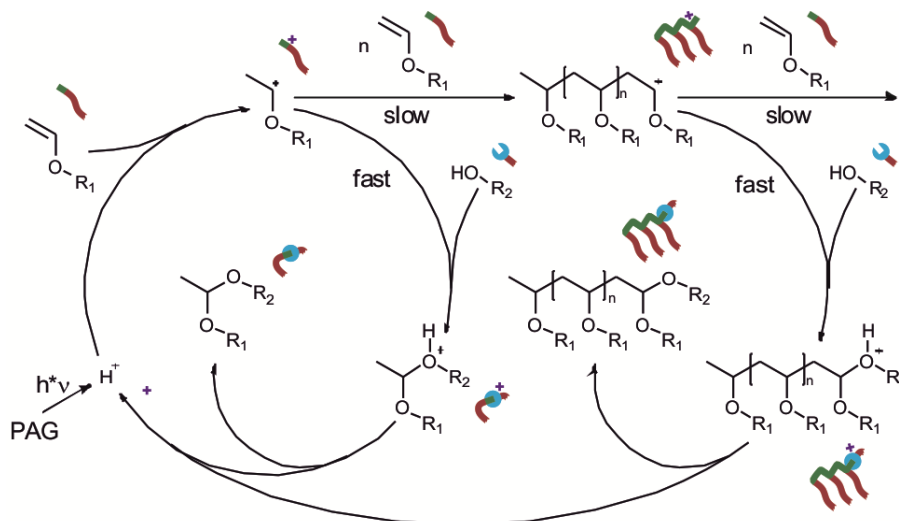


Figure 4.25. Schematic representation of the cationic phototransfer polymerization of vinyl ethers in the presence of alcohol.

As described in Chapter 4.1.2, the applied VEPUs have a high vinyl ether functionality ($f \approx 16.5$) and densely crosslink upon cationic polymerization. Generally, an increasing contribution of transfer reactions decreases the poly(vinyl ether) chain length and hence the crosslinking density. Furthermore, the functionality of the hydroxyl components has a tremendous influence on the cured network structure and its degradation behavior. Monofunctional alcohols lead to significantly decreased network densities and materials with comparably low mechanical modulus, while multifunctional alcohols in contrast lead to compensatory crosslinking via acetal bridges. The corresponding acetal units are susceptible for hydrolysis under acidic conditions and can be utilized to release the hydroxyl component or further reduce the crosslinking density, mechanical modulus, and cohesive strength. Conceptually, polyfunctional alcohols are best suited for structural applications and adjustment of mechanical material properties, while monofunctional alcohols are most effective for release purposes. Both approaches are discussed separately in the following using divergent and appropriate evaluation methods. Octanediol was exemplarily applied as multifunctional hydroxyl component and undecanol was used as monofunctional alcohol.

4.4.3 Addition of Difunctional Alcohols

The crosslinking cationic phototransfer polymerization of VEPUs in the presence of a diol, and the hydrolytic degradation of the corresponding acetal bridges in the formed network are schematically depicted in Figure 4.26.

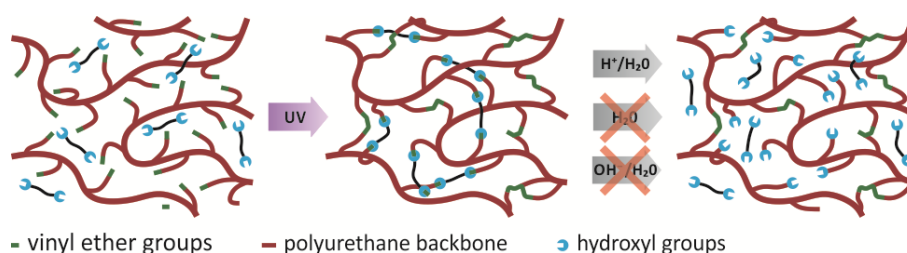


Figure 4.26. Schematic illustration of the diol-mediated cationic phototransfer polymerization of VEPUs and subsequent hydrolytic cleavage of acetal-bridges.

The cationic curing reaction of a VEPU in presence of octanediol was carried out in a UV/NIR-rheology experiment with an initial vinyl ether/hydroxyl group stoichiometry of $n_{VE}/n_{OH} = 1:0.5$. For reference purposes the cationic photocuring of VEPU was also conducted in the absence of octanediol. The mechanical storage modulus and the residual vinyl ether content were recorded simultaneously upon UV-irradiation at 25 °C and are plotted over time in Figure 4.27.

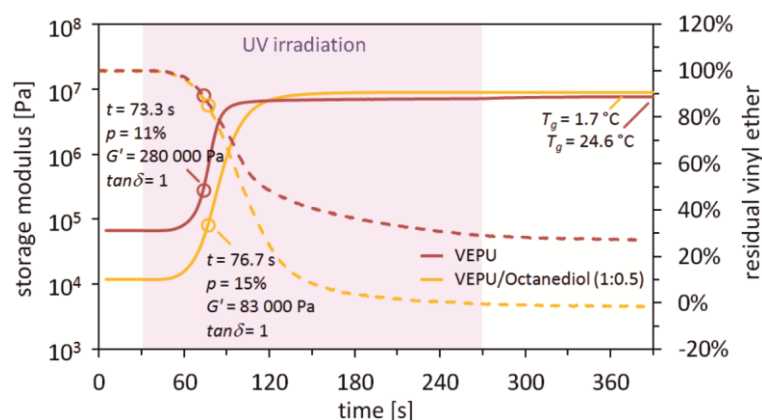


Figure 4.27. Storage moduli (dashed lines) and residual vinyl ether content (solid lines) of the curing reaction of VEPU (red) and VEPU/Octanediol (yellow) upon short UV-irradiation at 25 °C. Data were recorded simultaneously via UV/NIR-rheometry. Gelation is indicated by hollow circles. The displayed T_g s after curing were measured via DSC.

In terms of room temperature curing behavior, the addition of octanediol shows a beneficial effect. The starting viscosity becomes reduced by about one order of magnitude, what significantly enhances the molecular mobility and higher conversions

of vinyl ether can be achieved, which result in an increased mechanical modulus after curing. Theoretically, the chemical incorporation of polyol segments was expected to diminish the mechanical properties, as the newly formed acetal bridged network chain segments are comparably flexible and therefore should result in a slight plasticization. The presence of soft, less rigid linkages is confirmed by the reduced glass transition temperature, which is in congruence with the literature.¹⁹⁴ However, the increased conversion overcompensates the plasticization effect in terms of mechanical modulus as it allows an overall higher crosslinking density. To gain more understanding on the cationic phototransfer polymerization Figure 4.28 shows additional samples with varying stoichiometry of vinyl ether to hydroxyl groups ($n_{VE}/n_{OH} = 1:0, 1:0.5, 1:1$ and $1:1.5$) were prepared and cured at an elevated temperature of $70\text{ }^{\circ}\text{C}$, which is certainly above the expected T_{gs} .

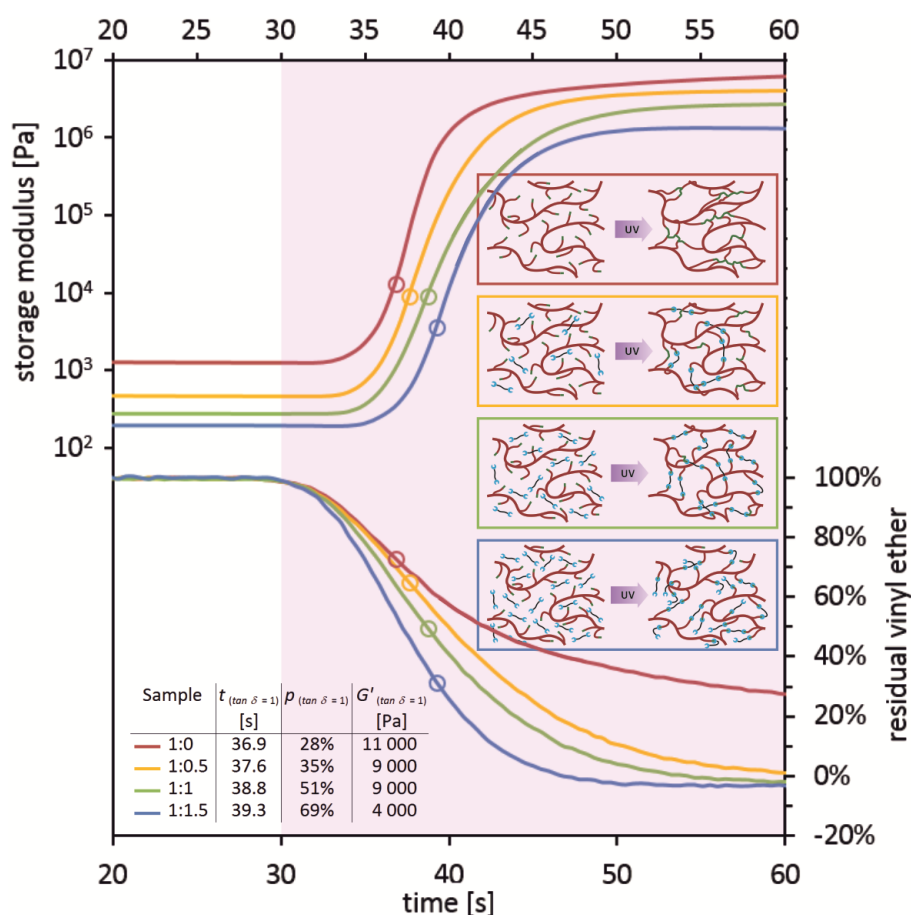


Figure 4.28. Rheological plots of the curing reaction of VEPUs and octanediol at $70\text{ }^{\circ}\text{C}$ and different stoichiometry. Gelation is indicated by hollow circles. Schematic illustrations are added to visualize the structural influence of the stoichiometry on the cured polymer network.

The elevated temperature avoids undesired vitrification of the samples and ensures an unimpeded progress of the reaction.¹⁷⁵ Consequently, the expected trend of decreasing plateau moduli with increasing octanediol content was observed. Also the conversion at sample gelation increases with the octanediol content, which is a clear indication for the chemical incorporation of the hydroxyl functional components into the cured network. If octanediol would not become covalently attached to the VEPU and simply act as physical softener, an octanediol swollen polymer gel would be obtained. In that case the conversion at gelation should be independent from the octanediol content and consistent for all samples.

Moreover, it was observed, that the cured glass/aluminum joint detaches easy and fast if it is swollen in an acidic solvent such as THF/HCl. In the following, the hydrolytic cleavage of acetal groups is investigated in more detail for the monofunctional alcohol approach, including the release efficiency and kinetics under different pH-conditions via extractive GC analysis.

4.4.4 Addition of Monofunctional Alcohols

Cationic phototransfer polymerization was carried out with a sample of VEPU and undecanol in a stoichiometry of $n_{VE}/n_{OH} = 1:0.5$. Figure 4.29 schematically depicts the curing reaction and the subsequent hydrolytic degradation of such formulations. It is indicated that the alcohol component can contain an additional, active moiety or be an active ingredient itself.

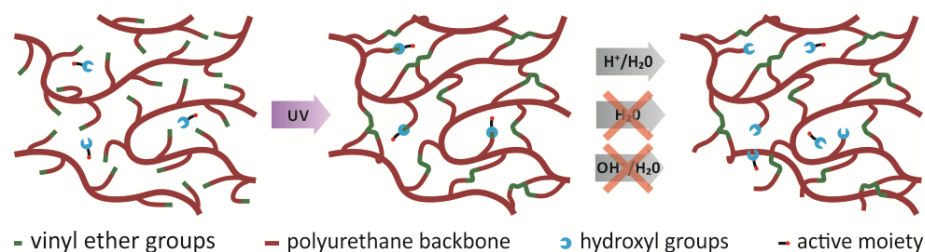


Figure 4.29. Schematic illustration of the curing and degradation reactions of the VEPU formulated with a monofunctional alcohol. The pH-sensitive hydrolytic cleavage can be utilized as controlled release mechanism for hydroxyl group containing active ingredients.

UV/NIR-rheology was performed at 25 °C to obtain cured sample films with a defined geometry (see Figure 4.30).

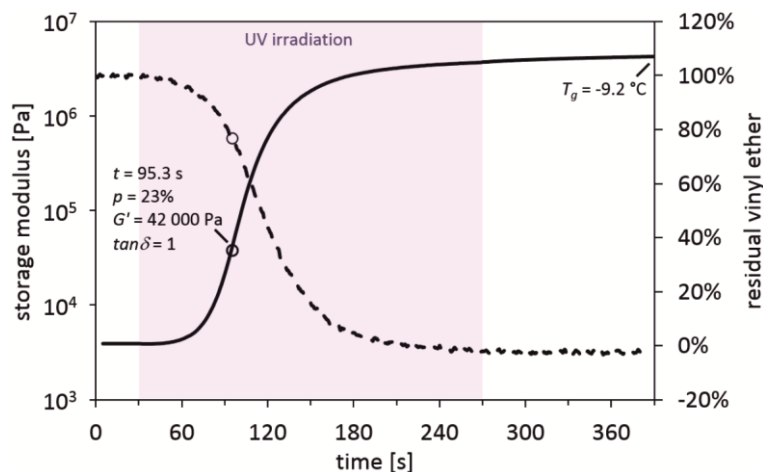


Figure 4.30. Rheological (solid line) and NIR spectroscopic plot (dashed line) of the UV-induced curing reaction of VEPU formulated with undecanol in a molar ratio of 1:0.5 (VE/OH).

As expected, the softening effect is more distinct in comparison to octanediol formulated VEPUs and results in a lower T_g and mechanical modulus. Gelation becomes more delayed at similar stoichiometry and occurs at a vinyl ether conversion of 23%. If the transfer reaction would proceed almost exclusively, the conversion at gelation must have been $> 50\%$ for the given stoichiometry. Therefore, it can be assumed that undecanol is not just incorporated at the early reaction stage but over the entire course of the reaction.

The resulting flexible but solid films were mechanically removed from the rheometer setup and treated with a small amount of triethylamine (TEA) to neutralize residual photoacid traces, which could catalyze the hydrolysis of acetal groups and distort further analytical investigations. ^{13}C magic angle spinning (MAS) NMR spectroscopy of the dried film was carried out to verify the formation of acetate linkages in the gelled polymer structure. In order to improve the quality of the ^{13}C MAS NMR spectra, cross polarization (CP) and insensitive nuclei enhanced by polarization transfer (INEPT) experiments have been performed, and the recorded spectra are shown in Figure 4.31.

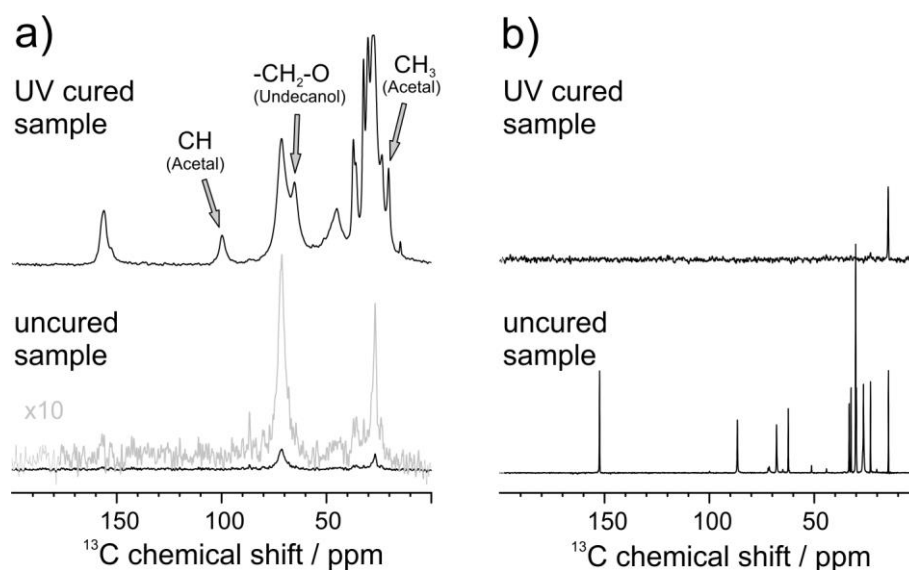


Figure 4.31. ^{13}C MAS NMR spectroscopy of the uncured and cured VEPU/undecanol (1:0.5) recorded at 10 kHz MAS spinning frequency. a) CP-MAS NMR spectra (1 ms CP contact time) and b) INEPT-MAS NMR spectra (optimized for 145 Hz ^1H - ^{13}C J-coupling).

Both applied MAS NMR techniques rely on polarization transfer from ^1H to ^{13}C sites for the signal enhancement. However, the CP-MAS measurement¹⁹⁵ using hetero-nuclear dipolar couplings for polarization transfer is sensitive only towards rigid sites of the material and discriminates peaks from highly mobile, liquid like regions. As expected, before curing the spectra of the low viscous VEPU/undecanol formulation only shows very weak signals from entangled segments of the formulation, whereas in the UV-cured sample the formation of acetal groups can be clearly observed. Furthermore, several peaks corresponding to covalently attached undecanol can be detected. For comparison some reference spectra are provided in Figure 4.32. In contrast to the CP-MAS experiment, the MAS-INEPT experiment¹⁹⁶ discriminates signals originating from rigid structures and primarily sites in mobile liquid-like environments are observed. Therefore, the INEPT-MAS spectrum of the uncured VEPU sample swollen in undecanol shows all expected VEPU signals together with the signals of undecanol, the latter being over emphasized due to its higher molecular mobility. Surprisingly, in the INEPT spectrum of the cured VEPU/undecanol a single peak can be observed, which can be assigned to the CH_3 group of undecanol. Obviously, the terminal methylene groups of the acetal-attached undecanol side-chains are sufficiently mobile to be detected via the INEPT-MAS method. It is important to note that for unattached undecanol in the swollen VEPU network all signals of undecanol would be observable in the $^{13}\text{C}\{^1\text{H}\}$ INEPT-MAS NMR. Accordingly, the INEPT-MAS

measurement of the cured material provides a clear evidence for approximately quantitative incorporation of undecanol in the polymer network.

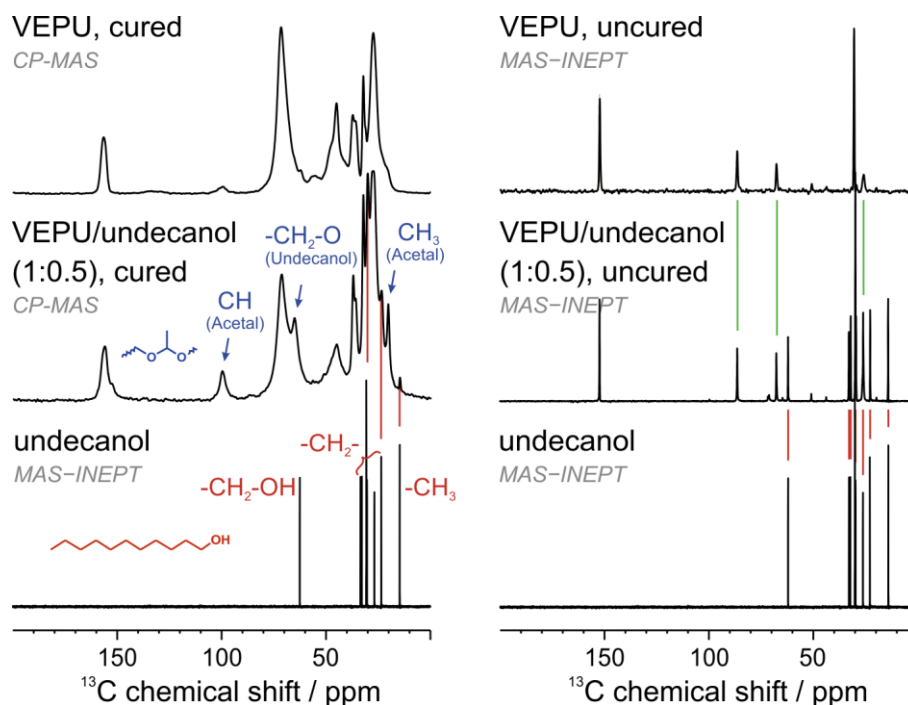


Figure 4.32. CP and INEPT MAS NMR spectra of the uncured and cured VEPU/undecanol (1:0.5) formulation in comparison to the uncured and cured pure VEPU and undecanol.

In Figure 4.32, peak assignments are provided for undecanol and crucial acetal structures. Some peaks from the undecanol backbone that are apart from the reaction center and do not shift upon the reaction can be identified in the CP spectrum of the cured VEPU/undecanol as they became incorporated in the rigid network structure. Also the UV-cured, pure VEPU exhibits a slight acetal peak at 100 ppm. This peak is presumably caused by hydrolysis of vinyl ether carbocations and subsequent acetal formation of the resulting hydroxyl groups. However, the low peak intensity compared to the cured VEPU/undecanol formulation reveals that this reaction is not of significance, although the displayed CP spectrum is generally not quantifiable. The right spectra break down the uncured VEPU/undecanol spectrum into the peak contributions of VEPU and undecanol, respectively.

To the best of our knowledge, these NMR investigations represent the first unambiguous spectroscopic proof of acetal formation in an insoluble, highly crosslinked material upon curing. In general, the insolubility of the polymer networks, which in our example is maintained even after pH-triggered hydrolysis of the acetal units, can be

highlighted and provide significant advantages for a variety of controlled release applications such as antimicrobial materials, active dressing for wound healing,¹⁹⁷ long lasting fragrances¹⁹⁸ or gastro-resistant drug carriers.^{199, 200}

Gas chromatographic analysis was performed with samples treated for several hours under different pH-conditions to investigate the release efficiency and kinetics. Figure 4.33 summarizes the relative extractable undecanol content from THF swollen polymer films depending on the addition of different ingredients and the extraction time.

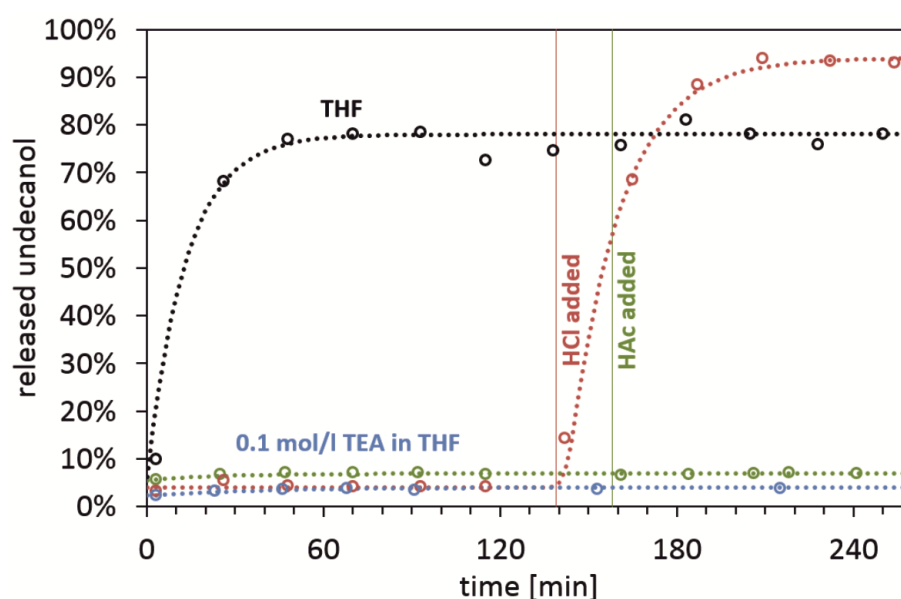


Figure 4.33. Efficiency and kinetics of undecanol release under different conditions.

The black curve shows the evolving undecanol concentration in the supernatant moist THF solution (0.36 mol/l H₂O). The extracted undecanol concentration increases within minutes to about 78% of the initially added amount. The result can be explained by residual photoacid from the UV-initiation, which obviously provides a sufficiently acidic medium to cause hydrolysis of acetal groups if the film becomes swollen in pre-moistened solvents. Therefore, the other polymer films (blue, green and red curve) were swollen in alkaline THF, containing 0.1 mol/l TEA, to neutralize residual acid from the photoinitiator. Under these conditions only 4 - 7% of undecanol were extractable, which most likely corresponds to the fraction of undecanol that has not been incorporated upon UV-curing. For one of these samples hydrochloric acid (red curve) was added after an extraction time of 139 min. Another sample was treated with acetic acid (green curve) after 158 min. In both cases a final acid concentration of

0.1 mol/l after neutralization of TEA was calculated. The weak acetic acid did not result in an increased extractable undecanol content. However, treatment with hydrochloric acid caused degradation of the acetal linkages and leads to the release of about 94% of the initial undecanol within 80 min.

4.4.5 Conclusion and Outlook

In summary, we have prepared crosslinked vinyl ether functional polyurethanes (VEPUs) via photoinduced cationic polymerization of vinyl ether side-groups in the presence of hydroxyl functional transfer agents. In this cationic phototransfer polymerization the transfer agents strongly influence the resulting polymer structure and flexibilized networks containing degradable, acid-labile acetal groups are obtained. Upon pH-decrease hydrolytic cleavage triggers the release of the original hydroxyl component and additionally cause softening of the material structure. The mechanical modulus before and after release can be adjusted by the polyurethane backbone and/or the structure and content of the transfer agent. Monofunctional alcohols are best suited for controlled release applications, while multifunctional transfer agents like diols are well suited for structural applications, such as engineering materials with debonding on command properties. Furthermore, we would like to emphasize that the crosslinked polymer networks remain insoluble, even after controlled hydrolytic release. This behavior could provide significant advantages for a variety of applications like antimicrobial materials, active tissues for wound healing, long lasting fragrances or gastro-resistant drug carriers.

4.5 Cationic Phototransfer Polymerization of Photocurable Polyhydroxyurethanes*

Vinyl ether functionalized polyhydroxyurethanes (VEPHUs), which contain vinyl ether and hydroxyl groups along their backbone were prepared via aminolysis of vinyl ether functional dicarbonates to provide a competitive and sustainable alternative for isocyanate based synthesis of polyurethanes. Low molecular weight prepolymers can be cured via a cationic phototransfer polymerization mechanism, under consumption of hydroxyl groups. This procedure allows the preparation of crosslinked PHUs with reduced hydroxyl content and provides an efficient method to overcome low molecular weights and high water absorption, which are the main drawbacks of classical PHUs. The curing behavior was monitored using UV/NIR-rheology and photo-DSC and the consumption of hydroxyl groups in the curing reaction was verified using IR spectroscopy and ^{13}C CP-MAS NMR spectroscopy.

4.5.1 Motivation

Conventional polyurethanes (PU) are based on isocyanate chemistry, which inherently involves the handling of hazardous materials (see Chapter 2.2.1). Most isocyanates used on an industrial scale are labeled toxic, and are typically synthesized from highly hazardous phosgene. To overcome the associated risks, a variety of synthetic pathways have been developed towards non-isocyanate polyurethanes (NIPU), which are summarized in several recent review articles.¹¹⁰⁻¹¹³ In this context polyhydroxyurethanes (PHU), which are prepared via ring-opening addition of primary, aliphatic amines to cyclic carbonates, are considered as one of the most promising material categories. Figure 4.34 shows the synthesis of conventional PUs and the alternative synthesis of PHUs.

* This section is based on the publication manuscript “*Cationic Phototransfer Polymerization of Photocurable Polyhydroxyurethanes*” by Stefan Kirschbaum, Katharina Landfester and Andreas Taden. Publication is withheld for the submission of the patent “*Kationische Phototransferpolymerisation*“, internal no. PT033452.

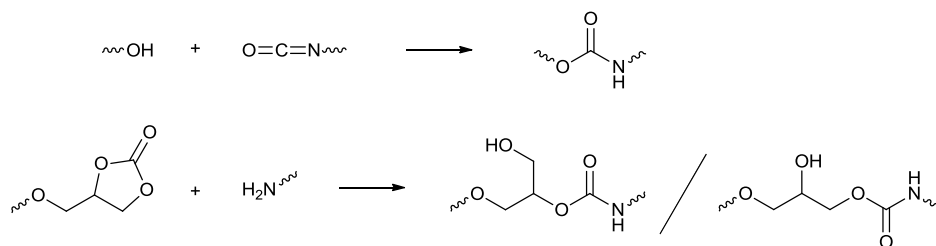


Figure 4.34. Syntheses of PUs and PHUs.

In contrast to common PUs the aminolysis of cyclic carbonates yield polyurethanes with hydroxyl groups close to the urethane groups. The isomer containing a secondary hydroxyl group is favored, if five-membered cyclic carbonates are applied.

The synthesis and properties of PHUs were extensively investigated in the last decade and is discussed in Chapter 2.2.2 in detail. The aminolysis readily proceeds at ambient conditions. Although, fast reactions at room temperature have been reported, most often catalysts and elevated temperatures are required for several hours in order to obtain high conversion. Obviously, the exchange of highly energetic isocyanates leads to a lack in reactivity, that strongly dependent on the specific amine and carbonate structure.^{116, 119, 201} Furthermore, second order kinetics with respect to both, the amine and the cyclic carbonate significantly slow the reaction down at high conversions.¹¹³ However, in polyaddition reactions high molecular weights are only obtained at very high conversions. Hence, the obtained molecular weights of PHUs are rather low compared to standard polyurethanes. Therefore, they are mainly applicable as prepolymers or in crosslinking formulations. The thermal and mechanical properties of PHUs were found to be similar or superior in many aspects^{116, 202} and intramolecular hydrogen bonding between the hydroxyl groups and the urethane carbonyl renders them chemically more resistant. However, the presence of polar hydroxyl groups leads to fundamentally increased water absorption.^{119, 201} Up to now high water absorption and low molecular weights are considered as key drawbacks that limit the utilization of PHUs.

Reactive post modification of the hydroxyl groups via esterification,^{203, 204} silylation,²⁰³ urethanization^{205, 206} or crosslinking through the addition of titanium alkoxides²⁰⁷ or diisocyanates²⁰² have already been reported. The use of isocyanates, of course, spoils the environmental benefits of PHUs. However, these reactions indicate the utility of additional hydroxyl groups. The preparation of hydroxyl functional polyurethanes is not possible via standard PU synthesis, due to the high reactivity of isocyanates towards

hydroxyl groups. In contrast, the high chemoselectivity of cyclic carbonates towards aminolysis even allows the graduation between primary and secondary amines.²⁰⁸

The synthesis and the unique curing behavior of vinyl ether side-chain functionalized polyurethanes (VEPUs) was reported in Chapter 4.1. Furthermore, the impact of hydroxyl functional transfer agents on the cationic curing reaction was discussed in Chapter 4.4. The resulting cationic phototransfer polymerization proceeds via a mixed-mode mechanism of step growth and chain growth similar to non-ideal thiol-ene reactions.

In this chapter, we now introduce the synthesis of a vinyl ether functionalized diglycidyl carbonate (VEDGC) and the subsequent ring-opening reaction with hexamethyldiamine (HMDA) to yield a linear, vinyl ether functionalized polyhydroxyurethanes (VEPHU). This VEPHU can be photocured with low energy requirements via a phototransfer polymerization mechanism as depicted in Figure 4.25. In this approach only low molecular weight PHU prepolymers are prepared via aminolysis and crosslinked under cationic conditions in a later step. Consequently, the molecular weight or crosslinking density limitation, which comes along with the isocyanate free synthetic procedure can be circumvented. Furthermore, free hydroxyl groups are consumed in the phototransfer process and result in the formation of acetal groups upon addition to vinyl ether carbocations. Previously described results (Chapter 4.4.4) have shown that large quantities of hydroxyl groups are consumed under cationic conditions and that the formed acetal linkages are stable in a wide pH-range from basic to weak acidic media. Therefore, water absorption is expected to be significantly reduced in comparison to common PHUs. However, upon hydrolysis large quantities of hydroxyl groups are generated while the crosslinking density is expected to drop significantly. This pH-triggered, switchable behavior is of particular interest for certain applications such as debonding on command. Nevertheless, the main objective is to provide a solution that overcomes the drawbacks associated with polyhydroxyurethanes, to provide a more competitive alternative for common isocyanate based polyurethanes.

4.5.2 Synthesis of the VEPHU

A vinyl ether functional diglycidyl carbonate (VEDGC) and a monofunctional glycidyl carbonate butyl vinyl ether (GCBVE) were synthesized from their corresponding alcohols via epoxidation with epichlorohydrin and subsequent CO₂ insertion as depicted in Figure 4.35.

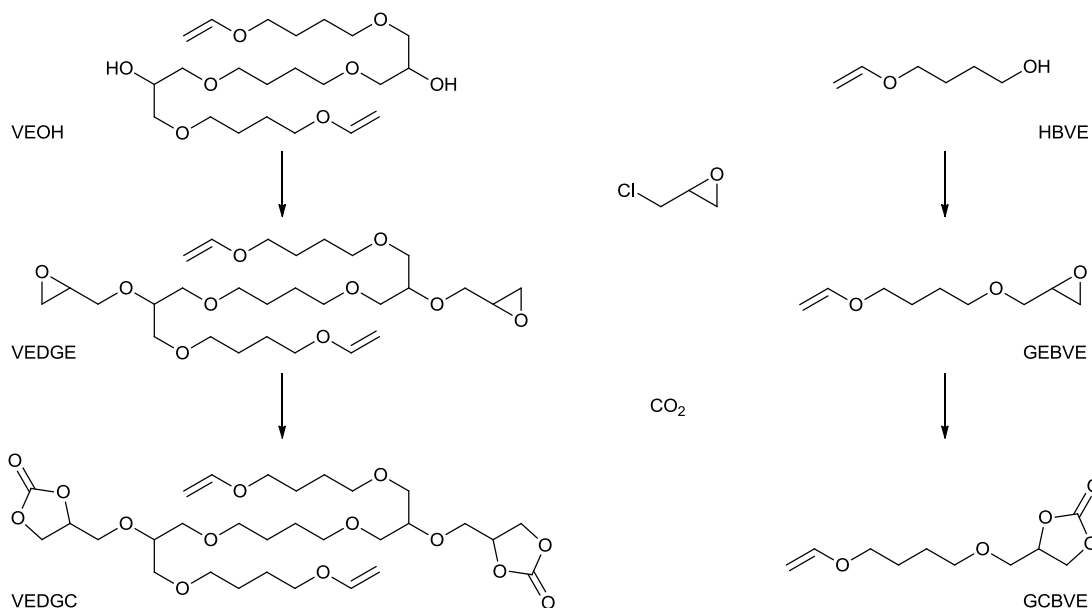


Figure 4.35. Synthesis of VEDGC and GCBVE.

VEDGC was synthesized as reactant for the VEPHU synthesis. GCBVE was prepared as low molecular weight amine-scavenger.

The diglycidyl carbonate is used as monomer in a ring-opening polyaddition reaction with hexamethylene diamine (HMDA) to yield a vinyl ether functional polyhydroxyurethane, whereas GCBVE serves as low molecular weight amine-scavenger of high mobility to convert residual amines into less nucleophilic urethanes. The VEPHU synthesis was conducted at 70 °C and is schematically depicted in Figure 4.36.

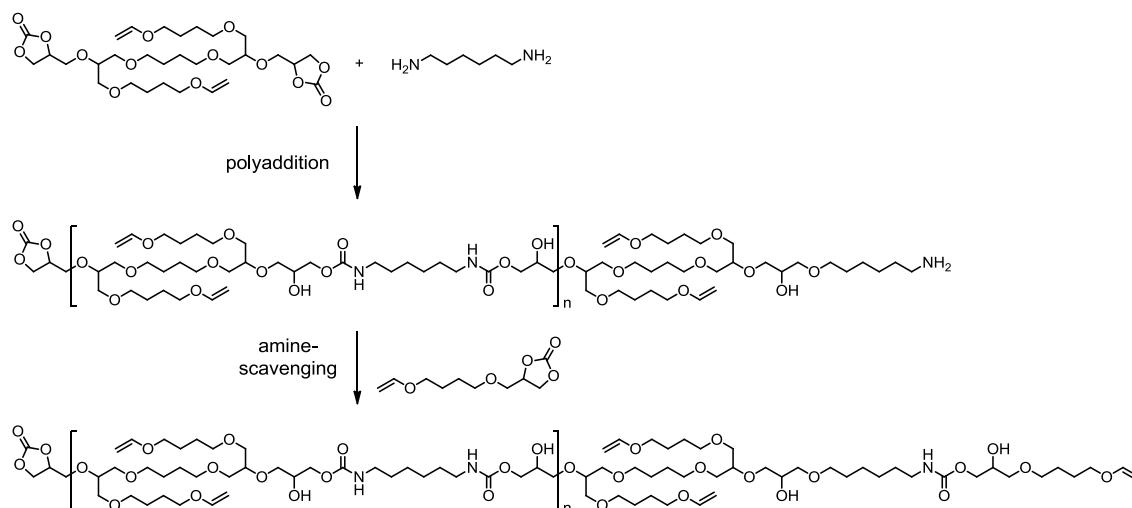


Figure 4.36. Schematic illustration of the VEPHU synthesis.

The carbonate conversion was monitored via IR spectroscopy. Figure 4.37 shows a time dependent plot of the carbonate conversion.

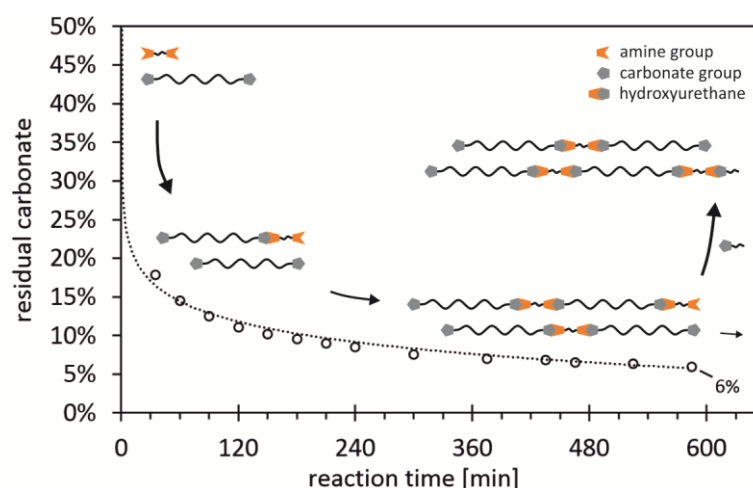


Figure 4.37. Evolution of the cyclic carbonate concentration during the VEPHU synthesis.

More than 80% of the cyclic carbonate groups are consumed within the first 30 min although HMDA is initially insoluble in VEDGC and the reaction takes place solely at the interface for several minutes until a homogeneous mixture was obtained. However, with increasing conversion the reaction slows down significantly and even after 10 h reaction time about 6% of residual carbonate and presumably an equivalent amount of amine is indicated.

Generally, increased concentrations of residual carbonate and amine end groups are no issue in common PHUs and the reduced molecular weight build up is not significant for

low molecular weight prepolymers. Anyway, a second mechanism will be employed to crosslink the material via vinyl ether side-groups. However, particularly the cationic curing reaction is inhibited by nucleophilic amine groups. Unfortunately, high amine conversions are hardly obtained due to second order kinetics with respect to both functional groups and the increasing molecular weight of reactive, oligomeric adducts. Hence, the effort to obtain tolerably low concentration of residual amine groups in a technically feasible procedure is disproportionately high.

To enable cationic polymerization, GCBVE was charged to the reaction after 10 h. Its low molecular weight and consequently high mobility enables the conversion of amine groups more efficiently compared to less mobile terminal glycidyl carbonate groups from the prepolymer. Furthermore, it can be applied in excess as residual GCBVE will be incorporated into the polymer structure upon cationic curing. Therefore, it also qualifies as reactive diluent. The addition of 30 mol% (13 wt%) GCBVE with respect to the initial amount of amine groups was sufficient to enable the photoinduced curing reaction in the presence of 5 wt% of 4,4'-dimethyl-diphenyliodonium hexafluorophosphate as photoinitiator. The relatively high concentration of photoinitiator had to be applied as the presence of residual epoxy groups in the VEDGC may yield secondary or tertiary amine groups, which are not reactive towards cyclic carbonates and remain as alkaline functional groups in the material and partially consume the acid generated upon decomposition of the photoinitiator. The reaction of amines with epoxides and cyclic carbonates is shown in Figure 4.38.

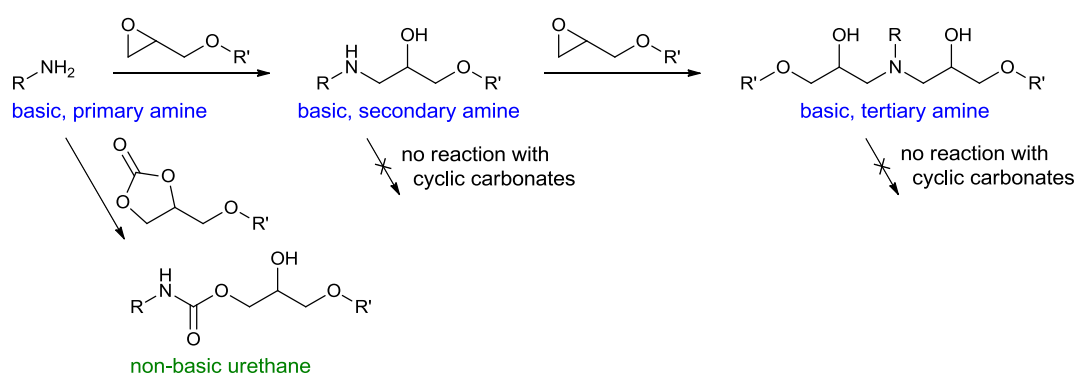


Figure 4.38. Reaction of amines with epoxides and cyclic carbonates.

The efficiency of GCBVE as amine-scavenger was also investigated using ^1H NMR spectroscopy in a more defined model reaction with hexylamine at room temperature (see Figure 4.39).

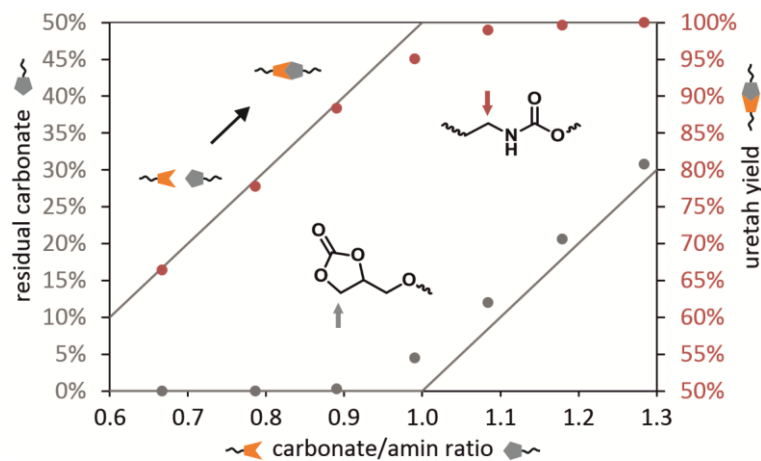


Figure 4.39. Amine-scavenging study.

The quantification of residual cyclic carbonate and generated urethane was performed via ^1H NMR spectroscopy.

The concentrations of residual cyclic carbonate and formed urethane groups were quantified via integration of the corresponding, indicated peaks (at 4.50 ppm and 3.17 ppm, respectively) in the ^1H NMR spectra relative to the hexyl- CH_3 group (0.89 ppm). The exact stoichiometry was calculated from the ratio of the hexyl- CH_3 group and the vinyl ether peak (6.45 ppm). An equimolar ratio of amine and carbonate results in about 95% conversion and about 5% residues. But already and excess of 10 mol% of GCBVE is sufficient to convert about 99% of the amine groups. Hence, it seems reasonable that an excess of 30 mol% of GCBVE is sufficient to reduce the free amine content in the VEPHU.

4.5.3 Cationic Curing of the VEPHU

The VEPHU was formulated with 5 wt% of the photoinitiator and the curing behavior at 25 °C was investigated using UV/NIR-rheology to simultaneously observe the mechanical property evolution and conversion of vinyl ether groups. The results are plotted in Figure 4.40a.

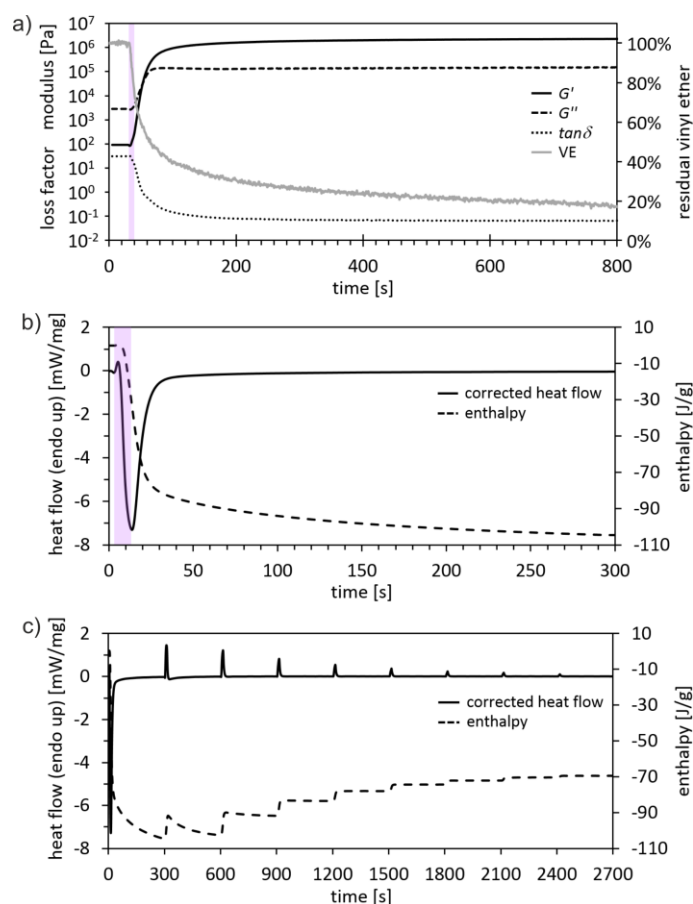


Figure 4.40. Curing profiles of the VEPHU.

a) UV/NIR-rheology investigation. b) Isothermal photo-DSC analysis. c) photo-DSC of nine successive irradiations.

The sample was irradiated for 10 s, indicated by the purple background. Fast evolution of mechanical properties was observed upon UV-irradiation and proceeds in the absence of light. Due to its living character, the cationic curing process is not limited to the irradiation period. Gelation ($\tan\delta = 1$) takes place after 23 s and 43% of vinyl ether group conversion, whereas after 60 s a conversion of 58% was reached, while the storage and loss moduli approach their limits. Moreover, the conversion of vinyl ether proceeds further for several minutes in the crosslinked, rubbery material, but no significant contribution to the mechanical properties was observed any more.

Complementary, isothermal photo-DSC measurements were performed. Figure 4.40b displays the corrected heat flow and the reaction enthalpy for the first irradiation and subsequent post-curing. The development of the reaction enthalpy is generally considered to be related to the conversion and shows a consistent shape over time in comparison to the NIR determined conversion. Figure 4.40c shows the same plot over

nine successive irradiations indicating that after 3 irradiations no further exothermal reaction enthalpy was observed. However, upon irradiation an endothermal heat flow corresponding to the photoinitiator decomposition was observed, which declines over several irradiations. As a result of the relatively high photoinitiator concentration, the total enthalpy is largely dependent on the overall irradiation time and a correlation to the conversion is rather difficult. Glass transition temperatures were determined in the same DSC experiment and showed a significant increase from $-50.4\text{ }^{\circ}\text{C}$ before irradiation to $-5.1\text{ }^{\circ}\text{C}$ after ten consecutive irradiations. Above T_g , the crosslinked material exists in a rubbery state, which allows sufficient molecular mobility to ensure an ongoing conversion that is likely to reach integrity without further external stimuli.

Structurally, the addition reaction results in the connection of exactly two functional moieties whereas the number of connected moieties at a knotting dot in the vinyl ether chain growth reaction depends on the kinetic chain length. On the other hand, the proton transfer shifts the reaction site between subsequent addition reactions. Such behavior has similarly been described for thiol-ene reactions, which proceed via a similar mechanism.^{57, 209} Furthermore, the network is not just more uniform it may also cure more tightly as the hydroxyl groups introduce additional networking sites along the backbone and hence reduce the segment length. Additionally, hydroxyl groups are consumed and product properties more similar to those of conventional PUs may be obtainable. Microscopic schemes for the UV-curing of VEPUs and VEHPUs are depicted in Figure 4.41.

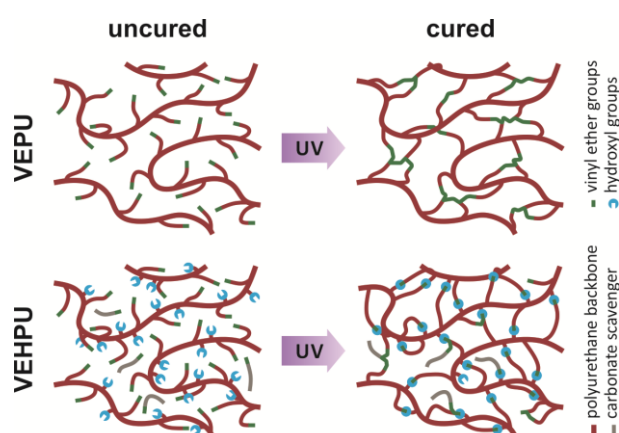


Figure 4.41. Schematic illustration of VEPUs and VEHPUs before and after UV-irradiation.

Figure 4.42 shows the IR spectra of the uncured and cured material.

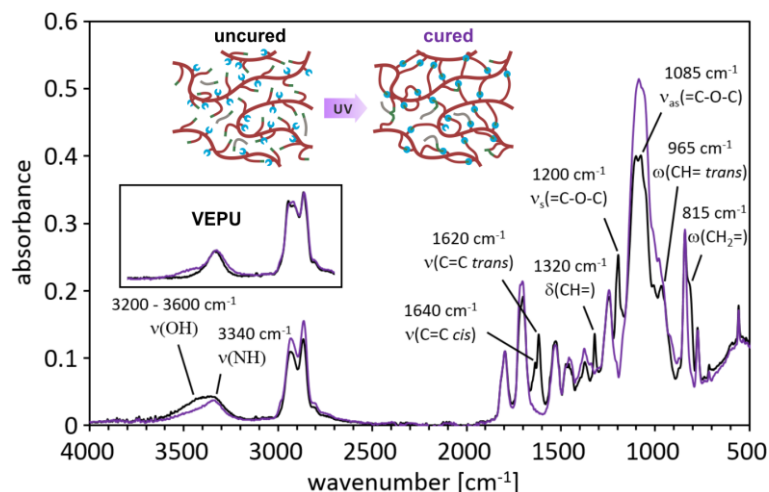


Figure 4.42. IR Spectra of the uncured VEPHU formulation and the cured VEPHU film.

The inserted box shows the partial spectra of the VEPU for comparison.

Complete conversion of the vinyl ether can be observed by total disappearance of several absorption bands. Furthermore, consumption of hydroxyl groups is indicated by the narrowed absorption in the range of 3200 to 3600 cm^{-1} . This absorption originates from overlapping absorption bands of OH and NH-groups. Before curing, the largely overlapping OH and NH stretching vibrations result in a broad absorption band. After curing one can identify the NH-peak tailing towards higher wavenumbers. Hence, the concentration of hydroxyl groups is significantly reduced in the cured sample. As reference spectra of a comparable urethane (VEPU) is displayed (see inserted box), which was synthesized via conventional PU synthesis and is consequently free of hydroxyl groups. Before curing the VEPU shows only the NH-absorption band and after curing a similarly small OH absorption band emerged. It can be speculated that delayed hydrolysis of carbocationic chain-ends results in the formation of new hydroxyl groups in both materials. Similar conclusions can be drawn from solid state ^{13}C NMR spectroscopy, which show a pronounced acetal peak for the cured VEPHU in comparison the cured VEPU (see Figure 4.43).

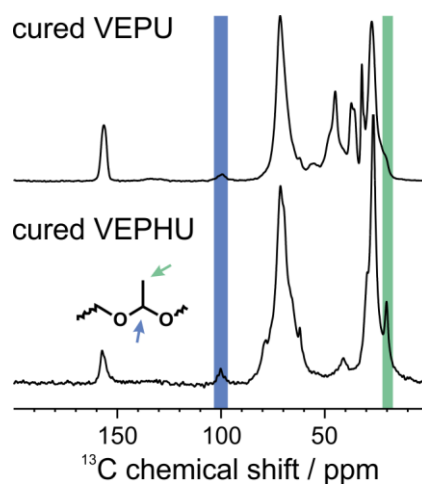


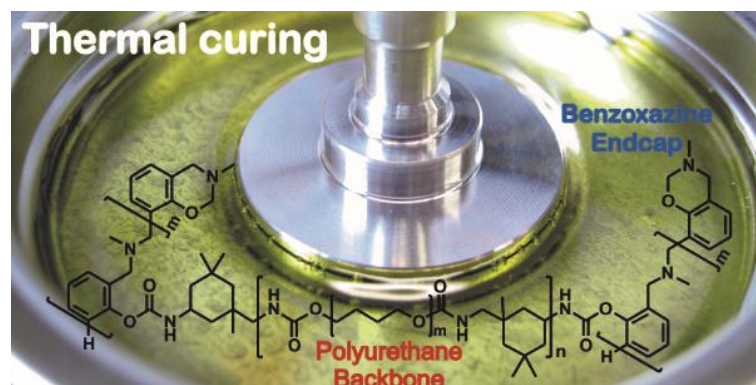
Figure 4.43. ^{13}C CP-MAS NMR spectra of the cured VEPHU in comparison to the cured VEPU. The spectrum indicates an increased acetal group content.

The presence of acetal groups within the cured polymer structure additionally offers a pH-responsive behavior. Therefore, the ratio of acetal structures to poly(vinyl ether) chains determines a critical parameter for the acid catalyzed degradability. Both structures are hard to quantify in crosslinked networks but are expected to indirectly correlate with the ratio of vinyl ether to hydroxyl groups ($n_{\text{VE}}/n_{\text{OH}}$). In general, VEPHUs based on the described VEDGC, which exhibits two vinyl ether and two cyclic carbonate groups, contain similar amounts of vinyl ether and hydroxyl groups ($n_{\text{VE}}/n_{\text{OH}} \approx 1$). However, the VE/OH-ratio of VEPHUs can be further shifted through incorporation of other dicarbonates or formulation with either vinyl ether or hydroxyl containing materials such as GCBVE, which was applied as amine-scavenger. Most of the GCBVE represents an excess over the amine. Therefore, the majority of the carbonate is not converted to hydroxyurethanes. In the present formulation 30 mol% of GCBVE were added and hence a VE/OH ratio of >1 results in the formation of network structures that are not entirely degradable due to the presence of significant poly(vinyl ether) structures. The VE/OH-ratio is a manipulation variable that allows to tune the relative content of degradable crosslinking points and hence influences the behavior upon acidic treatment. In other words this parameter allows the facile adjustment from slight degradation, which causes softening and increased swelling to almost complete degradation that causes disintegration of the material.

4.5.4 Conclusion and Outlook

In summary, we have introduced the synthesis of vinyl ether functional polyhydroxyurethanes (VEPHU) from a novel vinyl ether functional dicarbonate precursor. The vinyl ether functionality enables cationic UV-curing under consumption of hydroxyl groups and the generation of acetal crosslinking sites in a so-called phototransfer polymerization mechanism. The introduction of this second curing step provides a potential route to overcome the main drawbacks of common PHUs such as the limited molecular weight and high water absorption and hence improves the competitiveness as environmentally benign alternative for common isocyanate based polyurethanes. The main purpose of this chapter was the introduction of the synthetic procedure rather than the investigation of the final material properties. However, with respect to the degradation analytics described in Chapter 4.4.4, it can be assumed that VEPHUs nicely qualify as pH-responsive materials. More detailed degradation experiments are part of ongoing investigations and shall be published elsewhere.

4.6 Synthesis and Thermal Curing of Benzoxazine Functionalized Polyurethanes*



Benzoxazine (BOX) functionalized polyurethanes (PU) are introduced to provide a conceptually new thermal curing mechanism for polyurethanes. 3,4-dihydro-3-methyl-2H-1,3-benzoxazine (P-m) was carefully oligomerized through thermal treatment. In a straight forward synthesis the newly formed hydroxyl groups are used for end-capping reaction with isocyanate terminated polyurethane prepolymers. The isocyanate reactive hydroxyl content (IRH) of the benzoxazine oligomer was investigated in detail via ^1H NMR spectroscopy, HPLC-MS, indirect potentiometric titration, solvent variation as well as comparison with model substances and found to be strongly influenced by hydrogen bonding. The corresponding polyurethane/benzoxazine-hybrid materials (PU/BOX) can crosslink at elevated temperatures and do not suffer from shelf life issues or outgassing of blocked isocyanates. The thermally activated curing reaction was investigated via rheology and DSC. Significant improvements over state of the art systems based on phenol capped PU prepolymers are shorter curing times, increased moduli and drastically increased glass transition temperatures.

* This section is based on the publication "Synthesis and Thermal Curing of Benzoxazine Functionalized Polyurethanes" by Stefan Kirschbaum, Katharina Landfester and Andreas Taden, published in *Macromolecules* **2015**, 48, 3811-3816. Reprinted with permission. Copyright 2015 American Chemical Society.

4.6.1 Motivation

Polybenzoxazines are a class of thermosetting phenolic resins that recently gained increased interest due to their unusual set of competitive material properties.^{121, 122, 210} They combine typical properties of phenolic resins like high temperature resistance and high char yield with unique properties like low water uptake, high glass transition values (T_g) exceeding the curing temperatures and extremely strong mechanical performance. Benzoxazines are synthesized from abundant raw materials such as phenols, primary amines and formaldehyde proceeding water as a condensation product and can be polymerized through thermally activated ring-opening reaction.²¹¹ The polymerization proceeds without producing stoichiometric amounts of by-products, resulting in near zero shrinkage and yields Mannich bridged phenol resins. This structure comprising phenolic hydroxyl groups and tertiary amines allows the formation of various hydrogen bonds, including extremely stable intramolecular six-membered hydrogen bonds, is the key feature towards many unexpected properties that are characteristic for benzoxazines.^{135, 212, 213}

Polyurethanes, on the other hand, are among the most important tough engineering polymers and can be adjusted to serve a wide spectrum of properties.^{99, 100} This versatility is based on the segmented structure consisting of urethane rich hard segments and urethane poor soft segments that are easily generated through the polyaddition reaction of isocyanates and higher molecular weight polyols. In general polyurethanes possess good adhesion and abrasion resistance as well as excellent flexibility and are therefore principally suited to improve the toughness of benzoxazine resins.^{136, 214, 215} *Vice versa* benzoxazines can be used to introduce thermal curability to polyurethane prepolymers. Consequently, a clever combination of these very different polymer classes is expected to lead to hybrid materials with a beneficial set of properties. In fact it should be able to address a broad range of applications by tailoring hybrid materials either with high elasticity or high modulus, or anything in between.

The simplest approach for such a hybrid material is blending of benzoxazines with reactive, isocyanate terminated polyurethane prepolymers and subsequent thermal induction of the ring-opening polymerization of the benzoxazine.^{214, 216-218} The arising free hydroxyl groups of the benzoxazine polymer are reactive towards isocyanates and

yield aromatic urethanes. These phenol based urethanes are thermally labile and may reversibly dissociate at the curing temperature, and regenerated isocyanate functions additionally can react with urethane or urea units to reversibly form allophanates or biurets moieties. Upon cooling finally isocyanate free resins are formed at room temperature. However, simple blends of benzoxazines and reactive isocyanates are moisture-sensitive and exhibit limited stability and shelf life issues. Hence a different approach using blocked isocyanates was described. The isocyanate functionality was converted to thermally labile urethanes by use of bisphenol A²¹⁹, nitrophenol²²⁰ or butanone oxime²²¹. This approach renders the BOX/PU blend more stable and depending on the actual thermal stability of these urethanes and the applied polymerization temperature the urethane bonds can dissociate to regenerate free isocyanates. Unfortunately the blocking agents, which are often volatile organic compound (VOC), may be released from the material. Among these blocking agents phenol derivatives show special properties as free phenols are catalytically active for the polymerization reaction of benzoxazines.²²² Furthermore, they can be attacked by iminium ion intermediates to be incorporated in the network structure and hence covalently connect the PU prepolymers to the benzoxazine, even if dissociation did not occur.²¹⁹ However, these incorporated phenols dilute the benzoxazine network as they do not polymerize themselves and hence reduce the material performance. Another approach is the pre-curing of the polyurethane through multifunctional diols²²³ or moisture.²²⁴ The benzoxazine swollen polymer network then provides an improved dimensional stability at elevated temperatures for the benzoxazine curing reaction. The generated interpenetrating network (IPN) was shown to have a synergistic effect on the glass transition temperature due to intimate hydrogen bonding between both materials. Furthermore, it was observed that the presence of thermally labile allophanate or biureh groups regenerate low quantities of free isocyanate and allow the formation of covalent connections between both networks. Recently benzoxazines were covalently attached to a polyurethane structure previous to the benzoxazine curing reaction. Namely aliphatic hydroxyl group containing benzoxazines were synthesized for the direct incorporation in the polyurethane²²⁵ and furan functional benzoxazines were synthesized for the Diels-Alder addition reaction with maleimide functionalized polyurethanes.²²⁶ However, both approaches suffer from high synthetic effort.

In this contribution we introduce a straight forward synthetic approach that makes use of the inherent hydroxyl groups in benzoxazine oligomers. These oligomers can be generated through thermal treatment but are also obtained as by-product in crude benzoxazine resins. Their content is dependent on the actual synthetic conditions like temperature, reaction time or the dielectric constant of the solvent and hence can be adjusted without further synthetic effort.¹²⁴ The oligomer containing benzoxazine is then covalently attached to the polyurethane. Aliphatic isocyanate based polyurethanes renders the resulting phenolic urethane linkage relatively stable with approximate dissociation temperatures of >180 °C.¹⁰⁴ The use of methylamine based benzoxazines that polymerize at comparatively low temperatures²²⁷ and the presence of catalytically active phenolic hydroxyl groups in the benzoxazine oligomer allow the curing reaction to proceed below the deblocking temperature of the benzoxazine functionalization. Nevertheless, if dissociation occurs to some extent the free isocyanate may additionally catalyze the benzoxazine curing via stabilization of the iminium ion intermediate²²⁸ and is likely to yield a similar phenolic urethane upon addition due to the great excess of free hydroxyl groups.

Besides phosphorous NMR spectroscopy of derivatized, oligomerized benzoxazines,²²⁹ so far surprisingly little attention was paid to benzoxazine oligomers. Consequently, there is a lack of characterization and quantification. Therefore we developed an indirect potentiometric titration method that is capable to quantify the isocyanate reactive hydroxyl content (IRH) as well as the basic amine content in benzoxazines. This method was successfully applied to a series of benzoxazine oligomers and *N,N*-bis(3,5-dimethyl-2-hydroxybenzyl)methylamine (DMP₂-m) as model substance for polymerized benzoxazines and provides novel insights on the reactivity of phenolic hydroxyl groups in benzoxazine oligomers and polymers towards isocyanates and the importance of hydrogen bonding in benzoxazine-based systems.

4.6.2 Synthesis and Oligomerization of the P-m

The synthesis and polymerization reactions of P-m are displayed in Figure 4.44.

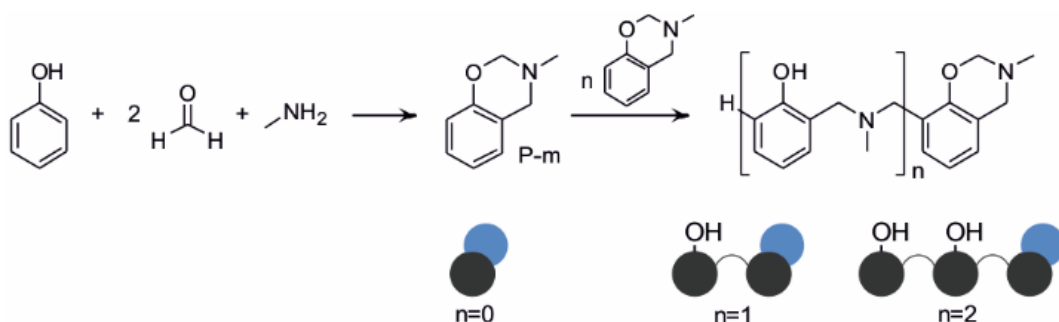


Figure 4.44. Synthesis and polymerization of P-m.

Additionally, to the idealized chemical structures the corresponding monomeric and oligomeric species are schematically depicted. Aromatic moieties are represented by a black circle, ring closed polymerizable units by a blue circle. The OH-groups are drawn explicitly, as they can serve as reaction sites for isocyanate groups.

Additionally, to the idealized linear polymerization reaction of unsubstituted, monofunctional benzoxazines the free para position leads to branching through substitution in the less favored para position.²³⁰ Hence, comparatively high molecular weight species can be generated and partially insoluble material is generated at high conversion. The free hydroxyl groups generated upon polymerization provide the opportunity of functionalization reactions. To gain more insights on the evolution of hydroxyl groups and their reactivity towards isocyanates, samples of the purified P-m were smoothly polymerized at 160 °C, while a sample was removed from the oven every 5 min. Up to 45 min reaction time all samples were completely soluble in xylene and chloroform, and were analyzed via ¹H NMR spectroscopy to observe the overall progress of the reaction. Figure 4.45 shows the spectra and structural assignments as well as plots of their intensities over the reaction time.

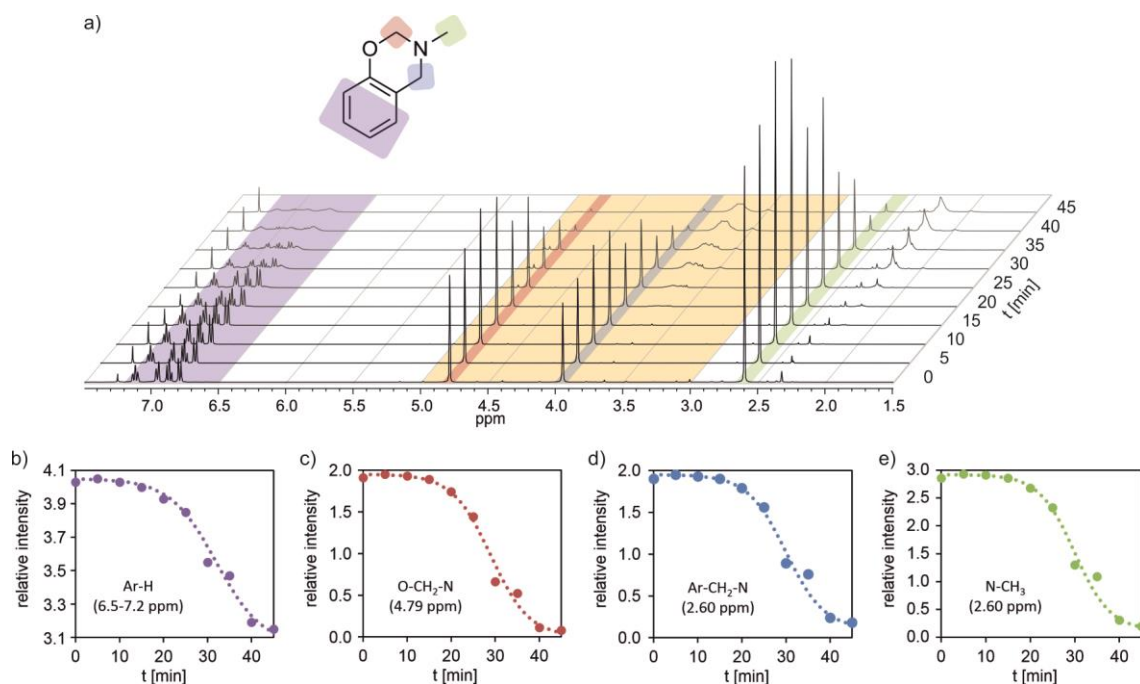


Figure 4.45. ¹H NMR study of the P-m polymerization.

a) stacked ¹H NMR spectra. b-e) Peak intensities over the reaction time.

All aliphatic CH₂ signals from educts and products appear in the spectral region of 3.0 ppm to 5.0 ppm. This region (yellow background, Figure 4.45a) was used as internal standard for the integration. The normalized peak intensities of signals, assigned to the educt, indicate a similar reaction profile with an overall conversion of about 90% after 45 min. Samples that have been treated for a longer time were partially insoluble in common organic solvents. The Mannich bridged structure of the main product was confirmed by HBMC-NMR spectroscopy (see Figure 5.30 in the Experimental Section). The same samples have also been investigated using an indirect potentiometric titration method. This method was shown to quantify the hydroxyl content of ordinary, electron rich phenols with good accuracy and in contrast to standard anhydride based titration methods, the procedure does not cause ring-opening or ring extension²³¹ of the benzoxazine. Also the reactivity of the aliphatic cyclohexyl isocyanate used for quantification is similar to that of IPDI and hence, was expected to be transferrable to the functionalization reaction. Additionally, a second equivalent point in the potential curve allows the quantification of basic amine due to different basicity of dibutylamine and the amine structures in benzoxazines. The results are shown in Table 4.3.

Table 4.3. Titration results of reference substances.

Sample	m (g)	$V_{ep1}-V_b$ (ml)	n_{OH} (mmol)	$n_{OH,th}$ (mmol)	recovery rate OH
Ph	0.1051	2.28	1.140	1.12	102%
	0.1251	2.68	1.340	1.33	101%
	0.1157	2.47	1.235	1.23	100%
DMP	0.1553	2.54	1.270	1.27	100%
	0.1533	2.55	1.275	1.25	102%
	0.1551	2.60	1.300	1.27	102%
DMP _{2-m}	0.1913	1.25	0.625	1.28	49%
	0.1831	1.19	0.595	1.22	49%
	0.1919	1.21	0.605	1.28	47%
Sample	$V_{ep2}-V_{ep1}$ (ml)	n_N (mmol)	w_N	$w_{N,th}$	recovery rate N
DMP _{2-m}	1.28	0.64	4.69%	4.68%	100%
	1.24	0.62	4.74%	4.68%	101%
	1.30	0.65	4.75%	4.68%	101%

The quantitative recovery rates for phenol and 2,4-dimethylphenol indicate that the method is reliable for ordinary, electron rich phenols. Phenolic structures in polybenzoxazines are rather electron rich and structurally related to dimethylphenol. Nevertheless, for DMP_{2-m} as model a substance for polybenzoxazines low recovery rates of about 48% were found. A possible explanation for this result is that only one hydroxyl group of DMP_{2-m} is reactive towards isocyanates, whereas the other hydroxyl group is involved in a very strong, intramolecular hydrogen bond with the Mannich bridge. The synthesis of DMP_{2-m} and its reaction with cyclohexyl isocyanate is depicted in Figure 4.46.

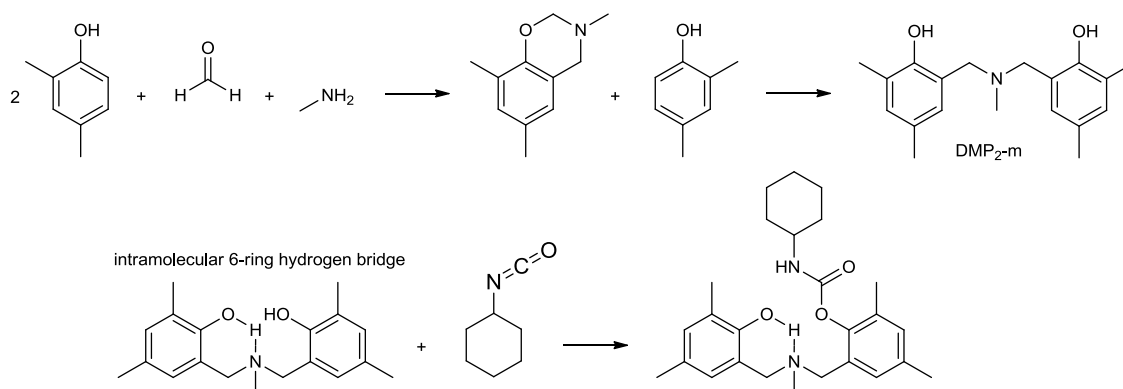


Figure 4.46. Synthesis of DMP_{2-m} and reaction with cyclohexyl isocyanate.

Intramolecular hydrogen bridges are assumed to significantly reduce the reactivity of one hydroxyl group.

This hypothesis was investigated using HPLC-MS spectroscopy of the reaction product of 1 mol DMP_{2-m} with 2 mol cyclohexyl isocyanate in xylene. Residual isocyanate was previously converted by an excess of DBA (2 mol). The chromatogram is shown in Figure 4.47.

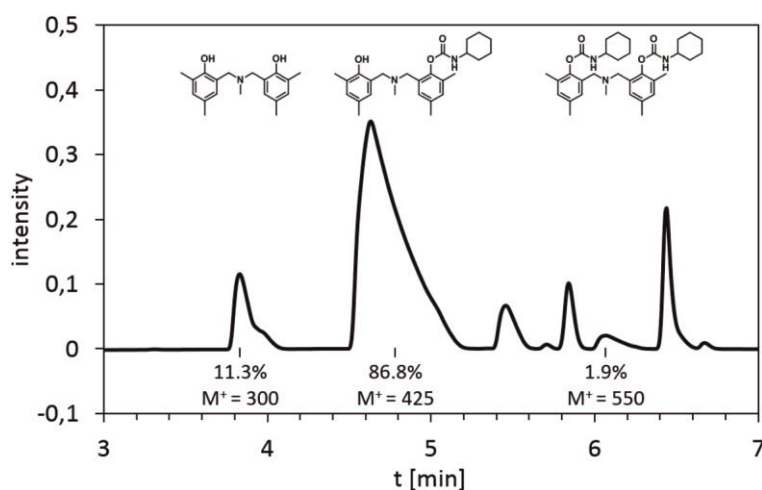


Figure 4.47. HPLC-MS analysis of the reaction product of DMP_{2-m} with cyclohexyl isocyanate.

UV-detectin was applied at 282 nm, which is a relative absorption maximum of DMP_{2-m}. Three peaks in the chromatogram were assigned to contain DMP_{2-m} fragments via mass spectroscopy and could be assigned to the residual DMP_{2-m} (3.83 min) as well as the mono- and diurethanized products (4.63 min; 6.06 min). The peaks were integrated for quantification, although the influence of the urethane groups on the absorption coefficient was not considered. For example the peak at 6.45 min corresponds to the urethane of cyclohexylisocyanate and dibutylamine indicates the

absorption of urethane structures at 282 nm. However, it is obvious that the reactivity of the second phenolic hydroxyl group of DMP₂-m is significantly reduced after the first hydroxyl group has been converted. This result also explains the recovery rate of about 48% via titration.

The relative, isocyanate reactive hydroxyl content (IRH) is an important parameter for the tailored design of PU/BOX-hybrids. Therefore, Figure 4.48 shows the plot of the IRH in conjunction with the relative, basic nitrogen content for the thermally treated P-m samples.

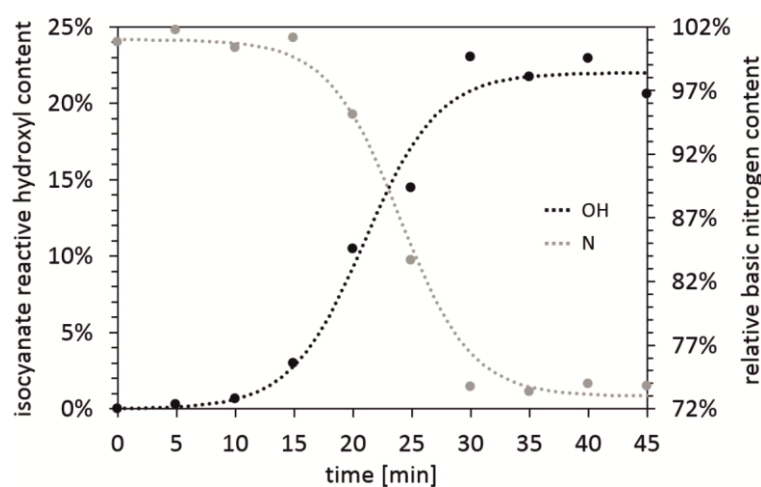


Figure 4.48. Isocyanate reactive hydroxyl content (IRH) and relative basic nitrogen content of P-m upon polymerization.

The isocyanate reactive hydroxyl content evolves similarly to the overall reaction profile, but remains low in comparison to the theoretical values. Only up to 21% of the theoretically possible hydroxyl content could be determined through the reaction with cyclohexyl isocyanate in xylene, even at high conversions of the benzoxazine. This results strongly suggest that most of the hydroxyl groups formed are trapped in very stable hydrogen bondings, for example six-membered intramolecular hydrogen bonding between the hydroxyl moiety and the Mannich bridge, and are therefore not accessible for the reaction with isocyanates. In fact the pronounced hydrogen bonding capabilities are widely recognized to be responsible for many unusual properties of polybenzoxazines.^{135, 212, 213} Hence, the comparably low IRH values seem plausible and may also be seen as measure to quantify the strength of hydrogen bonding in a given benzoxazine system. At the same time the basic nitrogen content is decreased by about 28% of the initial value. Due to this correlation it is assumed that the isocyanate reactive

4.6.3 Benzoxazine Functionalization of the Polyurethane

A polyurethane prepolymer with a theoretical average molecular weight of $M_n = 2000$ g/mol was synthesized from PTMO and IPDI. The molecular weight was confirmed via IR spectroscopic end group analysis (see Figure 5.34). The PTMO backbone was chosen due to its high compatibility with benzoxazines. Other polyols like polypropylenoxide (PPO, $M_n = 2000$ g/mol) caused undesired macro-phase separation upon polymerization of the hybrid material. However, in a previous publication our group has shown that the morphology of polyether containing benzoxazines can be adjusted by varying the amount and ratio of PTMO and PPG segments and that tailored micro-phase separation can be very beneficial for the toughness of resin materials.¹³⁶ The reactive, isocyanate terminated prepolymer was divided into two portions. One was directly charged with the oligomerized P-m and as a reference the other one was terminated with phenol and subsequently charged with the oligomerized P-m to obtain the same final content of polyurethane and benzoxazine resin (including phenol). The oligomerized P-m was determined to have a relative, isocyanate reactive hydroxyl content of 10.9% in xylene. This result matches with that obtained from the model polymerization. An overlay is shown in Figure 4.50.

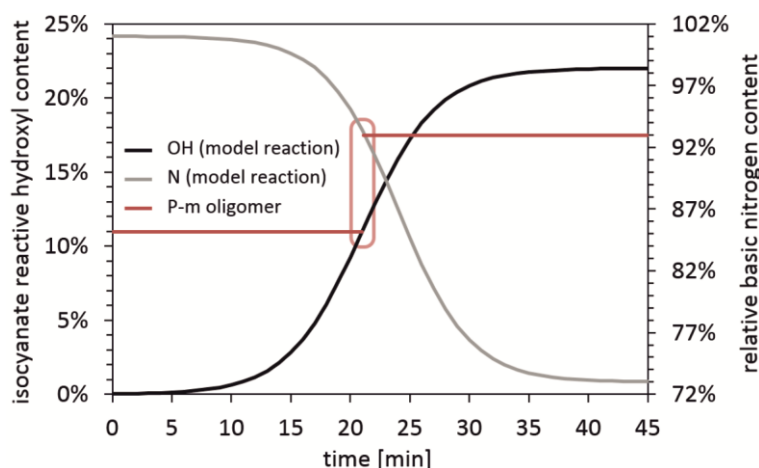


Figure 4.50. Titration results of the oligomerized P-m for the use as end-capping agent.

Both values similarly fit the model oligomerization reaction plots for the evolution of the isocyanate reactive hydroxyl content and the relative basic amine content.

Based on this result a formulation of 42 wt.% PU and 58 wt.% BOX would be necessary for a stoichiometric functionalization and an even greater excess of benzoxazine was expected to be necessary to avoid crosslinking due to oligomers

containing multiple hydroxyl groups. The synthetic pathway is schematically depicted in Figure 4.51.

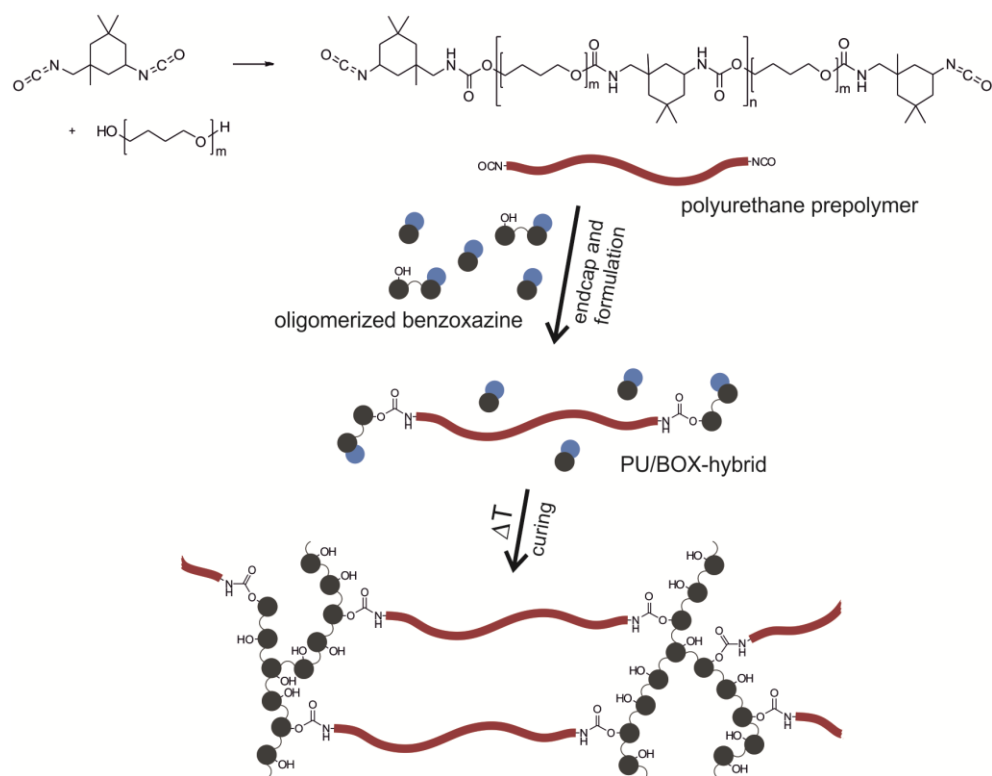


Figure 4.51. Synthesis and curing of PU/BOX-hybrid formulations.

In fact, IR spectroscopy indicated that a formulation of 70 wt.% PU and 30 wt.% oligomerized P-m was sufficient to completely convert the isocyanate groups without gelation. This formulation (PU/BOX 70/30) corresponds to a stoichiometry of $1/0.3 \text{ NCO/OH}_{\text{determined}}$ and a stoichiometry of $1/2.6 \text{ NCO/OH}_{\text{theoretically}}$. The reaction behavior shows that under synthetic conditions in bulk more hydroxyl groups are accessible for the reaction with isocyanates. In contrast to the unpolar xylene solvent utilized as reaction medium for the IRH determination the non-diluted polyurethane system provides a more viscous and polar, protic reaction environment that weakens the intramolecular hydrogen bonds and obviously increase the reactivity of phenolic hydroxyl groups in polybenzoxazines. To substantiate this hypothesis the hydroxyl content of DMP₂-m as model substance for polybenzoxazines was investigated under variation of different reaction parameters. In deed it was observed that more polar solvents, basic catalysts or more reactive aromatic isocyanates are capable to increase the hydroxyl content contributing to the urethane formation reaction. The reference hybrid material (PU-Phenol/BOX 70/30) was composed of 70 wt.% polyurethane,

6.6 wt.% of phenol and 23.4 wt.% of oligomerized P-m. In contrast to the PU/BOX 70/30 the use of phenol as end-capping agent prevents a covalent binding between the polyurethane and the oligomerized P-m upon formulation and provides a state of the art material that allows covalent attachment upon the thermally induced attack of benzoxazines to the terminal phenol moieties.

4.6.4 Curing of the Polyurethane/Benzoxazine-Hybrids

The curing reaction was conducted in the rheometer at 170 °C. Rheometric plots are shown in Figure 4.52.

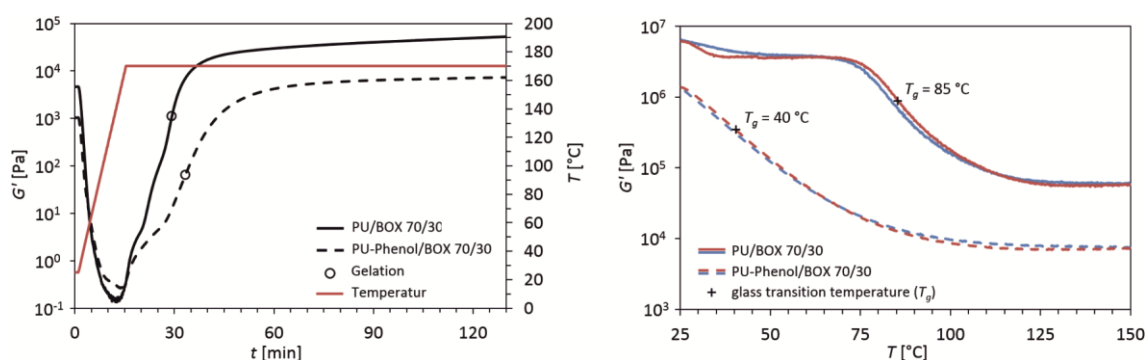


Figure 4.52. Curing of the PU/BOX-hybrids at 170 °C.

a) rheometric curing profile. b) Temperature dependence of the storage. The PU/BOX 70/30 cures faster and shows significantly improved mechanical properties in comparison to the state of the art PU-Phenol/BOX 70/30.

The storage modulus of the immediately benzoxazine functionalized polyurethane PU/BOX 70/30 evolves faster and reaches a final value that is about one order of magnitude higher than that of the phenol functionalized state of the art PU-Phenol/BOX 70/30 hybrid material. Furthermore, the pure PU/BOX 70/30 gels faster and the glass transition temperature (T_g) of the cured materials is more narrow and about 45 °C higher than that of the PU-Phenol/BOX 70/30. Especially, the difference in the T_g provides a tremendously improved thermal resistance. Another advantage is the far more distinct softening behavior at the glass transition, which is highly favorable and a clear demand for the majority of engineering processes and applications. The sharp decline of the storage modulus is related to the break-up of hydrogen bonds near the T_g . Generally, this effect is very strong for benzoxazines in comparison to most polymers whose properties do not depend as heavily on hydrogen bonding.¹²¹ The improved curing

profile as well as physical and thermal properties can be attributed to an unperturbed benzoxazine curing reaction. In contrast, if phenol is used for the PU-functionalization instead, the inactive but Mannich bridge accepting phenolic arenes dilute and weaken the polybenzoxazine network structure. This effect is expected to escalate with increasing phenol content, if lower molecular weight polyurethanes or higher polyurethane contents become applied. These results are substantiated via DSC in Figure 4.53.

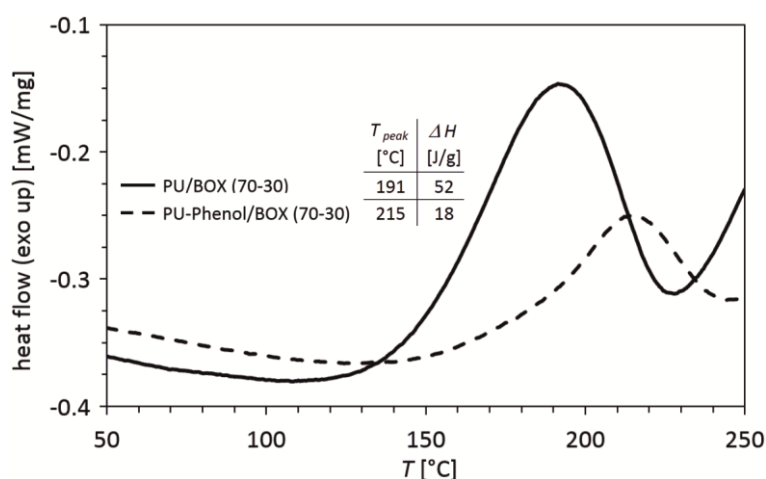


Figure 4.53. DSC measurement of the polyurethane/benzoxazine-hybrids.

The heat flow indicates a significantly increased reaction enthalpy for the curing reaction of the benzoxazine functionalized polyurethanes PU/BOX 70/30 in comparison to the phenol capped polyurethane PU-Phenol/BOX 70/30. The values for the determined reaction enthalpies are not very accurate as the thermal decomposition of polyurethanes starts before the baseline was reached after curing. However, the results clearly indicate a reduced reaction enthalpy for the phenol functionalized hybrid, which can be explained by dilution of the benzoxazine curing reaction with almost inactive phenolic structures. Also the curing reaction was shifted towards lower reaction temperatures for the benzoxazine capped hybrid.

4.6.5 Conclusion and Outlook

In summary, our PU/BOX-hybrid approach combines two totally different material classes in a straight forward and synergistic manner. We were able to achieve significantly improved reaction profiles and material properties compared to state of the

art polyurethane/benzoxazine-hybrids. The material design is extremely versatile and allows the tailored adjustment of product properties over a very broad range by simply changing the composition. Our investigations on the concentration and reactivity of hydroxyl groups clearly demonstrate the importance of hydrogen bonding in benzoxazine-based systems, and contribute to a better analytical understanding of the corresponding interaction strength. Strong differences cannot only be revealed and adjusted by different chemical structures, but also by choosing different reaction media, which is of tremendous importance for the post-modification of oligomerized and even polymerized benzoxazines. Finally, we want to emphasize that the capability of benzoxazine functionalized polyurethanes to attack electron rich phenolic structures and covalently bind to phenolic precursors like lignin in wood or phenol resins can be highly beneficial for many applications.

5 Experimental Section

5.1 Unique Curing Properties through Living Polymerization in Crosslinking Materials: Polyurethane Photopolymers from Vinyl Ether Building Blocks*

5.1.1 Materials

4-Hydroxybutyl vinyl ether (HBVE) (BASF, 99%, stabilized with 0.01% KOH) was stored over molecular sieve 4Å. Sodium (Merck, 99%) was cut into pieces under nitrogen atmosphere before use. 1,4-Butanediol diglycidyl ether (BDDGE) (Sigma-Aldrich, 95%), isophorone diisocyanate (IPDI) (Merck, 99%), polypropylene glycol (PPG) (Dow Chemical, Voranol 2000 L, 2000 g/mol), 1-heptanol (Acros Organics, 98%), dimethyltin dineodecanoate (Momentive, Fomrez catalyst UL-28), and 4,4'-dimethyl-diphenyliodonium hexafluorophosphate (Omnicat 440, IGM, 98%) were used as received.

5.1.2 Synthesis of Vinyl Ether Polyol (VEOH)

139.51 g (1.2 mol) of HBVE were placed in a 250 ml round-bottom flask equipped with a pressure equalizing dropping funnel containing 24.78 g (0.12 mol) of BDDGE. The apparatus was dried *in vacuo* and flushed with nitrogen. 7.00 g (0.3 mol) of sodium were added. After sodium was completely dissolved BDDGE was slowly added not exceeding 50 °C. The mixture was stirred at 50 °C for additional 30 min before 50 ml of water were added to hydrolyze residual alkoxide. The product was washed with brine and water several times and concentrated *in vacuo* to remove residual educts and water. Yield: 76%. Elemental analysis: C, 60.86; H, 9.71; O, 29.43 (calculated: C, 60.80; H,

* This section is based on the publication “*Unique Curing Properties through Living Polymerization in Crosslinking Materials: Polyurethane Photopolymers from Vinyl Ether Building Blocks*” by Stefan Kirschbaum, Katharina Landfester and Andreas Taden, published in *Angew. Chem. Int. Ed.* **2015**, 54, 5789-5792. Reprinted with permission. Copyright 2015 Wiley-VCH Verlag GmbH & Co. KGaA, Weinheim.

9.74; O, 29.45 for $C_{22}H_{42}O_8$). MS (ESI): $m/z = 457.4$ $[M+Na]^+$ (calculated: 457.3 for $C_{22}H_{42}O_8Na$), also a small signal of $m/z = 775.5$ indicates an oligomeric by-product ($n = 1$, see Figure 5.1) resulting from the addition of the product and HBVE to another BDDGE molecule (calculated: 775.5 for $C_{38}H_{72}O_{14}Na$).

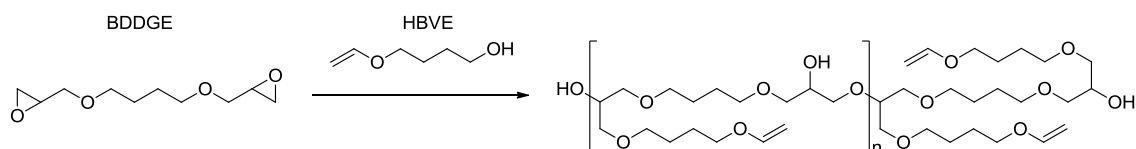


Figure 5.1. Oligomeric structures of VEPUs.

SEC is reported in Figure 5.2.

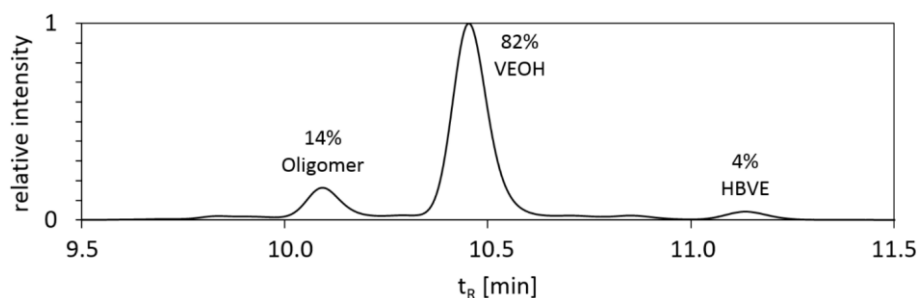


Figure 5.2. SEC analysis of the VEOH.

The chromatogram indicates the presence of residual HBVE and oligomers in the sample. For quantification the relative peak areas are displayed in the graph. An apparent number average molecular weight of $M_n = 650$ g/mol and a polydispersity index (PDI) of 1.1 were calculated. The deviation to the theoretical molecular weight is attributed to the difference in the hydrodynamic volume of the hydroxyl functional sample molecules to the polystyrene calibration standards in THF. From the relative peak areas a degree of oligomerization $n = 0.09$ can be calculated.

1H NMR ($CDCl_3$, 400 MHz): δ (ppm) = 1.6-1.8 (m, 12H, mid- CH_2 butyl), 2.69 (q, 2H, OH, H/D exchangeable), 3.4-3.55 (m, 16H, CH_2-O-CH_2), 3.70 (t, 4H, $CH_2-O-vinyl$), 3.94 (m, 2H, CH-O), 3.98 (dd, 1H, $CH_2=CH-O$ *trans*), 4.17 (dd, 1H, $CH_2=CH-O$ *cis*), 6.46 (dd, 1H, $CH_2=CH-O$ *gemi*). The spectrum is shown in Figure 5.3. Furthermore, a hydroxyl value of 260 mg_{KOH}/g_{sample} was determined via an acetylation method according to DGF C-V 17a (53). The corresponding molecular weight is 432 g/mol, if an OH functionality of 2 is assumed, which is in good accordance with the theoretical molecular weight of 434 g/mol.

5.1.3 Synthesis of the Hydrogenated Vinyl Ether Polyol (h-VEOH)

A solution of 500 ml VEOH (0.02 mol/l) in methanol was hydrogenated using the H-Cube continuous hydrogenation equipment HC-2.SS (ThalesNano). The required quantity of hydrogen is generated through electrolysis of water and consequently dried. The reactant solution was charged with hydrogen at 20 bar and 25 °C in a mixing chamber and passed with a constant flow rate of 1.2 ml/min through the reaction chamber containing a 10% Pd/C (CatCart 30) catalyst cartridge. Methanol was removed under reduced pressure. Yield: 98%. Elemental analysis: C, 60.29; H, 10.39; O, 29.32 (calculated: C, 60.25; H, 10.57; O, 29.18 for C₂₂H₄₆O₈). MS (ESI): $m/z = 461.5$ [M+Na]⁺ (calculated: 461.3 for C₂₂H₄₆O₈Na), also a small signal of $m/z = 781.6$ indicates the hydrated by-product, which was already present in the VEOH (calculated: 781.5 for C₃₈H₇₈O₁₄Na). ¹H (400 MHz, CDCl₃, 298 K) δ (ppm): 1.2 (t, 6H, CH₃), 1.64 (m, 12H, mid-CH₂ butyl), 2.46 (br, 2H, OH) 3.4-3.55 (m, 24H, CH₂-O-CH₂), 3.93 (tt, 2H, CH-O), 4.19 & 6.46 (residual vinyl ether, peak integration indicates 1-2% residue). The spectrum is shown Figure 5.3 in comparison to VEOH.

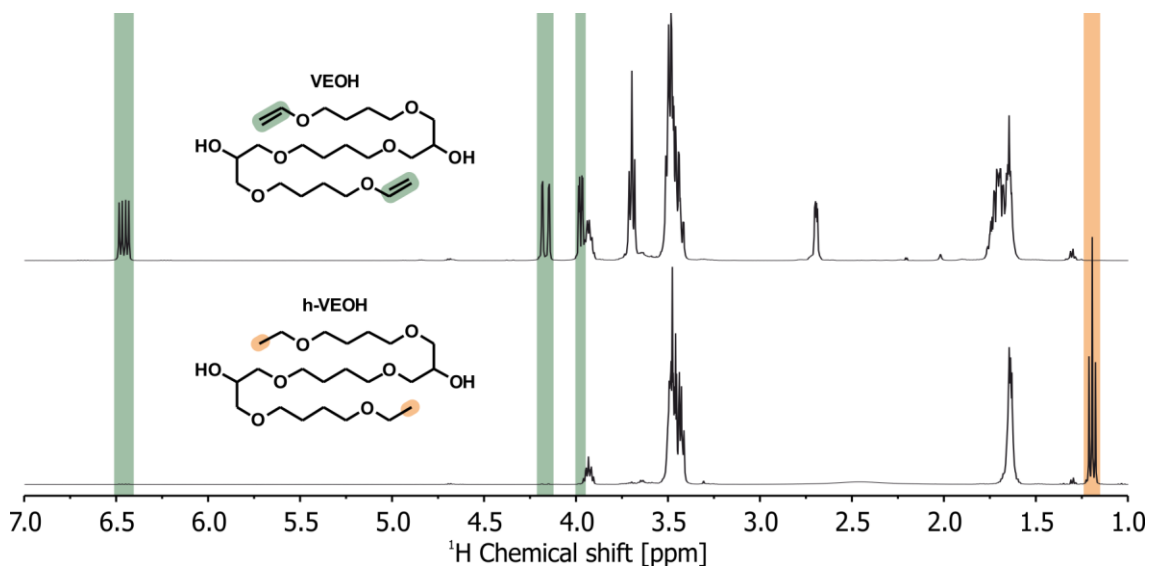


Figure 5.3. ¹H NMR spectra of VEOH and h-VEOH.

5.1.4 General Synthesis Procedure for Vinyl Ether Functionalized Polyurethanes (VEPUs)

The polyurethanes were synthesized in batches of 7 - 40 g each. The stoichiometry was calculated to yield a NCO-terminated prepolymer with a number average molecular

weight of $M_n = 5000$ g/mol. The polyols were placed in a small round bottom flask dried at 75 °C under vacuum. Then the aliphatic isocyanate component was added at 40 °C. A sample of the mixture was taken for IR spectroscopy. The band corresponding to the stretching vibration of $N=C=O$ at about 2250 cm^{-1} was integrated and correlated to the initial concentration of isocyanate groups. Then the catalyst was added (50 mg/100 g product, as a 50% solution in dry acetone) and the mixture was gently heated to 80 °C. After 1 h reaction time an aliquot was taken to confirm the desired isocyanate concentration via IR spectroscopy. 90% of the stoichiometric amount of the end-capping agent were added to avoid an excess of hydroxyl functionality in the product and after 30 min another sample was taken to confirm almost complete conversion of the isocyanate via IR spectroscopy. Yield: 95%. The SECs are reported in Figure 5.4 and IR spectra are provided in Figure 5.5.

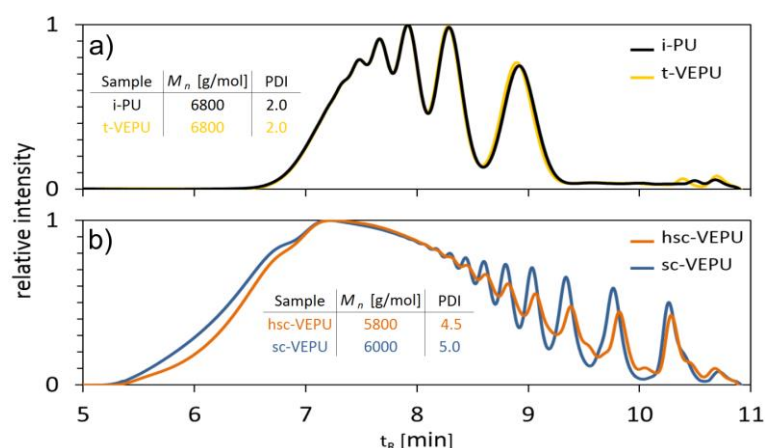


Figure 5.4. SEC analysis of the polyurethane prepolymers.

The molecular weights obtained are in good accordance with the theoretical number molecular weight of $M_n = 5000$ g/mol. The overall deviation to the higher apparent molecular weights are attributed to the difference in the hydrodynamic volume between polyurethanes and the polystyrene calibration standards. The same accounts for the difference between simple linear polyurethanes (a) and the side-chain functionalized polyurethanes with increased urethane group density (b). The broadened molecular weight distribution for the sc-VEPU and the hsc-VEPU is a consequence of the low molecular weight of the VEOH compared to the PPG, which results in a larger number of average repeating units and hence, generally causes increased PDIs in polyaddition reactions.

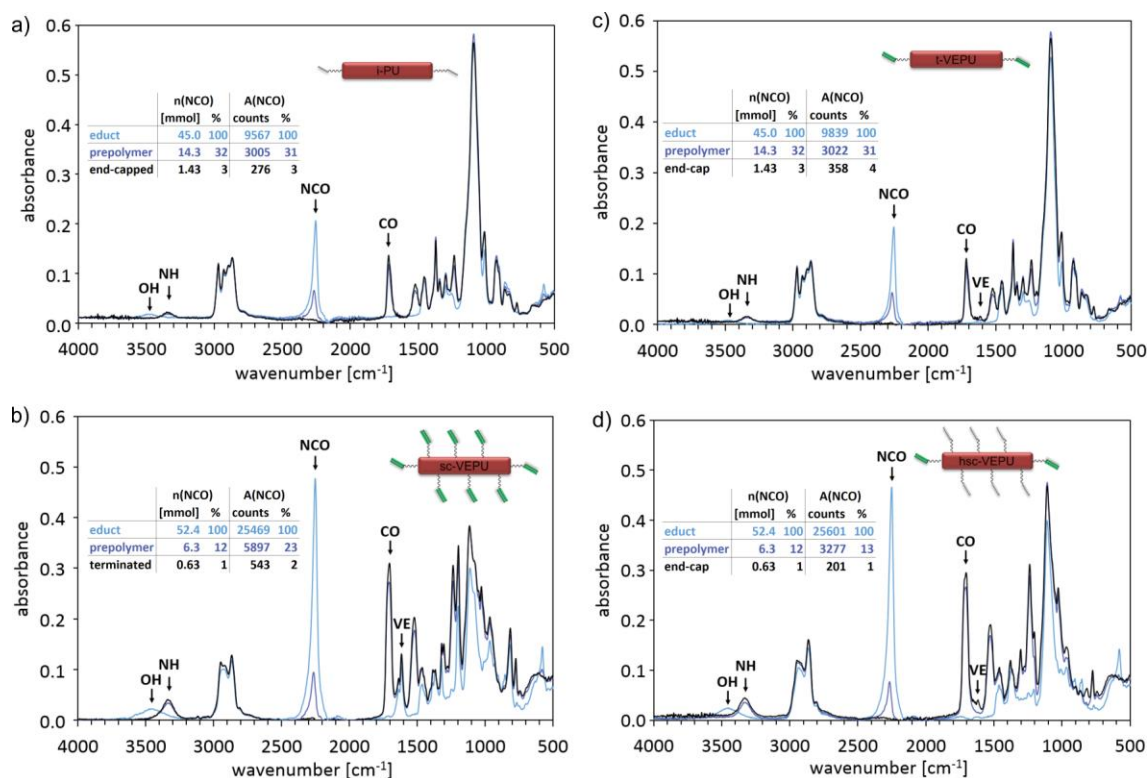


Figure 5.5. IR spectra for the synthesis of the i-PU (a), t-PU (b), sc-VEPU (c) and hsc-VEPU (d).

Spectra were recorded directly after the addition of the isocyanate (educt), before addition of the terminating agent (prepolymer) and after complete reaction with the terminating agent (terminated). Some structural relevant peaks are assigned. The integrated peak areas corresponding to the N=C=O stretching vibration at 2250 cm^{-1} are displayed in the top left corner of each diagram along with the associated molar amounts calculated from the stoichiometry. It can be observed that the reactions were well controlled for all prepolymers.

5.1.5 Formulation of the VEPUs with Photoinitiator

The polyurethane was formulated with 1 wt% of 4,4'-dimethyl-diphenyliodonium hexafluorophosphate and the mixture was dissolved in the same volume of acetone to support dissolving the photoinitiator in the viscous polyurethane. Acetone was subsequently removed *in vacuo*.

5.1.6 Size Exclusion Chromatography (SEC)

SEC was performed using a Waters Acquity APC system equipped with a set of three Waters APC XT columns (450/125/45 Å) and a Waters APC RI detector operated at 40 °C. THF was used as eluent at a flow rate of 0.5 ml/min. Calibration of molecular weights refers to polystyrene standards (162 - 1 210 000 Da provided by PPS).

5.1.7 UV/NIR-Rheology

The simultaneous measurement of viscoelastic properties and near-infrared spectra upon UV-initiation was performed using a similar rheometer setup as described by the group of Scherzer¹⁵⁷. An Anton Paar MCR 302 rheometer was used in combination with a Bruker MPA FT-NIR spectrometer and an Omnicure S 2000 SC light source, both triggered via the rheometer software. The sample was placed at the center of the quartz bottom plate and an aluminum plate with 25 mm diameter was used as mobile top plate at an initial gap of 0.3 mm. A normal force of zero was applied for automatic gap control upon sample shrinkage to avoid additional stress or delamination. A ramped measurement profile was applied to ensure linear viscoelastic behavior and to remain within instrument limitations, as the sample moduli increase over several orders of magnitude upon curing. Before UV-irradiation a sinusoidal strain of 10% was applied for 30 s with a frequency of 10 Hz. The UV-light source was set to irradiate for only 10 s. The intensity of 0.40 mW/cm² UVC (189 mW/cm² UVA-C) was controlled regularly above the quartz plate via a spectral radiometer (OpSyTec Dr. Göbel, see Figure 5.6). Upon UV-irradiation the strain was linearly reduced from 10% to 0.1% within 210 seconds and mechanical data were recorded at a rate of 1 s⁻¹ (no ramp was applied for the i-PU). Some samples were further irradiated for another 10 s and dark curing was recorded for 240 s at a constant strain of 0.1% after each irradiation. No attempt was made to remove dissolved gases from the samples and the measurements were carried out under instrumental air atmosphere (H₂O: 1.1 mg/m³). For comparison one experiment was performed under nitrogen atmosphere (N₂: <99.9996%, O₂: <0.5 ppm, H₂O: <1 ppm).

NIR spectra were recorded with a resolution of 16 cm⁻¹ at a constant sampling rate of about 2 spectra s⁻¹. The relative vinyl ether concentration was calculated from the integrated peak area of the C-H-stretching vibration at about 6200 cm⁻¹ (bond of integration = 6130 cm⁻¹ - 6250 cm⁻¹).^{150, 152} The average value for this peak in the spectra before irradiation was set to 100%.

5.1.8 Differential Scanning Calorimetry (DSC)

The DSC analysis was executed using a Netzsch Photo-DSC 204 F1 Phoenix equipped with an Omnicure S 2000 SC light source. Samples of 10 - 15 mg were prepared from the uncured materials. Measurement of the initial glass transition temperatures (T_{g0}) was performed using a modulated heating rate of 10 K/min with an amplitude of 0.5 K and a cycle time of 60 s from -75 °C to 60 °C. To initiate photo-curing the sample was exposed to UV-light for 10 s at the indicated curing temperatures and the isothermal heat flow was monitored for 5 min. The irradiation was repeated 9 times before the glass transition temperature (T_{g1} , determined from the reversible heat flow) and thermally induced post-curing (T_{Onset} , ΔH , determined from the irreversible heat flow) were examined using a similarly modulated heating rate of 10 K/min from -75 °C to 100 °C. The final glass transition temperature (T_{g2}) was determined from the second heating run after exposure to UV-light from -75 °C to 120 °C. An intensity of 0.16 mW/cm² UVC (194 mW/cm² UVA-C) was measured below the glass optics of the DSC-lid via a spectral radiometer (OpSyTec Dr. Göbel, see Figure 5.6), to get the best possible approximation of the intensity at the sample surface. During the entire measurement the measuring cell was purged with instrumental air (H₂O: 1.1 mg/m³) at a flow rate of 20 ml/min.

To determine the durability of the post-curing ability some samples were stored isotherm, at a constant purge gas (instrumental air, H₂O: 1.1 mg/m³) flow rate of 20 ml/min within the DSC setup. In addition to the defined storing time about 3 h passed between the first irradiation and the determination of the thermally induced post-curing process. 50 min need to be calculated for the 10 irradiation cycles. Afterwards the sample was cooled with -10 K/min and stored for 25 min at -75 °C. Additionally, an isotherm modulation was performed for 5 min before a modulated heating rate of 10 K/min was applied.

5.1.9 Comparability of UV/NIR-Rheology and Photo-DSC

Figure 5.6 shows the absorption spectrum of the photoinitiator in comparison to the emission spectra of the Omnicure S 2000 SC light sources, recorded in the rheometer and DSC setups. The absorption spectrum of Omnicat 440 was measured using a Perkin

Elsmar Lambda 850 UV/VIS spektrometer at a concentration of 24.4 g/l in acetonitrile and the emission spectra were recorded with a spectral radiometer (OpSyTec Dr. Göbel) as described in Chapter 5.1.7 and 0. Although the same type of light source with a similar lifecycle of the bulbs was used it can be seen that the relevant UVC intensity, which is responsible for the photoinitiator decomposition, is significantly higher in the rheometer. This observation can be explained by different setups in terms of optics and light guide fibers. Therefore, it needs to be emphasized that both evaluations are not totally comparable even when the irradiation time and temperature are equal.

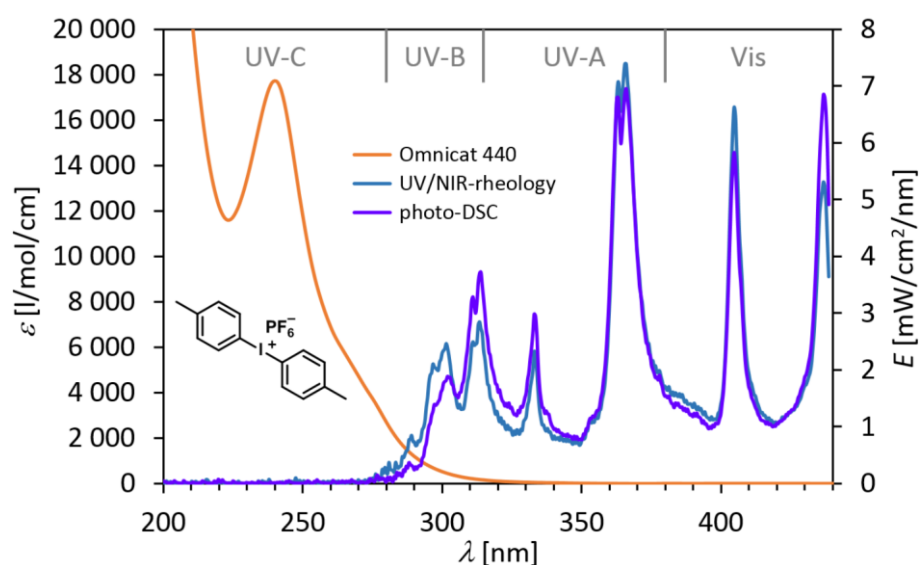


Figure 5.6. Emission spectra in the rheometer and DSC instrument in comparison to the absorption spectrum of the applied photoinitiator. The obtained curing data from both instruments are not totally comparable due to the divergent intensities in the relevant UVC spectral range.

5.2 Vinyl Ether-Functional Polyols as Building Blocks for UV-Curable Polyurethanes and Isocyanate-Free Polyhydroxyurethanes*

5.2.1 Materials

4-Hydroxybutyl vinyl ether (HBVE, BASF, 99%, stabilized with 0.01% KOH), epichlorohydrin (ECH, Solvay, 99.8%), tetrabutylammonium bromide (TBAB, Merck, 99%), tetraethylammonium bromide (TEAB, Merck, 99%), 1,4-butanediol diglycidyl ether (BDDGE, Sigma-Aldrich, 95%), di(trimethylolpropane) (di-TMP, Sigma-Aldrich, 97%), ethyl chloroformiate (Alfa Aesar, 97%), triethylamine (Acros Organics, 99%), ethylene glycol bis(3-aminopropyl) ether (EGBAPE, Huntsman, Jeffamine EDR-176), 3-aminopropyl vinyl ether (APVE, BASF, 99.7%), hexamethylene diisocyanate (HDI, Acros Organics, 99%), dimethyltin dineodecanoate (Momentive, Fomrez catalyst UL-28), methanol (VWR Chemicals), 10-[1,1'-biphenyl]-4-yl-2-(1-methylethyl)-9-oxo-9H-thioxanthenium hexafluorophosphate (Omnicat 550, IGM), dimercapto-1,8-dioxo-3,6-octane (DMDO, Arkema), pentaerythritoltetra(3-mercaptopropionat) (Bruno Bock, Thiocure PETMP, 95%) and 2,2'-Azobis(2,4-dimethylvaleronitrile) (Wako V65) were used as received.

5.2.2 Synthesis of 4-Glycidylether Butyl Vinyl Ether (GEBVE)

GEBVE was synthesized similar to a procedure described in the literature.⁸¹ 116.16 g (1 mol) of HBVE and 10.51 g (0.05 mol) of tetrabutylammonium bromide were placed in a 1 l round-bottom flask equipped with a dropping funnel. A mixture of 300 ml toluene and 300 ml 50 wt% aqueous NaOH was added. The reaction mixture was cooled with an ice bath to 5 °C. 148.16 g (2 mol) epichlorohydrin were added slowly

* This section is based on the publication manuscript "Vinyl Ether Functional Polyols as Building Blocks for UV-Curable Polyurethanes and Isocyanate-Free Polyhydroxyurethanes" by Stefan Kirschbaum, Katharina Landfester and Andreas Taden. Publication was withheld for the submission of the patent "Herstellung oder Härtung von Polymeren mittels Thiol-En Polyadditionsreaktionen", filed on 11.11.2015, filing no. EP 15194064.0, internal no. PT033463.

while stirring fast. After complete addition the emulsion was stirred for 16 h without cooling. The organic phase was washed several times with brine and water. Solvents were removed under reduced pressure and the product was purified via vacuum distillation to yield a clear, colorless liquid. Yield: 66%. Elemental analysis: C, 62.55; H, 9.50; O, 27.95 (calculated: C, 62.77; H, 9.36; O, 27.87 for $C_9H_{16}O_3$). MS (CI): $m/z = 190.2$ $[M+NH_4]^+$ (calculated: 190.1 for $C_9H_{16}O_3NH_4$). 1H NMR (400 MHz, $CDCl_3$, 298 K) δ (ppm): 1.72 (m, 4H, mid- CH_2 butyl), 2.61 (dd, 1H, CH_2 epoxide), 2.79 (dd, 1H, CH_2 epoxide), 3.14 (m, 1H, CH epoxide), 3.38 (dd, 1H, O- CH_2 -epoxy), 3.53 (m, 2H, CH_2 -O-glycidyl ether), 3.65-3.75 (m, 2H, CH_2 -O-vinyl + 1H, O- CH_2 -epoxy), 3.97 (dd, 1H, $CH_2=CH-O$ *trans*), 4.17 (dd, 1H, $CH_2=CH-O$ *cis*), 6.46 (dd, 1H, $CH_2=CH-O$ *gemi*) (see Figure 5.7). GC-FID analysis indicated a purity of 99%.

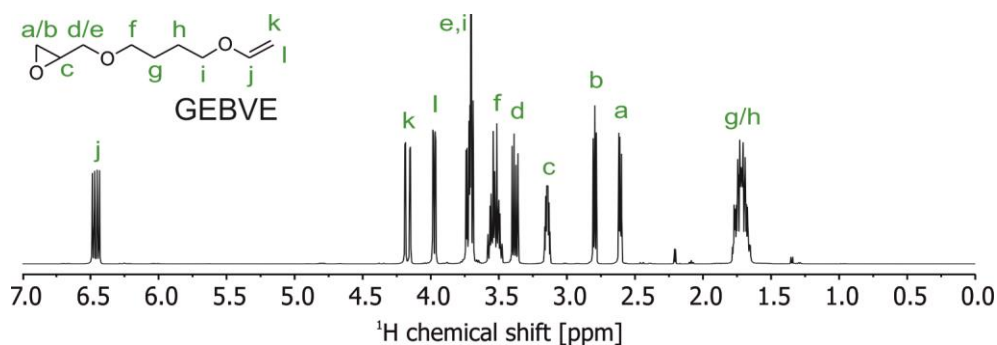


Figure 5.7. 1H NMR spectrum of GEBVE.

5.2.3 Synthesis of 4-Glycidylcarbonate Butyl Vinyl Ether (GCBVE)

GCBVE was synthesized via CO_2 insertion to 17.22 g (0.1 mol) of GEBVE using an atmospheric pressure process referring to that described by Caló et al.¹¹⁵ The reaction progress was observed by the disappearance of the epoxy peaks at 760 cm^{-1} and 910 cm^{-1} and the evolution of carbonate $C=O$ stretching vibration at 1780 cm^{-1} via IR spectroscopy. The product was dissolved in 50 ml ethyl acetate, washed with water several times and dried *in vacuo* to yield a clear, colorless liquid. Yield: 90%. Elemental analysis: C, 55.66; H, 7.65; O, 36.69 (calculated: C, 55.55; H, 7.46; O, 37.00 for $C_{10}H_{16}O_5$). MS (CI): $m/z = 234.2$ $[M+NH_4]^+$ (calculated: 234.1 for $C_{10}H_{16}O_5NH_4$). 1H NMR (400 MHz, $CDCl_3$, 298 K) δ (ppm): 1.70 (m, 4H, mid- CH_2 butyl), 3.55 (t, 2H, CH_2 -O-glycidylcarbonat), 3.61 (dd, 1H, O- CH_2 -cyclic carbonate), 3.69 (m, 2H, CH_2 -O-vinyl + 1H, O- CH_2 -cyclic carbonate), 3.98 (dd, 1H, $CH_2=CH-O$ *trans*), 4.17 (dd,

1H, CH₂=CH-O *cis*), 4.39 (dd, 1H, CH₂ cyclic carbonate), 4.50 (t, 1H, CH₂ cyclic carbonate), 4.81 (m, 1H, CH cyclic carbonate) 6.46 (dd, 1H, CH₂=CH-O *gemi*), 2.61, 2.80, 3.14, 3.38 (residual epoxy signals of about 3%) (see Figure 5.8). GC-FID analysis indicated a purity of 96% and 3% residual GEBVE.

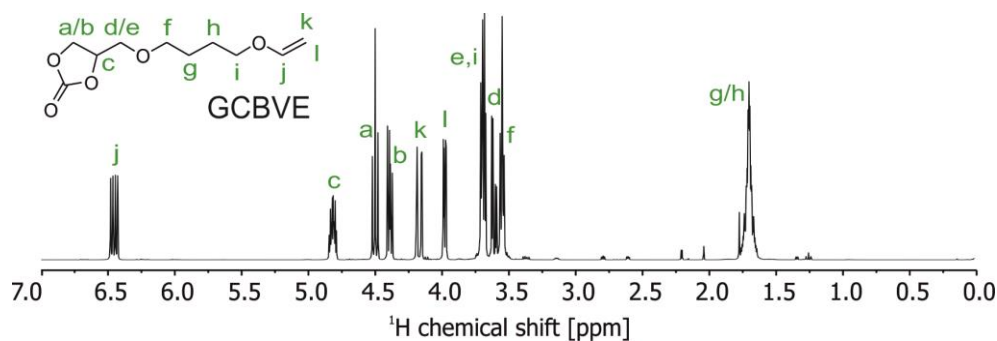


Figure 5.8. ¹H NMR spectrum of GCBVE.

5.2.4 Synthesis of 1,4-Butanedioldiglycidylcarbonate (BDDGC)

BDDGC was synthesized via CO₂ insertion to 24.27 g (0.12 mol) BDDGE using an atmospheric pressure process referring to that described in by Caló et al.¹¹⁵ The reaction progress was observed by the disappearance of the epoxy peaks at 760 cm⁻¹ and 910 cm⁻¹ and the evolution of carbonate C=O stretching vibration at 1780 cm⁻¹ via IR spectroscopy. The product was dissolved in 50 ml ethyl acetate, washed with water several times and dried *in vacuo* to yield a white solid. Yield: 81%. Elemental analysis: C, 49.51; H, 6.29; O, 44.20 (calculated: C, 49.65; H, 6.25; O, 44.10 for C₁₂H₁₈O₈). MS (CI): *m/z* = 308.1 [M+NH₄]⁺ (calculated: 308.1 for C₁₂H₁₈O₈NH₄). ¹H NMR (400 MHz, CDCl₃, 298 K) δ (ppm): 1.65 (m, 4H, mid-CH₂ butyl), 3.54 (t, 4H, CH₂-O-glycidylcarbonat), 3.59 (dd, 2H, O-CH₂-cyclic carbonate), 3.69 (dd, 2H, O-CH₂-cyclic carbonate), 4.39 (m, 2H, CH₂ cyclic carbonate), 4.50 (t, 2H, CH₂ cyclic carbonate), 4.82 (m, 2H, CH cyclic carbonate) (see Figure 5.9).

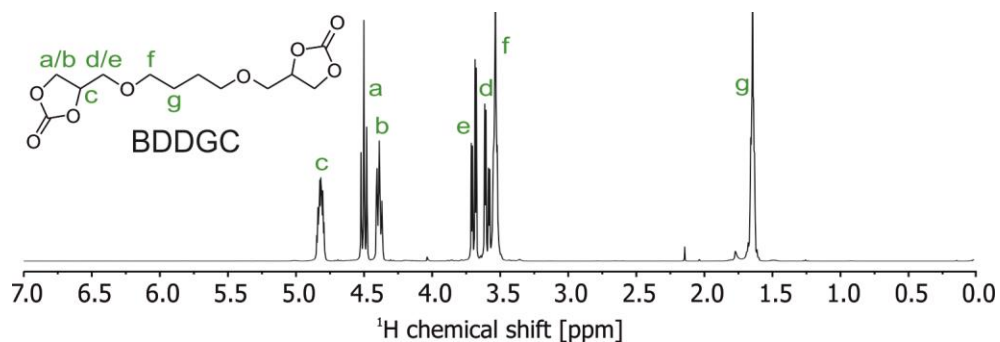


Figure 5.9. ¹H NMR spectrum of BDDGC.

5.2.5 Synthesis of di-Trimethylolpropanedicarbonate (di-TMPDC)

Di-TMPDC was synthesized according to the literature.²³² 37.55 g (0.15 mol) of di-TMP were dissolved in 1 l dry THF and cooled to -10 °C. 97.67 g (0.9 mol) of ethyl chloroformate were added dropwise at that temperature. Subsequently, triethylamine was added under the same conditions before the mixture was stirred without cooling overnight. The mixture was filtered and washed with water. The organic solution was concentrated under reduced pressure and the product was precipitated in diethyl ether and recrystallized from THF to yield a white solid. Yield: 76%. Elemental analysis: C, 55.69; H, 7.37; O, 36.94 (calculated: C, 55.62; H, 7.33; O, 37.05 for C₁₄H₂₂O₇). MS (CI): *m/z* = 320.1 [M+NH₄]⁺ (calculated: 302.2 for C₁₄H₂₂O₇NH₄). ¹H NMR (400 MHz, CDCl₃, 298 K) δ (ppm): 0.95 (t, 6H, CH₃), 1.49 (q, 4H, CH₂-CH₃), 3.49 (s, 4H, CH₂-O), 4.22 (dd, 8H, CH₂ cyclic carbonate) (see Figure 5.10).

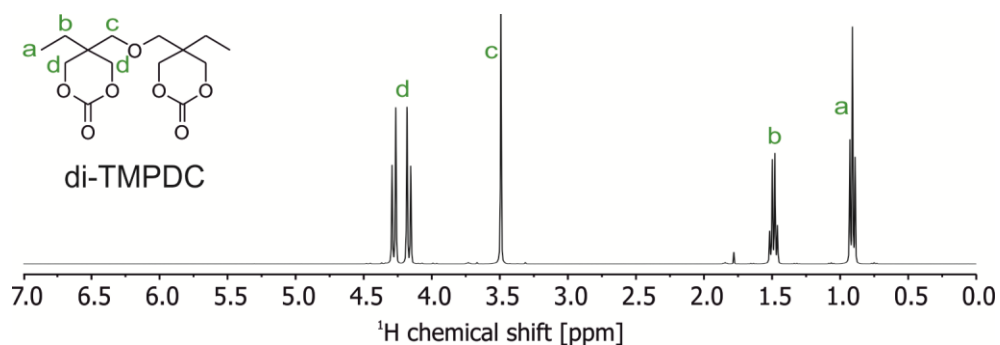


Figure 5.10. ¹H NMR spectrum of di-TMPDC.

5.2.6 Synthesis of the Vinyl Ether Polyol P1

3.26 g (18.5 mmol) of EGBAPE and 8.00 g (37.5 mmol) of GCBVE were mixed and heated to 80 °C under nitrogen atmosphere for 15 h. Conversion was followed via IR spectroscopy using the C=O stretching vibration of the six-membered carbonate and the urethane at 1735 cm⁻¹ and 1690 cm⁻¹, respectively. IR spectrum is provided in Figure 5.18, ¹H NMR and ¹³C NMR spectra are shown in Figure 5.11 and Figure 5.12, respectively and HPLC-MS analysis is provided in Figure 5.21.

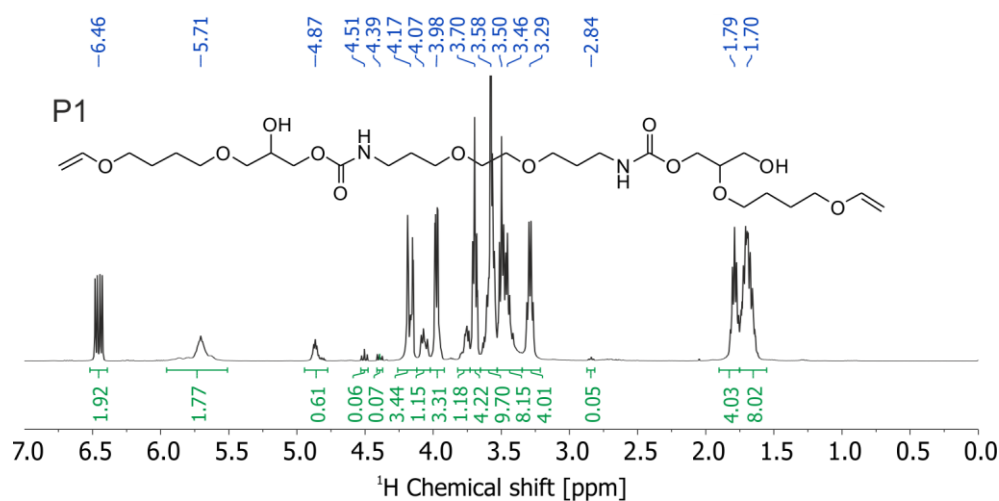


Figure 5.11. ¹H NMR spectrum of P1 (C₂₈H₅₂N₂O₁₂).

An idealized structure of the product is depicted within the spectrum. Upon ring-opening of the cyclic carbonate two isomeric structures can be formed as indicated in the displayed structure. The entire spectral region was set to equal 52 hydrogen atoms. Several hydrogen atoms with similar chemical shifts from the product, its isomers and by-products make it difficult to provide detailed assignments. However, some peaks are clearly related to the indicated structure such as vinyl ether peaks at 3.98 ppm, 4.17 ppm and 6.46 ppm.

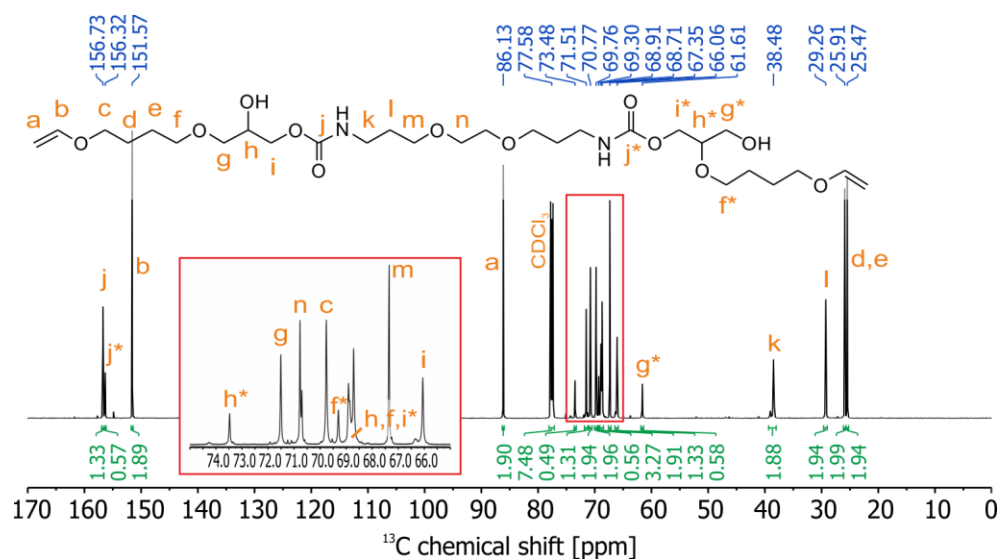


Figure 5.12. Quantifiable ^{13}C NMR spectrum of P1 ($\text{C}_{28}\text{H}_{52}\text{N}_2\text{O}_{12}$).

One isomeric structure of the product is depicted within the spectrum. The entire spectral region excluding the CDCl_3 -peak at 77.58 ppm was set to equal 28 carbon atoms. Upon ring-opening of the cyclic carbonate two isomeric structures of the glyceryl unit can be formed as depicted in the displayed molecule. The ratio of secondary hydroxyl groups to primary hydroxyl groups is about 70/30, which is consistent with the literature.^{82, 110}

5.2.7 Synthesis of the Vinyl Ether Polyol P2

14.15 g (50 mmol) of BDDGC and 11.13 g (110 mmol) of APVE were mixed and heated to 80 °C under nitrogen atmosphere for 22 h. Conversion was followed via IR spectroscopy using the $\text{C}=\text{O}$ stretching vibration of the five-membered carbonate and the urethane at 1780 cm^{-1} and 1690 cm^{-1} , respectively. IR spectrum is provided in Figure 5.19, ^1H NMR and ^{13}C NMR spectra are shown in Figure 5.13 and Figure 5.14, respectively and HPLC-MS analysis are provided in Figure 5.22

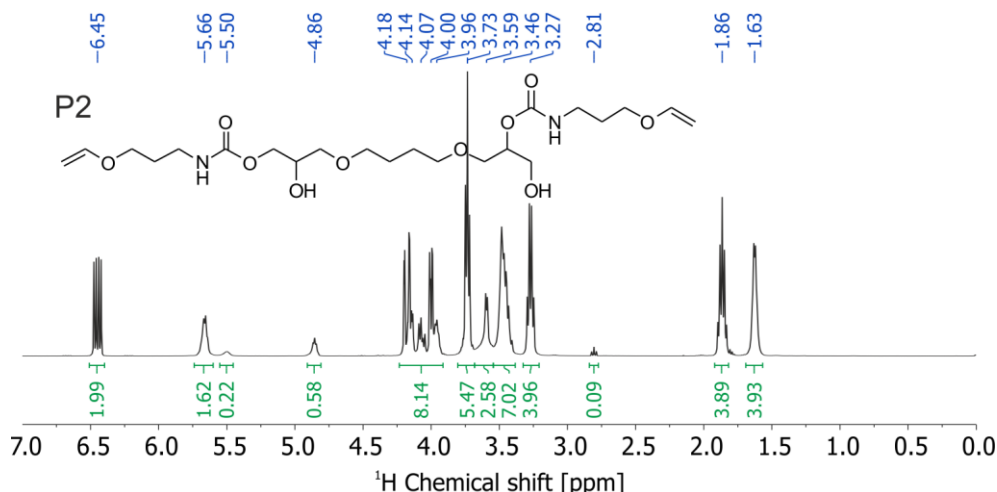


Figure 5.13. ^1H NMR spectrum of P2 ($\text{C}_{22}\text{H}_{40}\text{N}_2\text{O}_{10}$).

An idealized structure of the product is depicted within the spectrum. Upon ring-opening of the cyclic carbonate two isomeric structures can be formed as indicated in the displayed structure. The entire spectral region was set to equal 40 hydrogen atoms. Several hydrogen atoms with similar chemical shifts from the product, its isomers and by-products make it difficult to provide detailed assignments.

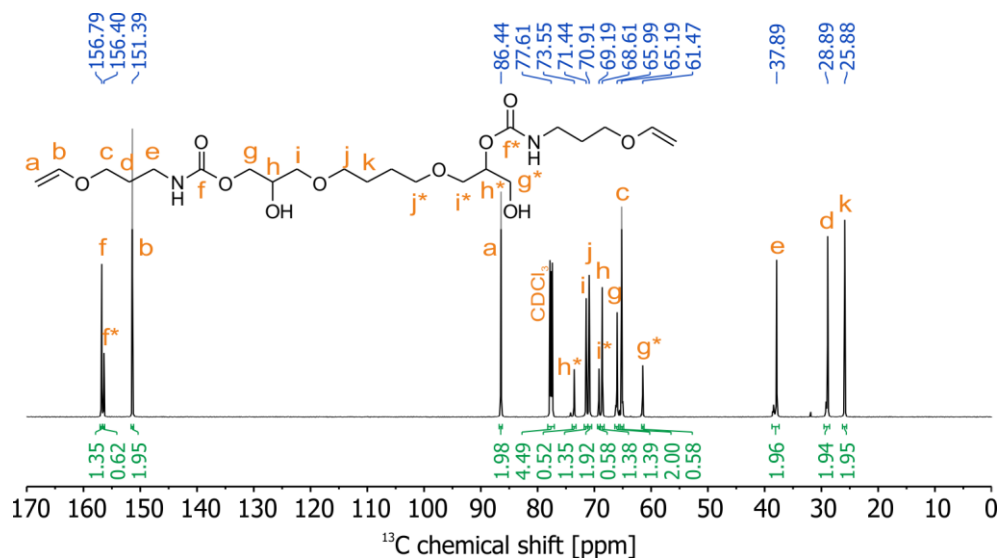


Figure 5.14. Quantifiable ^{13}C NMR spectrum of P2 ($\text{C}_{22}\text{H}_{40}\text{N}_2\text{O}_{10}$).

One isomeric structure of the product is depicted within the spectrum. The entire spectral region excluding the CDCl_3 -peak at 77.61 ppm was set to equal 22 carbon atoms. Upon ring-opening of the cyclic carbonate two isomeric structures of the glyceryl unit can be formed as depicted in the displayed molecule. The ratio of secondary hydroxyl groups to primary hydroxyl groups is about 70/30, which is consistent with the literature.^{82, 110}

5.2.8 Synthesis of the Vinyl Ether Polyol P3

9.10 g (30 mmol) of di-TMPDC and 6.09 g (60 mmol) of APVE were mixed and heated to 80 °C under nitrogen atmosphere for 22 h. Conversion was followed via

IR spectroscopy using the C=O stretching vibration of the five-membered carbonate and the urethane at 1780 cm^{-1} and 1690 cm^{-1} , respectively.. IR spectrum is provided in Figure 5.20, ^1H NMR and ^{13}C NMR spectra are shown in Figure 5.15 and Figure 5.16, respectively and HPLC-MS analysis are provided in Figure 5.23

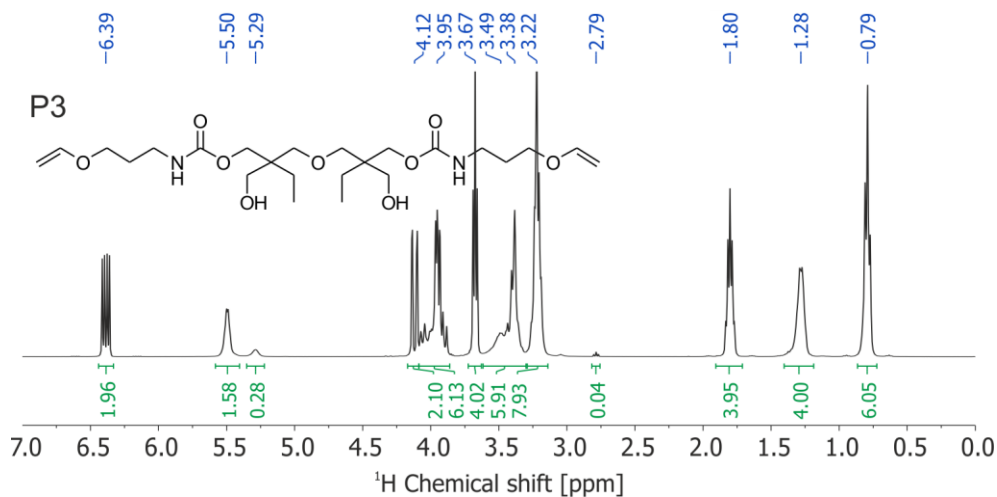


Figure 5.15. ^1H NMR spectrum of P3 ($\text{C}_{24}\text{H}_{44}\text{N}_2\text{O}_9$).

An idealized structure of the product is depicted within the spectrum. Upon ring-opening of the cyclic carbonate two isomeric structures can be formed as indicated in the displayed structure. The entire spectral region was set to equal 4 hydrogen atoms. Several hydrogen atoms with similar chemical shifts from the product, its isomers and by-products make it difficult to provide detailed assignments.

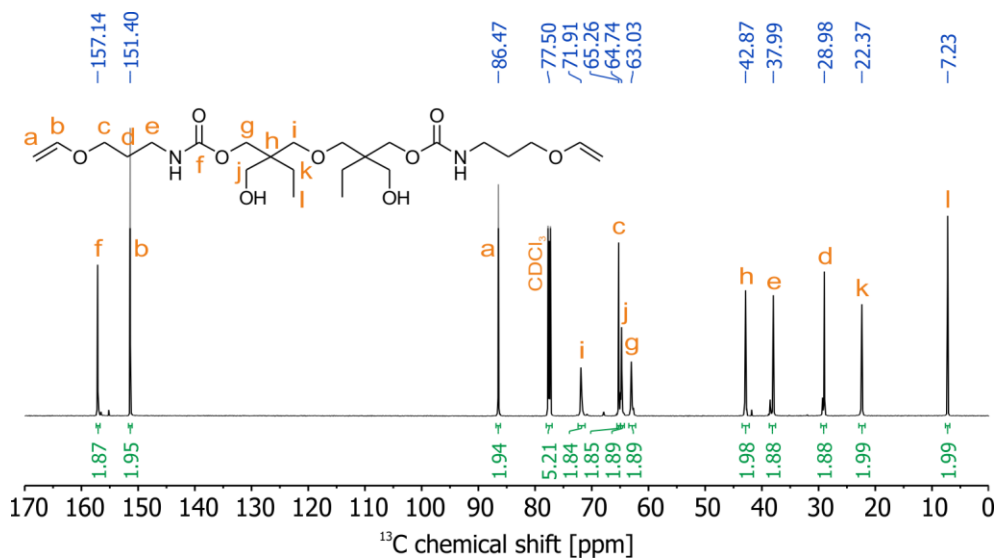


Figure 5.16. Quantifiable ^{13}C NMR spectrum of P3 ($\text{C}_{24}\text{H}_{44}\text{N}_2\text{O}_9$).

The structure of the product is depicted within the spectrum. The entire spectral region excluding the CDCl_3 -peak at 77.50 ppm was set to equal 24 carbon atoms. The symmetric six-membered carbonate does not form isomers upon ring-opening. Therefore the spectrum consists of less peaks.

5.2.9 Synthesis of the Vinyl Ether Functionalized Polyurethanes PU1, PU2, PU3

The polyurethanes PU1 - PU3 were synthesized in batches of 10-12 g from the corresponding vinyl ether polyols P1 - P3 using an excess of HDI. The stoichiometry was calculated to yield a NCO-terminated polymer with a number average molecular weight of $M_n = 2000$ g/mol. The polyols were placed in a small round bottom flask, dried at 75 °C under reduced pressure and cooled to 40 °C. HDI was added and a sample was subjected to IR spectroscopy. The band corresponding to the stretching vibration of N=C=O at about 2250 cm^{-1} was integrated and can be correlated to the initial isocyanate concentration. 25 mg dimethyltin dineodecanoate / 100 g batch were added as catalyst and the mixture was gently heated to 80 °C. The conversion of terminal isocyanate groups was monitored via IR spectroscopy. After 1h reaction time 0.5 g methanol were added to convert terminal isocyanate groups and 3 wt% of Omniscat 550 were added as photoinitiator after IR spectroscopy indicated the complete reaction. The excess of methanol was removed under reduced pressure

5.2.10 Synthesis of the Linear Polyhydroxyurethane PHU3

4.28 g (8.5 mmol) of P3, 1.55 g (8.5 mmol) of DMDO and 0.058 g (1 wt%) of 2,2'-Azobis(2,4-dimethylvaleronitrile) were placed in a 100 ml triple-necked flask and dissolved in 50 ml THF and purged with nitrogen. A Loctite 97034 equipped with an UVC 97327 light guide was joined to the centered neck and the reaction was induced via UV-irradiation for 900 s at room temperature while stirring with 500 rpm. THF was removed under reduced pressure and IR spectroscopy indicated consumption of vinyl ether and thiol functional groups (see Figure 5.17).

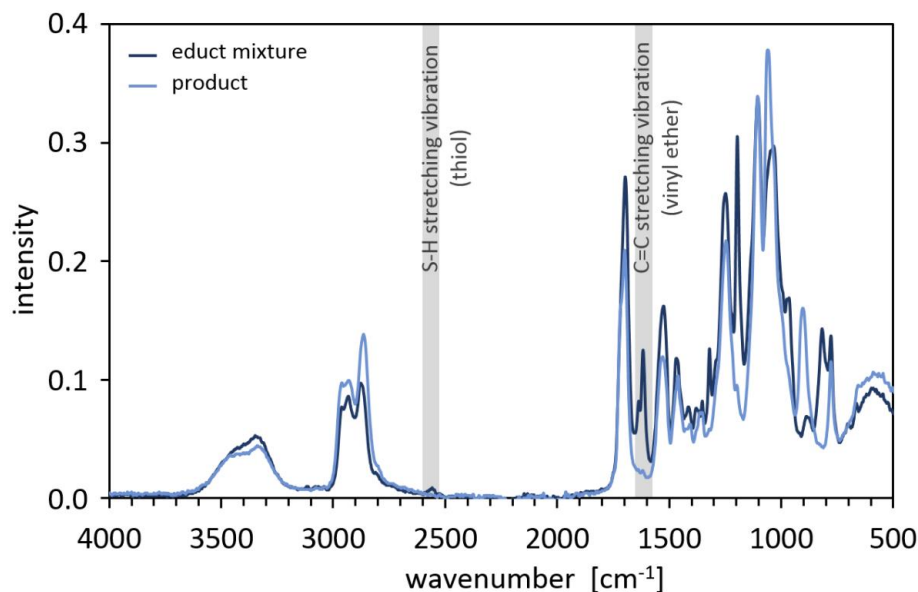


Figure 5.17. IR spectra of the polyhydroxyurethane (PHU3) synthesis.

The educt mixture shows the highlighted absorption bands of the SH stretching vibration (thiol) at 2560 cm^{-1} and the C=C stretching vibration (vinyl ether) at 1620 cm^{-1} . The reaction product after UV-induced thiol-ene reaction indicates the consumption of both functional groups.

5.2.11 Synthesis of the Crosslinked Polyhydroxyurethane c-PHU3

1.0086 g (2 mmol) of P3, 0.4319 g (1 mmol) of PETMA and 0.0073 g (0.5 wt%) of were mixed and a sample was cured in the rheometer setup.

5.2.12 UV/NIR-Rheology

Rheological and NIR spectroscopic investigations of the UV-induced curing reaction were performed using an Anton Paar MCR 302 rheometer coupled to a Bruker MPA FT-NIR spectrometer and an Omnicure S 2000 SC light source. The instrument was set up as previously described¹⁷⁵ in a plate/plate geometry using a quartz glass bottom plate and a disposable aluminum top plate with a diameter of 25 mm at an initial gap distance of 100 μm . A normal force of zero was applied to avoid stress caused from sample contraction or expansion. The measurement was performed at $75\text{ }^{\circ}\text{C}$ under instrumental air atmosphere (H_2O : 1.1 mg/m^3). Initially, data were recorded every 5 s with a sinusoidal strain of 10% at frequency of 10 Hz. The sample was then irradiated for 30 s with an intensity of 189 mW/cm^2 UVA-C. This intensity was determined at the surface of the quartz plate using a spectral radiometer (OpSyTec Dr. Göbel). Upon irradiation mechanical data were recorded at a rate of 1 s^{-1} and the sinusoidal strain was linearly

ramped to 0.5% within 210 s and kept constant for another 360 s. NIR spectra were recorded with a rate of about 2 s^{-1} at a resolution of 16 cm^{-1} . The conversion of the vinyl ether double bond was followed by the characteristic absorption of the C-H stretching vibration overtone at 6200 cm^{-1} (bond of integration = $6135 \text{ cm}^{-1} - 6250 \text{ cm}^{-1}$). The sample was subsequently cooled to $5 \text{ }^\circ\text{C}$ at a cooling rate of $2 \text{ }^\circ\text{C}/\text{min}$ and again heated to $75 \text{ }^\circ\text{C}$ with a heating rate of $2 \text{ }^\circ\text{C}/\text{min}$ for the determination of the glass transition temperatures.

For the non-living thiol-ene curing reaction the irradiation period was increased to 100 s in an otherwise equal method.

5.2.13 IR Spectroscopy

Measurements were carried using a Bruker ALPHA FT-IR spectrometer equipped with an ATR unit. 24 spectra were accumulated at a resolution of 4 cm^{-1} . IR spectra of several educts and products are provided in Figure 5.18 - Figure 5.20.

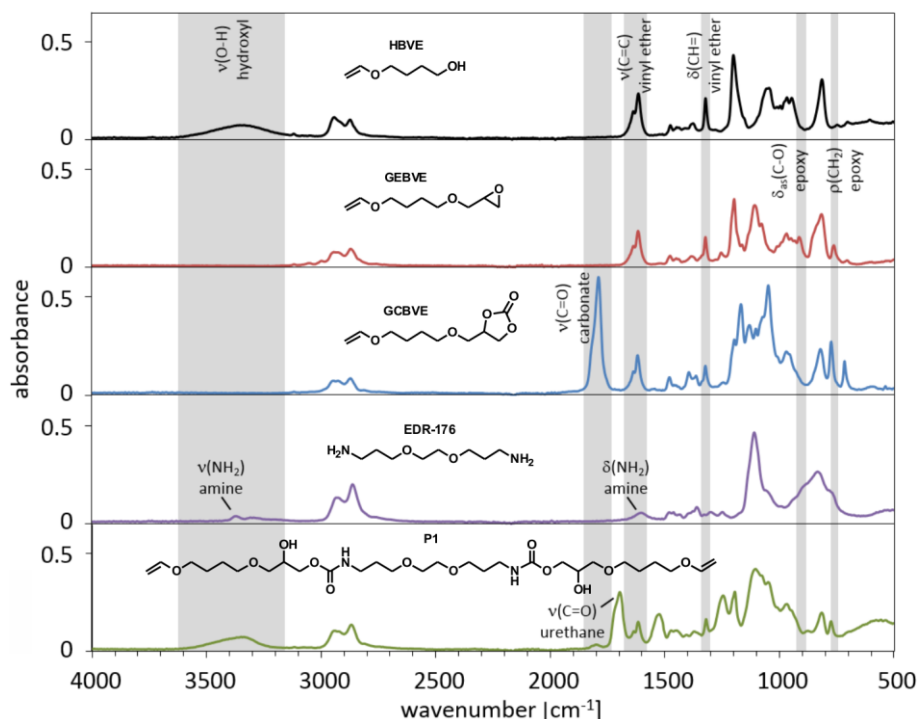


Figure 5.18. IR spectra of educts, intermediates and products related to the multi-step synthesis of the vinyl ether functionalized polyol P1. Some structural assignments are provided for important functional groups and the absorption bands are highlighted in the spectrum. The appearance and disappearance of these bands was used to monitor the reaction progress.

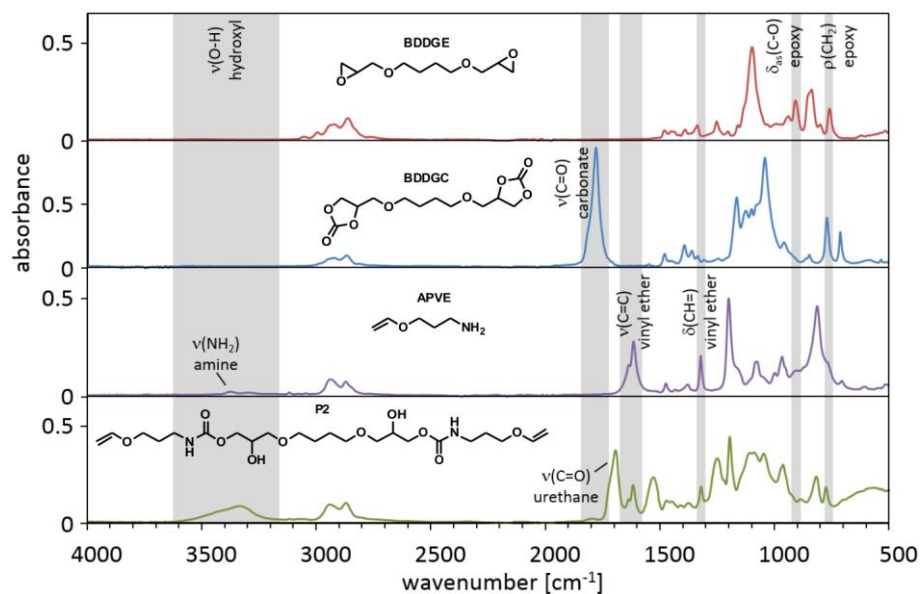


Figure 5.19. IR spectra of educts, intermediates and products related to the multi-step synthesis of the vinyl ether functionalized polyol P2. Some structural assignments are provided for important functional groups and the absorption bands are highlighted in the spectrum. The appearance and disappearance of these bands was used to monitor the reaction progress.

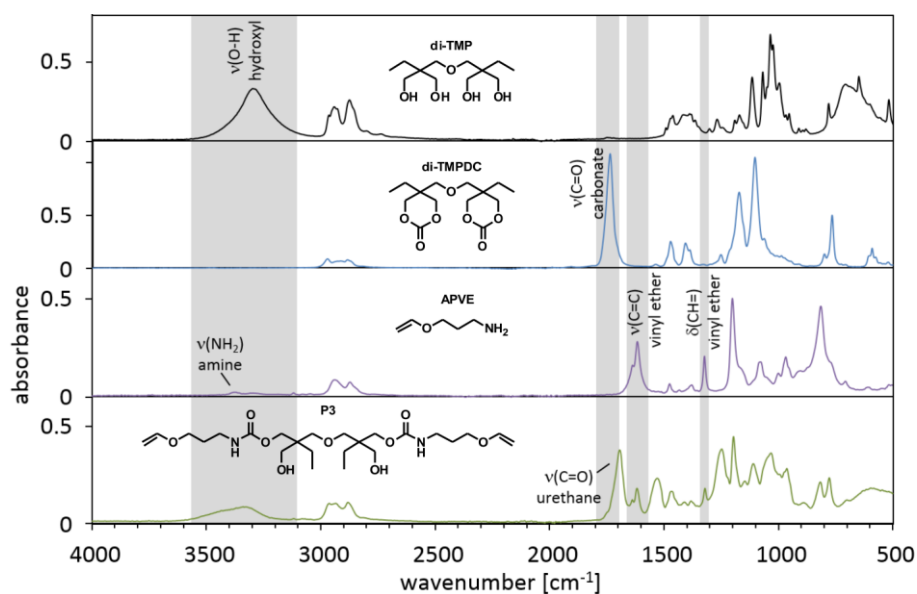


Figure 5.20. IR spectra of educts, intermediates and products related to the multi-step synthesis of the vinyl ether functionalized polyol P3. Some structural assignments are provided for important functional groups and the absorption bands are highlighted in the spectrum. The appearance and disappearance of these bands was used to monitor the reaction progress.

5.2.14 GC-FID Analysis

The degree of purity of GEBVE and GCBVE was determined using an Agilent GC HP6890 gas chromatograph equipped with a FID-detector. Chromatographic separation was performed on an Agilent DB-5 column.

5.2.15 ^1H NMR Spectroscopy

^1H NMR spectra were recorded with a Bruker Avance 400 MHz NMR spectrometer at 298 K using CDCl_3 as solvent. 32 scans were accumulated at a relaxation time of 10 s. ^1H NMR spectra of the synthesized epoxide, cyclic carbonates and polyols are provided in Figure 5.7 - 5.11, 5.13 and 5.15.

5.2.16 ^{13}C NMR Spectroscopy

Quantifiable ^{13}C NMR spectra were recorded with an Agilent Technologies DD2 600 MHz NMR spectrometer at 298 K in an inverse gated decoupled methodology. CDCl_3 was used as solvent and 4 g/l of chromium(III) acetylacetonate were added as relaxation agent. 2000 scans were accumulated at a relaxation time of 10 s. ^{13}C NMR spectra of the vinyl ether polyols (P1-P3) are provided in Figure 5.12, 5.14 and 5.16.

5.2.17 HPLC-MS Analysis

Chromatographic measurements were performed with a Waters Acquity UPLC system equipped with a Symmetry C18, 5 μm , 3.9 mm x 150 mm column and a RI detector W410. The samples were dissolved in methanol and 10 μL of that solution were injected. A mixture of water and methanol (50/50 v/v) with 1 g/l ammonium acetate was used for isocratic elution with a flow rate of 1 ml/min. The same chromatographic procedure was performed using a Thermo Scientific LTQ XL linear ion trap mass spectrometer as detector. Electrospray ionization (ESI) was applied and the mass spectrometer was operated in positive ion mode scanning from 50 – 2000 m/z . For quantification the RI detected chromatogram was used, whereas product peaks were identified via molar mass assignments. The RI chromatograms with assigned molecular weights are provided in Figure 5.21 - 5.23.

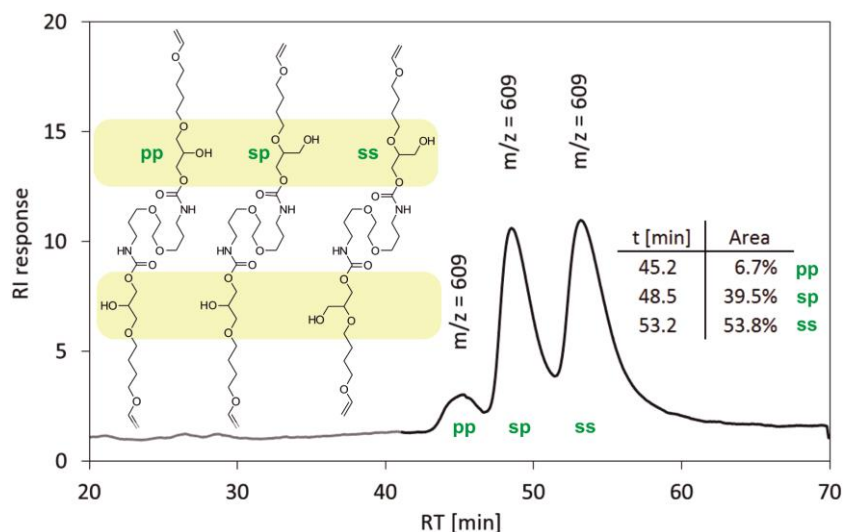


Figure 5.21. HPLC-RI chromatogram of P1.

Quantification was realized via the integrated peak areas. All three peaks were identified to be isomers of the expected product with a molecular ion peak of $[M+H]^+ = 609$ g/mol (calculated: 609 g/mol for $C_{28}H_{53}N_2O_{12}$). The product is generated through ring-opening reaction of two independent carbonate units and hence contains two hydroxyl groups. Each hydroxyl group either emerges as the primary hydroxyl group containing isomer (p) or more likely as secondary hydroxyl group containing isomer (s). Hence, three isomers of the product are possible: ss, sp (equal to ps) and pp. Based on a probability of 70/30 (s/p) a ratio of 49/42/9 (ss/sp/pp) is expected for the three isomers. This ratio is in good accordance with the experimental values displayed in the inserted table.

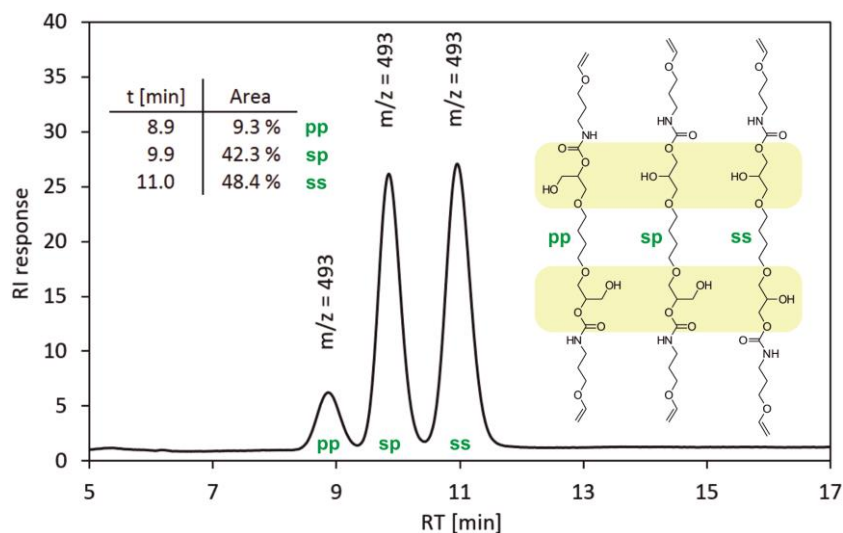


Figure 5.22. HPLC-RI chromatogram of P2.

Quantification was realized via the integrated peak areas. All three peaks were identified to be isomers of the expected product with a molecular ion peak of $[M+H]^+ = 493$ g/mol (calculated: 493 g/mol for $C_{22}H_{41}N_2O_{10}$). The product is generated through ring-opening reaction of two independent carbonate units and hence contains two hydroxyl groups. Each hydroxyl group either emerges as the primary hydroxyl group containing isomer (p) or more likely as secondary hydroxyl group containing isomer (s). Hence, three isomers of the product are possible: ss, sp (equal to ps) and pp. Based on a probability of 70/30 (s/p) a ratio of 49/42/9 (ss/sp/pp) is expected for the three isomers. This ratio is in good accordance with the experimental values displayed in the inserted table.

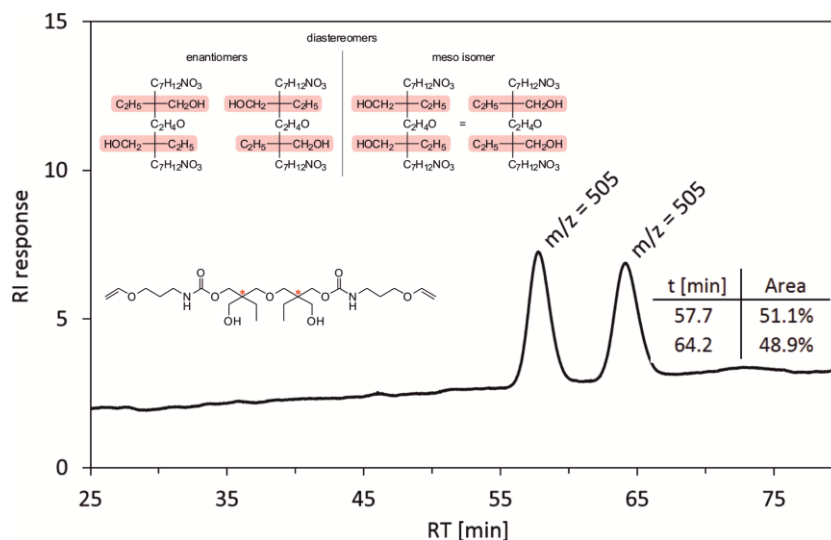


Figure 5.23. HPLC-RI chromatogram of P3.

Quantification was realized via the integrated peak areas. Both peaks were identified to be isomers of the expected product with a molecular ion peak of $[M+H]^+ = 505$ g/mol (calculated: 505 g/mol for $C_{24}H_{45}N_2O_9$). The product is not expected to contain constitutional isomers. However as two chiral centers are present in the molecule two diastereomeric structures are obtained that can be chromatographically separated.^{233, 234} Therefore, we assume that the peaks represent one diastereomer each. As the cyclic carbonate can be attacked from both sides with equal probabilities a ratio of 50/50 seems reasonable.

5.2.18 SEC Analysis

Chromatographic measurements were carried out using a Waters Alliance 2695 Separations Module equipped with two Agilent PLgel 10 μ m Mixed-B columns (300 x 7.5 mm) and a Waters 2414 RI detector. The sample was dissolved in THF and eluted with a mixture of THF and diethylamine (0.1 Vol.-%) at a flow rate of 0.5 ml/min. Determined molecular weights refers to a calibration with polystyrene standards (162 - 2 520 000 Da, Polymer Standards Service).

5.3 Synergistic and Sequential Dual Curing Mechanism for Vinyl Ether Functional Polyurethanes*

5.3.1 Materials

4-Hydroxybutyl vinyl ether (HBVE) (BASF, 99%, stabilized with 0.01% KOH) was stored over molecular sieve 4Å. Sodium (Merck, 99%). The oxidized surface was cut away under nitrogen atmosphere before use. 4,4'-dimethyl-diphenyliodonium hexafluorophosphate (Omnicat 440, IGM, 98%) was sieved. 1,4-Butanediol diglycidyl ether (BDDGE) (Sigma-Aldrich, 95%), polypropylene glycol (PPG) (Dow Chemical, Voranol 2000 L, 2000 g/mol), hexamethylene diisocyanate (HDI, Acros Organics, 99%) and dimethyltin dineodecanoate (Momentive, Fomrez catalyst UL-28) were used as received.

5.3.2 Synthesis of the Vinyl Ether Functional Polyol (VEOH)

VEOH was synthesized through the addition of deprotonated HBVE to BDDGC according to the procedure described in Chapter 5.1.2.

5.3.3 Synthesis of the Reactive Vinyl Ether Functional Polyurethane (rVEPU)

18.00 g (9.0 mmol) of PPG and 1.96 g (4.5 mmol) of VEOH were charged to a 50 ml flask, dried at 75 °C *in vacuo* and flushed with nitrogen. 3.05 g (18.1 mmol) of HDI and 0.0127 g of dimethyltin dineodecanoate were added at 15 °C and the temperature was gently increased to 80 °C. The reaction progress was controlled via IR spectroscopy (see Figure 5.24). After the desired NCO value was reached 0.23 g of 4,4'-dimethyl-diphenyliodonium hexafluorophosphate were added at 40 °C while stirring fast.

* This section is based on the publication manuscript “*Synergistic and Sequential Dual Curing Mechanism for Vinyl Ether Functional Polyurethanes*” by Stefan Kirschbaum, Katharina Landfester and Andreas Taden. Publication was withheld for the submission of the patent “*Härtungsverfahren für Polyurethane*“, filed on 11.11.2015, filing no. EP 15194065.7, internal no. PT033407.

Dissolved gases were removed under reduced pressure and the sample was filled to the top edge of a small glass vial and sealed tight.

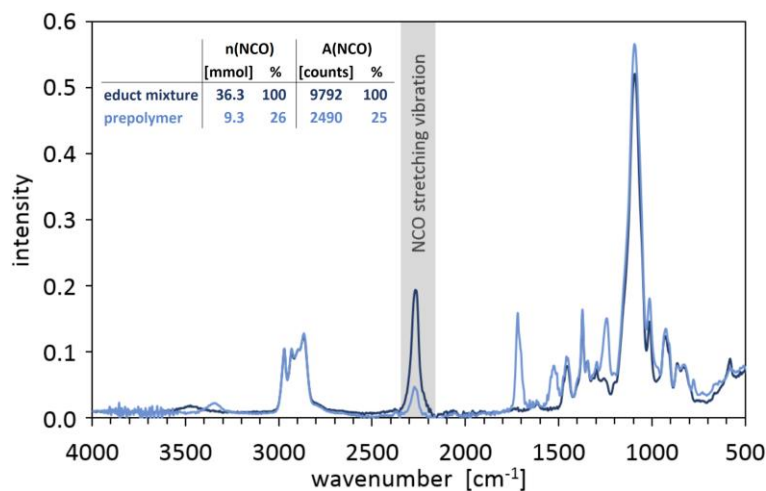


Figure 5.24. IR spectra of the rVEPU synthesis.

Samples were taken directly after homogenization of the educt mixture at 15 °C and after 1 h reaction time at 80 °C (prepolymer). The NCO stretching vibration at 2250 cm⁻¹ was integrated to check for the desired conversion and molecular weight via spectroscopic end group analysis.

5.3.4 UV/NIR-Rheology

Measurements were carried out using an Anton Paar MCR 302 rheometer in conjunction with a Bruker MPA FT-NIR spectrometer and an Omnicure S 2000 SC light source as described in a previous publication.¹⁷⁵ Oscillatory measurements were performed at a deformation of 0.1 %, a frequency of 10 Hz and an initial gap of 0.3 mm with an applied normal force of $F_n = 0$ N. The measurement cell was purged with instrumental air (water content = 1.1 mg/m³) and tempered to 60 °C. Data were recorded every 5 s before irradiation and every second upon irradiation. The light source was automatically switched on after 30 s for 50 s (189 mW/cm² UVA-C). NIR spectra were recorded with a sampling rate of 2 s⁻¹. After 1800 s (30 min) in total the measurement cell was opened and purging with instrumental air was stopped to allow humidity diffusion. Mechanical data were recorded every 60 s and NIR spectra were recorded every 15 min for another 120 hours.

5.4 Cationic Phototransfer Polymerization: pH-Responsive Acetal-Based Polymer Networks*

5.4.1 Materials

4-Hydroxybutyl vinyl ether (HBVE) (BASF, 99%, stabilized with 0.01% KOH) was stored over molecular sieve 4Å. Sodium (Merck, 99%) was stored in paraffin oil and oxidized surface was removed. 1,4-Butanediol diglycidyl ether (BDDGE) (Sigma-Aldrich, 95%), isophorone diisocyanate (IPDI) (Merck, 99%), dimethyltin dinedecanoate (Momentive, Fomrez catalyst UL-28), octanediol (Acros Organics, 98%), undecanol (Acros Organics, 98%) and 4,4'-dimethyl-diphenyliodonium hexafluorophosphate (Omnicat 440, IGM, 98%) were used as received.

5.4.2 Synthesis of the Vinyl Ether Functional Polyol (VEOH)

VEOH was synthesized through the addition of sodium 4-(vinylloxy) butanolate to 1,4-butanediol diglycidyl ether according to the procedure described in Chapter 5.1.2.

5.4.3 Synthesis of the Vinyl Ether Functional Polyurethane (VEPU)

A vinyl ether side-chain functionalized polyurethane prepolymer with an number average molecular weight of $M_n = 5000$ g/mol was synthesized from VEOH, an excess of IPDI and HBVE as end-capping agent as described in Chapter 5.1.4. Subsequently, the VEPU was dissolved in an equal volume of acetone and formulated with 2 wt.% of Omnicat 440 as photoinitiator with respect to the pure VEPU and octanediol or undecanol as listed in Table 5.1. The solvent was removed under reduced pressure (100 mbar).

* This section is based on the publication manuscript “*Cationic Phototransfer Polymerization: pH-Responsive Acetal-Based Polymer Networks*” by Stefan Kirschbaum, Robert Graf, Katharina Landfester and Andreas Taden. Publication is withheld for the submission of the patent “*Kationische Phototransferpolymerisation*“, internal no. PT033452.

Table 5.1. Formulations of VEPU with octanediol or undecanol

Sample	$m(\text{VEPU})$ [g]	$n(\text{vinyl ether})$ [mmol]	$m(\text{alcohol})$ [g]	$n(\text{OH})$ [mmol]	$m(\text{PI})$ [g]
VEPU/Octanediol (1:0)	3.00	9.49	-	-	0.06
VEPU/Octanediol (1:0.5)	3.00	9.49	0.35	4.74	0.06
VEPU/Octanediol (1:1)	3.00	9.49	0.69	9.49	0.06
VEPU/Octanediol (1:1.5)	3.00	9.49	1.04	14.23	0.06
VEPU/Undecanol (1:0.5)	3.00	9.49	0.82	4.74	0.06

The theoretical equivalent weight of VEPU was calculated to be 316.2 g/mol vinyl ether.

5.4.4 UV/NIR-Rheology

An Anton Paar MCR 302 rheometer coupled to an Omnicure S 2000 SC light source and a Bruker MPA FT-NIR spectrometer was operated in a plate/plate setup using a disposable aluminum top plate with a diameter of 25 mm and a quartz glass bottom plate. An optical fiber light guides was used to irradiate the sample perpendicular to its surface through the quartz glass plate. The NIR spectrometer was also equipped with light guides in a way that the beam penetrates the sample from the bottom, angular to its surface and is collected at the angle of reflection. The detailed instrument setup is described in more detail in a previous publication.¹⁷⁵ The initial sample thickness was set to 300 μm and a normal force of $F_n = 0$ N was applied to avoid stress caused from sample shrinkage via an automatic gap control. Mechanical data were recorded in an oscillatory mode with a sinusoidal strain of 10% and a frequency of 10 Hz at a sampling rate of 1/s. After 30 s UV-irradiation was performed for 240 s while the lamp was operated at a power level of 20%. An intensity of 0.40 mW/cm^2 UVC (189 mW/cm^2 UVA-C) was determined at a power level of 100% on top of the quartz glass plate using a Dr. Göbel OpSyTec spectral radiometer. NIR spectra were recorded with a resolution of 16 cm^{-1} at a constant sampling rate of about 2 spectra/s. The C-H stretching vibration peak of the vinyl ether at 6200 cm^{-1} was integrated and used to calculate the amount of residual vinyl ether groups. All measurements were carried out under instrumental air atmosphere (humidity = 1.1 mg/m^3).

5.4.5 Differential Scanning Calorimetry (DSC)

DSC experiments were carried out using a Netzsch Photo-DSC 204 F1 Phoenix equipped with an Omnicure S 2000 SC light source to determine the glass transition temperature T_g of the cured VEPU samples. 15 g \pm 2 g sample were placed in an open DSC pan. The samples were first heated to 70 °C for 1 min to obtain a leveled surface and cooled to 25 °C. This temperature was kept isotherm for 20 min before the sample was irradiated for 240 s (at a power level of 20%) with UV-light and post-curing was allowed to proceed for another 21 min. Subsequently, the samples were cooled to -75 °C with a rate of 10 °C/min, conditioned at that temperature for 20 min and heated to 150 °C with a rate of 10 °C/min. Measurements were conducted using instrumental air (humidity = 1.1 mg/m³) as purge gas with a flow rate of 20 ml/min. The light source provided a maximum intensity of 0.16 mW/cm² UVC (194 mW/cm² UVA-C), measured at a power level of 100% using a Dr. Göbel OpSyTec spectral radiometer) below the glass optics of the DSC-lid and was operated at a power level of 20%.

5.4.6 Solid State ¹³C NMR Spectroscopy

The ¹³C MAS NMR measurements have been performed on a Bruker Avance II console operating at 300.15 MHz ¹H Larmor frequency using a commercial ¹H-X double resonance MAS probe supporting zirconia MAS rotors of 4mm outer diameter. All measurements have been performed at ambient conditions, 10 kHz MAS spinning and 62.5 kHz RF nutation frequency on both frequency channels, the latter corresponding to a 90° pulse length of 4 μ s. For each CP-MAS experiment, 10 000 transients with a repetition time of 3 s and 1ms CP contact time have been acquired, using high power SPINAL 64 ¹H decoupling during ¹³C signal acquisition. For the INEPT-MAS NMR spectra, 4000 transients were sufficient to obtain good signal to noise with ¹H decoupling during acquisition. The delays in the refocused INEPT sequence were optimized to acquire maximal signal intensity for a ¹H-¹³C J coupling of 145 Hz corresponding to the known value of an aliphatic proton-carbon bond. The cured samples were prepared in the rheometer setup using consistent curing conditions. These films were mechanically removed, swollen in 1 ml of 0.1 mol/l triethylamine solution in humid THF (0.36 mol/l H₂O) and subsequently solvents were removed under reduced pressure (100 mbar).

5.4.7 Extractable Alcohol Content (GC Analysis)

Cured samples were prepared in the rheometer setup using consistent curing conditions. Sample films were mechanically removed, punched with a cutting tool to have a diameter of 20 mm, rolled up and placed in a GC vial. 1.5 ml moist THF (0.36 mol/l H₂O) was added, the vial was sealed tight, shaken by hand and placed in the autosampler. The vial was manually shaken every 20 min. For some samples only 1 ml of THF with 0.1 mol/l triethylamine was added to the sample and after about 2 h the medium was acidified upon addition of 0.5 ml acidic THF solution with a concentration of 0.5 mol/l acidic acid or hydrochloric acid. The syringe was flushed with THF and 1 µl of the sample solution. Subsequently, 15 sample pumps of 10 µl were performed for sample homogenization and 1 µl was injected at a split ratio of 20:1. Successive gas chromatographic measurements were carried out at an Agilent Technologies 7820A GC System equipped with a HP-5, 30 m x 0.32 mm, 0.25 µm column and a FID detector. The injection liner was set to 300 °C and the oven was set to 180 °C. After 2 min the oven temperature was ramped with a rate of 10 °C/min to 300 °C and kept constant at that temperature for at least 5 min. Undecanol shows a well resolved signal at a retention time of 1.98 min and was quantified via an external calibration (see Figure 5.25).

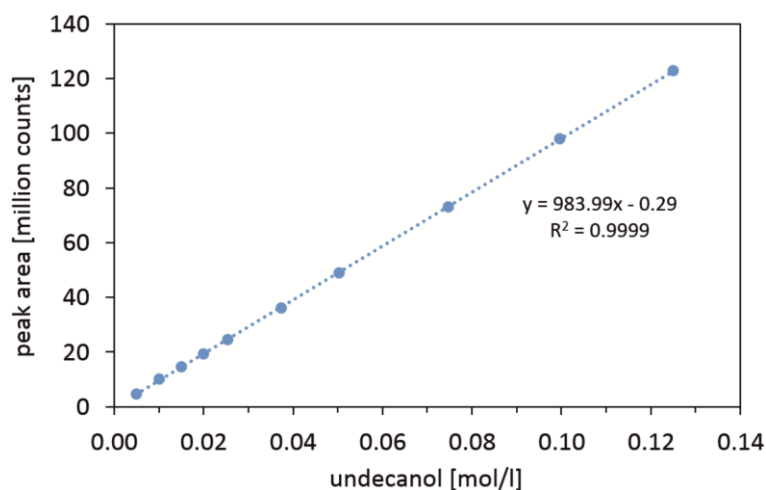


Figure 5.25. Calibration plot for undecanol.

The calibration shows a linear dependency of the undecanol concentration to the determined peak area in a range of 0.005 mol/l - 0.125 mol/l with high accuracy.

5.5 Cationic Phototransfer Polymerization of Photocurable Polyhydroxyurethanes*

5.5.1 Materials

4-Hydroxybutyl vinyl ether (HBVE) (BASF, 99%, stabilized with 0.01% KOH) was stored over molecular sieve 4Å. Sodium (Merck, 99%) was cut under nitrogen atmosphere. Epichlorohydrin (ECH) (Solvay, 99.8%), tetrabutylammonium bromide (TBAB) (Merck, 99%), tetraethylammonium bromide (TEAB) (Merck, 99%), 1,4-butanediol diglycidyl ether (BDDGE) (Sigma-Aldrich, 95%), hexamethylenediamine (HMDA) (Merck, 99%), 4,4'-dimethyl-diphenyliodonium hexafluorophosphate (Omnicat 440, IGM, 98%) and hexylamine (Merck, 99%) were used as received.

5.5.2 Synthesis of 4-Glycidylcarbonate Butyl Vinyl Ether (GCBVE)

GCBVE was synthesized according to the procedure described in Chapter 5.2.3.

5.5.3 Synthesis of the VEOH

VEOH was synthesized according to the procedure described in Chapter 5.1.2.

5.5.4 Synthesis of the Vinyl Ether Diglycidylcarbonate (VEDGC)

VEDGC was synthesized similarly to GCBVE via epoxidation and subsequent CO₂ insertion, starting from VEOH in a two-step synthesis. A 250 ml round-bottom flask equipped with a dropping funnel was charged with 13.04 g (30 mmol) of VEOH and 0.3211 g (1.5 mmol) of tetrabutylammonium bromide (TBAB). 50 ml toluene and 50 ml

* This section is based on the publication manuscript "Cationic Phototransfer Polymerization of Photocurable Polyhydroxyurethanes" by Stefan Kirschbaum, Katharina Landfester and Andreas Taden. Publication is withheld for the submission of the patent "Kationische Phototransferpolymerisation", internal no. PT033452.

aqueous NaOH (50 wt.%) were added. The emulsion was placed in an ice bath and 148.16 g (2 mol) epichlorohydrin (ECH) was added slowly with stirring. Stirring was continued for 24 h, while the emulsion was left to warm up. The organic phase was washed with brine and water several times and solvents were removed under reduced pressure. This epoxidation procedure was repeated using the same amounts of toluene, NaOH, TBAB and ECH to increase the conversion. The epoxidized VEOH was then subjected to a CO₂ insertion reaction similar to the procedure described by Caló.¹¹⁵ The reaction was monitored via IR spectroscopy. The product was cooled down and dissolved in 50 ml ethyl acetate upon complete conversion. The solution was washed with water several times to remove the catalyst and solvents were removed under reduced pressure. Overall yield: 66%. Elemental analysis: C, 56.86; H, 8.35; O, 34.80 (calculated: C, 56.77; H, 7.35; O, 35.29 for C₂₂H₄₂O₈). MS (EI): $m/z = 634.3$ [M]⁺ (calculated: 634.3 for C₃₀H₅₀O₁₄), also mol peaks of 590 g/mol, 534 g/mol and 216 g/mol were observed. Structures of the indicated by-products are shown in Figure 5.26.

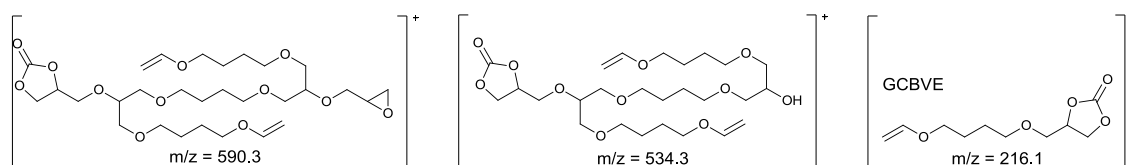


Figure 5.26. By-products indicated by MS analysis.

5.5.5 Synthesis of the Vinyl Ether Functionalized Polyhydroxyurethane (VEPHU) and Subsequent Amine-scavenging

1.003 g (8.63 mmol) of hexamethylene diamine and 6.697 g (10.55 mmol) of VEDGC were placed in a 50 ml flask. The mixture was stirred for 10 h at 70 °C. The conversion of the carbonate was observed via IR spectroscopy using the C=O stretching vibration at 1795 cm⁻¹. Also the generation of the urethane can be observed either at 1700 cm⁻¹ or at 1530 cm⁻¹ (full spectra are provided in Figure 5.27, whereas the carbonate conversion is plotted over time in Figure 4.37). GCBVE was added in portions of 10 mol% with respect to the initial amount of amine and the reaction was allowed to proceed for another hour. Samples were taken and formulated with 5wt% of 4,4'-dimethyl-diphenyliodonium hexafluorophosphate as photoinitiator for qualitative polymerization tests until the formulation could be cured under UV-irradiation. In total

1.145 g (5.30 mmol, 30 mol%, 13 wt%) GCBVE were added and the entire product was formulated with the photoinitiator.

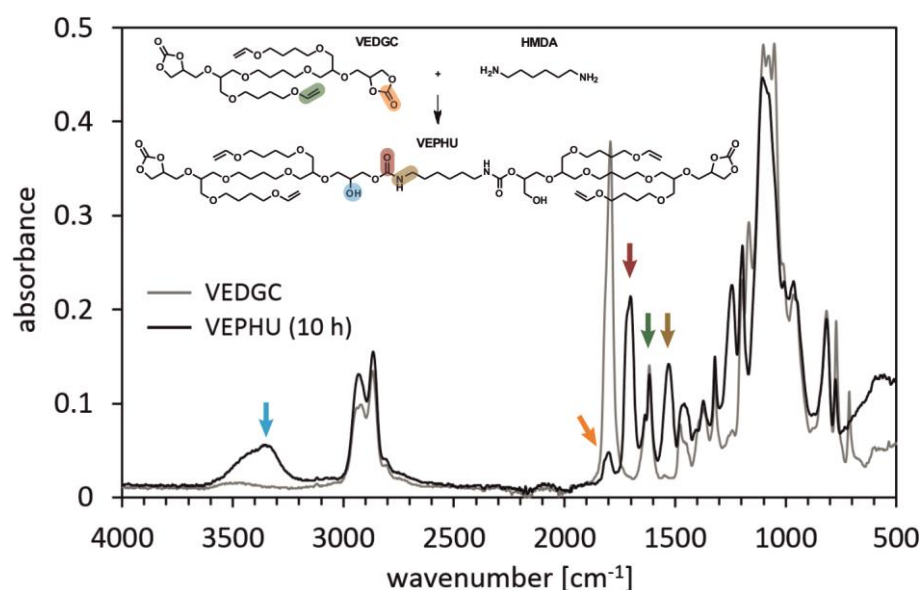


Figure 5.27. IR Spectra of VEDGC and the VEPHU batch after 10 h reaction time.

The crude mixture of this reaction was heterogeneous. Therefore, no representative, initial spectrum could be recorded. For compensation, a spectrum of the pure VEDGC was recorded. The integrated peak areas of the carbonate absorption band were compared to the carbonate peak area of VEDGC, reduced by a factor for the dilution with HMDA to get a rough approximation of the carbonate conversion.

5.5.6 Amine-scavenging Study

3 g of GCBVE were mixed with hexylamine in different stoichiometries and stirred for 24 h at room temperature before samples were subjected to ¹H NMR spectroscopy.

5.5.7 ¹H NMR Spectroscopy

Spectra were recorded with a Bruker Avance 400 MHz NMR spectrometer at 298 K using CDCl₃ as solvent. 32 scans were accumulated at a relaxation time of 10 s. The spectra of VEOH, VEDGE and VEDGC are shown in Figure 5.28.

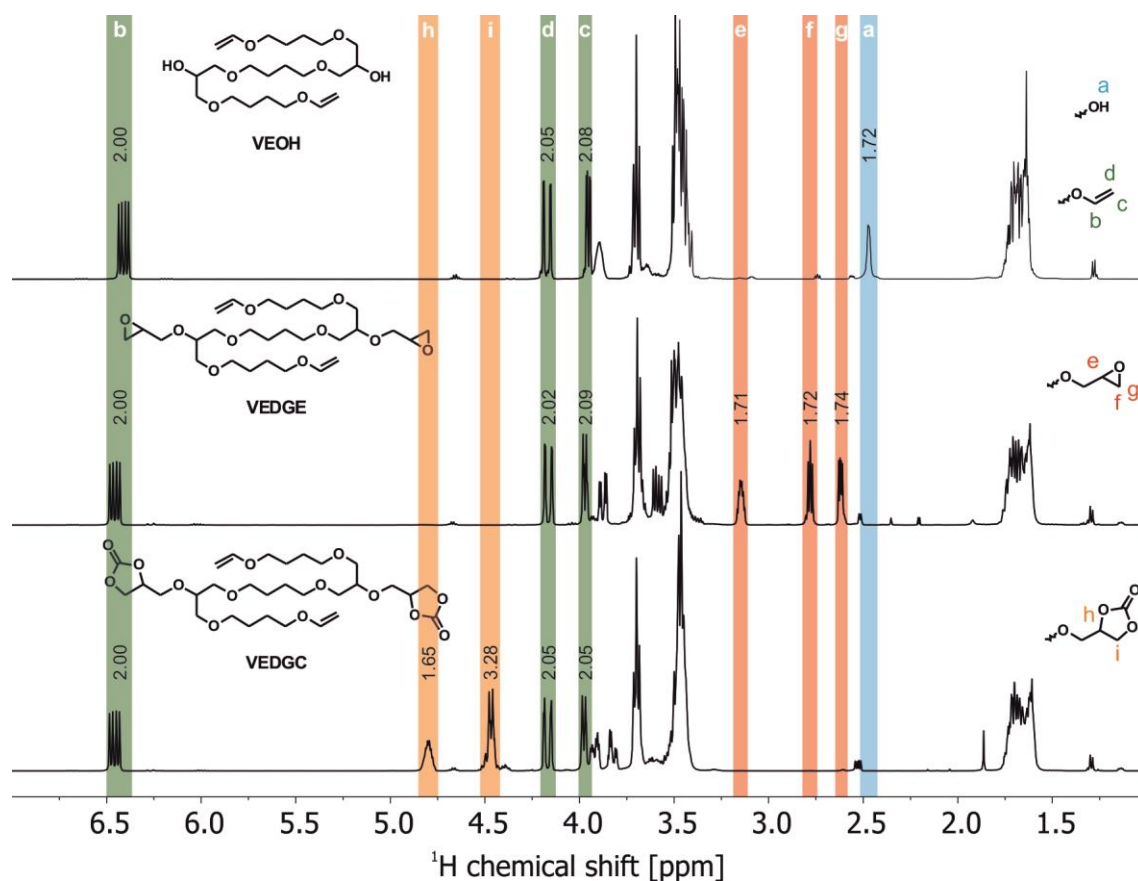


Figure 5.28. ^1H NMR spectra of VEOH, VEDGE and VEDGC.

In ^1H NMR spectroscopy hydroxyl groups are hard to quantify and only a reduced relative peak area of 1.72 was observed in the spectrum of VEOH. However, the hydroxyl value of 260 indicates about 2 hydroxyl groups per mol VEOH. Nevertheless, the relative epoxy peak area in the spectrum of VEDGE shows a similarly reduced value of 1.72 after two epoxidation steps (conversion = 86%). After the first epoxidation step the integrated peaks area was only 1.56. The VEDGC finally indicates a glycidyl carbonate functionality of 1.65 at an overall conversion of 83% (conversion of the CO_2 insertion reaction = 96%). The obtained functionality is sufficient to synthesize prepolymers with an average, theoretical molecular weight of 4000 g/mol with a large share of terminal hydroxyl groups. Therefore, tedious and environmentally questionable further epoxidations or purification procedures were omitted.

5.5.8 Solid State ^{13}C NMR Spectroscopy

The ^{13}C CP-MAS NMR measurements have been performed on a Bruker Avance II console operating at 300.15 MHz ^1H Larmor frequency using a commercial ^1H -X double resonance MAS probe supporting zirconia MAS rotors of 4mm outer diameter. All measurements have been performed at ambient conditions, 10 kHz MAS spinning and 62.5 kHz RF nutation frequency on both frequency channels, the latter corresponding to a 90° pulse length of 4 μs . 10 000 transients with a repetition time of 3 s and 1ms CP contact time have been acquired, using high power SPINAL 64

^1H decoupling during ^{13}C signal acquisition. The cured samples were mechanically removed from the rheometer experiment, swollen in 1 ml of 0.1 mol/l triethylamine solution in humid THF (0.36 mol/l H_2O) and subsequently solvents were removed under reduced pressure (100 mbar).

5.5.9 IR Spectroscopy

Spectra were recorded using a Bruker ALPHA FT-IR spectrometer equipped with an ATR crystal, a SiC light source and a DTGS detector. 24 scans were accumulated at a resolution of 4 cm^{-1} . Spectra of the uncured VEPHU and the cured VEPHU film from the rheology experiment were recorded 24 h after curing and were dried under reduced pressure at room temperature one hour previous to the measurement.

5.5.10 UV/NIR-Rheology

Rheological measurements were performed using an Anton Paar MCR 302 rheometer coupled to an Omnicure S 2000 SC light source and a Bruker MPA FT-NIR spectrometer. The light source was triggered to photoinduce the curing reaction, whereas the near-infrared (NIR) spectrometer was applied to monitor the vinyl ether conversion via integration of the C-H-stretching vibration band at 6200 cm^{-1} . The instrument setup was described in detail in a previous publication.¹⁷⁵ For oscillatory measurements a sample of 200 μm thickness was placed between a quartz glass bottom plate and a disposable aluminium top plate with a diameter of 20 mm. A normal force of $F_n = 0$ was applied over the course of reaction to minimize axial stress upon sample shrinkage. Initially a sinusoidal strain of 10% was applied at a frequency of 10 Hz. After 30 s the light source was switched on for an irradiation period of 10 s. At the same time the strain was logarithmically ramped from 10% to 0.1% within 210 s to maintain linear viscoelastic behaviour. Mechanical data were recorded at a sampling rate of 1 s^{-1} , whereas NIR spectra with a resolution of 16 cm^{-1} were continuously recorded at a sampling rate of about 2 s^{-1} . The measurement was performed at $25\text{ }^\circ\text{C}$, under instrumental air atmosphere (H_2O : 1.1 mg/m^3) and UV-irradiation was conducted at a light intensity of 0.40 mW/cm^2 UVC (189 mW/cm^2 UVA-C, determined using an OpSyTec Dr. Göbel spectral radiometer).

5.5.11 Differential Scanning Calorimetry (DSC)

DSC analysis was performed using a Photo-DSC 204 F1 Phoenix (Netzsch) equipped with an Omnicure S 2000 SC light source. 10 ± 2 mg of the uncured material were charged to an open aluminum pans. A complex measurement profile was applied to UV-cure the sample and determine the glass transition temperature before and after curing. Cooling and heating rates were always performed at a rate of 10 K/min. The sample was cooled to -75 °C and conditioned for 30 min before it was heated to 60 °C. Then the sample was cooled to 25 °C and conditioned for 25 min, before it was irradiated with an intensity of 0.16 mW/cm² UVC (194 mW/cm² UVA-C, determined using an OpSyTec Dr. Göbel spectral radiometer) for 10 s. Irradiation was repeated 10 times after an isotherm of 5 min each. Subsequently, the sample was cooled to -75 °C and after 30 min conditioning time finally heated to 120 °C. The entire measurement was conducted under with instrumental air (H₂O: 1.1 mg/m³) as purge gas at a flow rate of 20 ml/min.

5.6 Synthesis and Thermal Curing of Benzoxazine Functionalized Polyurethanes*

5.6.1 Materials

Phenol (99%, Acros Organics), dimethylphenol (DMP) (98%, Alfa Aesar), paraformaldehyde (96%, Acros Organics), methylamine 40% in water (Acros Organics), dimethyltin dineodecanoate (Fomrez UL-28, Momentive), cyclohexyl isocyanate (98%, Alfa Aesar), dibutylamine (99%, Merck), isophorone diisocyanate (IPDI) (Merck, 99%), polytetramethylenoxide (PTMO, $M_n = 650$ g/mol) (PolyTHF 650 S, BASF) were used as received.

5.6.2 Synthesis of 3,4-Dihydro-3-methyl-2H-1,3-benzoxazine (P-m)

94.11 g (1 mol) Phenol, 66.06 g paraformaldehyde (equivalent to 2.2 mol formaldehyde), 190 g (50 wt.%) toluene and 31.06 g (1 mol) methylamine 40% in water were placed in a flask equipped with a magnetic stirrer, a water separator and a reflux condenser. The mixture was heated to reflux till water separation stopped. The product was washed with an aqueous solution of sodium hydroxide (2 mol/l) and water several times. Solvent was evaporated under reduced pressure to yield the crude P-m.

5.6.3 Oligomerization of P-m

A 250 ml Flask was charged with 22 g of crude P-m, heated to 70 °C and purged with nitrogen. The flask was then placed in an oil bath of 160 °C for 6 min under vigorous stirring. The oligomerization was visually monitored by the increasing viscosity and stopped through abrupt cooling in an ice bath. Indirect potentiometric titration indicates

* This section is based on the publication “*Synthesis and Thermal Curing of Benzoxazine Functionalized Polyurethanes*” by Stefan Kirschbaum, Katharina Landfester and Andreas Taden, published in *Macromolecules* **2015**, 48, 3811-3816. Reprinted with permission. Copyright 2015 American Chemical Society.

10.9% isocyanate reactive phenol structures and 93.0% of the theoretical basic nitrogen content.

5.6.4 Vacuum Distillation of P-m

72 g of the crude P-m were vacuum distilled to obtain the pure, low viscous and colorless P-m. Condensate was collected at a reduced pressure of 0.8 mbar and a vapor temperature of 85 - 87 °C. In the course of distillation the temperature of the residue needs to be increased to ensure a constant condensate flow due to enrichment of oligomers and by products and at some point fast and exothermic curing of the residue occurs. Yield: 83%. Elemental analysis: C, 72.5; H, 7.5; N, 9.4; O, 10.5 (calculated: C, 72.46; H, 7.43; N, 9.39; O, 10.72 for C₉H₁₁NO). ¹H NMR (400 MHz, CDCl₃, 298 K) δ (ppm): 2.60 (s, 3H, N-CH₃), 3.95 (s, 2H, Ar-CH₂-N), 4.79 (s, 2H, O-CH₂-N), 6.79 - 7.12 (m, 4H, Ar-H). The spectrum is shown in Figure 5.29.

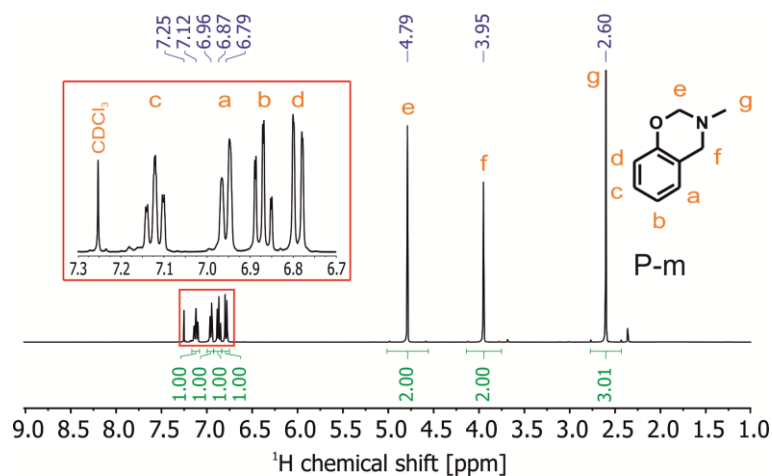


Figure 5.29. ¹H NMR spectrum of the vacuum distilled P-m in CDCl₃.

5.6.5 Polymerization Study of P-m

Samples of 0.3 g distilled P-m each were flushed with nitrogen, sealed and placed in an oven of 160 °C. Every 5 min a sample was removed from the oven and immediately cooled in a water bath. The samples were subsequently subjected to ¹H NMR (400 MHz, CDCl₃, 298 K) spectroscopy and indirect potentiometric titration. Additionally, a HBMNMR spectrum of the sample after 45 min thermal treatment was recorded and is shown in Figure 5.30.

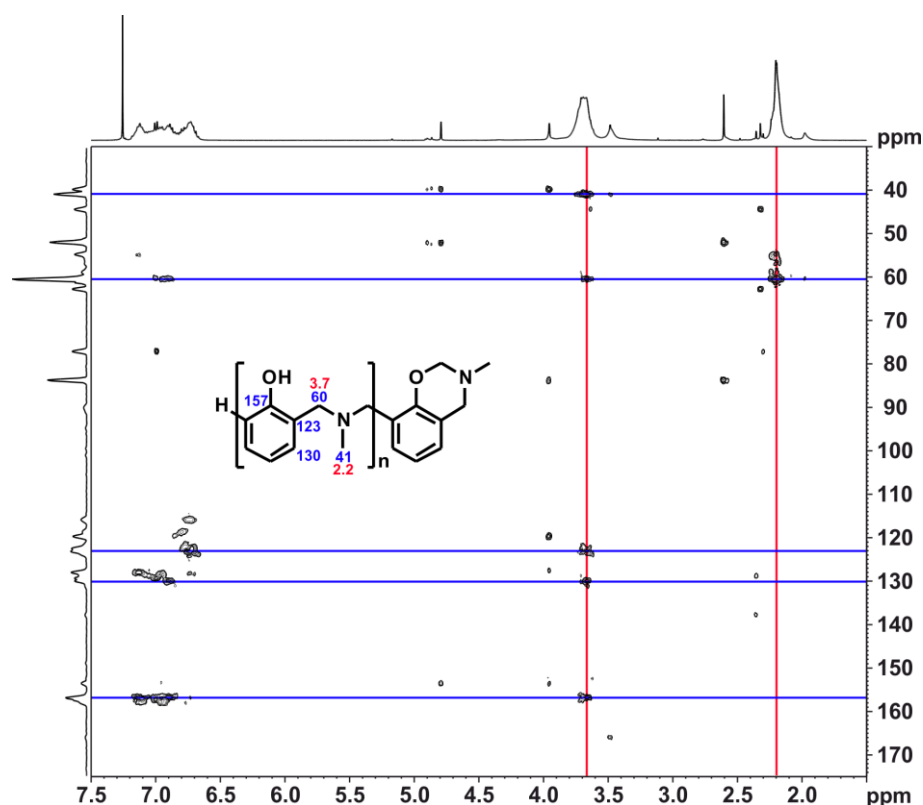


Figure 5.30. HMBC-NMR spectrum of the P-m sample after 45 min of thermal treatment at 160 °C. The spectrum reveals that the depicted structure applies to the main product.

5.6.6 Synthesis of N,N-bis(3,5-dimethyl-2-hydroxybenzyl)methylamine (DMP₂-m)

DMP₂-m was synthesized referring to the procedure to this described by Dunkers.²³⁵ 36.65 g 2,4-dimethylphenol (0.3 mol), 9.91 g paraformaldehyde (equivalent to 0.33 mol formaldehyde), 57 g (50 wt.%) toluene and 11.65 g (0.15 mol) methylamine 40% in water were placed in a flask equipped with a magnetic stirrer, a water separator and a reflux condenser. The mixture was heated to reflux till water separation stopped. Solvent was evaporated under reduced pressure. The bulk material was heated to 150 °C for 1 h. The product was then recrystallized from diethyl ether till white crystals were obtained. Elemental analysis: C, 75.9; H, 8.5; N, 4.7; O, 10.9 (calculated: C, 76.22; H, 8.42; N, 4.68; O, 10.69 for C₁₉H₂₅NO₂). MS (APCI): m/z = 300.4 [M+H]⁺ (calculated: 300.4 for C₁₉H₂₆NO₂). ¹H NMR (400 MHz, CDCl₃, 298 K) δ (ppm): 2.21 (s, 6H, Ar-CH₃), 2.22 (s, 3H, N-CH₃), 2.23 (s, 6H, Ar-CH₃) 3.64 (s, 4H, Ar-CH₂-N), 6.73 (s, 2H, Ar-H), 6.87 (s, 2H, Ar-H) 5-9 (br, 2H, OH). The spectrum is shown in Figure 5.31.

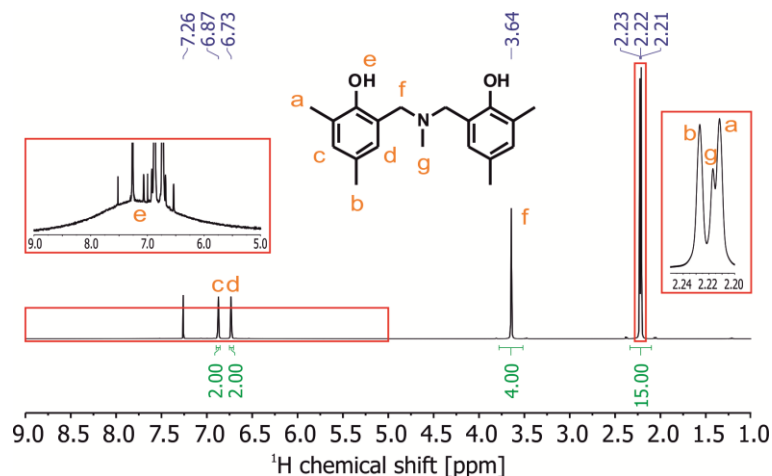


Figure 5.31. ^1H NMR spectrum of DMP₂-m in CDCl_3 .

5.6.7 Indirect Potentiometric Titration

An aliquot of the sample containing approximately 0.4 - 2.0 mmol of phenolic hydroxyl groups was placed in a 40 ml screw cap glass. The sample was dissolved in 5 ml of dry xylene before 0.02 g of dimethyltin dodecanoate and 5 ml of cyclohexyl isocyanate solution (0.5 mol/l in dry xylene) were added. The glass was flushed with nitrogen and sealed tight. The samples were stored in an oven at 80 °C for 60 min. At room temperature 7 ml of dibutylamine solution (0.5 mol/l in xylene) were added. The sample was then transferred to a 400 ml beaker using 15 ml xylene and 50 ml isopropyl alcohol and was subjected to a potentiometric titration with aqueous hydrochloric acid 0.5 mol/l, while the potential of the solution was recorded using a solvotrode (Metrohm 6.0229.010 or Mettler Toledo DGI113-SC). For some titrations also different reaction conditions such as other catalysts, solvents or isocyanates were used as indicated. Blank samples and phenol were applied as reference with every sample series. Figure 5.32 exemplarily shows a corresponding titration plot.

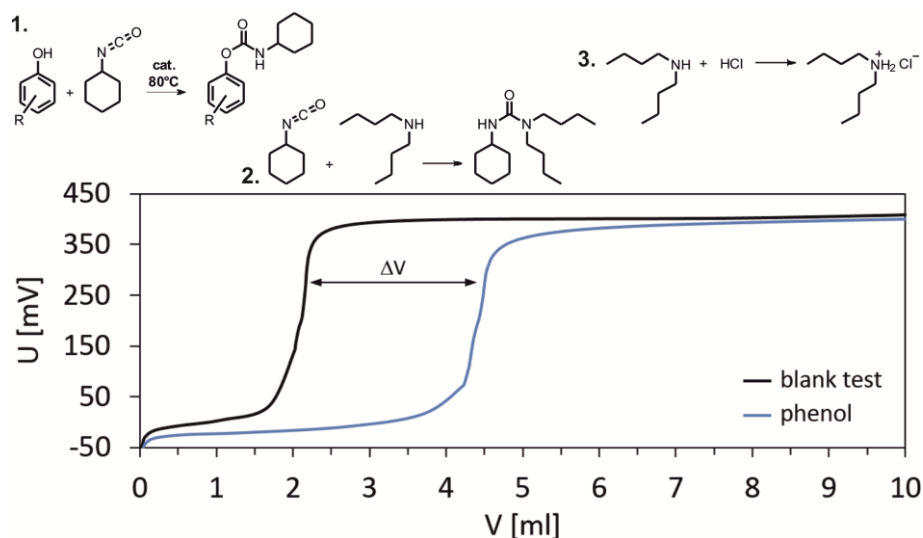


Figure 5.32. Titration plot of phenol and the blind sample.

The difference in volume consumed until the equivalent point is reached is directly proportional to the amount of isocyanate that is consumed by the sample.

Samples containing basic amine groups may show a second equivalent point (EP). Hence, the basic amine content may be quantifiable without extra effort. Figure 5.33 exemplarily shows a titration plot of DMP₂-m.

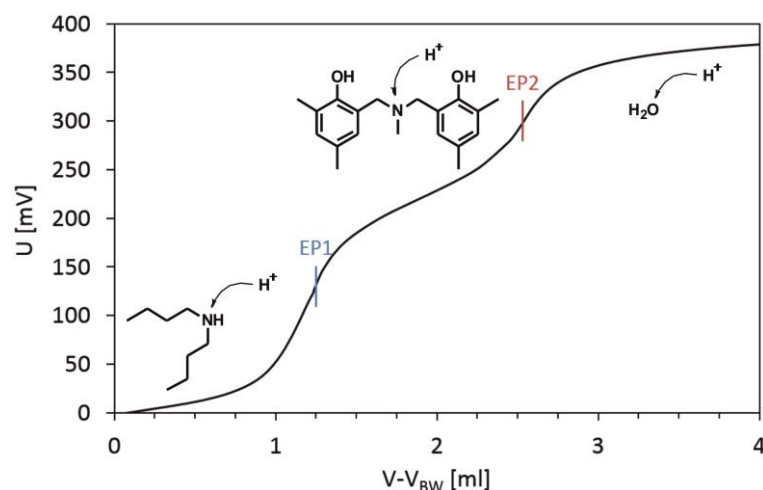


Figure 5.33. Titration plot of DMP₂-m.

The DMP₂-m structure contains an amine that differs in its basicity from the DBA and hence shows a second equivalent point (EP2) in the potential curve. Hence, the EP2 can be used to quantify the basic amine content of samples.

5.6.8 Synthesis of PU/BOX-Hybrids

47.08 g (72.4 mmol) PTMO were dried at 75 °C under reduced pressure. 24.00 g (108 mmol) IPDI were added at 40 °C. A sample was taken for IR spectroscopy. Then

0.09 g (125 mg / 100 g sample) of dimethyltin dodecanoate were added and the mixture was heated to 80 °C until the desired intensity of the N=C=O stretching vibration band at about 2250 cm⁻¹ was achieved. Subsequently, aliquots of the sample were taken for end-capping reactions. 5.83 g (70 wt.%) were reacted with 2.50 g (30 wt.%) of the oligomerized P-m. Another aliquot of 10.00 g (70 wt.%) was reacted with 0.94 g (6.6 wt.%) of phenol to end-cap the reactive isocyanate groups. 3.34 g (23.4 wt.%) of the oligomerized P-m were added to the phenol capped PU, after almost complete conversion of the isocyanate was confirmed by IR spectroscopy. The corresponding IR spectra are shown in Figure 5.34.

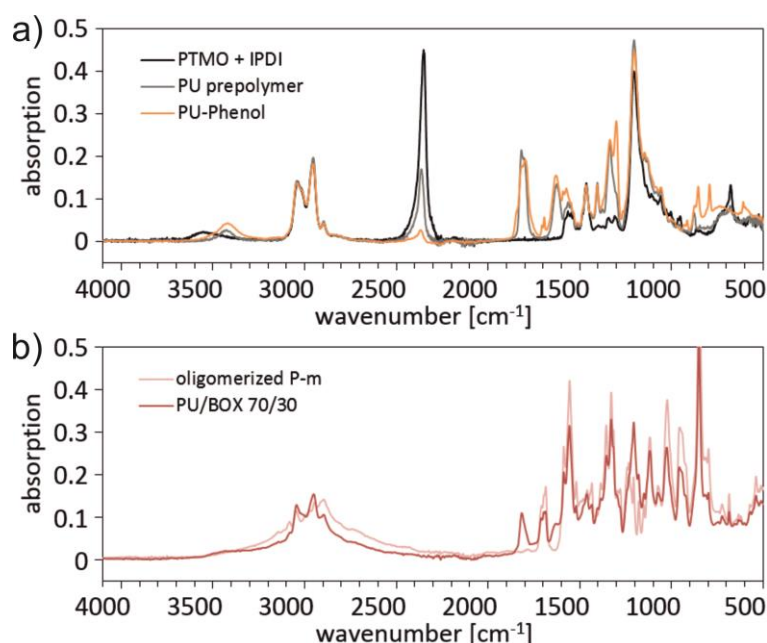


Figure 5.34. IR Spectra of the polyurethane/benzoxazine-hybrid syntheses.

The characteristic N=C=O stretching vibration shows an intensive signal at 2250 cm⁻¹. Graph a) shows the spectra of the polyurethane formulation before reaction, after synthesis of the prepolymer and after end-cap with phenol. The isocyanate absorption of the prepolymer is in good agreement with the theoretical value and confirms the average molecular weight of about 2000 g/mol. Almost complete conversion of the isocyanate was achieved after termination of the prepolymer with phenol. The prepolymer was subsequently formulated with the oligomerized P-m. Graph b) shows the spectrum of the same PU prepolymer immediately end-capped with the oligomerized P-m (PU/BOX 70/30) in comparison to the spectrum of the pure, oligomerized P-m. The missing absorption band at 2250 cm⁻¹ indicates complete conversion of the isocyanate.

5.6.9 Curing of PU/BOX-Hybrids and Rheological Investigation

The thermally induced curing reaction of the polyurethane/benzoxazine-hybrids was performed and monitored in a rheological plate/plate setup using an Anton Paar MCR

302 rheometer. Disposable aluminum cups with a diameter of 53 mm were charged with 1.5 g of the sample and used as bottom plate. Disposable aluminum top plates with a diameter of 25 mm were used at a gap distance of 0.35 mm. The starting values were monitored for 1 min at 25 °C, at a sinusoidal strain of 10% and a frequency of 1 Hz. The temperature was then increased with a rate of 10 °C/min to 170 °C and the sample was cured for 120 min at that temperature, whereas the sample deformation was ramped linearly from 10% to 0.2% to remain within the instrument limitation and to maintain linear viscoelastic behavior as the moduli increase over several orders of magnitude upon curing. Subsequently, a normal force of zero was applied to allow automatic gap control and minimize stress from thermal contraction or expansion of the solidified sample. The temperature was then decreased with a rate of 10 °C/min to 25 °C. After 60 min post-curing time at room temperature the thermal properties of the cured sample were investigated. Therefore, the sample was heated with a rate of 2 °C/min to 150 °C, kept at that temperature for 5 min and cooled with a rate of 2 °C/min.

5.6.10 HPLC-MS Analysis

0.6455 g DMP₂-m (2.16 mmol), 0.5400 g cyclohexyl isocyanate (4.31 mmol) and 0.02 g of dimethyltin dodecanoate were dissolved in 10 ml dry xylene. The glass was flushed with nitrogen and sealed tight. The sample was stored in an oven at 80 °C for 60 min. Subsequently, 0.2770 g dibutylamine (2.14 mmol) were added at room temperature. A sample of this mixture was subjected to HPLC-MS analysis. The HPLC-MS measurement was performed using a Waters Acquity UPLC system coupled to a Thermo Scientific LTQ XL linear ion trap mass spectrometer. Chromatographic separation was achieved using an Acquity UPLC BEH C18 column. Mobile phase A was composed of water containing 0.1% formic acid, whilst mobile phase B consisted of acetonitrile and 0.1% formic acid. The gradient elution program employed was: 100 - 0% A from 0 to 10 min at a flow-rate of 0.2 ml/min. The UV-detector was set to measure in the range of 200 - 400 nm. Atmospheric pressure chemical ionization (APCI) was applied and the mass spectrometer was operated in positive ion mode scanning from 100 – 2000 *m/z*.

6 Summary

This thesis deals with the introduction of a cationic photocuring mechanism to polyurethane chemistry. The objective was realized via incorporation of vinyl ether functional side-chains along the polymer backbone. Merging polyurethanes with vinyl ethers results in novel photopolymers, which easily overcome the drawbacks that are typically associated with common vinyl ether monomers. Generally, photopolymers are important technology enablers, which seem to enjoy ever-growing interest. This development is currently fueled by numerous exciting technologies like stereolithography, nanoimprint lithography or 3D-inkjet printing and the broad availability of energy-efficient, light sources. Important aspects, including fundamental physicochemical basics and a brief review on the state-of-the-art are discussed in Chapter 2. The modular synthesis of polyurethanes enables photopolymers with adjustable molecular mobility, crosslinking density, and mechanical properties, which in combination with cationic polymerization feature exceptional curing characteristics. Different materials with unique curing behaviors and material properties are presented in Chapter 4. The work is divided in coherent parts and the individual sections are summarized separately in the following. Collectively, the presented photopolymers are particularly interesting for challenging assembly processes even of non-transparent substrates, dimensional stable and non-tacky, semi-cured intermediates and improved interlayer adhesion, which is of high value for additive manufacturing techniques. Consequently, these new materials go far beyond a simple replacement for common photocurable epoxides and polyurethane acrylates and can be seen as driver for new processes and applications.

Unique Curing Properties through Living Polymerization in Crosslinking Materials: Polyurethane Photopolymers from Vinyl Ether Building Blocks

Vinyl ether functional polyols (VEOHs) were prepared in an addition reaction of hydroxybutyl vinyl ether to butanediol diglycidyl ether and utilized as building blocks to synthesize vinyl ether side-chain functionalized polyurethane prepolymers (VEPUs) of high functionality. The dependency of their molecular and mechanical photocuring

profiles on the backbone structure and vinyl ether functionality were investigated in formulations with common cationic photoinitiators. In addition to the initial curing reaction, special emphasis was put on *dark curing*, multi-stage irradiation curing and thermally induced post-curing. It was found, that propagating, cationic chain ends turn into trapped, dormant species upon vitrification of the crosslinking polymer networks, which remain living but inactive for days, even in the presence of residual vinyl ether. Propagation can be reactivated through heating above the glass transition temperature. Moreover, the actual properties of the entirely cured material were shown to be adjustable by the process conditions such as light dose and temperature profile.

Vinyl Ether-Functional Polyols as Building Blocks for UV-Curable Polyurethanes and Isocyanate-Free Polyhydroxyurethanes

A straight forward and easily scalable synthetic approach towards VEOHs based on the ring-opening addition of cyclic carbonates with primary, aliphatic amines was introduced. This process is technically feasible as it avoids tedious work-up procedures and oligomeric by-products. Moreover, various structures can be realized with a high design flexibility. These polyols inherently contain urethane groups, which beneficially contribute to the product properties and consequently lower the quantities of isocyanates that are required in the VEPUs synthesis. The polyol structure was carefully evaluated and subsequent VEPUs were subjected to photocuring. Furthermore, one urethane containing VEOH was exemplarily utilized to prepare linear and crosslinked polyhydroxyurethanes (PHUs) via thiol-ene addition. In comparison to the classical PHU synthesis, the final molecular weight build up proceeds via radical mediated thiol-ene addition, which is advantageous to obtain high molecular weight PHUs and enables storage stable and photocurable one component formulations.

Synergistic and Sequential Dual Curing Mechanism for Vinyl Ether Functional Polyurethanes

An isocyanate terminated, vinyl ether functional polyurethane prepolymer was prepared as novel dual cure material. Dual cure describes the combination of two independent curing mechanism within one material and is often utilized for multi-stage curing materials. The reported polymers can undergo photoinduced cationic curing via vinyl

ether groups and moisture-induced curing of isocyanates. Both curing mechanisms are externally triggered and proceed independently. Although their combination is highly synergistic. Generally, cationic polymerization is sensitive towards nucleophiles such as water. However, the presence of reactive isocyanate groups ensures an almost nucleophile free, *self-drying* reaction medium that provides robust and efficient photopolymerization conditions. On the other hand, the cationic curing reaction enables fast thickening or setting to facilitate the dimensional stability that is often required while the slow moisture-curing reaction proceeds. Photopolymers with subordinate moisture-curing can be designed to shift the generation of polar structure and strong intermolecular interactions after the application. This is of particular interest for processes like 3D-inkjet printing, where thin cross sections and high flow rates require low viscosities. In this context, the presence of unselectively reactive isocyanates after application may improve interlayer adhesion.

Cationic Phototransfer Polymerization: pH-Responsive Acetal-Based Polymer Networks

The effect of hydroxyl functional transfer agents on the cationic polymerization of VEPU was investigated using undecanol and octanediol as model substances. If a sufficiently large amount of hydroxyl groups is present the overall curing mechanism shifts from pure chain growth towards a mixed mode reaction with significant contribution of step growth similar to unideal thiol-ene reactions. This so-called cationic phototransfer polymerization yields flexibilized polymer networks, which contain acid-labile acetal groups. Sophisticated ^{13}C MAS NMR spectroscopy was applied to verify the expected network structure containing acetal bridges formed via incorporation of the alcohol components. Moreover, the release efficiency and degradation kinetics were evaluated under different pH-conditions. This work is of particular interest for medical applications as the hydroxyl functional load is released from an insoluble carrier and the body is not charged with additional ingredients. Furthermore, from a technical point of view, these materials also qualify for debonding on command applications.

Cationic Phototransfer Polymerization of Photocurable Polyhydroxyurethanes

A vinyl ether di(cyclic carbonate) was prepared as precursor for the synthesis of vinyl ether functional polyhydroxyurethanes (VEPHUs). These prepolymers inherently contain both vinyl ether and hydroxyl groups and can be photocured via cationic phototransfer polymerization. Common PHUs are currently seen as most promising, sustainable alternative for isocyanate based PUs, but suffer from limited molecular weight and high water absorption. However, the introduced, photocuring VEPHUs provides an efficient route to overcome these drawbacks via consumption of polar hydroxyl groups and additional crosslinking. Hence, their improved competitiveness is expected to promote the implementation of environmentally benign PHU as substitute for common isocyanate based polyurethanes.

Synthesis and Thermal Curing of Benzoxazine Functionalized Polyurethanes

Instead of the vinyl ether functional groups, this section deals with the introduced of benzoxazine functional groups to polyurethane chemistry. Novel polyurethane/benzoxazine-hybrid materials were prepared via end-cap reaction of polyurethane prepolymers with phenolic groups of oligomerized benzoxazines. The thermal stability of these covalent attachment is largely dependent on the type of isocyanate and benzoxazine used and is expected to be rather high for materials derived from aliphatic isocyanates and benzoxazines. Depending on the actual composition these materials can be used as thermally curing polyurethanes or as toughener in benzoxazine resins. Significantly improved reaction profiles and material properties were observed in comparison to state of the art polyurethane/benzoxazine-hybrids. Moreover, detailed spectroscopic and potentiometric investigations demonstrated that very strong hydrogen bonds may have a strong impact on the reactivity of free hydroxyl groups in ring opened benzoxazines. This influence was also investigated in a model reaction using different catalysts or solvents and is generally of high importance for the post-modification of oligomerized or polymerized benzoxazines.

In a nutshell, the introduced material classes of VEOHs and VEPUs provide a number of specific reactions with tremendous value for material chemistry originating from their vinyl ether functional groups. Especially, cationic polymerization, acid mediated addition of alcohols and the radical mediated thiol-ene addition were utilized in this thesis. The focus of investigation was to provide new synthetic pathways towards novel functional materials with advanced curing behavior. Sophisticated analytical techniques were established to observe the photochemical conversions and obtain a comprehensive understanding of the structure-property relationships. The findings of this work are of high industrial interest and expected to promote existing and emerging applications. In fact vinyl ether polyurethanes can be considered as a novel photopolymer class which can be adapted over a broad range to fulfill various demanding requirements and hence shows great prospect as future technology enabler.

7 References

1. Hohmann-Marriott, M. F.; Blankenship, R. E. *Annual Review of Plant Biology* **2011**, 62, (1), 515-548.
2. Berner, R. A. *Nature* **2003**, 426, (6964), 323-326.
3. The Nobel Prize in Physics 2014. http://www.nobelprize.org/nobel_prizes/physics/laureates/2014/ (06.09.2015),
4. Commission Regulation (EC) No 244/2009. Union, E., Ed. 2009.
5. Commission Regulation (EU) No 1194/2012. Union, E., Ed. 2012.
6. 2015 International Year of Light and Light-based Technologies. <http://www.light2015.org/Home/About.html> (11.10. 2015),
7. Nocera, D. G. *Accounts of Chemical Research* 2012, 45, (5), 767-776.
8. Balzani, V.; Bergamini, G.; Ceroni, P. *Angewandte Chemie International Edition* **2015**, 54, (39), 11320-11337.
9. Bach, T. *Angewandte Chemie International Edition* **2015**, 54, (39), 11294-11295.
10. Crivello, J. V. *Journal of Polymer Science Part A: Polymer Chemistry* **1999**, 37, (23), 4241-4254.
11. Sangermano, M.; Razza, N.; Crivello, J. V. *Macromolecular Materials and Engineering* **2014**, 299, (7), 775-793.
12. Crivello, J. V.; Reichmanis, E. *Chemistry of Materials* **2013**, 26, (1), 533-548.
13. Fouassier, J.-P., *Photoinitiation, Photopolymerization, and Photocuring: Fundamentals and Applications*. Hanser/Gardner Publications: Cincinnati, 1995.
14. Fouassier, J. P.; Lalevée, J., *Photoinitiators for Polymer Synthesis*. Wiley-VCH: Weinheim, 2012.
15. Decker, C. *Polymer International* **1998**, 45, (2), 133-141.
16. Decker, C. *Pigment & Resin Technology* **2001**, 30, (5), 278-286.
17. Decker, C. *Macromolecular Rapid Communications* **2002**, 23, (18), 1067-1093.
18. *European Markets for Radiation Curable Coatings (B919-01)*. Frost & Sullivan: London, 2006.
19. Tieke, B., *Makromolekulare Chemie: Eine Einführung*. Wiley-VCH: Weinheim, 2005; Vol. 2. Auflage.
20. Wendel, B.; Rietzel, D.; Kühnlein, F.; Feulner, R.; Hülder, G.; Schmachtenberg, E. *Macromolecular Materials and Engineering* **2008**, 293, (10), 799-809.
21. Ahn, S. H.; Guo, L. J. *ACS Nano* **2009**, 3, (8), 2304-2310.
22. Khang, D.-Y.; Kang, H.; Kim, T.-I.; Lee, H. H. *Nano Letters* **2004**, 4, (4), 633-637.
23. Hua, F.; Sun, Y.; Gaur, A.; Meitl, M. A.; Bilhaut, L.; Rotkina, L.; Wang, J.; Geil, P.; Shim, M.; Rogers, J. A.; Shim, A. *Nano Letters* **2004**, 4, (12), 2467-2471.
24. Lessard, R. A.; Manivannan, G. *Proceedings of SPIE* **1995**, 2405, 2-23.

25. Trentler, T. J.; Boyd, J. E.; Colvin, V. L. *Chemistry of Materials* **2000**, 12, (5), 1431-1438.
26. Moszner, N. *Macromolecular Symposia* **2004**, 217, (1), 63-76.
27. Ilie, N.; Jelen, E.; Clementino-Luedemann, T.; Hickel, R. *Dental Materials Journal* **2007**, 26, (2), 149-155.
28. Crivello, J. V., Cationic Polymerization - Iodonium and Sulfonium Salt Photoinitiators. In *Advances in Polymer Science*, Springer: Berlin, 1984; Vol. Vol. 62, pp 1-48.
29. Neckers, D. C., *Mechanistic Organic Photochemistry*. Reinhold Publishing: New York, 1967.
30. Kissinger, M.; Michel, J., *Excited States and Photochemistry of Organic Molecules*. VCH Publishers: New York, 1995.
31. Hollas, J. M., *Modern Spectroscopy*. 4th ed. ed.; John Wiley & Sons: Chichester, 2004.
32. Hof, M., Basics of Optical Spectroscopy. In *Handbook of Spectroscopy*, Wiley-VCH: 2005; pp 37-47.
33. Hesse, M.; Meier, H.; Zeeh, B., *Spektroskopische Methoden in Organischer Chemie*. 2nd ed. ed.; Thieme: Stuttgart, 2007.
34. Saunders, C.; Lopata, V.; Barnard, J.; Stepanik, T. *Radiation Physics and Chemistry* **2000**, 57, (3-6), 441-445.
35. Fouassier, J. P., Excited-State Reactivity in Radical Polymerization Photoinitiators. In *Radiation Curing in Polymer Science and Technology*, Elsevier: 1993; Vol. Vol. II, pp 1-61.
36. Hageman, H. J. *Progress in Organic Coatings* **1985**, 13, (2), 123-150.
37. Monroe, B. M.; Weed, G. C. *Chemical Reviews* **1993**, 93, (1), 435-448.
38. Yağci, Y.; Reetz, I. *Progress in Polymer Science* **1998**, 23, (8), 1485-1538.
39. Dektar, J. L.; Hacker, N. P. *Journal of the American Chemical Society* **1990**, 112, (16), 6004-6015.
40. Crivello, J. V. *Annual Review of Materials Science* **1983**, 13, (1), 173-190.
41. Dektar, J. L.; Hacker, N. P. *Journal of Organic Chemistry* **1990**, 55, (2), 639-647.
42. Crivello, J. V.; Jang, M. *Journal of Photochemistry and Photobiology A: Chemistry* **2003**, 159, (2), 173-188.
43. Crivello, J. V. *Journal of Macromolecular Science, Part A* **2009**, 46, (5), 474-483.
44. Ledwith, A. *Polymer* **1978**, 19, (10), 1217-1219.
45. Tehfe, M.-A.; Lalevée, J.; Gigmès, D.; Fouassier, J. P. *Macromolecules* **2010**, 43, (3), 1364-1370.
46. Aoshima, S.; Kanaoka, S. *Chemical Reviews* **2009**, 109, (11), 5245-5287.
47. Lechner, M. D.; Gehrke, K.; Nordmeier, E. H., *Makromolekulare Chemie*. Birkhaeuser Verlag: Basel, 2003; Vol. 3. Auflage.
48. Elias, H.-G., Ionische Polymerisationen. In *Makromoleküle: Chemische Struktur und Synthesen*, Wiley-VCH: Weinheim, 2009; Vol. 6. Auflage, pp 214-261.

49. Penczek, S.; Kubisa, P.; Matyjaszewski, K., *Cationic Ring-Opening Polymerization of Heterocyclic Monomers*. Springer: Berlin, 1980.
50. Lapin Stephen, C., Radiation-Induced Cationic Curing of Vinyl-Ether-Functionalized Urethane Oligomers. In *Radiation Curing of Polymeric Materials*, American Chemical Society: 1990; Vol. Vol. 417, pp 363-381.
51. Lapin, S. *Polymeric materials science and engineering* **1989**, 61, 302-306.
52. Szwarc, M. *Nature* **1956**, 178, (4543), 1168-1169.
53. Miyamoto, M.; Sawamoto, M.; Higashimura, T. *Macromolecules* **1984**, 17, (3), 265-268.
54. Ligon, S. C.; Husár, B.; Wutzel, H.; Holman, R.; Liska, R. *Chemical Reviews* **2014**, 114, (1), 557-589.
55. Jacobine, A. F., Thiol-ene photopolymers. In *Radiation Curing in Polymer Science and Technology*, Elsevier: London, 1993; Vol. Vol. III, pp 219-268.
56. Hoyle, C. E.; Lee, T. Y.; Roper, T. *Journal of Polymer Science Part A: Polymer Chemistry* **2004**, 42, (21), 5301-5338.
57. Hoyle, C. E.; Bowman, C. N. *Angewandte Chemie International Edition* **2010**, 49, (9), 1540-1573.
58. Hoyle, C. E.; Lowe, A. B.; Bowman, C. N. *Chemical Society Reviews* **2010**, 39, (4), 1355-1387.
59. Kade, M. J.; Burke, D. J.; Hawker, C. J. *Journal of Polymer Science Part A: Polymer Chemistry* **2010**, 48, (4), 743-750.
60. Carothers, W. H. *Chemical Reviews* **1931**, 8, (3), 353-426.
61. Elias, H.-G., Polykondensationen und Polyadditionen. In *Makromoleküle: Chemische Struktur und Synthesen*, Wiley-VCH: Weinheim, 2009; Vol. 6. Auflage, pp 417-486.
62. Henríquez, C.; Bueno, C.; Lissi, E. A.; Encinas, M. V. *Polymer* **2003**, 44, (19), 5559-5561.
63. Kolb, H. C.; Finn, M. G.; Sharpless, K. B. *Angewandte Chemie International Edition* **2001**, 40, (11), 2004-2021.
64. Barner-Kowollik, C.; Du Prez, F. E.; Espeel, P.; Hawker, C. J.; Junkers, T.; Schlaad, H.; Van Camp, W. *Angewandte Chemie International Edition* **2011**, 50, (1), 60-62.
65. Gress, A.; Völkel, A.; Schlaad, H. *Macromolecules* **2007**, 40, (22), 7928-7933.
66. ten Brummelhuis, N.; Diehl, C.; Schlaad, H. *Macromolecules* **2008**, 41, (24), 9946-9947.
67. Reppe, W. *Chemie Ingenieur Technik* **1950**, 22, (17), 361-373.
68. Reppe, W. *Justus Liebig's Annalen der Chemie* **1956**, 601, (1), 81-138.
69. Reppe, W. Verfahren zur Herstellung von Vinyläthern. DE 550403 C, 19.05.1932.
70. Reppe, W. Verfahren zur Darstellung von Vinyläthern DE 584840 C, 25.09.1933.
71. Lapin, S., Radiation-Induced Cationic Curing of Vinyl Ethers. In *Radiation Curing*, Springer: 1992; pp 241-271.
72. Brochure: The broadest portfolio of vinyl monomers. BASF, Ed. 2013.

73. Vinyl Ether Terminated Monomers: Reactive Agents for RadCure. https://www.sigmaaldrich.com/content/dam/sigmaaldrich/docs/Aldrich/General_Information/vinyl_ether_terminated_monomers.pdf (05.09.2015),
74. Adelman, R. L. *Journal of the American Chemical Society* **1953**, 75, (11), 2678-2682.
75. Okimoto, Y.; Sakaguchi, S.; Ishii, Y. *Journal of the American Chemical Society* **2002**, 124, (8), 1590-1591.
76. Watanabe, W. H.; Conlon, L. E. Vinyl Transesterification US 2760990 A, 28.08.1956.
77. Smith, M. A.; Wagener, K. B. *American Chemical Society, Polymer Preprints, Division of Polymer Chemistry* **1987**, 28, 264-265.
78. Handerson, S.; Schlaf, M. *Organic Letters* **2002**, 4, (3), 407-409.
79. Winternheimer, D. J. Vinyl Ether Synthesis. Dissertation, University of California, Los Angeles, 2010.
80. Karcher, M.; Henkelmann, J. Verfahren zur Herstellung von Aminovinylethern. EP 514710 A2, 07.05.1992.
81. Mangold, C.; Dingels, C.; Obermeier, B.; Frey, H.; Wurm, F. *Macromolecules* **2011**, 44, (16), 6326-6334.
82. Webster, D. C. *Progress in Organic Coatings* **2003**, 47, (1), 77-86.
83. Tordeux, M.; Dorme, R.; Wakselman, C. *Synthetic Communications* **1983**, 13, (8), 629-633.
84. Satoh, K.; Kamigaito, M.; Sawamoto, M. *Macromolecules* **2000**, 33, (3), 748-753.
85. Hon, Y.-S.; Lee, C.-F.; Chen, R.-J.; Szu, P.-H. *Tetrahedron* **2001**, 57, (28), 5991-6001.
86. Kipnis, F.; Soloway, H.; Ornfelt, J. *Journal of the American Chemical Society* **1951**, 73, (4), 1783-1784.
87. Reppe, W.; Baur, K. Verfahren zur Herstellung von Alkyl- bzw. Aryloxyäthylidenestern und Acetalen DE 566033 C, 08.12.1932.
88. Summers, L. *Chemical Reviews* **1955**, 55, (2), 301-353.
89. Allinger, N. L.; Glaser, J. A.; Davis, H. E.; Rogers, D. W. *The Journal of Organic Chemistry* **1981**, 46, (4), 658-661.
90. Kamachi, M.; Tanaka, K.; Kuwae, Y. *Journal of Polymer Science Part A: Polymer Chemistry* **1986**, 24, (5), 925-929.
91. Knolle, W.; Janovský, I.; Naumov, S.; Mehnert, R. *Radiation Physics and Chemistry* **1999**, 55, (5-6), 625-631.
92. Matsumoto, A.; Nakana, T.; Oiwa, M. *Die Makromolekulare Chemie, Rapid Communications* **1983**, 4, (5), 277-279.
93. Decker, C.; Decker, D. *Journal of Macromolecular Science, Part A* **1997**, 34, (4), 605-625.
94. Bevington, J. C.; Huckerby, T. N.; Jenkins, A. D. *Journal of Macromolecular Science, Part A* **1999**, 36, (12), 1907-1922.

95. Fujimori, K.; Organ, P. P.; Costigan, M. J.; Craven, I. E. *Journal of Macromolecular Science: Part A - Chemistry* **1986**, 23, (5), 647-655.
96. Decker, C.; Decker, D. *Polymer* **1997**, 38, (9), 2229-2237.
97. Zhang, L.; Liu, L.; Chen, Y. *Journal of Applied Polymer Science* **1999**, 74, (14), 3541-3547.
98. Bayer, O. *Angewandte Chemie* **1947**, 59, (9), 257-272.
99. Delebecq, E.; Pascault, J.-P.; Boutevin, B.; Ganachaud, F. *Chemical Reviews* **2012**, 113, (1), 80-118.
100. Chattopadhyay, D. K.; Raju, K. V. S. N. *Progress in Polymer Science* **2007**, 32, (3), 352-418.
101. Szycher, M., *Szycher's Handbook of Polyurethanes*. CRC Press Boca Raton, 2012; Vol. Vol. 2.
102. Meier-Westhues, U., *Polyurethane - Coatings, Adhesives and Sealants*. Vincentz Network: Hannover, 2007; Vol. Vol. 2.
103. Simon, J.; Barla, F.; Kelemen-Haller, A.; Farkas, F.; Kraxner, M. *Chromatographia* **1988**, 25, (2), 99-106.
104. Wicks Jr, Z. W. *Progress in Organic Coatings* **1975**, 3, (1), 73-99.
105. Wicks, D. A.; Wicks Jr, Z. W. *Progress in Organic Coatings* **1999**, 36, (3), 148-172.
106. Wicks, D. A.; Wicks Jr, Z. W. *Progress in Organic Coatings* **2001**, 41, (1-3), 1-83.
107. Anastas, P. T.; Boethling, R.; Voutchkova-Kostal, A., *Green Processes, Designing Safer Chemicals*. Wiley-VCH: Weinheim, 2013; Vol. 9.
108. Kreye, O.; Mutlu, H.; Meier, M. A. R. *Green Chemistry* **2013**, 15, (6), 1431-1455.
109. Keller, H. *Strukturbildung in Polyurethandispersionen und -filmen*. Johannes Gutenberg-Universität, Mainz, 2014.
110. Nohra, B.; Candy, L.; Blanco, J.-F.; Guerin, C.; Raoul, Y.; Mouloungui, Z. *Macromolecules* **2013**, 46, (10), 3771-3792.
111. Blattmann, H.; Fleischer, M.; Bähr, M.; Mülhaupt, R. *Macromolecular Rapid Communications* **2014**, 35, (14), 1238-1254.
112. Guan, J.; Song, Y.; Lin, Y.; Yin, X.; Zuo, M.; Zhao, Y.; Tao, X.; Zheng, Q. *Industrial & Engineering Chemistry Research* **2011**, 50, (11), 6517-6527.
113. Kathalewar, M. S.; Joshi, P. B.; Sabnis, A. S.; Malshe, V. C. *RSC Advances* **2013**, 3, (13), 4110-4129.
114. Darensbourg, D. J.; Holtcamp, M. W. *Coordination Chemistry Reviews* **1996**, 153, 155-174.
115. Caló, V.; Nacci, A.; Monopoli, A.; Fanizzi, A. *Organic Letters* **2002**, 4, (15), 2561-2563.
116. Tomita, H.; Sanda, F.; Endo, T. *Journal of Polymer Science Part A: Polymer Chemistry* **2001**, 39, (1), 162-168.
117. Wang, K.; Wu, W.; Zhu, X.; Yu, Q. *Designed Monomers and Polymers* **2012**, 15, (1), 31-39.

118. Darensbourg, D. J.; Horn Jr, A.; Moncada, A. I. *Green Chemistry* **2010**, 12, (8), 1376-1379.
119. Diakoumakos, C. D.; Kotzev, D. L. *Macromolecular Symposia* **2004**, 216, (1), 37-46.
120. Clements, J. H. *Industrial & Engineering Chemistry Research* **2003**, 42, (4), 663-674.
121. Ishida, H., Chapter 1 - Overview and Historical Background of Polybenzoxazine Research. In *Handbook of Benzoxazine Resins*, Hatsuo, I.; Tarek, A., Eds. Elsevier: Amsterdam, 2011; pp 3-81.
122. Ghosh, N. N.; Kiskan, B.; Yagci, Y. *Progress in Polymer Science* **2007**, 32, (11), 1344-1391.
123. Takeichi, T.; Kawauchi, T.; Agag, T. *Polym. J* **2008**, 40, (12), 1121-1131.
124. Ishida, H.; Liu, J.-P., Chapter 2 - Benzoxazine Chemistry in Solution and Melt. In *Handbook of Benzoxazine Resins*, Hatsuo, I.; Tarek, A., Eds. Elsevier: Amsterdam, 2011; pp 85-102.
125. Gu, Y.; Li, M., Chapter 3 - Molecular Modeling. In *Handbook of Benzoxazine Resins*, Hatsuo, I.; Tarek, A., Eds. Elsevier: Amsterdam, 2011; pp 103-110.
126. Jubsilp, C.; Takeichi, T.; Rimdusit, S., Chapter 7 - Polymerization Kinetics. In *Handbook of Benzoxazine Resins*, Hatsuo, I.; Tarek, A., Eds. Elsevier: Amsterdam, 2011; pp 157-174.
127. Kim, H.; Ishida, H., Chapter 12 - Hydrogen Bonding of Polybenzoxazines. In *Handbook of Benzoxazine Resins*, Hatsuo, I.; Tarek, A., Eds. Elsevier: Amsterdam, 2011; pp 237-261.
128. Chirachanchai, S.; Phongtamrug, S.; Laobuthee, A.; Tashiro, K., Chapter 4 - Mono-Substituted Phenol-Based Benzoxazines: Inevitable Dimerization Via Self-Termination and Its Metal Complexation. In *Handbook of Benzoxazine Resins*, Hatsuo, I.; Tarek, A., Eds. Elsevier: Amsterdam, 2011; pp 111-126.
129. Kirschbaum, S.; Landfester, K.; Taden, A. *Macromolecules* **2015**, 48, (12), 3811-3816.
130. Ning, X.; Ishida, H. *Journal of Polymer Science Part A: Polymer Chemistry* **1994**, 32, (6), 1121-1129.
131. Low, H. Y.; Ishida, H. *Polymer* **1999**, 40, (15), 4365-4376.
132. Hemvichian, K.; Ishida, H. *Polymer* **2002**, 43, (16), 4391-4402.
133. Shen, S. B.; Ishida, H. *Polymer Composites* **1996**, 17, (5), 710-719.
134. Kim, H. J.; Brunovska, Z.; Ishida, H. *Journal of Applied Polymer Science* **1999**, 73, (6), 857-862.
135. Wirasate, S.; Dhumrongvaraporn, S.; Allen, D. J.; Ishida, H. *Journal of Applied Polymer Science* **1998**, 70, (7), 1299-1306.
136. Sawaryn, C.; Landfester, K.; Taden, A. *Polymer* **2011**, 52, (15), 3277-3287.
137. Sawaryn, C.; Landfester, K.; Taden, A. *Macromolecules* **2010**, 43, (21), 8933-8941.
138. Sawaryn, C.; Landfester, K.; Taden, A. *Macromolecules* **2011**, 44, (14), 5650-5658.

139. Sawaryn, C.; Landfester, K.; Taden, A. *Macromolecules* **2011**, 44, (19), 7668-7674.
140. Ehrenstein, G. W.; Riedel, G.; Trawiel, P., *Praxis der Thermischen Analyse von Kunststoffen*. Hanser Verlag: München, 2003; Vol. Vol. 2.
141. Wunderlich, B., *Thermal Analysis of Polymeric Materials*. Springer: Heidelberg, 2005.
142. Menczel, J. D.; Prime, R. B., *Thermal Analysis of Polymers: Fundamentals and Applications*. John Wiley & Sons: New Jersey, 2009.
143. Höhne, G. W. H.; Hemminger, W. F.; Flammersheim, H.-J., *Differential Scanning Calorimetry*. Springer: Heidelberg, 2003; Vol. Vol. 2.
144. Wight, F. R.; Hicks, G. W. *Polymer Engineering & Science* **1978**, 18, (5), 378-381.
145. Schmolzer, S., Brochure: Untersuchungen an UV-härtenden Systemen mittels Photo-Dynamischer Differenzkalorimetrie (Photo-DSC). Netzsch-Gerätebau: 2012.
146. Photocalorimetry - Photo-DSC: Method, Technique, Applications. Netzsch-Gerätebau, Ed. 2015.
147. Decker, C.; Moussa, K. *Die Makromolekulare Chemie* **1988**, 189, (10), 2381-2394.
148. Yang, D. B. *Journal of Polymer Science Part A: Polymer Chemistry* **1993**, 31, (1), 199-208.
149. Kirschbaum, S. Syntheses, characterization and evaluation of photoinitiator-functionalized poly(meth)acrylates by SET-LRP. FH Aachen, 2012.
150. Scherzer, T.; Buchmeiser, M. R. *Macromolecular Chemistry and Physics* **2007**, 208, (9), 946-954.
151. Asmussen, S.; Schroeder, W.; dell'Erba, I.; Vallo, C. *Polymer Testing* **2013**, 32, (7), 1283-1289.
152. Workman, J.; Weyer, L., Alkenes and Alkynes. In *Practical Guide and Spectral Atlas for Interpretive Near-Infrared Spectroscopy*, 2nd ed.; CRC Press: 2012; pp 33-38.
153. Mezger, T. G., *Das Rheologie Handbuch*. Vincentz Network: Hannover, 2012; Vol. Vol. 4.
154. Mezger, T. G., *The Rheology Handbook*. 2nd ed. ed.; Vincent Network: Hannover, 2006.
155. Khan, S. A.; Plitz, I. M.; Frantz, R. A. *Rheola Acta* **1992**, 31, (2), 151-160.
156. Schall, J. D.; Jacobine, A. F.; Woods, J. G.; Coffey, R. N. In *Photorheometry: A Tool for Characterizing High-Performance Adhesives and Coatings* RadTech Europe Conference, Vienna, 13.-15.11.2007, Vienna.
157. Scherzer, T.; Schröder, M. W. *Proc. RadTech Europe 2009 Conference* **2009**.
158. Botella, A.; Dupuy, J.; Roche, A.-A.; Sautereau, H.; Verney, V. *Macromolecular Rapid Communications* **2004**, 25, (12), 1155-1158.
159. Chang, M.-H.; Das, D.; Varde, P. V.; Pecht, M. *Microelectronics Reliability* **2012**, 52, (5), 762-782.
160. Jandt, K. D.; Mills, R. W. *Dental Materials* **2013**, 29, (6), 605-617.

161. Choi, S.-J.; Yoo, P. J.; Baek, S. J.; Kim, T. W.; Lee, H. H. *Journal of the American Chemical Society* **2004**, 126, (25), 7744-7745.
162. Yoo, P. J.; Choi, S.-J.; Kim, J. H.; Suh, D.; Baek, S. J.; Kim, T. W.; Lee, H. H. *Chemistry of Materials* **2004**, 16, (24), 5000-5005.
163. Choi, S.-J.; Kim, H. N.; Bae, W. G.; Suh, K.-Y. *Journal of Materials Chemistry* **2011**, 21, (38), 14325-14335.
164. Crivello, J. V.; Lam, J. H. W. *Macromolecules* **1977**, 10, (6), 1307-1315.
165. Guo, L. J. *Advanced Materials* **2007**, 19, (4), 495-513.
166. Cheng, X.; Guo, L. J.; Fu, P. F. *Advanced Materials* **2005**, 17, (11), 1419-1424.
167. Sawamoto, M.; Higashimura, T. *Makromolekulare Chemie. Macromolecular Symposia* **1986**, 3, (1), 83-97.
168. Namikoshi, T.; Hashimoto, T.; Kodaira, T. *Journal of Polymer Science Part A: Polymer Chemistry* **2004**, 42, (12), 2960-2972.
169. Feng, P.; Li, W.; Zou, Y. *Journal of Applied Polymer Science* **2014**, 131, (15), 40501.
170. Lim, Y. H.; Heo, G. S.; Rezenom, Y. H.; Pollack, S.; Raymond, J. E.; Elsabahy, M.; Wooley, K. L. *Macromolecules* **2014**, 47, (14), 4634-4644.
171. Dahlquist, C. A., Tack. In *Adhesion Fundamentals and Practice*, 1969; pp 143-151.
172. Paul, C. W., Pressure-Sensitive Adhesives (PSAs). In *Handbook of Adhesion Technology*, Silva, L. F. M. d.; Öchsner, A.; Adams, R. D., Eds. Springer: Berlin, 2011; pp 341-372.
173. Radke, W.; Müller, A. H. E. *Makromolekulare Chemie. Macromolecular Symposia* **1992**, 54-55, (1), 583-594.
174. Roos, S. G.; Müller, A. H. E.; Matyjaszewski, K. *Macromolecules* **1999**, 32, (25), 8331-8335.
175. Kirschbaum, S.; Landfester, K.; Taden, A. *Angewandte Chemie International Edition* **2015**, 54, (19), 5789-5792.
176. Pham, H. Q.; Marks, M. J., Epoxy Resins. In *Kirk-Othmer Encyclopedia of Chemical Technology*, John Wiley & Sons: 2000.
177. Mezger, T. G., Oszillationsversuche. In *Das Rheologie Handbuch*, Vincentz Network: Hannover, 2012; pp 138-218.
178. Chattopadhyay, D. K.; Sreedhar, B.; Raju, K. V. S. N. *Polymer* **2006**, 47, (11), 3814-3825.
179. Crivello, J. V. *Journal of Polymer Science Part A: Polymer Chemistry* **2007**, 45, (18), 4331-4340.
180. Crivello, J. V. *Journal of Polymer Science Part A: Polymer Chemistry* **2007**, 45, (16), 3759-3769.
181. Jian, Z.; Yong, H.; Ming, X.; Jun, N. *Progress in Organic Coatings* **2009**, 66, (1), 35-39.
182. Weikard, J.; Sonntag, M.; Mundstock, H. Coating composition containing UV-curable urethane (meth)acrylates containing isocyanate groups and urethane (meth)acrylates containing hydroxyl groups. US 6500876 B2, 31.12.2002.

183. Jacobine, A. F.; Nakos, S. T.; Salamon, P. A.; Chu, H.-K. Polyurethane Compositions Containing Both Radiation and Moisture Curable Groups. US 6844376 B1, 18.01.2005.
184. Bruchmann, B.; Beck, E.; Renz, H.; Königer, R.; Schwalm, R.; Lokai, M.; Reich, W. Coating agents which can be hardened by the addition of isocyanate groups as well as by the radiation-induced addition of activated C-C double covalent bonds. EP 1144476 B1, 14.12.1999.
185. Lin, Y.; Stansbury, J. W. *Journal of Polymer Science Part A: Polymer Chemistry* **2004**, 42, (8), 1985-1998.
186. Wuts, P. G. M.; Greene, T. W., Protection for the Hydroxyl Group, Including 1,2- and 1,3-Diols. In *Greene's Protective Groups in Organic Synthesis*, John Wiley & Sons: 2006; pp 16-366.
187. Ruckenstein, E.; Zhang, H. *Journal of Polymer Science Part A: Polymer Chemistry* **2000**, 38, (10), 1848-1851.
188. Heller, J.; Penhale, D. W. H.; Helwing, R. F. *Journal of Polymer Science: Polymer Letters Edition* **1980**, 18, (4), 293-297.
189. Zhang, H.; Ruckenstein, E. *Journal of Polymer Science Part A: Polymer Chemistry* **2000**, 38, (20), 3751-3760.
190. Hashimoto, T.; Ishizuka, K.; Umehara, A.; Kodaira, T. *Journal of Polymer Science Part A: Polymer Chemistry* **2002**, 40, (22), 4053-4064.
191. Dingels, C.; Müller, S. S.; Steinbach, T.; Tonhauser, C.; Frey, H. *Biomacromolecules* **2013**, 14, (2), 448-459.
192. Pohlit, H.; Bellinghausen, I.; Schömer, M.; Heydenreich, B.; Saloga, J.; Frey, H. *Biomacromolecules* **2015**, 16, (10), 3103-3111.
193. Tonhauser, C.; Schüll, C.; Dingels, C.; Frey, H. *ACS Macro Letters* **2012**, 1, (9), 1094-1097.
194. Sangermano, M.; Malucelli, G.; Morel, F.; Decker, C.; Priola, A. *European Polymer Journal* **1999**, 35, (4), 639-645.
195. Metz, G.; Wu, X. L.; Smith, S. O. *Journal of Magnetic Resonance, Series A* **1994**, 110, (2), 219-227.
196. Nowacka, A.; Bongartz, N. A.; Ollila, O. H. S.; Nylander, T.; Topgaard, D. *Journal of Magnetic Resonance* **2013**, 230, 165-175.
197. Boateng, J. S.; Matthews, K. H.; Stevens, H. N. E.; Eccleston, G. M. *Journal of Pharmaceutical Sciences* **2008**, 97, (8), 2892-2923.
198. Hofmeister, I.; Landfester, K.; Taden, A. *Angewandte Chemie International Edition* **2015**, 54, (1), 327-330.
199. Ganta, S.; Devalapally, H.; Shahiwala, A.; Amiji, M. *Journal of Controlled Release* **2008**, 126, (3), 187-204.
200. Mura, S.; Nicolas, J.; Couvreur, P. *Nat Mater* **2013**, 12, (11), 991-1003.
201. Tomita, H.; Sanda, F.; Endo, T. *Journal of Polymer Science Part A: Polymer Chemistry* **2001**, 39, (6), 860-867.
202. Kihara, N.; Endo, T. *Journal of Polymer Science Part A: Polymer Chemistry* **1993**, 31, (11), 2765-2773.

203. Ochiai, B.; Inoue, S.; Endo, T. *Journal of Polymer Science Part A: Polymer Chemistry* **2005**, 43, (24), 6613-6618.
204. McCabe, R. W.; Taylor, A. *Chemical Communications* **2002**, (9), 934-935.
205. Ochiai, B.; Sato, S.-I.; Endo, T. *Journal of Polymer Science Part A: Polymer Chemistry* **2007**, 45, (15), 3408-3414.
206. Ochiai, B.; Sato, S.-I.; Endo, T. *Journal of Polymer Science Part A: Polymer Chemistry* **2007**, 45, (15), 3400-3407.
207. Kihara, N.; Kushida, Y.; Endo, T. *Journal of Polymer Science Part A: Polymer Chemistry* **1996**, 34, (11), 2173-2179.
208. Ochiai, B.; Nakayama, J.-i.; Mashiko, M.; Kaneko, Y.; Nagasawa, T.; Endo, T. *Journal of Polymer Science Part A: Polymer Chemistry* **2005**, 43, (23), 5899-5905.
209. Cramer, N. B.; Bowman, C. N., Chapter 1: Thiol-ene and Thiol-yne Chemistry in Ideal Network Synthesis. In *Thiol-X Chemistries in Polymer and Materials Science*, The Royal Society of Chemistry: 2013; pp 1-27.
210. Yagci, Y.; Kiskan, B.; Ghosh, N. N. *Journal of Polymer Science Part A: Polymer Chemistry* **2009**, 47, (21), 5565-5576.
211. Dunkers, J.; Ishida, H. *Journal of Polymer Science Part A: Polymer Chemistry* **1999**, 37, (13), 1913-1921.
212. Dunkers, J.; Zarate, E. A.; Ishida, H. *The Journal of Physical Chemistry* **1996**, 100, (32), 13514-13520.
213. Kim, H.-D.; Ishida, H. *The Journal of Physical Chemistry A* **2002**, 106, (14), 3271-3280.
214. Sawaryn, C.; Kreiling, S.; Schönfeld, R.; Landfester, K.; Taden, A., Chapter 35 - Benzoxazines for Industrial Applications Comparison with Other Resins, Formulation and Toughening Know-How, and Water-Based Dispersion Technology. In *Handbook of Benzoxazine Resins*, Hatsuo, I.; Tarek, A., Eds. Elsevier: Amsterdam, 2011; pp 605-620.
215. Prisacariu, C., *Polyurethane Elastomers: From Morphology to Mechanical Aspects*. Springer: Wien, 2011.
216. Takeichi, T.; Guo, Y.; Agag, T. *Journal of Polymer Science Part A: Polymer Chemistry* **2000**, 38, (22), 4165-4176.
217. Takeichi, T.; Guo, Y. *Polymer Journal* **2001**, 33, (5), 437-443.
218. Rimdusit, S.; Pirstpindvong, S.; Tanthapanichakoon, W.; Damrongsakkul, S. *Polymer Engineering & Science* **2005**, 45, (3), 288-296.
219. Jamshidi, S.; Yeganeh, H.; Mehdipour-Ataei, S. *Polymers for Advanced Technologies* **2011**, 22, (11), 1502-1512.
220. Jamshidi, S.; Yeganeh, H.; Mehdipour-Ataei, S. *Polymer International* **2011**, 60, (1), 126-135.
221. Liu, Y.; Zhang, X.; Gao, N. *Polymer Engineering & Science* **2015**, 55, (3), 604-613.
222. Ishida, H.; Rodriguez, Y. *Journal of Applied Polymer Science* **1995**, 58, (10), 1751-1760.

223. Cui, Y.; Chen, Y.; Wang, X.; Tian, G.; Tang, X. *Polymer International* **2003**, 52, (8), 1246-1248.
224. Rimdusit, S.; Sudjidjune, M.; Jubsilp, C.; Tiptipakorn, S. *Journal of Applied Polymer Science* **2014**, 131, (13), 40502.
225. Baqar, M.; Agag, T.; Ishida, H.; Qutubuddin, S. *Polymer* **2011**, 52, (2), 307-317.
226. Gaina, C.; Ursache, O.; Gaina, V.; Varganici, C. D. *J Polym Res* **2014**, 21, (11), 1-11.
227. Sudo, A.; Du, L. C.; Hirayama, S.; Endo, T. *J Polym Sci Pol Chem* **2010**, 48, (13), 2777-2782.
228. Sudo, A.; Mori, A.; Endo, T. *Journal of Polymer Science Part A: Polymer Chemistry* **2011**, 49, (10), 2183-2190.
229. Chutayothin, P.; Ishida, H. *European Polymer Journal* **2009**, 45, (5), 1493-1505.
230. Burke, W. J.; Bishop, J. L.; Glennie, E. L. M.; Bauer, W. N. *The Journal of Organic Chemistry* **1965**, 30, (10), 3423-3427.
231. Kudoh, R.; Sudo, A.; Endo, T. *Macromolecules* **2009**, 42, (7), 2327-2329.
232. Yang, L.-Q.; He, B.; Meng, S.; Zhang, J.-Z.; Li, M.; Guo, J.; Guan, Y.-M.; Li, J.-X.; Gu, Z.-W. *Polymer* **2013**, 54, (11), 2668-2675.
233. Helmchen, G.; Strubert, W. *Chromatographia* **1974**, 7, (12), 713-715.
234. Agrawal Y, K.; Patel, R. *Reviews in Analytical Chemistry* **2002**, Vol. 21, (4), 285.
235. Dunkers, J.; Ishida, H. *Spectrochimica Acta Part A: Molecular and Biomolecular Spectroscopy* **1995**, 51, (5), 855-867.

8 Appendix

8.1 List of Abbreviations and Symbols

^{13}C NMR	carbon-13 nuclear magnetic resonance
^1H NMR	proton nuclear magnetic resonance
APVE	3-aminopropyl vinyl ether
BDDGC	4,1-butanedioldiglycidylcarbonate
BDDGC	butanedioldiglycidyl carbonate
BDDGE	butanediol diglycidylether
BOX	benzoxazine
CP	cross polarization
DABCO	1,4-diazabicyclo[2.2.2]octane
DBTL	dibutyltin dilaurate
ΔH_{pc}	post-curing enthalpy
di-TMP	di-trimethylolpropane
di-TMPDC	di-trimethylolpropanedicarbonate
DMC	dimethyl carbonate
DMDEE	2,2'-dimorpholinyl diethyl ether
DMDO	dimercapto-1,8-dioxa-3,6,-octane
DMP	2,4-dimethylphenol
DMP _{2-m}	polybenzoxazine reference substance based on dimethylphenol and methylamine
DMSO	dimethyl sulfoxide
ECH	epichlorohydrin
EGBAPE	ethylene glycol bis(3-aminopropyl) ether
EP	equivalent point
GC-FID	gas chromatography with flame ionization detector
HBVE	4-hydroxybutyl vinyl ether
HDI	hexamethylene diisocyanate
HMDA	hexamethylene diamine
HOMO	highest occupied molecular orbital
HPLC-MS	combined high performance liquid chromatography mass spectrometry
HS	hard segment
IC	internal conversion
INEPT	insensitive nuclei enhanced by polarization transfer
IPDA	isophorone diamine
IPDI	isophorone diisocyanate
IR	infrared

IRH	isocyanate reactive hydroxyl content
ISC	intersystem crossing
LED	light emitting diode
LUMO	lowest unoccupied molecular orbital
MAS	magic angle spinning
MDI	methylene diphenyl diisocyanate
M_n	number average molecular weight
M_p	peak molecular weight
NIPU	non-isocyanate polyurethane
NIR	near infrared
p	conversion
PAG	photoacid generator
PDI	polydispersity index
PETMP	pentaerythritoltetra(3-mercaptopropionate)
PHU	polyhydroxyurethane
PI	photoinitiator
P-m	benzoxazine from phenol and methylamine
PPG	polypropylene glycol
PU	polyurethane
PUA	polyurethane acrylate
r	copolymerization parameter
R	organic substituent
S_0	singlet ground state
S_1	first excited singlet state
$\Sigma\Delta H_c$	total curing enthalpy
SEC	size exclusion chromatography
SS	soft segment
t	time
T_1	first excited triplet state
TBAB	tetrabutylammonium bromide
T_c	curing temperature
TDI	toluene diisocyanate
TEA	triethylamine
TEAB	tetraethylammonium bromide
T_g	glass transition temperature
T_{pc}	onset temperature of the post-curing reaction
UV	ultraviolet
VEDGC	vinyl ether diglycidylcarbonate
VEPU	vinyl ether functional polyurethane
VR	vibrational relaxation

8.2 Scientific Contributions

Conferences

- Oral presentation “Vinyl Ether Functionalized Polymers - Photopolymers with Unique Properties”, Group Seminar - Physical Chemistry of Polymers, Max Planck Institute for Polymer Research, Mainz, 13.05.2015
- Poster presentation “Polyurethane Photopolymers - Unique Curing Properties Introduced via Vinyl Ether Building Blocks”, European Scientific Advisory Board Meeting, Henkel Adhesive Technologies, Düsseldorf, 23.-24.02.2015
- Oral presentation “Polyurethane Photopolymers Based on Vinyl Ether Building Blocks”, Review Meeting Henkel/MPI Cooperation, Düsseldorf, 30.-31.10.2014
- Oral presentation “Photoinduced Crosslinking of Waterbased Polyurethane Systems via Cationic Cure”, 3rd European Symposium of Photopolymer Science, Vienna, 09.-12.09.2014
- Oral presentation “Functionalized Polyurethane Dispersions”, Group Seminar - Physical Chemistry of Polymers, Max Planck Institute for Polymer Research, Mainz, 07.04.2014
- Oral presentation “Cationic Polymerization of Films from Dispersed Phase”, Review Meeting Henkel/MPI Cooperation, Düsseldorf, 17.-18.10.2013

Patents

- Andreas Taden, Stefan Kirschbaum, Katharina Landfester, Kationische Phototransferpolymerisation, *in preparation*, internal no. PT033452
- Andreas Taden, Stefan Kirschbaum, Jan-Erik Damke, Katharina Landfester, Härtingsverfahren für Polyurethane, 11.11.2015, filing no. EP 15194065.7, internal no. PT033407
- Andreas Taden, Stefan Kirschbaum, Katharina Landfester, Verfahren zur Herstellung oder Härtung von Polymeren mittels Thiol-En Polyadditionsreaktionen, 11.11.2015, filing no. EP 15194064.0, internal no. PT033463
- Andreas Taden, Stefan Kirschbaum, Katharina Landfester, Alkenyletherpolyole, 09.09.2014, filing no. EP 14184099.1, internal no. PT032591

Publications

- Stefan Kirschbaum, Katharina Landfester, and Andreas Taden, Cationic Phototransfer Polymerization of Photocurable Polyhydroxyurethanes, *withheld for patent submission (PT033452)*
- Stefan Kirschbaum, Robert Graf, Katharina Landfester, and Andreas Taden, Cationic Phototransfer Polymerization: pH-Responsive Acetal-based Polymer Networks for Controlled Release and Degradation, *withheld for patent submission (PT033452)*
- Stefan Kirschbaum, Katharina Landfester, and Andreas Taden, Synergistic Dual Cure Materials based on Vinyl Ether Functional Polyurethanes, *withheld for patent submission (PT033407)*
- Stefan Kirschbaum, Katharina Landfester, and Andreas Taden, Vinyl Ether-Functional Polyols as Building Blocks for Photocurable Polyurethanes and Isocyanate-Free Polyhydroxyurethanes, *withheld for patent submission (PT033463)*
- Stefan Kirschbaum, Katharina Landfester, and Andreas Taden, Synthesis and thermal curing of benzoxazine functionalized polyurethanes, *Macromolecules* **2015**, 48, 3811-3816
- Stefan Kirschbaum, Katharina Landfester, and Andreas Taden, Unique Curing Properties through Living Polymerization in Crosslinking Materials: Polyurethane Photopolymers from Vinyl Ether Building Blocks, *Angew. Chem. Int. Ed.* **2015**, 54, 5789-5792; Einzigartige Härtungseigenschaften durch lebende Polymerisation in vernetzenden Materialien: Polyurethan-Photopolymere aus Vinylether-Synthesebausteinen, *Angew. Chem.* **2015**, 127, 5881-5885

8.3 Danksagung (Acknowledgement)

8.4 Lebenslauf (Curriculum Vitae)

